The rational design of pyrrolobenzodiazepine derivatives

Maciej Kaliszczak

Thesis presented for degree of Doctor of Philosophy

The University of Edinburgh

2009

Declaration

I hereby declare that this thesis was composed by myself and that the work contained therein is my own, except where explicitly stated otherwise in the text.

Maciej Kaliszczak

April 2009

Biography

Before undertaking my PhD at the Edinburgh Cancer Research Center / University of Edinburgh (United Kingdom), I have completed a Degree (BSc) in cellular biology and physiology (mention" bien" eq. 2*i* honours degree) at the University of Rouen (France) in 2003. During my degree, I had been awarded a summer Scholarship (2002), allowing me to gain some laboratory experience at the MRC – (Cambridge, United Kingdom) working on the optimization of phosphotriesterase activity by selection of different genotypes under Dr. Andrew Griffith's supervision. I have also been awarded a travel award, in 2004, which allowed me to go on a five month placement at the Food Research Centre - London, Canada investigating the expression of spider silk and human antibodies in tobacco under Prof. Jim Brandle's supervision.

While working towards a Master degree (MSc) in cellular biology and physiopathology at the University of Rouen (France) in 2004/2005, I was awarded a regional scholarship and therefore, was able to pursue a one year placement at the "Laboratoire de Micro-Environnement et Renouvellement Cellulaire Intégré" (M.E.R.C.I) – (University of Medicine, Rouen, France). The project involved the evaluation of the effect of a proteasome inhibitor PS-341 on CD 133+ differentiation and proliferation using the hematopoietic stem cell model under Prof. Jean Pierre Vannier's supervision which led to the award of MSc. in 2005.

Acknowledgements

I would like to thank Cancer Research UK (CR-UK) for their financial support that has enabled me to complete these studies and the Edinburgh Cancer Research Center / University of Edinburgh for awarding me the studentship. I am also grateful to Spirogen Ltd and Ipsen Ltd (Prof. David E. Thurston, Dr. Philip Howard and Dr. Dyeison Antonow) for providing me with the different compounds and allowing me the investigation of the molecular modeling approach in the London school of Pharmacy, London. I would also like to thank the EORTC-PAMM group which has enabled me to present my data at the PAMM group meeting in Berlin in 2007.

I am grateful to everyone in the Pharmacology and Drug Develpment group (Dr. Shahida Din, Ms. Janet Mc Pherson, Dr. Katan Patel, Dr. Celine Filippi, Ms. Rhona E Aird, Mr. Kenny McLeod, Ms. Marian Thomson, Dr. Elidth Reid and Dr. Ian Mayer) and others of the Edinburgh Cancer Research Center not only for their technical assistance and academic advice they have given me during my studies but also for the great friendships I have made along the way. I would also like to thank Dr. Simon Langdon for his assistance with the *in vivo* work as well as the people of the aninal unit, Dr. Colin James (London shool of Pharmacy, London) for his assistance with the molecular modeling and Dr. Tony Gutierrez (the Scottish Association for Marine Science Dunstaffnage Marine Laboratory Oban, Argyll United Kingdom) for his assistance in the measurements of the surface activity parameter.

Thanks also to my girlfriend, Sophie, my mum and other members of my family, my friends for their wonderful support, always being supportive and

interested in my work (or at least pretending to be). Finally, I would like to thank my supervisors, Dr. Sylvie M. Guichard and Prof. Duncan I. Jodrell, from whom I have received an essential help in order to fulfill this work.

Abstract

Pyrrolobenzodiazepine (PBD) derivatives interact with the minor-groove of DNA to form mono-adducts (monomers) or cross-links (dimers). They show remarkable activity *in vitro* and *in vivo* in a wide range of tumour types and one dimer, SJG-136 is currently in clinical development. Preclinical studies have shown that SJG-136 is a P-gp substrate limiting its anti-tumour activity. The work presented in this thesis identifies key physicochemical properties influencing both the interaction of PBDs with ABC transporters P-gp, MRP1 and BCRP and their growth inhibitory potency. A testable hypothesis for further optimisation of PBDs is proposed.

The biological activity of 4 dimers and 12 monomers was assessed using several *in vitro* models presenting differential expression of ABC transporters. Biological endpoints were the growth inhibitory effect determined using a sulforhodamine B assay and γ-H2AX foci formation. In addition PBD transport was evaluated using a Caco-2 transwell assay.

P-gp substrate specificity was restricted to dimers. The MW, the number of (N+O) atoms (>8), a polar surface area (>75 $Å^2$) and hydrogen bonding energy (>10) could discriminate substrates among the PBDs. P-gp polymorphism was also evaluated. The mutation in position 2677 (G/T) was associated with reduced sensitivity to the PBDs. When combined mutations in position 3435/2677 were linked, the transporter abrogated this apparent gain of function. The impact of MRP1 was identified for all dimers and 1/12 monomers. In addition, the cooperative role of glutathione in the resistance mediated by MRP1 to the PBDs was revealed. The presence of a carbonyl moiety at the extremity was shown to discriminate the

substrate for MRP1 among the monomers. A structure-activity-relationship study showed that negatively charged (N+O) atoms and a greater number of aromatic rings confer greater dependency to BCRP. BCRP polymorphism was also evaluated. The T482 mutant was associated with an increase in drug transport.

The cytotoxicity of the PBDs correlated to the interaction of the DNA as measured by ΔTm. Compounds, being non surface active, with a greater polar surface area and number of aromatic rings and a lower solvent accessible surface area were associated with a greater cytotoxicity. Van-der-waals energy and the electrostatic forces were identified *in silico* as predictable features involved in the DNA binding. New PBDs were designed and were predicted to be associated with a greater affinity for DNA and with minimal interaction with ABC transporters.

Contents

1 Chapter 1: INTRODUCTION

1.1 Targeting DNA as a treatment for cancer

The term chemotherapy refers generally to the use of drugs that kill dividing cancer cells as a treatment for cancer. More than half of people diagnosed with cancer are treated with chemotherapy worldwide. This strategy has been used since the 1940s, when nitrogen mustard was used for the first time as a treatment for cancer. Since then, many drugs have been developed against different targets within the cell. Such compounds include anti-metabolites, monoclonal antibodies, cyclin and tyrosine kinase inhibitors, topo-isomerase inhibitors, vinca alkaloids, and cancer antibiotics. Despite the wide range of chemotherapeutic agents, cancer remains unbeaten. Therefore, there is a continuing need to develop more chemotherapeutic agents in order to eradicate cancer.

Compounds that react with DNA, commonly referred to as alkylating agents, as they attach an alkyl group to DNA, are used clinically to treat many types of tumours. Many alkylating agents have been developed such as nitrogen mustards, nitrosourea and alkyl sulfonates. Alkyltating-like agents, that do not alkyl DNA, *i.e* platinum compounds have also been shown to damage DNA in a similar manner (Cruet-Hennequart, Glynn et al. 2008). They may exert their anti-tumour activity by inhibiting the separation of the 2 strands which prevents replication, transcription and segregation, but also prevent transcription factors from recognizing their specific sequences (Lawley and Phillips 1996; Dronkert and Kanaar 2001).

Alkylating agents can be categorised according to the way that they bind to DNA. Some agents can form mono-adducts with one strand of DNA such as

ecteinascidin-743 (ET-743), irofulven and hedamycin (Kelner, McMorris et al. 1987; Hansen, Yun et al. 1995; Zewail-Foote and Hurley 1999) (Figure 1). These compounds would be referred as mono-functional DNA alkylators or mono-alkylating agents. Others can create 2 adducts, *i.e* bi-functional agents, within the same strand of DNA such as the platinum compounds and will be commonly referred as intrastrand cross-linking agents (Fichtinger-Schepman, van der Veer et al. 1985). Finally, agents can form adducts on the 2 opposite strands of DNA and, thereby are referred to as interstrand cross-linking agents (ICLs). For instance, Mitomycin C and bizelesin exert their anti-tumour activity mainly by inducing ICLs (Iyer and Szybalski 1963; Iyer and Szybalski 1964; Thompson and Hurley 1995) (Figure 1).

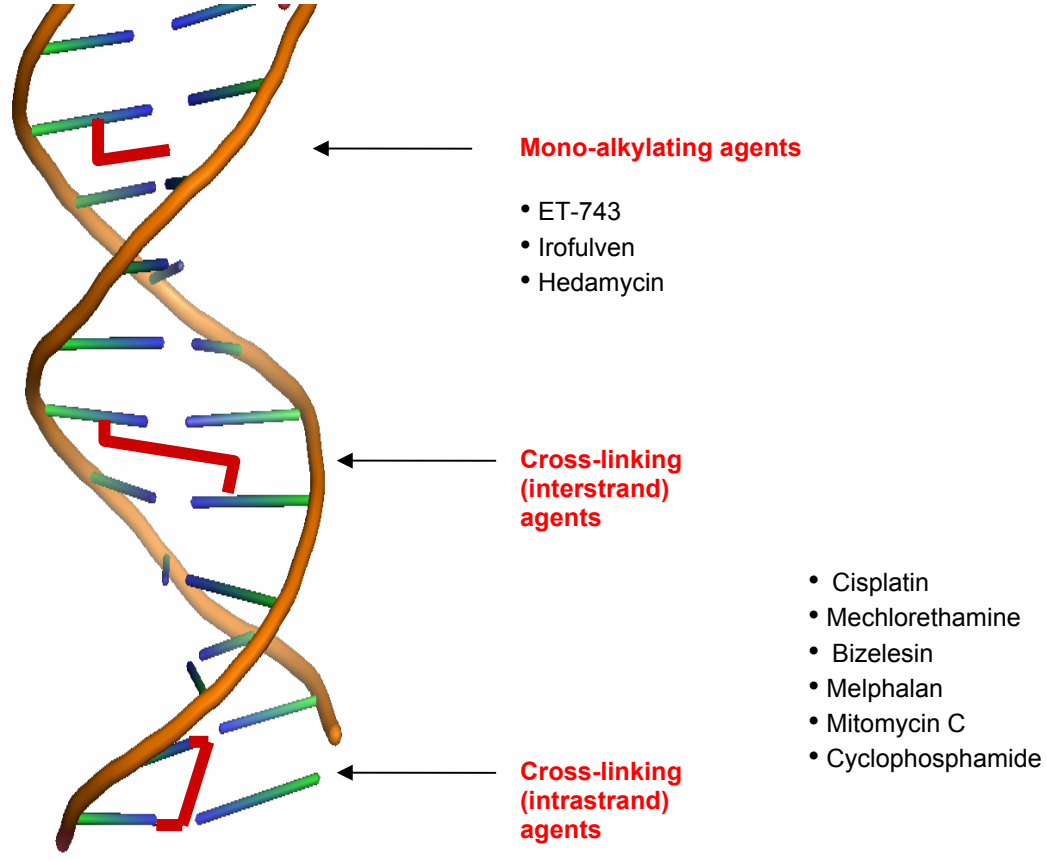

Figure 1. Different classes of alkylating agents. The list of chemotherapeutic agents is not exhaustive as only few examples have been illustrated. It is noteworthy pointing out that some agents, such as cisplatin can form interstrand cross-links but also intrastrand cross-links.

Alkylating agents can bind in the major groove of DNA such as the platinum compounds. However, major groove binders are easily recognised by DNA repair machinery and their anti-tumour activity is significant only when given at high doses. Another class of compounds has been developed which fit in the minor groove of DNA. The damage is less well recognised by DNA repair machinery and adducts would remain through the cell cycle. While in S phase, the replication fork would stall on drug-DNA adducts and the cell may then undergo apoptosis. In cell lines deficient in cell cycle checkpoints, replication would carry on, leading to chromosomal instability and to mitotic catastrophe (Akkari, Bateman et al. 2000) (Tercero and Diffley 2001).

1.2 Pyrrolobenzodiazepines

Pyrrolo[2,1-c][1,4]benzodiazepines (PBDs) are a family of anti-tumour antibiotics produced by various streptomyces species (Thurston 1993). PBDs include anthramycin, DC-81 and tomaymycin (Figure 2).

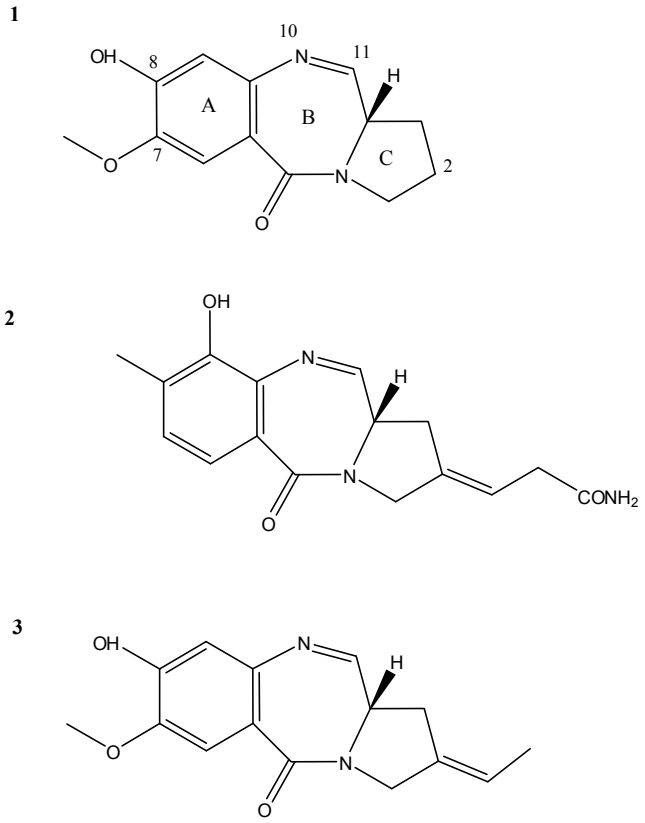

Figure 2. Structures of the naturally occurring PBD-monomers DC-81 (**1**), anthramycin (**2**) and tomaymycin (**3)**

PBDs are tricyclic molecules containing a chiral centre (at their C11 position), which provides them with a right-handed twist. This creates a shape, which allows these molecules to fit perfectly within the minor groove of DNA (Figure 3).

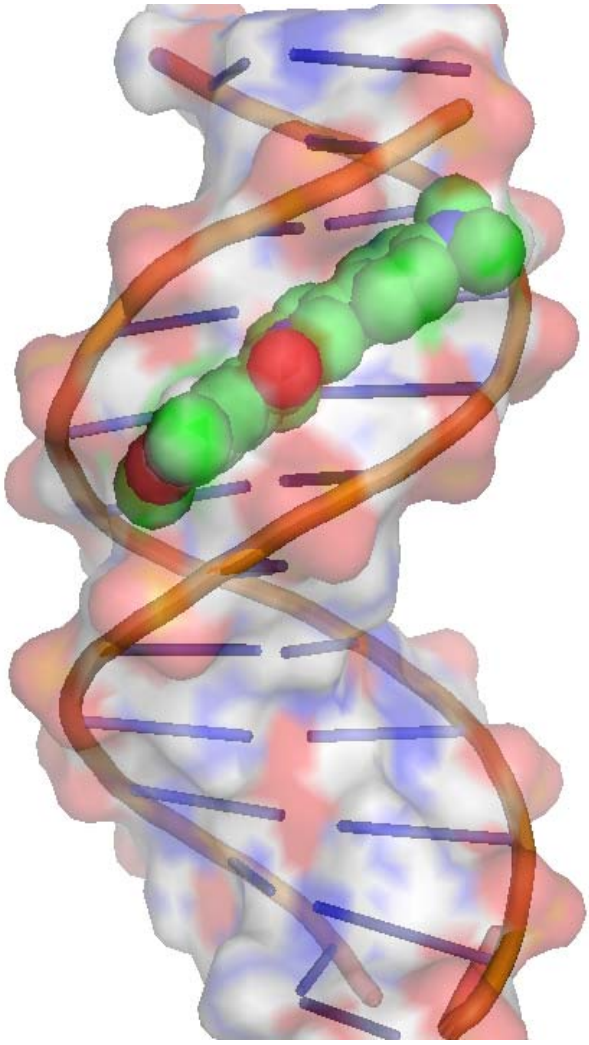

Figure 3. Interaction between a pyrrolobenzodiazepine derivative within the minor groove of DNA. The optimisation of the complex PBD-DNA has been minimised *in silico* using a molecular modelling approach. The carbon skeleton of the PBD is represented in green. The double helix of DNA has been represented as a cartoon in order to simplify the viewing. The sugar phosphate backbone of DNA is in brown and the complimentary bases in blue.

PBD/DNA adducts are formed (aminal bond) exclusively between the N10-C11 imine / carbinolamine moiety of the PBD and the exocyclic NH_2 group of a guanine (Figure 4) (Puvvada, Forrow et al. 1997).

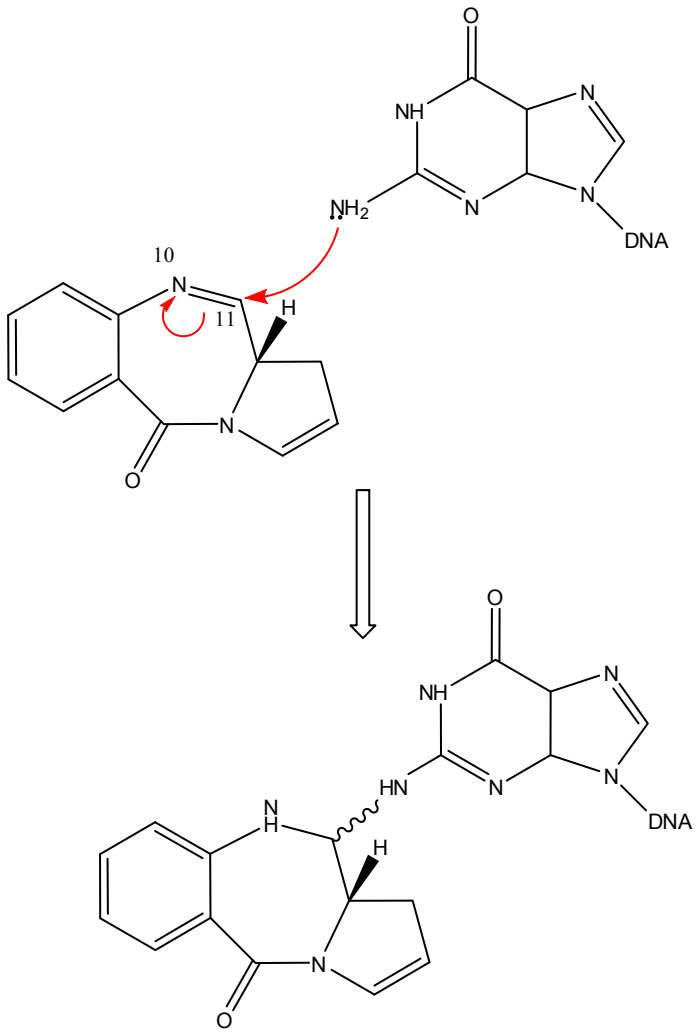

Figure 4. Mechanism of binding of the PBDs to DNA: the N10-C11 imine / carbinolamine moiety of the PBD bind to the C2-amino position of a guanine residue.

The binding sites of the naturally occurring PBDs have been extensively studied and most of adducts were found at a specific sequence A**G**A-5'. In addition, tomaymycin has been shown to bind to G**G**A-5' and T**G**A-5'. The flanking sequence has also been shown to influence the binding properties (Puvvada, Forrow et al. 1997). Upon binding to their specific sequence, PBDs exert their anti-tumour activity by inhibiting RNA polymerase and preventing other transcription factors,

such as sp1, to bind to their specific sequence resulting in a transcription blockage (Puvvada, Hartley et al. 1993; Puvvada, Forrow et al. 1997; Baraldi, Cacciari et al. 2000).

During the last decade much effort has been put into extending the pyrrolobenzodiazepines so that they span a greater number of base pairs with enhanced sequence selectivity. One approach involved coupling two PBD units, via their C8-positions, to produce novel sequence-selective DNA interstrand cross-linking agents (ICLs) (Gregson, Howard et al. 2001).

A new challenging synthetic route was developed to produce SJG-136 (Figure 5), the first compound in this family to enter clinical development (Gregson, Howard et al. 2001). Its chemical structure comprises 2 subunits of C2-exo-methylene-subsituted DC-81. It spans 6 DNA base pairs with a preference for binding to 5'-Pu-**G**ATC-Py-3' sequences (Gregson, Howard et al. 2001; Hartley, Spanswick et al. 2004). It exhibits a broad spectrum of cytotoxicity across the NCI60 cell line panel and pre-clinical studies have highlighted the potency of this agent *in vivo* in a number of tumour types (Alley, Hollingshead et al. 2004; Pepper, Hambly et al. 2004).

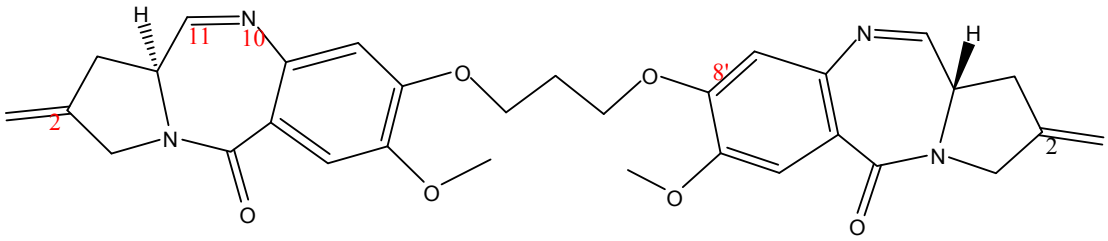

Figure 5. Chemical structure of SJG-136

Other PBD-dimers have been synthesised showing differential sequence specificity for DNA, *i.e* base pair spanning and induced biological activity (Figure 6).

DSB-120

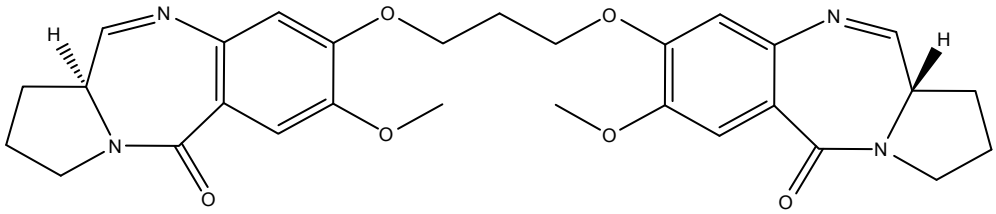

DRG-16

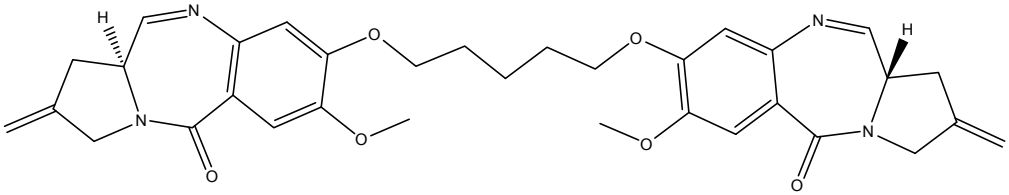

ELB-21

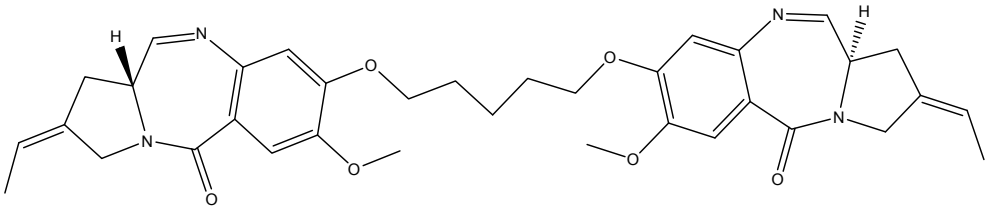

Figure 6. Chemical structure of pyrrolobenzodiazepine dimers DSB-120, DRG-16 and ELB-21

The structure of DSB-120 differs from SJG-136 in the absence of saturated carbons at the C2/C2' positions. The region which links the 2 subunits comprises 3 CH_2 groups. It allows the compound to bind, similarly to SJG-136, to 5'-Pu-**G**ATC-Py-3' sequences and cross-link opposite-strand guanines (Figure 7.A.) (Smellie, Bose et al. 2003). DSB-120 was shown to be a potent cytotoxic agent *in vitro* against a panel of human colon carcinomas whithout being able to show activity *in vivo* (Walton, Goddard et al. 1996).

The structures of ELB-21 and DRG-16 differ from SJG-136 in the length of the linker region between the two subunits containing 5 CH_2 groups as opposed to 3. They span a sequence of one additional base pair (n =7) and cross-link 5'-Pu-**G**A*(G/A)*TC-Py-3' (Figure 7.B.) (Smellie, Bose et al. 2003). These two compounds have been tested against Gram-positive bacteria and, when compared to SJG-136, shown higher activity (Hadjivassileva, Thurston et al. 2005). DRG-16 was also assessed in the NCI60 cell line panel and was significantly more cytotoxic than SJG-136 (Gregson, Howard et al. 2004).

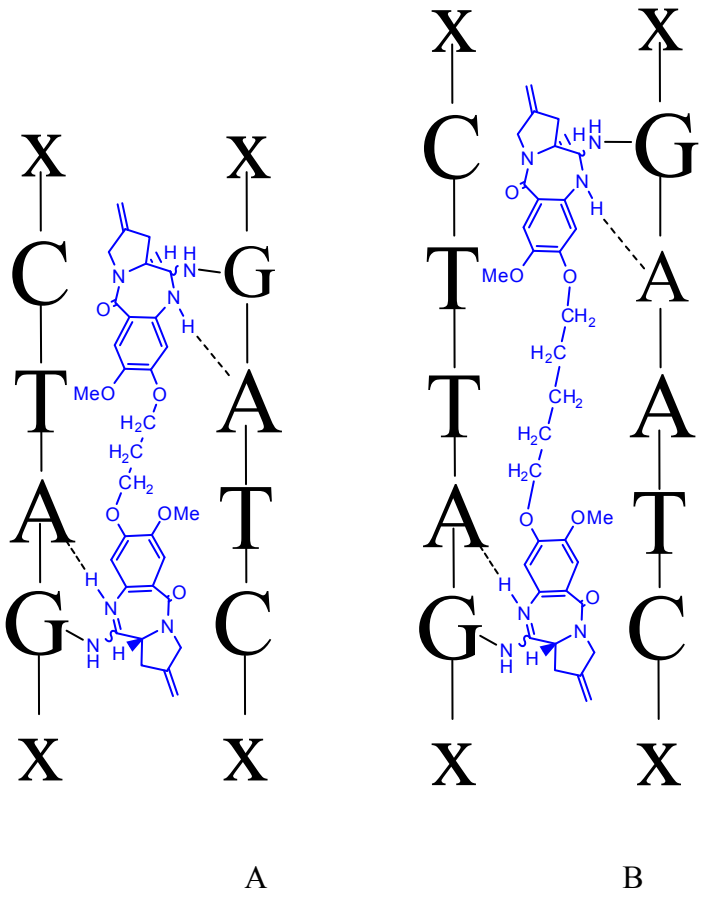

Figure 7. Mechanism for interstrand cross-linking of DNA by (A) PBD-dimer SJG-136 and (B) PBD-dimer DRG-16. Due to the number of CH_2 goups of the linker region, DSB-120 (n =3) would follow the pattern described by A and bind to 6 base pairs. ELB-21 with a greater number of CH_2 groups (n=5) would follow the pattern described by B and span a 7 base pairs sequence. X is used to denote any flanking base.

The complex formed by the PBD-dimers with DNA has been modelled *in silico* and minimal or no distortion of the secondary structure of DNA was observed (Gregson, Howard et al. 2001).

The synthesis of PBD monomers has also been undertaken and some have shown significant growth inhibitory effects *in vitro* (Cooper, Hagan et al. 2002). The chemical structures of a selection of PBDs, derived from a PBD skeleton, are presented in Figure 8.

The structure of the PBD-monomers has been modified at the C2 extremity (R1) in all derivatives of this library and at the C8 extremity (R2) in SJG-244.

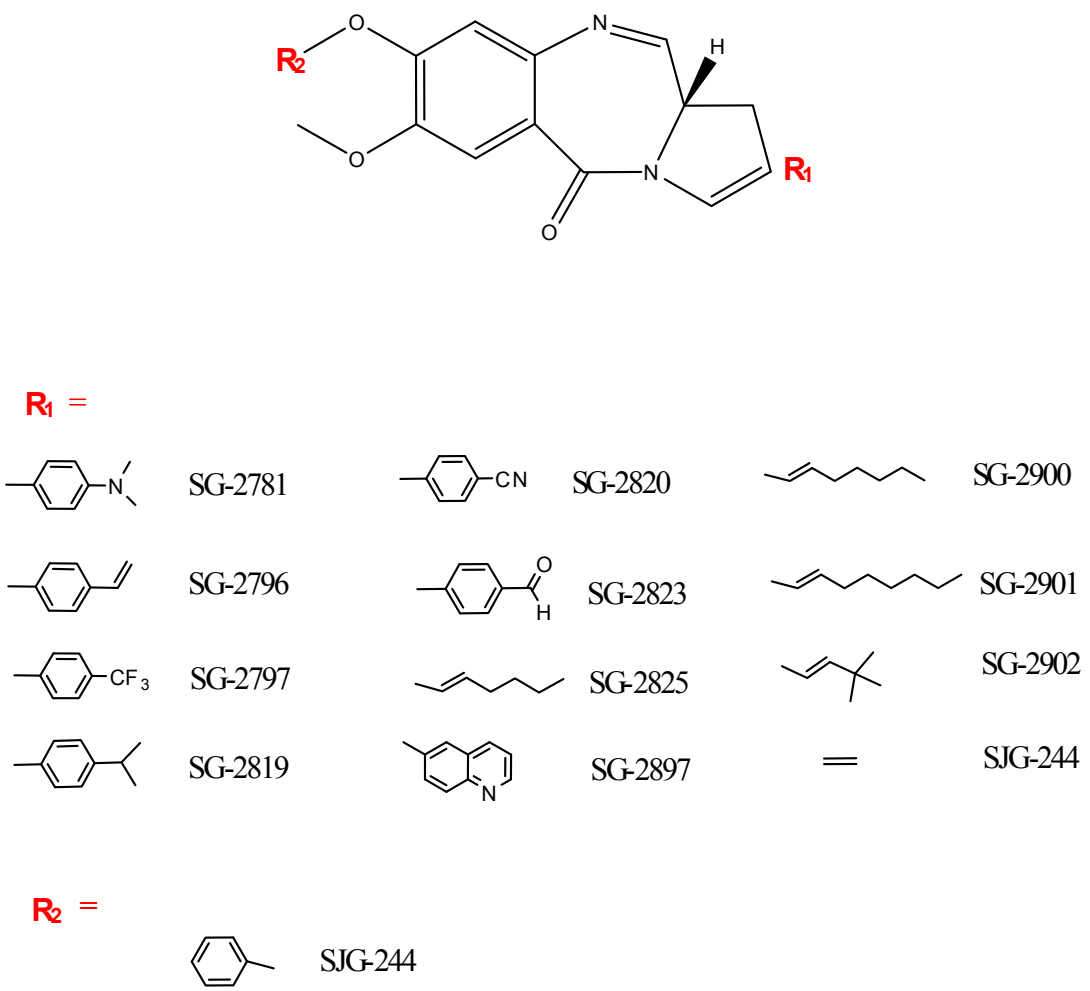

Figure 8. Chemical structure of the PBD-monomers.

We can discriminate 3 groups among the C2 paralogues: PBD-monomers with C2-aryl substituent (SG-2781, SG-2796, SG-2797, SG-2819, SG-2820 and SG-2823), PBD-monomers with a poly-carbonated chain, *i.e* sibiromycin analogues (SG-2825, SG-2900, SG-2901 and SG-2902) and, finally a PBD-monomer with a quinoline substituent (SG-2897) at the C2 extremity. Antonow and colleagues have shown that PBD-monomers were associated with a high affinity for DNA as

determined by the thermal denaturation studies (ΔTm) suggesting that the C2 moiety would participate in the overall affinity for DNA (personal communication).

1.3 DNA repair machinery

Besides their ability to bind to specific sequences of DNA preventing the interaction of different enzymes (Martin, Ellis et al. 2005), Arnould and colleagues have shown that the PBD-dimer, SJG-136 was associated with the formation of H2AX foci, a surrogate marker of double strand DNA breaks (DSB) (Arnould, Spanswick et al. 2006).

Indeed, ICLs can induce the formation of DSB when a replication fork collides with a cross-link or by repair intermediates during homologous recombination (Niedernhofer, Odijk et al. 2004). In early response to the DSB, Histone H2AX is phosphorylated at serine 139. This signal allows γ-H2AX (phosphorylated H2AX) to migrate to the site of damage and recruit other DNA repair factors involved in DNA damage-signalling pathway (Rogakou, Pilch et al. 1998; Paull, Rogakou et al. 2000). Thus the formation of γH2AX foci, has been widely used a surrogate marker of this type of damage and was observed after SJG-136 treatment (Figure 9) (Arnould, Spanswick et al. 2006).

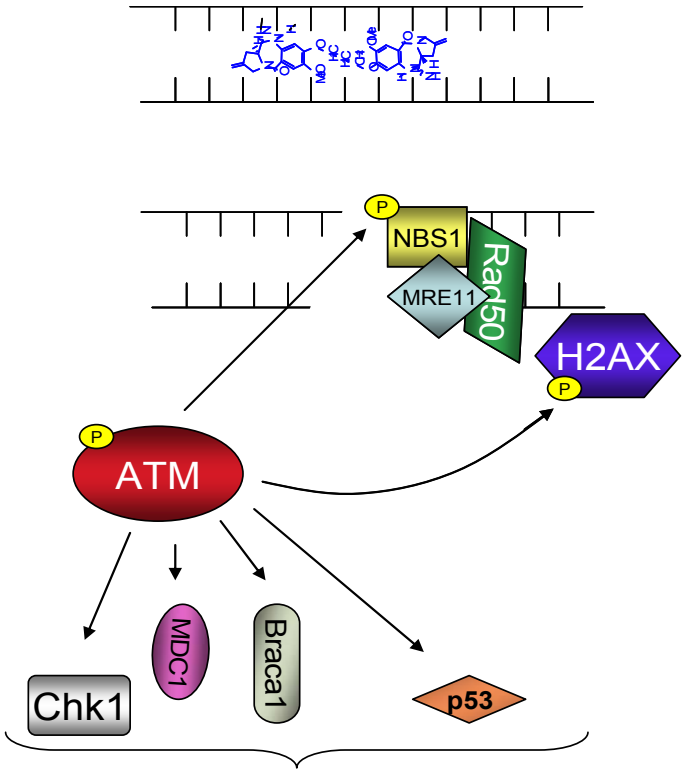

Figure 9. H2AX foci formation following treatment with PBD-dimer, SJG-136. SJG-136 interacts with the minor groove of DNA which potentially creates a cell cycle dependent double strand break. In an early response to DNA damage, the complex formed by NBS-MRE11 and RAD50 is recruited. ATM is activated as a monomer, phosphorylates NBS1 in return, which allows the complex to translocate to the site of damage. ATM phosphorylates also Histone H2AX involved in cell survival and other multiple substrates such as CHK1, MDC1, Braca1 and P53 implied in cell cycle checkpoint activation, DNA repair or Apoptosis.

The ability of the cell to repair DNA ICLs is a critical factor determining cytotoxicity. The nucleotide excision repair (NER) pathway (XPF-ERCC1) and the homologous recombination (HR) repair pathway (Rad51 paralogues) are both involved in the repair of ICLs (De Silva, McHugh et al. 2000). Any defect in these particular pathways would result potentially in increased cytotoxicity induced by ICL forming agents (Damia, Imperatori et al. 1996).

The repair of damage induced by major groove binders such as melphalan relies in a greater extend on the HR and the NER pathways than the cytotoxicity induced by minor groove binders such as the PBDs (Clingen, De Silva et al. 2005). Helical distortion is a major factor for the recruitment of DNA repair protein (Dip, Camenisch et al. 2004). Minor groove binders such as PBDs inducing a minimal or no distortion of DNA, could be less well recognised by the repair machinery and therefore repaired less readily (Gregson, Howard et al. 2001). This could result in greater cytotoxicity.

While the HR pathway remains a significant repair mechanism to the damage to DNA induced by the PBDs (Figure 10) (Clingen, De Silva et al. 2005), using PBDs in tumours, deficient in the HR proteins, would potentially result in a more significant cytotoxicity. A number of cancers have been related to genetic disorders involving proteins associated with the HR pathway such as ataxia telangiectasia, Bloom syndrome, Nijmegen breakage syndrome and Fanconi anemia (Thompson and Schild 2002). Tumour suppressor genes BRCA1, BRCA2 and Rad51 are involved in HR and have been used as predictive biomarkers in the response to chemotherapeutic agents (Bryant, Schultz et al. 2005; Soares, Escargueil et al. 2007). The impact of the PBDs in HR-deficient cells has not been elucidated to date.

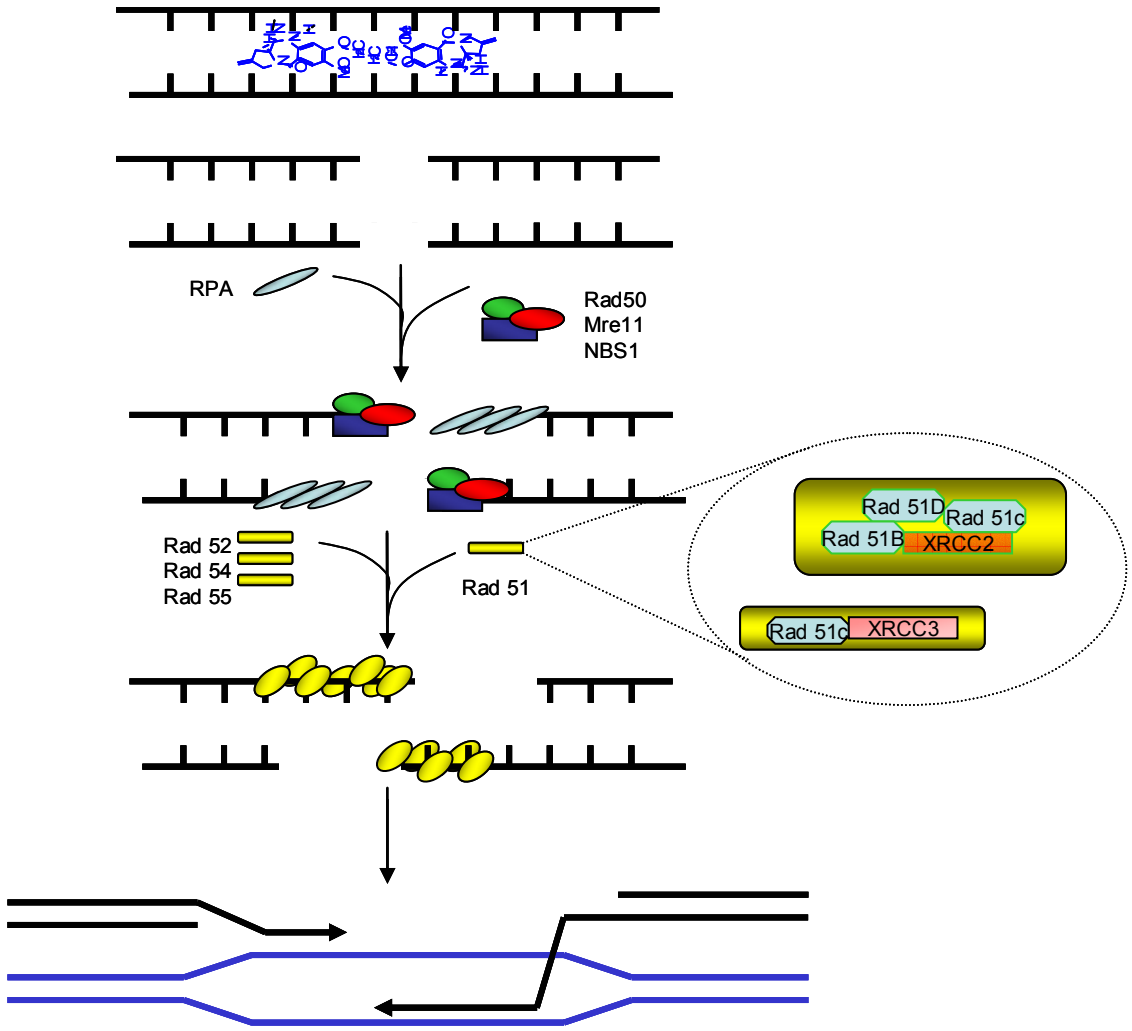

Figure 10. Homologous recombination (HR) pathway induced by the treatment of the pyrrolobenzodiazepine-dimer, SJG-136 and its mono-functional counterpart, mmy-SJG. PBDs are alkylating agents inducing damage to DNA. The MRN complex and RFA are rapidly recruited at the site of damage and coat the single-stranded DNA. This signal triggers the recruitment of Rad 51 paralogues with a prevalent role for XRCC2 in the repair induced by the PBDs. The recruitment of a homologous sequence of DNA allows a DNA polymerase to synthesise *de novo* the complementary sequence.

PBD-monomers have been shown not to produce any ICL in contrast to the PBD-dimers. However, Clingen and colleagues have reported, a similar increased sensitivity of the XRCC2 and XRCC3 mutants following the treatment of the mono-functional counterpart of SJG-136, mmy-SJG (Clingen, De Silva et al. 2005). To

date, no data has been reported on DSB induced by the PBD-monomers. While ET-743 does not cross-link DNA, it has shown a cell cycle dependency and formation of DSB (Niedernhofer, Odijk et al. 2004). The specific mechanism of the activity of the PBD-monomers remains to be elucidated.

1.4 ABC transporters and MDR phenotype

The PBD derivatives have shown promise in preclinical models of cancer. However, one of them, SJG-136 has been shown to be substrate of an ABC transporter, P-glycoprotein, potentially limiting its anti-tumour activity (Guichard, Macpherson et al. 2005).

Permeability-glycoprotein (P-gp) is a member of the large ATP binding cassette (ABC) super-family of transport proteins. ABC transporters are highly conserved phylogenetically from prokaryotes to humans and constitute a structurally related group of transmembrane proteins. They are localised in the intra- or extra-cellular membranes. They transport a wide range of substrates including endogenous metabolites as well as xenobiotics. Their over-expression has been linked to the multidrug resistance phenotype, termed MDR, which is considered to be a major cause of failure of chemotherapy.

Three major ABC transporters, modifying the uptake of drugs, have been documented: P-gp also termed multidrug resistance 1 (mdr1) or ABCB1, ABCC1 commonly referred as multi-drug resistance protein 1 (MRP1) and ABCG2 also named breast cancer resistance protein (BCRP). In addition to conferring the MDR

phenotype, these ABC transporters are expressed differentially in healthy tissues throughout the body (Figure 11). From the tissue distribution, ABC transporters are thought to participate in the absorption and secretion of endogenous and exogenous substances as well as providing pharmacological sanctuaries such as the brain and testes (Choi 2005) (Figure 11).

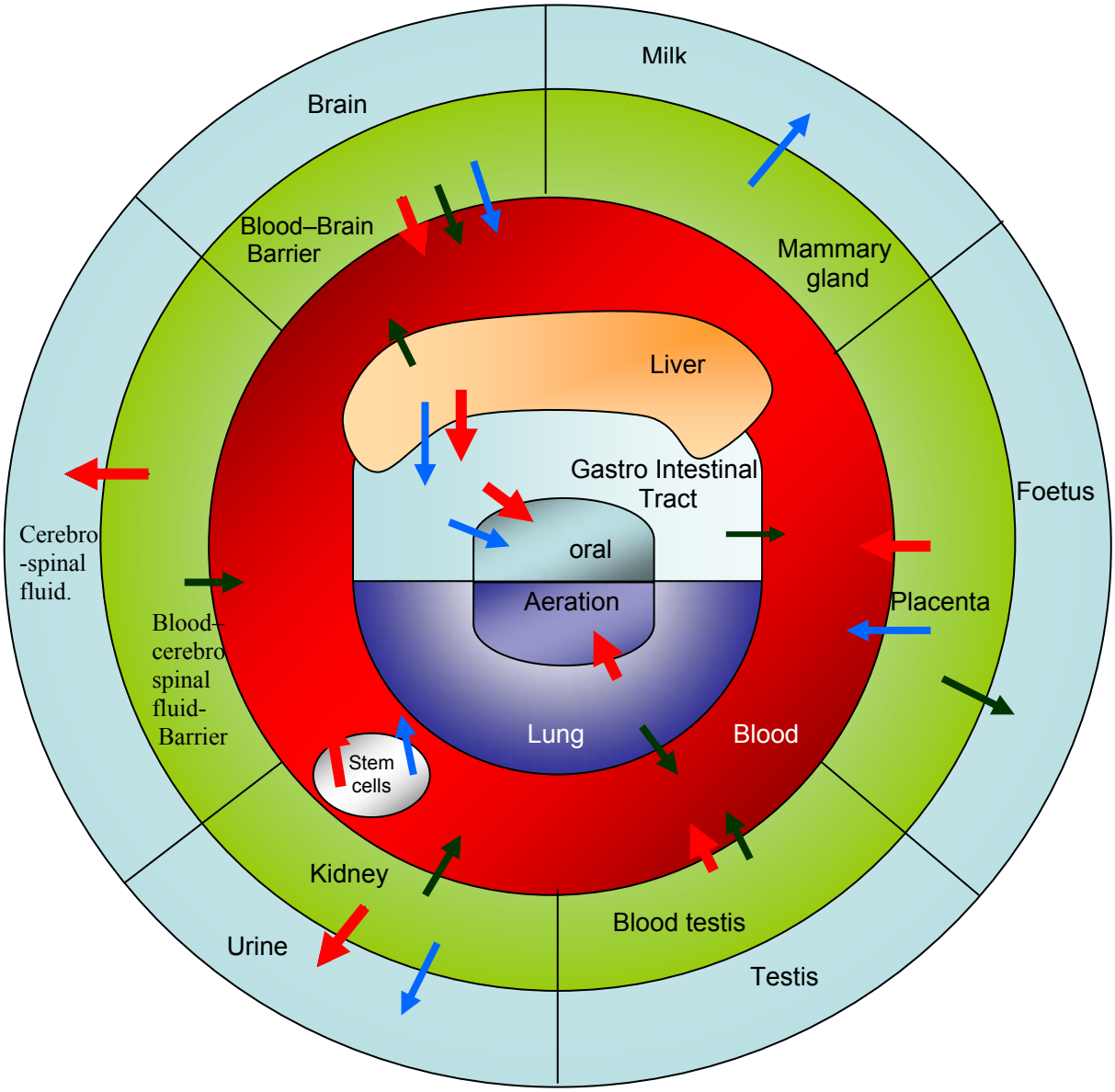

Figure 11. Physiological localisation of the ABC transporters. Model modified from Szakacs et al *(Szakacs, Paterson et al. 2006).* P-gp is represented in a red arrow, MRP1 in a green arrow and ABCG2 in a blue arrow.

1.4.1 P-gp or ABCB1

1.4.1.1 P-gp structure and mechanism

P-gp was the first ABC transporter to be discovered (1976) (Juliano and Ling 1976). It is a 170-kDA glycoprotein, comprising 1280 amino-acids, encoded by the ABCB1 gene in humans, mdr1 (also called mdr1b) and mdr3 (also called mdr1a) genes in rodents (Germann 1996; Krishna and Mayer 2000). It consists of two homologous subunits joined by a linker region (Ambudkar, Dey et al.). Each subunit contains six predicted trans-membrane domains and short hydrophilic N and C-terminal segments. The C-terminal, of each subunit, contains the sequences for a nucleotide–binding domain (NBD), which is involved in the binding and hydrolysis of ATP. The ATP binding cassette (ABC) commonly referred as ABC motifs (Walker A, Walker B and Walker C motifs) is highly conserved not only throughout different species but also among the different transporters of the ABC super-family. Both NBDs of P-gp are necessary for substrates to be expelled out of the cell (Figure 12) (Ambudkar, Dey et al.).

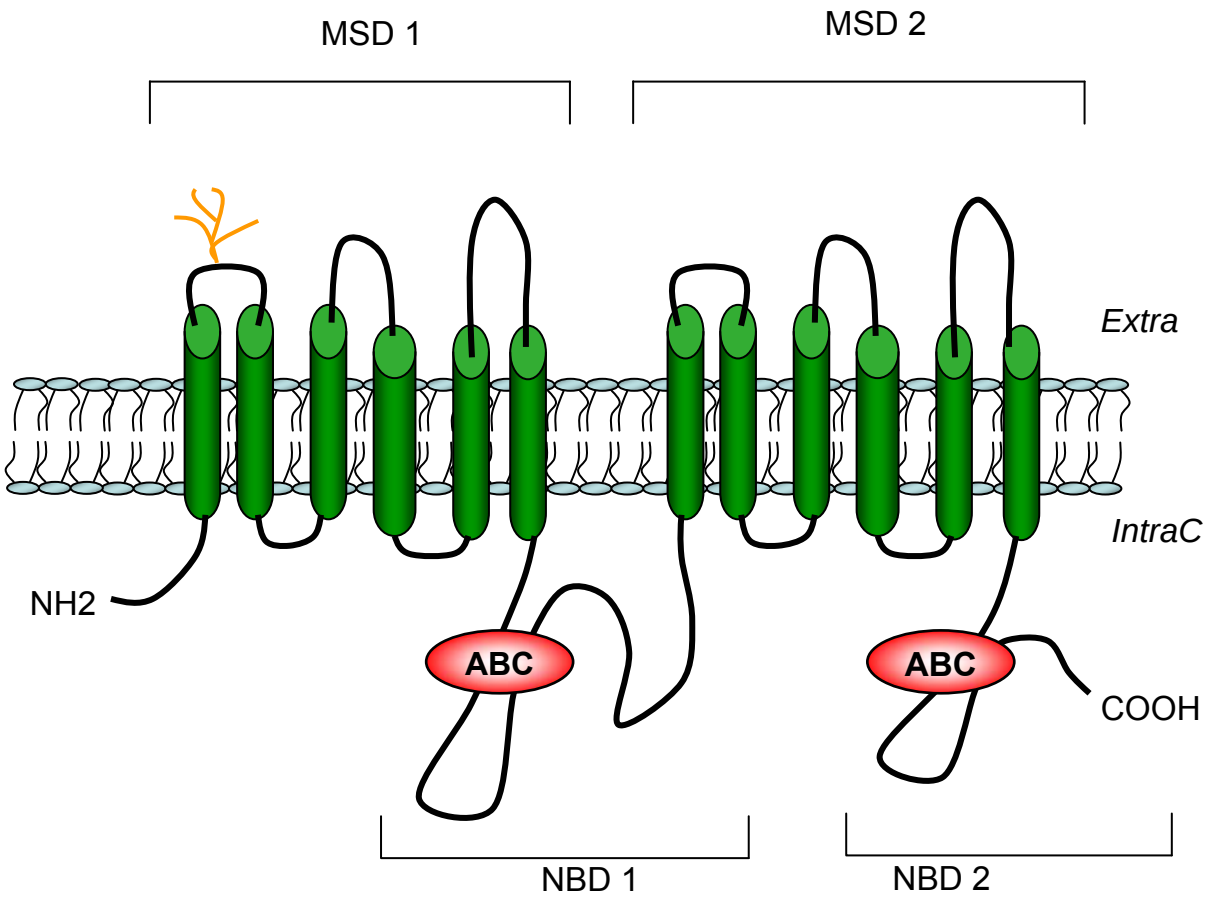

Figure 12. A membrane topology model of P-gp. P-gp contains two nucleotide binding domains (NBD) and two membrane-spanning domains (MSD) including 6 predicted trans-membrane α-helices. The putative N-glycosylation site is predicted to be in the extracellular loop as indicated. The ATPase binding cassette (ABC) is necessary for the binding and hydrolysis of ATP, required for the activity of the transporter.

The most widely accepted model is that P-gp uses the energy of ATP hydrolysis to extrude xenobiotics from the cell. According to this hypothesis, molecules diffuse down a concentration gradient into the cell. Substrates may be expelled from the membrane itself or may first be transported from the cytosol to the bilayer. The flippase model suggested by Gottesman *et al.*, proposes that the drugs are transported from the inner to the outer leaflet of the bilayer and then extruded (Gottesman and Pastan 1993). Although an alternative mechanism has been suggested, in which the intracellular pH and the membrane potential may alter the

trans-membrane partitioning or even the intracellular sequestering of the drugs, a large body of evidence favours the ATP-dependent active transport model (Roepe 1995) (Figure 13).

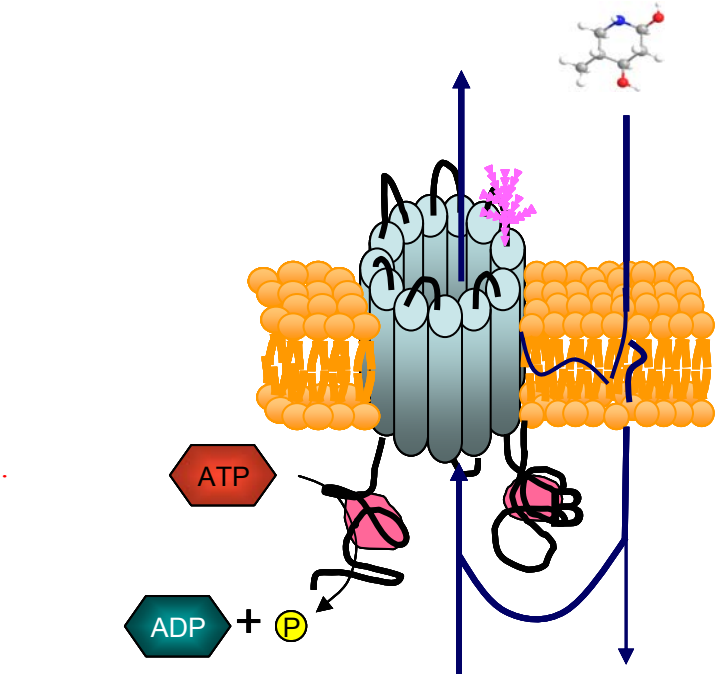

Figure 13. Representation of the transport activity of P-gp. A compound passes through the membrane by passive diffusion, is recognised by the transporter and by hydrolysis of ATP is extruded out of the cell. The substrate recruitment by P-gp from the cytosol or directly from the membrane bilayer is still a matter of debate. Both potential mechanisms have been shown.

The "overall ABCB1 activity" controlling P-gp-dependent drug transport depends on two parameters: (*i*) the level of expression of the ABCB1 gene controls the amount of protein that is synthesised in the cells, and (*ii*) the functionality of the ABCB1-encoded P-gp determines which substrates are recognised and the extent of transport.

The first parameter, the level of expression of ABCB1, has been analysed extensively, particularly because the sensitivity of tumour cells to chemotherapy

often correlates inversely with increased ABCB1 expression. ABCB1 over-expression can be attributed partially to gene amplifications (Chen, Chin et al. 1986; Yoshimoto, Iwahana et al. 1988), but also to transcriptional activation, by rifampicin for example (Greiner, Eichelbaum et al. 1999).

1.4.1.2 P-gp substrate specificity

Compounds that interact with the P-gp efflux pump represent a wide spectrum of chemical structures and belong to different therapeutic classes: anticancer drugs, HIV-protein inhibitors, antibiotics, immunosuppressant and antihypertensive drugs (Ambudkar, Dey et al. 1999). Compounds recognised by the transporter are relatively basic molecules carrying a positive charge at physiological pH. Their hydrophobicity allows them to pass trough cellular membranes by passive diffusion, thus being in close proximity to the transporter.

Knowledge of the factors that determine P-gp substrate specificity is crucial for the rational design of new drugs. Different attempts have been made to find a common set of functional features required for a substrate to interact with P-gp. The lipophilicity ($\log P > -1$), the molecular weight and several general parameters have shown to be related to a positive interaction with P-gp (Dellinger, Pressman et al. 1992; Ueda, Okamura et al. 1992; Gottesman and Pastan 1993; Bain and LeBlanc 1996; Schinkel, Wagenaar et al. 1996; Kim, Leake et al. 2001). These studies provide very general models based on overall properties. As such they are useful for screening the probability of a class of molecules to follow the same pattern and could help in the design of new compounds. However, evaluation of the specific structural

features responsible for activity (substrate specificity), the pharmacophores, provides a more detailed understanding of the action and could allow more detailed engineering of the new compounds. Seelig suggested a formalism based entirely on specific arrangements of hydrogen bonding moieties and may differentiate substrates and non-substrates (Seelig 1998). Partitioning into the membrane (as determined by the surface activity) was also suggested as the rate limiting step for interaction with P-gp and that the number and strength of hydrogen bonds would determine the potential dissociation of the complex (Seelig and Landwojtowicz 2000). The ligand modulation efficiency could be therefore correlated to P-gp structural recognition elements such as hydrogen bonding potential, the presence of a basic nitrogen and planar aromatic ring (Hamilton, Yazdanian et al. 2001; Didziapetris, Japertas et al. 2003).

1.4.1.3 ABCB1 polymorphism

Allelic differences in individual ABCB1 gene sequences may be associated with or causative of different expression levels (Germann, Schoenlein et al. 1994) as well as a differential functionality of the transporter. To date, genetic variations of the human ABCB1 gene have been extensively studied and 50 Single Nucleotide Polymorphisms (SNPs) and 3 insertion / deletion polymorphisms in the ABCB1 gene have been reported (Saito, Iida et al. 2002; Weinshilboum 2003). A main linkage disequilibrium comprising of three SNPs has been associated with altered pharmacokinetics of drug substrates (Figure 14):

- the synonymous SNP at position 1236 located in the exon 12: a C to T variant which refers to the glutamic acid in position 412
- the synonymous SNP at position 3435 located in the exon 26 : a C to T variant which refers to the isoleucine in position 1145
- the non-synonymous SNP at position 2677 located in the exon 21
  - a G to T variant which changes the amino acid from an alanine to a serine (commonly referred as 893)
  - a G to A variant which changes the amino acid to a threonine (commonly referred as 2677)

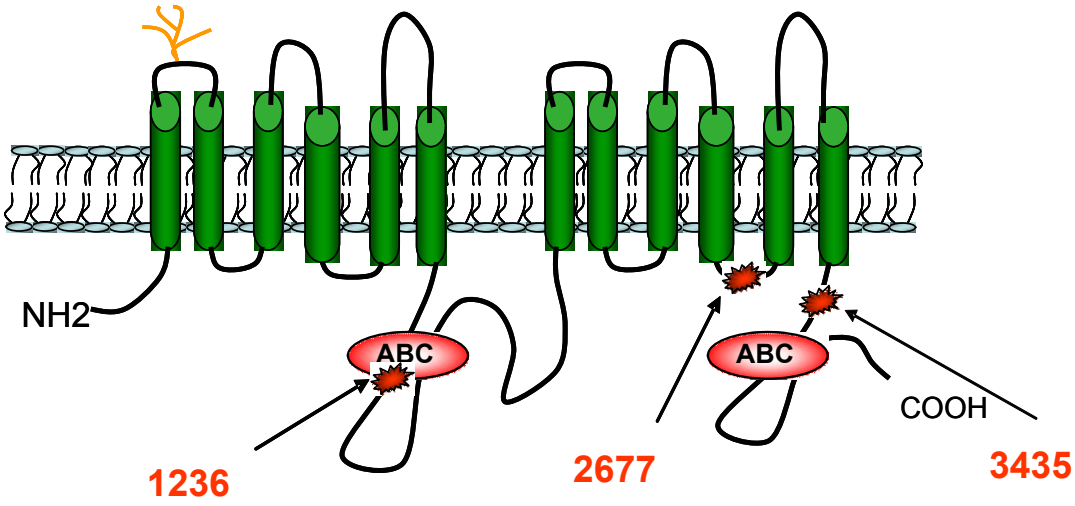

Figure 14. Cartoon showing the localisation of the three main SNPs of ABCB1 influencing the pharnacokinetics of drug substrates.

The haplotype combining the 3 different SNPs has been widely reported and is predominant in Chinese, Malaysian and Indian populations. However, most studies have focused on the evaluation of the impact on each individual SNP on tumour predisposition and the pharmacokinetics of chemotherapeutic treatment; but

it is evident from the literature that no real consensus can be found. For instance, the C3435T polymorphism has been shown to be associated with a higher risk of developing colon cancer and renal epithelium tumours while other studies have shown a differential incidence on disease disposition such as drug resistant epilepsy (Sills, Mohanraj et al. 2005; Kim, Kim et al. 2006). The impact of C3435T polymorphism on ABCB1 protein expression and function, as well as the reported influence on drug pharmacokinetics (PK), has been widely studied but still remains a matter of debate. For instance, a lower *in vivo* fexofenadine $AUC_{0–4\ h}$ was associated with 3435TT genotype when compared to the CC variant (Kim, Leake et al. 2001) while another study reported no difference (Drescher, Schaeffeler et al. 2002). The 3435TT homozygous genotype has also been associated with reduced protein function in peripheral blood cells, an increase of plasma levels of the substrate digoxin, as well as a lower rhodamine 123 efflux (Hoffmeyer, Burk et al. 2000; Hitzl, Drescher et al. 2001). Decreased ABCB1 mRNA expression in leukocytes and in the duodenum has been associated with the TT genotype (Hoffmeyer, Burk et al. 2000). Gottesman and colleagues have suggested that this silent polymorphism would influence the timing of co-translational folding, *i.e.* adopting its spatial functional conformation, and insertion of P-gp into the membrane, altering its substrate and inhibitor binding sites (Kimchi-Sarfaty, Oh et al. 2007).

The few studies that have evaluated the influence of the SNP at position 1236 in the pharmacokinetic effect on drug substrates of ABCB1 led to different results depending on the substrates: Anglicheau and colleagues reported an increase in the $AUC_{0–4\ h}$ of cyclosporine associated with the 1236TT genotype. In contrast, Goto

and colleagues have shown no difference in concentration / dose ratio of tacrolimus among the different genotypes (Goto, Masuda et al. 2002). Finally, Schaich and colleagues have shown that patients with glioblastoma treated using temozolomide had an improved overall survival if they were 1236CC carriers (Schaich, Kestel et al. 2008).

The ABCB1 2677G>T polymorphism (also called 893 Ala-Ser mutation) has been associated with a higher risk of developing diseases such as lung cancer (Gervasini, Carrillo et al. 2006). The homozygous genotype TT (893serine) has been shown to be associated with an enhanced *in vitro* digoxin efflux in stably transfected NIH3T3 and with an *in vivo* lower fexofenadine $AUC_{0-4\ h}$ compared to the GG genotype (Fairchild, Moscow et al. 1990; Kim, Leake et al. 2001). Another study suggested that the amino-acid substitution at position 893 would alter the ATPase activity and maybe the substrate specificity of the transporter (Sakurai, Onishi et al. 2007). Using a series of sf9 transfected cells and a wide variety of ABCB1 substrates, the same study showed that the 2677A variant (threonine) was associated with a higher ATPase activity while compared with its 2677G and 2677T variant counterparts.

However when both SNPs at position 3435 and 2677 were considered, an increased fexofenadine $AUC_{0-4\ h}$ was associated with 3435CC individuals which could be attributed to a prevalent impact of the 2677TT genotype. More recently, Sissung and colleagues have shown a combined effect of the association of the 3 SNPs: when treated for androgen-independent prostate cancer with docetaxel, patients carrying the haplotype 1236C-2677G-3435C linked alleles had improved

overall survival. The same set of patients carrying the haplotype 2677T-3435T had a shorter median survival.

The polymorphisms of 1236, 2677 and 3435 also exhibit wide ethnic differences in the allele frequency (Drescher, Schaeffeler et al. 2002; Kroetz, Pauli-Magnus et al. 2003). Therefore, consideration of these differences may suggest dose modifications to correct for altered bio-availability of the chemotherapeutic agents leading to a better clinical outcome.

1.4.1.4 P-gp - localisation

P-gp is not only expressed in tumour cells but also in normal tissues such as the gastrointestinal tract, liver, kidney, testis, lung and the placenta. P-gp was also found in the endothelial cells of the blood-brain barrier (Figure 11). In addition, P-gp was found at the apical side in polarized cells. These localisations clearly suggest the potential for P-gp to act as a protective mechanism against the uptake of toxic xenobiotics (Ambudkar, Dey et al. 1999; Silverman 1999).

1.4.1.5 P-gp and clinical outcome

Over-expression of P-gp may lead to worse cancer treatment outcome and most of the time to a reduced overall survival of cancer patients. In the UK, colorectal cancer is the most common cancer after breast and lung, with more than 35,000 cases diagnosed each year. It is the second most common cause of death from cancer in the UK after lung cancer, with around 16,000 deaths each year (data

from CRUK). Colorectal cancer is one of the tumor types associated with the highest proportion of P-gp positivity; 74% of untreated colorectal tumors expressed P-gp compared to 43% of normal colorectal specimens, suggesting that colon epithelium acquires high expression of P-gp in the course of carcinogenesis (Shen LZ 1999; Lorke, Kruger et al. 2001). In AML, while 30% of patients over-express P-gp at diagnosis, it increases to 50% at relapse, potentially due to exposure to chemotherapeutic agents (such as idarubicin, VP-16, ARA-C) substrates of P-gp (Han, Kahng et al. 2000).

One of the PBD derivatives, SJG-136 has been shown to be a substrate of P-gp, thus limiting its anti-tumour activity. Its chemical structure does fit in the general characteristics for compounds to be substrates of this specific transporter. However, the impact of P-gp on the anti-tumour activity of the other PBDs is unknown. Determining the specific features involved in the substrate specificity of this class of compounds should allow the rational design of new derivatives with enhanced anti-tumour activity.

ABCB1 polymorphism has been shown to alter the substrate specificity for many classes of compounds. The evaluation of the impact of the three main SNP on the anti-tumour activity of the PBDs should allow targeting defined tumours according to their genotypes with specific PBDs.

1.4.2 MRP1 or ABCC1

Numerous *in vitro* drug selected cell lines and some clinical situations have highlighted the critical role of P-gp in the resistance phenotype. However, there is a growing body of evidence that other mechanisms of MDR might occur. Indeed, some tumour types such as lung cancer were shown to acquire drug resistance without the expression of P-gp.

(Lai, Goldstein et al. 1989). The study of a multidrug resistant lung cancer cell line, H69AR, revealed that despite the lack of P-gp expression, the cell line had a cross resistant profile similar to the cells that express P-gp [7-9, 11](Mirski, Gerlach et al. 1987; Slovak, Hoeltge et al. 1988; Reeve, Rabbitts et al. 1990) (Cole 1990). While investigating the protein responsible for this MDR phenotype, Cole and colleagues identified the multidrug resistance protein 1 (MRP1) (Cole, Bhardwaj et al. 1992).

1.4.2.1 MRP1 structure

MRP1 is a 190-kDA glycoprotein comprising 1531 amino-acids, encoded by ABCC1 gene in humans and in rodents. The amino acid sequences contains only ~15% homology with P-glycoprotein and unlike other ABC transporters, MRP1 contains three membrane spanning domains (MSDs) as supposed to 2 (Figure 15) (Cole, Bhardwaj et al. 1992; Grant, Valdimarsson et al. 1994; Muller, Bakos et al. 1996; Hipfner, Almquist et al. 1997).

MSD1 and MSD2 are typical of ABC transporters, with 6 transmembrane α-helices with a COOH terminal intracellular. MDS0 contains only 5 transmembrane α- helices and it has been shown to be involved in the processing and the trafficking of the protein from the endoplasmic reticulum to plasma membrane. The NH_2

terminal is in this case, extracellular and is glycosylated. The core region contains the elements for substrate specificity and drug transport (Westlake, Cole et al. 2005).

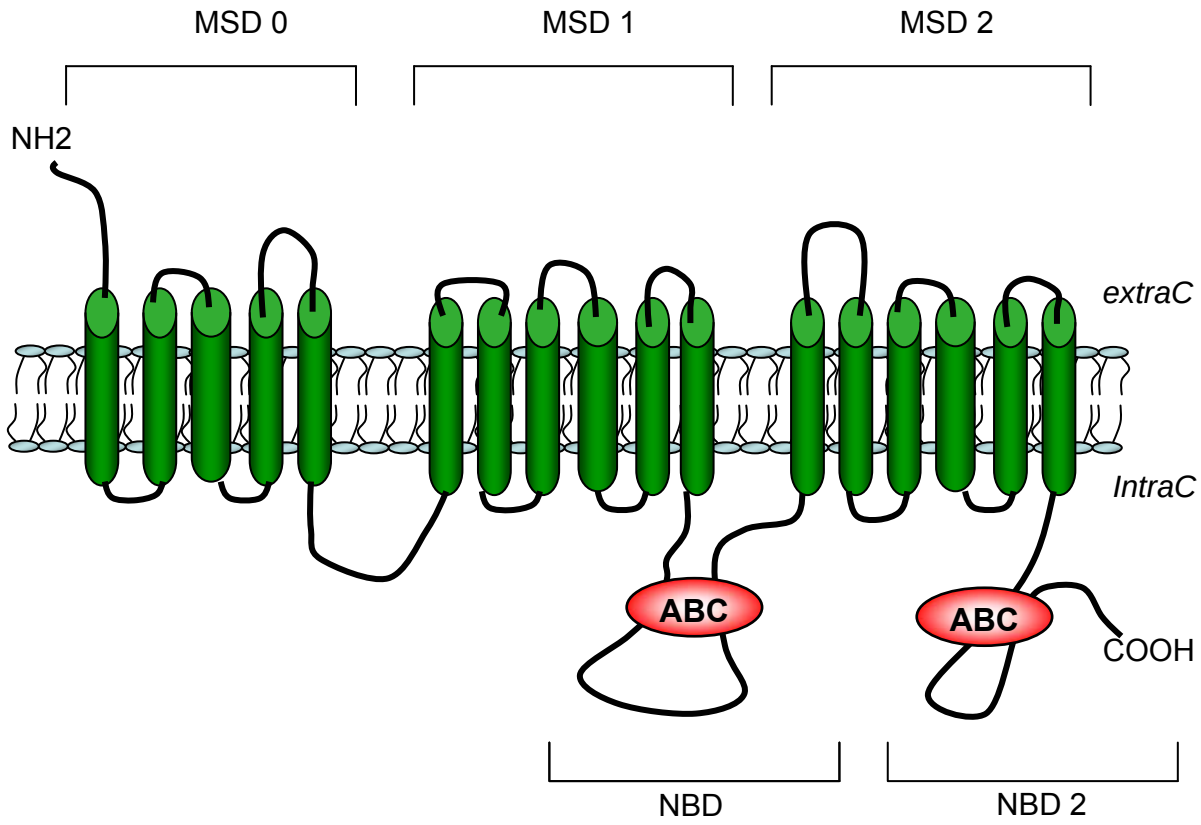

Figure 15. Cartoon of the predicted topology of MRP1. The upper panel shows the predicted topology of the MSDs. The lower panel indicates the nucleotide binding domains containing the ATP binding Cassette. The NH_2 terminal is predicted to be localised in the extracellular compartment.

1.4.2.2 MRP1 substrate specificity

Before its molecular identity was revealed, MRP1 was mistaken for the so called multi-specific organic anion transporter (MOAT) (Zaman, Lankelma et al. 1995). MOAT (also called GS-X pump) had first been found in a variety of cells types such as erythrocytes, hepatocytes and cardiac cells (Keppler, Leier et al. 1997). MRP1 is involved in the detoxification process of many organic anions (Jedlitschky, Leier et al. 1994; Leier, Jedlitschky et al. 1994; Muller, Meijer et al. 1994). Such

negatively charged molecules can not be recognised by P-gp. Similarly, MRP1 eliminates a wide range of exogenous drugs which may or may not be conjugated to glutathione (GSH), sulphate or glucuronide in order to be extruded out of the cell (Jedlitschky, Leier et al. 1996; Hipfner, Deeley et al. 1999; Konig, Nies et al. 1999). Besides the extrusion of exogenous added drugs, MRP1 is involved in the transport of a multitude of molecules endogenously produced in cells during normal physiological processes. For instance, the precursor Leucotriene A4 (LTA4) is transformed by coupling with GSH in its mature form Leucotriene C4 (LTC4). The conjugation process allows the latter to be extruded out of the cell by MRP1 and play its role in the allergic and inflammatory response

1.4.2.3 GSH as a cofactor

While coupling to GSH seems to be a prerequisite for some molecules to be transported out of the cell, GSH can also act as a cofactor / activator to MRP1 for other molecules (Figure 16). In both cases, the continuous synthesis of GSH by GSH-synthetase and γ-Glu-Cys-synthetase is essential for the transporter to be active and transport the substrates out of the cell (Figure 16).

In tumour cells, the multidrug phenotype is often associated with an over-expression of both the transporter and the enzymes involved in GSH synthesis (Ishikawa, Wright et al. 1994; Lautier, Canitrot et al. 1996).

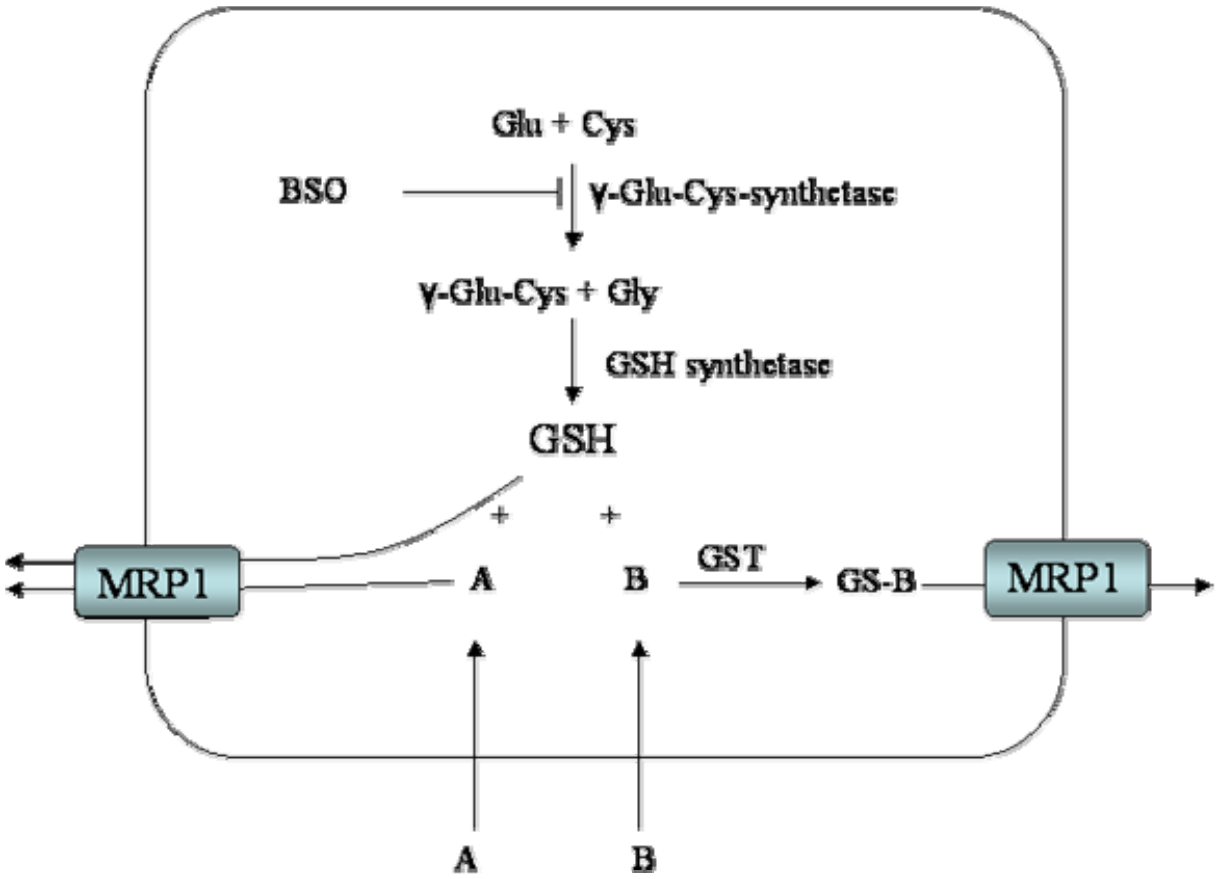

Figure 16. Model showing the combine role of MRP1 and glutathione (GSH) in the multidrug resistance phenotype. Some drugs (A) use GSH as a cofactor in order to be extruded out of the cell by the transporter. GSH is being extruded as well. Other drugs (B) can be conjugated to GSH by glutathione *S*-transferase (GST) and are then transported by MRP1. In both cases, drug transport is dependent on the continued synthesis of GSH, which can be blocked by DL-buthionine (*S, R*)-sulfoximine (BSO). Some compounds are turned into MRP1 substrates by conjugation to glucuronate or sulfate, whereas some other substrates do not require conjugation.

Some chemotherapeutics have been shown to be differentially affected by the availability of GSH. For example, the sensitivity to vinca alkaloids such as vinblastine or vincristine was restored more effectively by inhibition of the synthesis of GSH by BSO than the sensitivity to the anthracyclines such as doxorubicin in H69AR cells, where no P-gp is detectable (Lautier, Canitrot et al. 1996; Deeley and Cole 2006) (Cole 1990).

To date, only minor determinants of MRP1 substrate specificity have been identified: amphiphilic anions are more likely to be conjugated not only to

glutathione but also to glucuronide or sulphate (Jedlitschky, Leier et al. 1996; Zaman, Cnubben et al. 1996; Keppler, Leier et al. 1997; Loe, Deeley et al. 1998) whereas neutral or cationic lipophiles would be extruded out of the cell by MRP1, requiring GSH as a cofactor (Rappa, Lorico et al. 1997; Loe, Deeley et al. 1998). The determination of the distinct physico-chemical properties involved in the direct binding to MRP1 or in the conjugation to GSH would allow the establishment of structure-activity relationships to circumvent the detoxification process driven by MRP1.

1.4.2.4 Glutathione *S*-transferase

The conjugation process has been shown to be the prerequisite for many compounds to be extruded out of the cell by MRP1 (Table 1).

Conjugation to GSH can occur spontaneously in some instances but it is typically catalysed by one or several members of the multigene family of iso-enzymes: the glutathione *S*-transferases (GSTs) consisting of at least six classes in humans (α, μ, π, θ, ω and ξ) (Salinas and Wong 1999; Hayes, Flanagan et al. 2005) (Townsend and Tew 2003). The comparison of the amino-acid sequence has shown a relatively high structural heterogeneity of the enzymes involved in the detoxification process and differential substrate specificity has been demonstrated (O'Brien and Tew 1996; Hou, Honaker et al. 2007).

GST substrates	Reference
Chlorambucil	(Ciaccio, Tew et al. 1990; Ciaccio, Tew et al. 1991; Meyer, Gilmore et al. 1992)
Melphalan	(Dulik, Fenselau et al. 1986; Bolton, Colvin et al. 1991)
Cyclophosphamide	(Yuan, Smith et al. 1991)
Acrolein	(Yuan, Smith et al. 1991)
1,3-bis(2-chloroethyl)-1-nitrosourea	(Smith, Evans et al. 1989; Berhane, Hao et al. 1993)
Thiotepa	(Dirven, Dictus et al. 1995)
Ethacrynic Acid	(Yuan, Smith et al. 1991)
Base Propenals *	(Tan, Meyer et al. 1988)
Hydroxyalkenals *	(Tan, Meyer et al. 1988)
Hydroperoxides *	(Clark, Smith et al. 1973)

Table 1. Known anticancer drugs and metabolites that are GST substrates. * Metabolites generated from DNA free radical damage. Table modified from M.L. O'Brien and K.D. Tew, 1996 (O'Brien and Tew 1996).

For instance, the conjugation of melphalan and chlorambucil to glutathione are most likely to be catalysed by GST α while the μ iso-enzyme is associated with the detoxification of nitrosourea. In addition, over-expression of GSTπ has been found in cancer cells resistant to doxorubicin (Goto, Ihara et al. 2001) (Bolton, Colvin et al. 1991).

The differential expression of the GSTs has also been shown to be related to tumorigenicity. The level of expression at both the mRNA and protein level of the 6 classes of GSTs has been evaluated among the NCI60 panel and one of them, GSTπ

has been found to be the most predominant (Tew, Monks et al. 1996). Its expression has not only been found *in vitro* but also in human cancer tissues. Since the induction of GSTπ has been linked to the exposure to carcinogens, its detection is currently being employed as a preneoplastic and neoplastic marker (Tsuchida and Sato 1992) (Sato 1989). In addition, its expression is correlated with a negative clinical outcome and a reduced patient survival (Satoh, Nishida et al. 2001).

A few studies have suggested that GSTs sequester the drugs without GSH-conjugation but the most widely accepted model is that GST, by lowering the pKa of the cysteine of GSH (pKa > 9.5) to a more physiological value (pKa~7), would catalyse the formation of a thiol-ether bond with the drug at its electrophilic centre.

Electrophilicity is a major characteristic of most DNA alkylating agents and a number of these can conjugate to GSH.

1.4.2.5 MRP1 localisation

MRP1 is ubiquitous throughout the body with relatively high levels found in the lung, kidneys, testis, skeletal muscle, and peripheral blood mononuclear cells while relatively low levels are found in liver (Figure 11) (Cole, Bhardwaj et al. 1992; Leslie, Deeley et al. 2005). The localisation of MRP1 in polarized cell is found mainly at baso-lateral membranes apart from brain capillary endothelial cells where it is found at the apical side (Peng, Cluzeaud et al. 1999; Chan, Lowes et al. 2004).

1.4.2.6 MRP1 and clinical outcome

Clinical studies have documented the expression of MRP1 among solid and haematological cancers and, in some cases, have reported a correlation between MRP1 expression and a negative response to treatment and disease outcome (Schaich, Soucek et al. 2005). For instance, when treated for adeno-carcinoma, with epirubicin or paclitaxel, patients with an unfavourable clinical outcome were characterised by increased level of MRP1 mRNA (Ohishi, Oda et al. 2002). More recently, MRP1 expression was associated with poor prognosis in patients with nasopharyngeal carcinoma treated with 5-fluorouracil (Larbcharoensub, Leopairat et al. 2008).

The interaction of the PBDs with MRP1 is unknown. However, their physico-chemical properties would suggest a potential interaction for the transporter limiting their anti-tumour activity. PBDs exert their anti-tumour activity by interacting with DNA due to their relative electrophilicity. However, this property would also allow the PBDs to undergo a detoxification process mediated by the GSTs, limiting even more their biological activity. Determining the specific features involved in the substrate specificity to MRP1 and to the GSTs should allow the rational design of new PBD derivatives with enhanced anti-tumour activity.

1.4.3 ABCG2 or BCRP

ABCG2 was first identified 10 years ago by Doyle and colleagues (1998) in breast cancer cell lines selected with Doxorubicin (MCF7 AdVp) (Doyle, Yang et al. 1998). Because of its first localisation, this discovery led its name of breast resistance cancer protein or BCRP. A number of cell lines, selected for mitoxantrone resistance, have shown a multidrug resistance phenotype whilst expressing neither P-gp nor MRP1. Indeed, mitoxantrone resistant cell lines were not only highly resistant to mitoxantrone but have shown a transport activity with antracyclines (doxorubicin and daunorubicin) without being resistant to the vinca-alkaloids such as vinblastine (Taylor, Dalton et al. 1991; Nakagawa, Schneider et al. 1992; Ross, Yang et al. 1999) (Klimecki, Futscher et al. 1994) (Hazlehurst, Foley et al. 1999). Miyake and colleagues confirmed the presence of ABCG2 in mitoxantrone-resistant colon carcinoma cells (S1-M1-80) and named the protein MXR, relating to the mitoxantrone resistance phenotype (Miyake, Mickley et al. 1999).

1.4.3.1 ABCG2 structure

ABCG2 is a half-transporter of 72kDa comprising 655 amino-acids. It contains a single MSD with six putative trans-membrane-domains, a single NBS with three potential *N*-glycosylation sites (Figure 17). It needs to homo-dimerise in order to exert functional transport activity (Doyle, Yang et al. 1998) (Kage, Tsukahara et al. 2002). Little is known about the structural determinants responsible for the interaction with the different ABCG2 substrates: the trans-membrane domains (TMDs) are common to the other ABC transporters P-gp and MRP1 and are

responsible for binding (Figure 17) (Taguchi, Kino et al. 1997; Taguchi, Morishima et al. 1997; Hafkemeyer, Dey et al. 1998). It has recently been suggested that, in contrast to P-gp, ABCG2 has at least two symmetrical binding sites (Clark, Kerr et al. 2006).

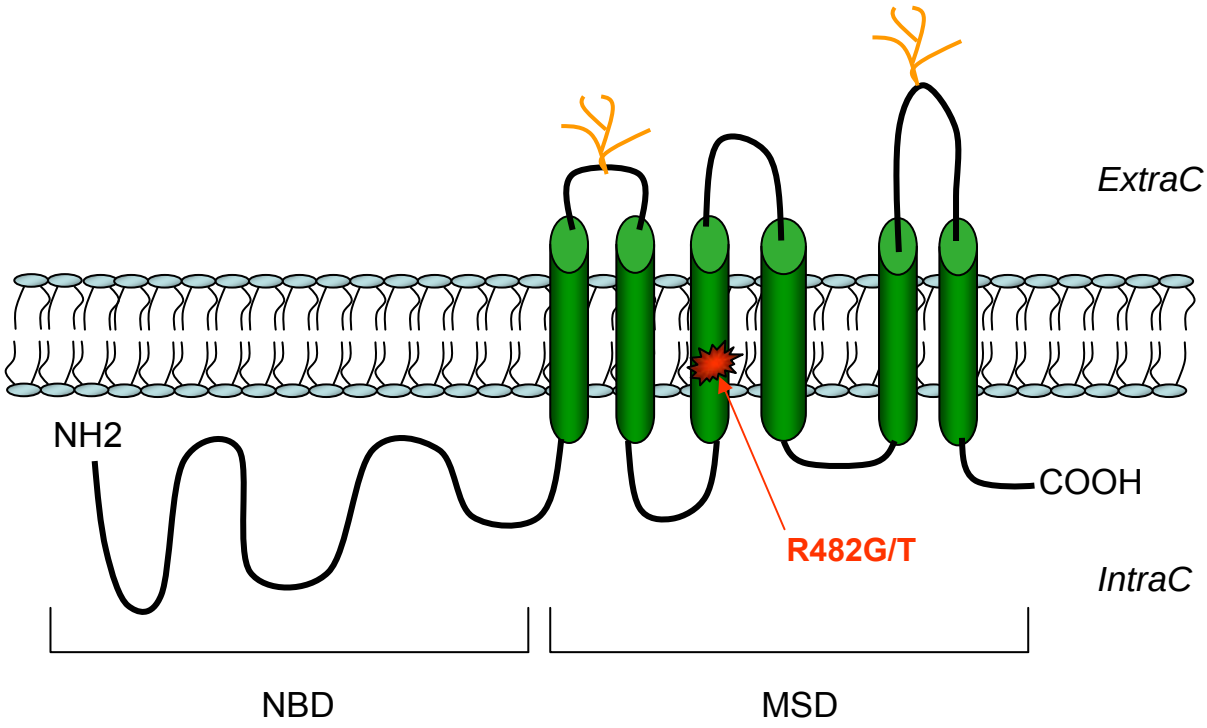

Figure 17. A membrane topology model of ABCG2. ABCG2 contains one nucleotide binding domain (NBD) followed by one membrane-spanning domain (MSD) with 6 predicted transmembrane α-helices. Two or 3 putative N-glycosylation sites are predicted to be in the extracellular loops as indicated. A single nucleotide polymorphism at position 482 has been shown to alter the function of the transporter. R corresponds to the arginine, G to guanine and T to threonine.

1.4.3.2 ABCG2 substrate specificity

Compounds that interact with ABCG2 represent a wide spectrum of chemical structures. ABCG2 is involved in the removal of anticancer drugs, but also of therapeutic agents such as antibiotics, HIV-protease inhibitors, folates and porphyrins (Honjo, Hrycyna et al. 2001; Chen, Robey et al. 2003; Imai, Asada et al. 2003; Mitomo, Kato et al. 2003) (Gupta, Zhang et al. 2004) (Janvilisri, Shahi et al.

2005; Shafran, Ifergan et al. 2005; Krishnamurthy and Schuetz 2006). Similarly to MRP1, ABCG2 recognises a wide range of drugs which can be conjugated to glutathione, glucuronide and with a preferential substrate specificity for sulphated compounds (Suzuki, Suzuki et al. 2003). In addition, compounds conjugated to glutamate may also be recognised by the transporter. For instance, inside the cells, folyl-poly-γ-glutamate synthetase (FPGS) conjugates glutamate to methotrexate (MTX). The poly-glutamylated form (MTX-Glu 2-3) was shown to be extruded by ABCG2 (Zeng, Chen et al. 2001). Its role is physiological extrusion of chemotherapeutic agents is additional as ABCG2 is primarily involved in the transport of endogenous substrates such as the steroids hormones estrone-3-sulfate the precursor of the biologically active oestrogen as well as the mature form 17β-estradiol-17-β-D-glucuronide (E217βG) (Chen, Robey et al. 2003).

Since the transporter was identified only a decade ago, only a few studies have attempted to determine the physico-chemical properties involved in ABCG2 substrate specificity. In 2006, Nagakawa showed by investigating a series of camptothecin (CPT) analogues that a hydroxyl group at position 10 or 11 are prerequisites for the compounds to be recognised by ABCG2. Moreover, the authors suggested that planar structure with conjugated π-orbitals may be critical for the interaction with the active site of the ABCG2 protein (Nakagawa, Saito et al. 2006).

1.4.3.3 ABCG2 polymorphism

A single amino-acid change at position 482 has been associated with altered substrate specificity. To date, no real consensus has been reached regarding the

impact of this particular mutation on drug efflux. For instance, the cell lines expressing the mutated form of the transporter (R482T or R482G) have shown a greater resistance to mitoxantrone and doxorubicin as well as an increase of the transport of rhodamine 123 compared to the cell lines expressing the wild type (Honjo, Hrycyna et al. 2001; Allen, Jackson et al. 2002) (Table 2). This specific mutation has therefore been considered as ‘‘gain of function’’ (Ozvegy, Varadi et al. 2002). In contrast, other studies have reported a “loss of function” for resistance to methotrexate indicating the critical role of this residue in the substrate specificity of the transporter (Volk, Farley et al. 2002; Chen, Robey et al. 2003). Finally, Robey and colleagues have recently shown that the transport of the ABCG2 substrate, pheophorbide A was not affected by this mutation (Robey, Steadman et al. 2004). In addition, stable transfectants expressing wild-type ABCG2 with an arginine at amino acid 482 were resistant to mitoxantrone, camptothecin and its metabolite SN-38, while cells transfected with mutant ABCG2 with a glycine or threonine at the same position were resistant to the anthracyclines and rhodamine 123 (Robey, Honjo et al. 2003). Allen *et al.* have postulated that the loss of the negatively charged arginine may impact on the substrate specificity of ABCG2, suggesting that the wild-type protein would not recognise compounds with a positive charge (Allen, Jackson et al. 2002). However, a compound predicted to carry a net positive charge at physiologic pH, pheophorbide A (PhA) has been shown to be a substrate for wild-type and mutant ABCG2. Thus, the role of amino acid 482 in substrate specificity of the transporter remains to be elucidated.

		ABCG2 - 482		
	Study	Wild type (Arginine)	Mutated (Threonine)	Mutated (Glutamine)
Substrates				
Doxorubicin (Robey, Honjo et al. 2003)	*Cytotoxicity*	+	+++	+++
Daunorubicin (Robey, Honjo et al. 2003)	*flow cytometry*	+	0	0
	Cytotoxicity	+	++	++
Epirubicin (Robey, Honjo et al. 2003)	*Cytotoxicity*	+	++	++
Rhodamine 123 (Robey, Honjo et al. 2003)	*flow cytometry*	+	0	0
Methotrexate (Volk, Farley et al. 2002) (Chen, Robey et al. 2003)	*vesicles*	++	0	0
MTX-Glu2 (Volk, Farley et al. 2002) (Chen, Robey et al. 2003)	*vesicles*	++	0	0
MTX-Glu (Volk, Farley et al. 2002) (Chen, Robey et al. 2003)	*vesicles*	++	0	0
Folic Acid (Chen, Robey et al. 2003)	*vesicles*	++	0	0
Mitoxantrone (Robey, Honjo et al. 2003)	*flow cytometry*	+	+	+
	Cytotoxicity	+	+++	+++
Topotecan (Volk, Farley et al. 2002)	*Cytotoxicity*	++	++	+
SN-38 (Volk, Farley et al. 2002)	*Cytotoxicity*	++	++	+
Pheophorbide A (Robey, Steadman et al. 2004)	*flow cytometry*	+	+	+
Etoposide (Robey, Honjo et al. 2003)	*Cytotoxicity*	+	++	++
Inhibitors				
Novobiocin (Robey, Honjo et al. 2003)	*flow cytometry*	+	++	++
FTC (Robey, Steadman et al. 2004)	*flow cytometry*	++	++	++
Tariquidar (Robey, Steadman et al. 2004)	*flow cytometry*	+	+	+

Table 2. Differential impact of the single nucleotide polymorphism of ABCG2 at position 482 on the substrate specificity of compounds substrates and inhibitors of the transporter. The presence of an arginine at position 482 is considered as the wild type form. The presence of a threonine or a glutamine at the same position is considered as the mutated form of the transporter. The detail of the measurement has been reported. 0 refers to a compound being not substrate for the transporter. (+) refers to a compound being substrate / inhibitor for the transporter. Compounds labelled with a greater number of (+) correspond to a greater interaction with ABCG2.

1.4.3.4 ABCG2 localisation

ABCG2 is highly expressed in tissues such as human placenta and to a lesser extent in liver, small intestine and colon, ovary, veins, capillaries, kidney, adrenal, lung and hematopoietic stem cells (Doyle, Yang et al. 1998; Litman, Brangi et al. 2000) (Faneyte, Kristel et al. 2002) (Krishnamurthy and Schuetz 2006) (Figure 11). ABCG2 was found predominantly at the apical side of polarised cells. This specific tissue and cell localisation suggests a protective role for ABCG2 similar to P-gp.

1.4.3.5 ABCG2 and clinical outcome

In addition to its physiological localisation, ABCG2 is also expressed in a wide range of tumours such as acute myelogenous leukemia (AML) (Galimberti, Guerrini et al. 2004), acute lymphoblastic leukemia (ALL) (Sauerbrey, Sell et al. 2002), adenocarcinomas (Faneyte, Kristel et al. 2002) and bladder tumours (Diestra, Condom et al. 2003). Many studies have evaluated the clinical relevance of the expression of ABCG2 in the response to chemotherapy without reaching a consensus. For instance, in leukemia, Benderra *et al*, have shown that, when treated daunorubicin and mitoxantrone for AML, patients expressing ABCG2 were found to have the poorest prognosis (Benderra, Faussat et al. 2004). In contrast, Sauerbrey *et al,* were not able to shown any correlation between the expression of the transporter and prognosis to childhood ALL (Sauerbrey, Sell et al. 2002). In breast cancer, Burger *et al*, have correlated ABCG2 expression and the clinical outcome after treatment with anthracyclines (Burger, Foekens et al. 2003) while 2 studies from Kanzaki *et al* (Kanzaki, Toi et al. 2001) and, Faneyte *et al* (Faneyte, Kristel et al.

2002), did not shown any correlation. Finally, in lung cancer, ABCG2 expression was associated with positive response to platinum-based chemotherapy and survival (Yoh, Ishii et al. 2004).

Compounds recognised by ABCG2 are relatively diverse and physico-chemical features involved in ABCG2 substrate specificity for one class of compounds may not be applicable to all. The impact of ABCG2 on the cytotoxicity of the PBD derivatives is unknown. Determining the specific physico-chemical properties for this class of compounds would help designing new PBD derivatives with enhanced anti-tumour activity.

ABCG2 polymorphism has been shown to alter the substrate specificity for many classes of compounds. The evaluation of the impact of the main SNP on the anti-tumour activity of the PBDs should allow targeting defined tumours according to their genotype with specific PBDs.

1.5 ABC transporters overlapping substrate specificity

Taken together, the ABC transporters, P-gp, MRP1 and ABCG2 transport a wide variety of chemotherapeutic agents inducing a MDR phenotype. Compounds may be recognised only by one or several ABC transporter suggesting in some cases overlapping substrate specificity (Table 3).

It has been established that P-gp preferentially extrudes hydrophobic cationic and/or neutral molecules. MRP1 and ABCG2 extend their spectrum to organic anions, including phase II conjugated metabolites.

Some compounds have shown substrate specificity for all 3 transporters such as epirubicin, etoposide, irinotecan and methotrexate. It is evident that these compounds do not share the property of being cationic, neutral and anionic simultaneously. A rational screening of the chemical structures involved in the substrate specificity of a specific ABC transporter appears necessary. Moreover, the features involved in the substrate specificity to an ABC transporter might differ between classes of compounds.

	P-gp	MRP1	ABCG2
Vinca alkaloids	Vinblastine	Vinblastine	
	Vincristine	Vincristine	
Anthracyclines	Daunorubicin	Daunorubicin	Daunorubicin
	Doxorubicin	Doxorubicin	Doxorubicin
	Epirubicin	Epirubicin	Epirubicin
Epipodophyllotoxins	Etoposide	Etoposide	Etoposide
	Teniposide		Teniposide
Taxanes	Docetaxel		
	Paclitaxel		
Kinase inhibitors	Imatinib	Imatinib	Imatinib
			Flavopiridol
Camptothecins	Irinotecan	Irinotecan	Irinotecan
	SN-38	SN-38	SN-38
Thiopurine			Topotecan
Other	Bisantrene		Bisantrene
		Arsenite	
	Colchicine	Colchicine	
	Methotrexate	Methotrexate	Methotrexate
	Mitoxantrone	Mitoxantrone	Mitoxantrone
	Saquinivir	Saquinivir	
	Ritinonavir	Ritinonavir	
	Actinomycin D		
			Azidothymidine

Table 3. Overlapping substrate specificity of the ABC transporters P-gp, MRP1 and ABCG2. Only a few examples of substrates are listed. Boxes were left blank where no data are available or no significant interactions were reported.

1.6 Circumventing MDR phenotype

Many compounds have been classified according to their substrate specificity to ABC transporters, thus explaining their chemo-resistance in a wide variety of tumour samples.

The strategy to block the different transporters appears appealing in the clinic. Much progress has been made in the identification of the tumour type and the level of expression of the different ABC transporters may be easily analysed prior to any treatment. Combination of treatment with a specific inhibitor appears to be a good strategy to circumvent the multidrug resistance phenotype. However, over the years, several generations of P-gp inhibitors have raised hopes only to fail in clinical trials (Szakacs, Paterson et al. 2006; Szakacs, Varadi et al. 2008). The first generation modulators such as verapamil, cyclosporine A and quinine were generally ineffective and toxic. In an attempt to reduce the toxic side effects, a second generation of inhibitors such as PSC-833, an analogue of cyclosprine D, was developed. However, drug-drug interactions that limited drug clearance and chemotherapeutic metabolism were accountable for the failure of these modulators into the clinic. In addition, pharmacokinetics interactions were generally unpredictable and therefore many patients were under dosed while some others were overdosed. More recently, a third generation of modulators such as tariquidar was tested in clinical trials without being able to overcome the issues mentioned above (Kurnik, Sofowora et al. 2008)].

Therefore, defining the features responsible for the specific interaction for the different ABC transporters and designing compounds which are not substrates of any of the transporters appears to be the best strategy to circumvent the multidrug resistance phenomenon.

1.7 Aims of the project

In view of the apparent activity of the PBDs and the potential to design new derivatives, I propose to identify the structural factors responsible for ABC transporter substrate specificity in order to design out these features in future derivatives. In addition, I propose to try to identify the structural factors responsible for the activity of the PBDs. Limiting the impact of the ABC transporters and improving the activity should allow the rational design of new PBDs with enhanced anti-tumour characteristics. Finally, I propose to try to identify predictive biomarkers, which could enhance further the potential anti-tumour activity of the PBDs. The derivatives studied will comprise both PBD-dimer analogues of the clinical candidate SJG-136 and PBD-monomers.

The thesis will include:

- In silico *work, identifying features in the set of compounds studied presenting important chemical features previously published as affecting ABC transporter substrate specificity as well as identifying the physico-chemical properties involved in PBD related activity*

- *Biological studies, evaluating the differential cytotoxicity of the compounds in a panel of cell lines expressing differential levels of the transporters. In addition, the co-exposure to specific inhibitors will confirm ABC transporter substrate specificity.*

- *A comparative study between ABC transporter dependency observed* in vitro *and ABC transporter dependency predicted from* in silico. *New chemical features may be proposed to explain the ABC transporter substrate specificity of PBDs. In addition, a correlation study comparing the biological activity and the features identified* in silico *may identify a structure activity relationship of the PBDs*

- *Since ABCB1 and ABCG2 polymorphism can influence the substrate specificity of the transporter, specific experiments will be carried out investigating the impact of the major ABC transporters polymorphisms using cell lines expressing different genotypes.*

- *The activity of the PBDs has been shown to be related to the ability for the cell to repair DNA damage. Therefore, the impact of the homologous repair (HR) machinery on the anti-tumour activity of the PBDs will be evaluated using HR deficient cell lines.*

2 Chapter 2: MATERIALS AND METHODS

2.1 Materials

The pyrrolo[2,1-*c*][1,4]benzodiazepine derivatives (PBDs) were synthesised *de novo.* The multiple step synthesis has been described in full elsewhere (Antonow, Cooper et al. 2007). Briefly, PBD-monomers were synthesised from commercially available 6-nitroveratric acid. The C2-aryl PBDs derivatives were obtained via Suzuki coupling from the advanced synthetic intermediate 1 (Figure 18).

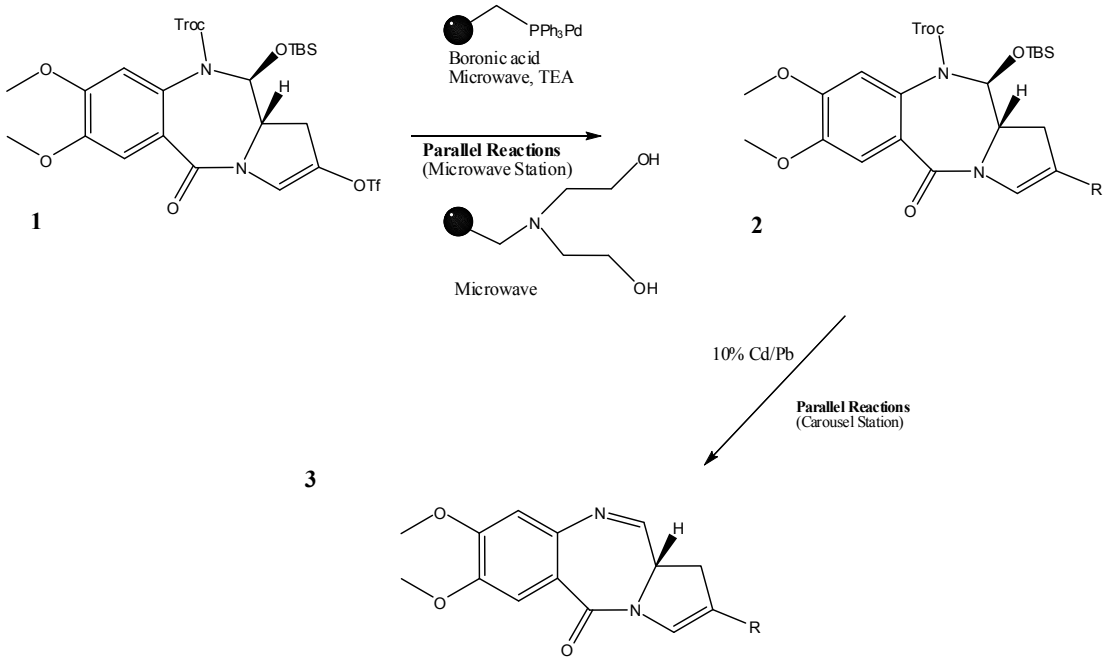

Figure 18. Chemical synthesis of the PBD-monomers. The insertion of different substituents at the C2-position of the PBD triflate intermediate **1** to give intermediates of type **2** followed by conversion to the PBD imine sub-libraries used in this study.

A diverse set of commercially available boronic acids and pinacol esters were subject to the coupling conditions using microwave conditions (10 min, 100 °C).

PS-PPh3Pd was employed as a solid-supported palladium catalyst to facilitate workup (on-bead reagents can be removed from the reaction mixture without chromatographic purification). After complete consumption of triflate **1**, *N*, *N*diethanolaminomethyl polystyrene (PS-DEAM) was added to sequester any unreacted boronic acid/pinacol esters (microwave radiation, 10 min, 100 °C), and a phase separator cartridge then used to isolate the Suzuki products of type **2**. Finally, the N10-Troc group was cleaved under mild conditions using a 10% Cd/Pb couple leading to elimination of the C11-OTBS group to afford the target C2-substituted N10-C11 PBD imines used in this study (**3**).

The PBD-dimers were synthesised from the commercially available *trans*-4-hydroxy-L-proline and followed the first steps of B-ring cyclisation strategy first reported by Fukuyama and colleagues (Fukuyama 1993). The full chemical synthesis has been reported elsewhere (Gregson, Howard et al. 2001). Both PBD-dimers and PBD-monomers were received on dry ice and stored as a powder at -20°C. Aliquots (~1-3mg) were dissolved in dimethylsulfoxide (DMSO) at 40 mM and stored at −80°C.

L-Glutathione reduced (dissolved in ultrapure sterile water) and Trichloroacetic acid ACS reagent (TCA), were obtained from Sigma-Aldrich and stored at 4°C. Verapamil hydrochloride, 3,3′-Methylene-bis(4-hydroxycoumarin) (dicumarol), L-Buthionine-sulfoximine (BSO) and Fumitremorgin C (FTC), were also obtained from Sigma-Aldrich. Aliquots were stored in DMSO at −20°C. MK-571 was obtained from BioMol. Aliquots were stored in ultrapure water at −80°C. Calcein AM and Lucifer yellow were obtained from Molecular Probes (invitrogen)

and stored at −20°C and 4°C, respectively. G418 sulfate was obtained from Calbiochem and stored in 100 mM Hepes, (pH = 7.3) at 4°C.

Mdr1 rabbit polyclonal antibody was obtained from Santa Cruz and stored at 4°C. The mouse monoclonal antibody to an external MDR1 epitope (4E3), MRP1 mouse monoclonal antibody and secondary FITC-goat polyclonal to mouse antibody were obtained form Abcam (United Kingdom). ABCG2 mouse antibody (BXP-21) was obtained from Alexis BioChemical. Phospho-histone H2AX (Ser 139) rabbit antibody was obtained from Cell Signalling. Aliquots of primary and secondary antibodies were stored at −20°C.

Transwell plates with Polyethylene Terephthalate (PET) Membrane (Millicell 24) were obtained from Millipore and stored at RT. Hanks buffer balanced saline (HBSS) was obtained from Fisher / Thermo Scientific HyClone and stored at RT.

2.2 Methods.

2.2.1 Cell culture

Colon cancer cell lines HCT 116, HCT-15, adenocarcinoma cell line Caco-2, melanoma cell line SK-MEL5 and lung cancer cell line A549 were obtained from the American Type Cell Culture Collection (ATCC) (Rockville, MD) and European Collection of Cell Cultures (Salisbury, UK). Ovarian cancer cell line A2780 and drug resistant sub-clones $A2780^{AD}$ were provided by the National Cancer Institute (NCI, Bethesda, USA). Murine fibroblasts (3T3 GP+E86 and 3T3 transfected with c-DNA expressing the different genotypes of mdr1 were kindly provided by Dr. E. Schuetz from St. Jude's Children Research Hospital, Memphis TN, USA. Breast

cancer cell line MCF7 and drug resistant sub-clones MCF7-MX were kindly provided by Dr. E. Schneider from the University of Maryland, USA. Chinese hamster ovarian cells (CHO), VC-8 and V-79 were kindly provided by Prof. M. Zdzienicka from N. Copernicus University, Bydgoszcz, Poland. Breast cancer cell line MDA-MB-231 transfected with an empty vector (MDA-MB-231 / V8) and MDA-MB-231 transfected with c-DNA expressing the different genotypes of ABCG2 (MDA-MB-231 / R12 and MDA-MB-231 / T3) were kindly provided by Dr. D. Ross from the University of Maryland, USA. HCT 116, HCT-15, A2780 and $A2780^{AD}$ were grown in monolayer in RPMI 1640 medium supplemented with 5% v/v fetal calf serum. 3T3 GP+E86, Caco-2, A549, MDA-MB-231 cells were grown in DMEM medium supplemented with 10% v/v fetal calf serum (FCS). VC-8 and V-79 were grown in Ham's F-10 medium supplemented with 10% FCS. All cells were maintained at 37°C in a humidified atmosphere containing 5% CO_2. $A2780^{AD}$ cells are derived from the parental A2780 cell line and are resistant to doxorubicin. They were obtained by stepwise incubation of increasing concentration of doxorubicin (adriamycin) (Hamilton, Winker et al. 1985). The cells were maintained in the presence of 10^{-7} M doxorubicin and were drug-free one week prior to any experiment. MCF7-MX cells are derived from the parental MCF7 cell line and are resistant to mitoxantrone. They were obtained by stepwise incubation of increasing concentration of mitoxantrone (Nakagawa, Schneider et al. 1992). They were maintained in 10^{-8} M mitoxantrone and were drug-free one week prior to any experiment. MDA-MB-231 cells were maintained in 1 mg / mL of G418 sulfate and were antibiotic-free one week prior to any experiment. All cells were tested

regularly for mycoplasma contamination and were mycoplasma-free for the period of the study.

2.2.2 Growth inhibition assay

Drug concentrations that inhibited 50% of cell growth (IC_{50}) were determined using a sulforhodamine B (SRB) technique (Skehan, Storeng et al. 1990). Cells were plated on day 1 in 96-well plates. The cell density was 2000 cells/well for HCT 116, 3T3 GP+E86, 3500 cells/well for HCT-15, A2780, A549, MDA-MB-231, MCF7, VC-8 and V-79, 5000 cells/well for $A2780^{AD}$ and MCF7-MX cells/well in a volume of 150 µL / well. All cell lines were treated on day 2 except A2780 and $A2780^{AD}$ which were treated on day 3. When cells were pre-treated with different inhibitors (verapamil, MK-571, FTC, dicumarol) they were seeded in 100 µL medium and treated 1 h before drug exposure (24h prior to the experiment for BSO) in a final volume of 50 µL. After 24h drug exposure, cells were washed once with cold phosphate buffer saline (PBS) and placed in 200 µL of drug-free medium for 72 h after the end of drug exposure. The cells were then fixed with trichloracetic acid and stained with sulforhodamine B. Optical densities were measured at 540 nm with a Biohit BP-800 (Bio-Hit, Helsinki, Finland). Growth inhibition curves were plotted as percentage of control cells and IC_{50}s were determined by Graphpad Prism 4 Software (Graphpad Software, San Diego, CA) by fitting a sigmoidal curve with variable slope.

2.2.3 Statistical methods

Comparisons between mean values were performed using a two-sided *t* test after verification of the homogeneity of variances. Confidence intervals of 95% confidence were used for IC_{50} data. Correlations were established using Graphpad Prism 4 Software and the coefficient correlation significance verified with a linearity test.

2.2.4 Calcein-AM assay

Cells (5×10^5) were aliquoted in glass tubes to a final volume of 100 µL. 50 µL of increasing concentrations of verapamil or MK-571 diluted in the appropriate tissue culture media were added to the tubes and incubated for 15 minutes at 37°C. The master stock of calcein-acetoxymethylester (calcein-AM) (1 mM) was diluted 1/1000 in the appropriate tissue culture medium. 50 µL of calcein-AM (1 µM) was added to each tube (final concentration of 250 nM) and incubated at 37°C for 15 minutes. The reaction was stopped by placing the samples on ice. The samples were then centrifuged for 5 minutes (at 200 x g at 4°C), the media removed and replaced by 200 µL cold (4°C) medium. The washing step was repeated 3 times. The cells were re-suspended in a final volume of 500 µL cold (4°C) medium. The calcein retention, i.e. fluorescence was measured using a FACScalibur (BD Biosciences) using an excitation of 488 nm and an emission filter at 515 nm (FL-1 channel). The voltages were set up to display the population within the FSC and SSC channels. The population was gated to exclude debris and aggregates and the intensity of the histogram distribution of the FL-1 fluorescence in the population of cells analysed (10 000 cells) was recorded.

2.2.5 Immunostaining for γ-H2AX

Exponentially growing cells were seeded in chamber slides on day 1. The cell density was 50 000 cells / chamber in a 4 chamber slide in a volume of 500 µL / chamber. The cells were treated on day 3 with 10 nM DRG-16, 1 µM SG-2901, increasing concentrations of SG-2900 (100 nM, 1 µM and 10 µM) and 0.1 nM SG-2897. When cells were pre-treated with verapamil, they were treated with 5 µg / mL verapamil starting 1 h before drug exposure in a final volume of 700 µL. Cells were washed in PBS. Cells were incubated in 2% paraformaldehyde (PFA) in PBS for 10 minutes, washed in PBS, permeabilised in 0.1% triton X100, diluted in PBS at RT for 10 min, washed, blocked with PBS containing 1% bovine serum albumin (BSA) (BDH) and 5% goat serum (Jackson Immunolaboratories, West Grove, PA), and incubated overnight at 4°C with an anti-phosphohistone H2AX antibody (Millipore, United Kingdom), washed, incubated with a FITC, AlexaFluor 488-conjugated goat anti-mouse IgG antibody (Invitrogen, Paisley, UK) for 1 hour at room temperature, and washed in PBS. Slides were mounted with Vectashield Mounting Medium containing or not DAPI (4',6 diamidino-2-phenylindole) (Vector Labs, UK) and visualized with a Leitz Laborlux UV microscope (Wetzlar, Germany) using a 40x or 100x objective fitted with a Spot Insight 4 camera (Diagnostic Instruments, Sterling Heights, MI). The intensity of fluorescence was evaluated with Photoshop CS3 (Adobe).

2.2.6 Caco-2 model of permeability, optimisation of the system

The Caco-2 model of permeability, *i.e.* the transwell assay, has been widely used in the drug discovery and drug development area. It has allowed many groups to measure the permeability of their test compounds.

Human colon carcinoma Caco-2 cells are grown, on permeable supports, for 21 days to allow them to differentiate as enterocytes and express the different ABC transporters at the surface. P-glycoprotein/ABCB1 and ABCG2/BCRP are located at the apical side while MRP1/ABCC1 is found at the basal side in polarised cells (Figure 19) (Evers, Zaman et al. 1996; Anderle, Niederer et al. 1998; Xia, Liu et al. 2005).

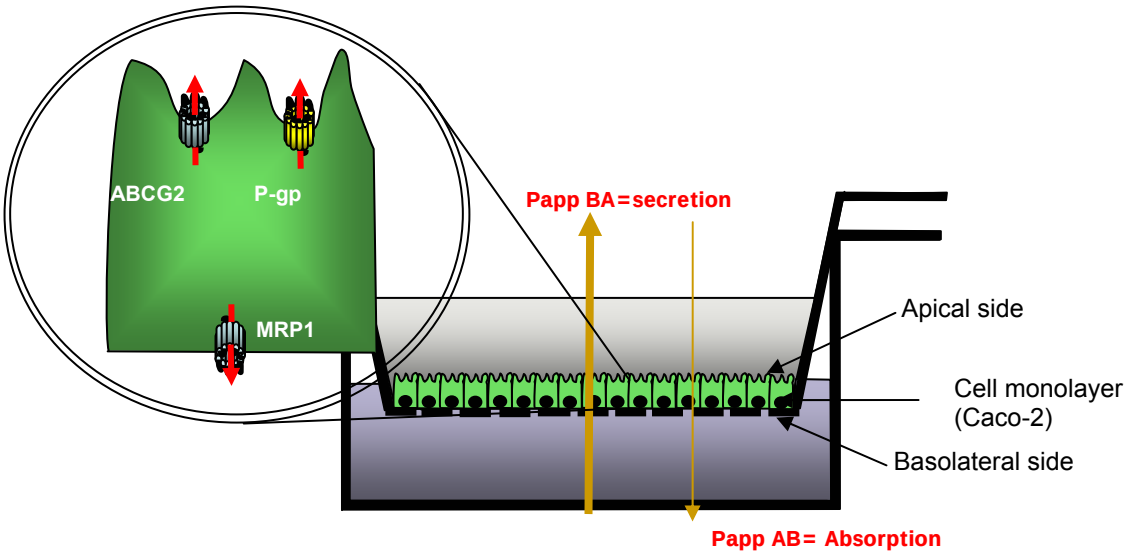

Figure 19. Representation of the transwell assay. After 21 days, Caco-2 cells differentiate as enterocytes and express the different ABC transporters: P-gp and ABCG2 at the apical side and MRP1 at the basal side.

The assay consists of measuring the permeability (for a test compound) from the apical to the basal side (A-B) which corresponds to the absorption (passive

transport) and compare it to the secretion which corresponds to the permeability from the basal to the apical side (B-A) (active transport). It has been shown that if a compound has a ratio (B-A)/(A-B) greater than 3, it can be considered as being actively transported by P-glycoprotein (Szakacs, Paterson et al. 2006).

The reliability of the results generated using this assay is dependent on several factors:

- Confluence of the cell monolayer which will avoid passive diffusion of the compound through the membrane
- Differentiation and passage number of the cells: membrane and culture media might have a different impact on the cell growth and differentiation but can also influence the level of expression of the transporters (Anderle, Niederer et al. 1998)
- Confirmation of the mass balance of the compound to ensure that intracellular metabolism has not biased significantly on the results generated.

Therefore, the transwell assay was optimised in order to evaluate the impact of the different ABC transporters on the permeability of the PBD derivatives.

2.2.6.1 Accuracy of seeding density.

The assay allows the Caco-2 cells to grow for 21 days and differentiate as a tight monolayer of enterocytes. In order to avoid leakiness of the monolayer but also formation of a multilayer membrane, the number of cells seeded is critical. It is important to dissociate the cells correctly as a unicellular cell suspension in order to seed exactly the same number of cells. The Caco-2 cells need longer to dissociate

(10 / 15 min) in presence of trypsin. This step is crucial as the cells could be seeded as clumps resulting in a non homogeneous membrane. After trypsinisation, 2 methods were used to optimise the dissociation: media was added to the flask and a 5 mL pipette and a pump are used. Pipeting up and down (at least 10 times) allowed an initial dissociation of the cells. The cells were then passed through a needle (at least 5 times) with a syringe to obtain a unicellular suspension. A microscope and coulter counter (Beckman Coulter, Fullerton, USA) were used to verify whether the cells were well dissociated. Indeed, the latter allows the visualisation of the proportion of the cells within a given size (9-21µm diameter) range. This optimisation process was done even when the cells were passage routinely.

It has been shown that the passage number of the cells has an impact on their differentiation (levels of mRNA, protein expression). Therefore, Caco-2 cells with an identical passage number (p4) were used in all experiments.

Different numbers of seeded cells have been suggested by different groups (20 000 cells / cm^2 – 100 000 cells / cm^2) (Crowe and Lemaire 1998; Malago, Koninkx et al. 2003; Shah and Khan 2004). Therefore, the number of seeded cells has been optimised "*in house*".

2.2.6.2 Measuring the viability of the system

The Trans Epithelial Electric Resistance (TEER) measurement technology has been used widely in order to verify the confluence of the cell monolayer (Ranaldi, Islam et al. 1992; Takahashi, Kondo et al. 2002). It allows an accurate measurement of the resistance of the membrane. Briefly, as confluence increases

over time, the level of resistance exerted by the cells increases and reaches a plateau when cells are confluent.

In this study, different densities of Caco-2 cells were seeded into transwell upper chambers. The relative resistance of the cell monolayer was measured on alternate days using an Epithelial Voltohmmeter (EVOM) (World Precision Instruments, USA). The cells were grown for up to 21 days (Figure 20).

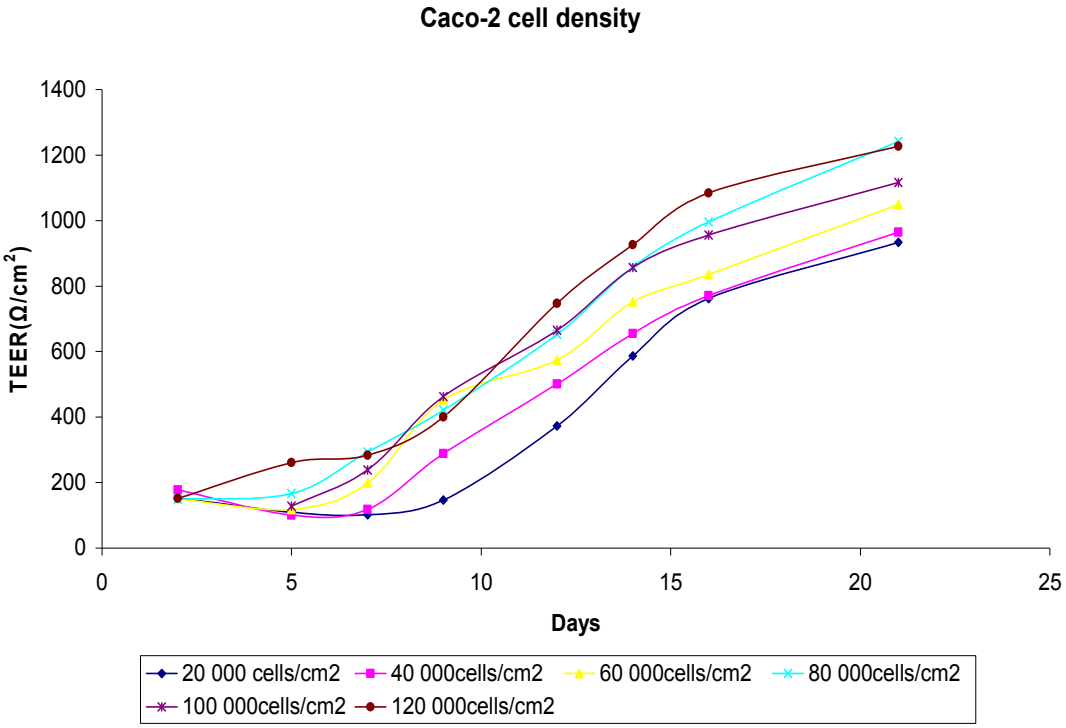

Figure 20. Impact of the cell density on the TEER of the membrane overtime. The Caco-2 cells were seeded at different cell density ranging from 20 000 cells / cm^2 up to 120 000 cm^2 into each transwell membrane. The TEER was measured every other day up to 21 days. The values are means of n = 4 wells. The SD has not been represented for reasons of clarity.

A general pattern was seen for all cell densities: the TEER was first relatively steady for up to 7 days (from mean $_{TEER}$ = 160 ± 12 at day 2 to mean $_{TEER}$ = 200 ± 80 at day 7) followed by an exponential increase up to 16 days (mean $_{TEER}$ = 900 ± 130).

Finally, the resistance slowly increase until day 21 (mean $_{TEER}$ = 1100 ± 130). This pattern could be explained by 2 weeks of cell growth until reaching confluence at day 16. The cells would differentiate thereafter.

At 16 days, the resistance is proportional to the number of cells seeded (r^2 = 0.9, P $_{value}$ < 0.005). At 21 days, the relationship between the resistance and the cell density of cells seeded is less significative (r^2 = 0.75, P $_{value}$ < 0.05). For instance, the cell density of 80 000 cells / cm^2 has shown a greater TEER (1242 Ω / cm^2) than cell densities of 100 000 cells / cm^2 and 120 000 cells / cm^2 (1117 and 1227 Ω / cm^2, respectively). These results suggest that at high density (100 000 and 120 000 cells / cm^2), the cells might have formed several layers and / or the cell membrane might have been disrupted. Therefore, at such density, the TEER would not be representative of the integrity of the cell monolayer suitable for the transwell assay.

2.2.6.3 Importance of the differentiation process

A monolayer associated with a TEER greater than 300 Ω / cm^2 was shown to be suitable for the transwell assay to be performed (Markowska, Oberle et al. 2001; Tirumalasetty and Eley 2006). In our case, the TEER reached 300 Ω / cm^2 after only 14 days for all the cell densities. Therefore, other studies were performed to assess whether the system was "ready" at 14 days in terms of transporter expression.

For this purpose, the mRNA level of the different ABC transporters was compared after 14 and 21 days (Figure 21) (data kindly generated by Janet McPherson, CRUK, Edinburgh, UK, personal communication). The level of P-gp transporter (normalised by housekeeping gene RPII) increases with the cell density up to 100 000 cells / cm^2 (CD5) (r^2 = 0.86, P $_{value}$ = 0.025). The expression decreases

when the cells are seeded at a density = 120 000 cells / cm^2 (CD6) suggesting a down regulation of the mRNA of P-gp. Additionally, the level of P-gp was not significantly different between 14 and 21 days in culture when cells were seeded at 80 000 cells / cm^2 (CD4).

Levels of MRP1 were unaffected by the different seeding densities and between day 14 and day 21.

Finally, the levels of ABCG2 mRNA were not significantly affected by seeding densities at day 21. When the cells were seeded at 80 000 cells / cm^2 (CD4) for 14 days, the level of ABCG2 was significantly lower than the level after 21 days ($P_{value} = 0.01$).

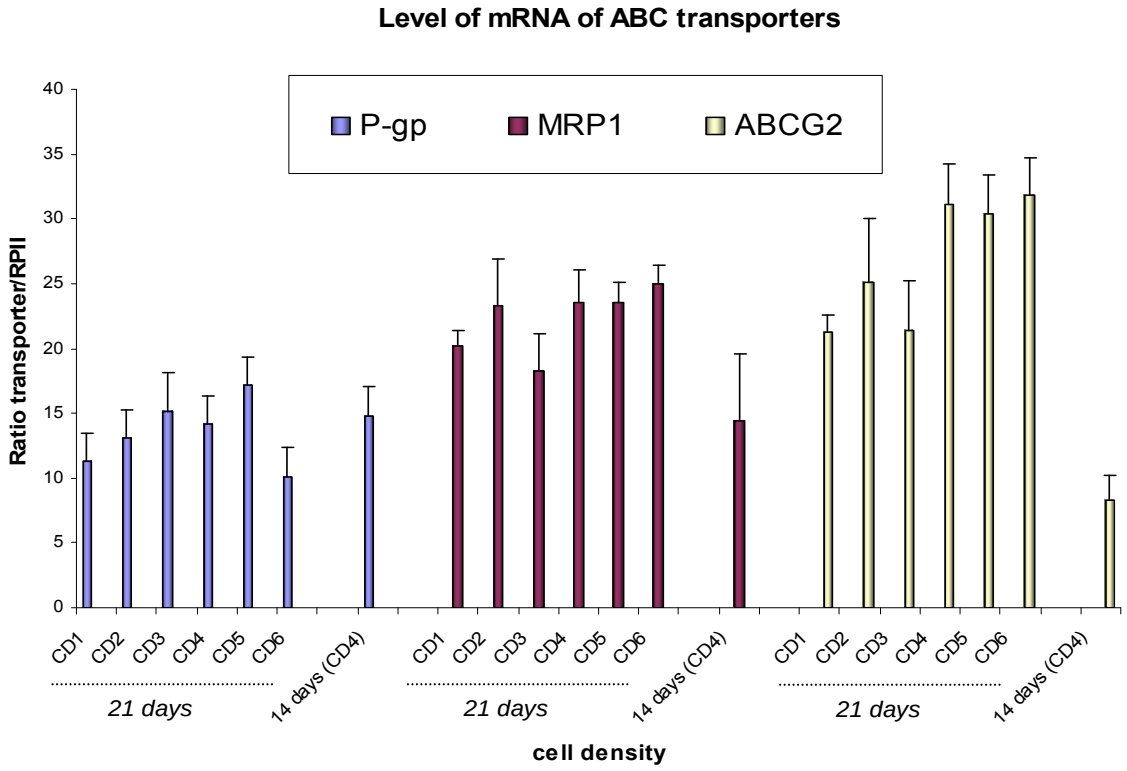

Figure 21. Impact of the seeding cell density on the level of mRNA of the different ABC transporters after 14 days and 21 days. CD 1 is the Cell Density 1 (20 000 cells / cm^2), CD 2 = 40 000 cells / cm^2, CD 3 = 60 000 cells / cm^2, CD 4 =80 000 cells / cm^2, CD 5 = 100 000 cells / cm^2 and CD 6 = 120 000 cells / cm^2. Results are means ± SEM of triplicate.

Overall, these data confirm that the transwell system is "ready" after 21 days, *i.e*. cells differentiating as enterocytes and expressing a sufficient level of the different ABC transporters (optimal level of ABCG2 after 21 days). In addition, A TEER value of 300 Ω / cm^2 should not be considered as being representative of adequately differentiated cells. The cells should be considered as suitable for the assay when TEER values are between 850 and 1100 Ω / cm^2.

2.2.6.4 Caco-2 transwell assay

Caco-2 cells were seeded at 80 000 cells / cm^2 for 21 days and the TEER was verified to be between 850 and 1100 Ω / cm^2 prior to all experiments. The cells were washed 3 times with HBSS before drug treatment. The PBDs were diluted, on the same day, at a concentration of 10 µM for the PBD-dimers and 100 µM for the PBD-monomers, in HBSS. These concentrations have been defined according to the sensitivity of the mass spectrometer which can detect accurately concentrations in the µM range.

The standard procedure for drug treatment is to add 9/10 of the volume of Hanks buffer in each chamber and 1/10 of (10 times drug concentration in HBSS) at the time of the experiment. However, in order to allow full homogenisation of the drug within the chamber, the protocol was modified as follows: the entire volume (1x drug concentration in HBSS) was prepared prior to the experiment and then added to the appropriate chamber. The cells were then placed on a shaker at 60 rpm at 37°C for 2 hours to allow complete homogenisation.

A standard curve of drug concentrations was determined for each PBD derivative analysed, using an LC/MS method (Figure 22) (results kindly generated by Dr. Katan Patel, CRUK, Edinburgh, UK).

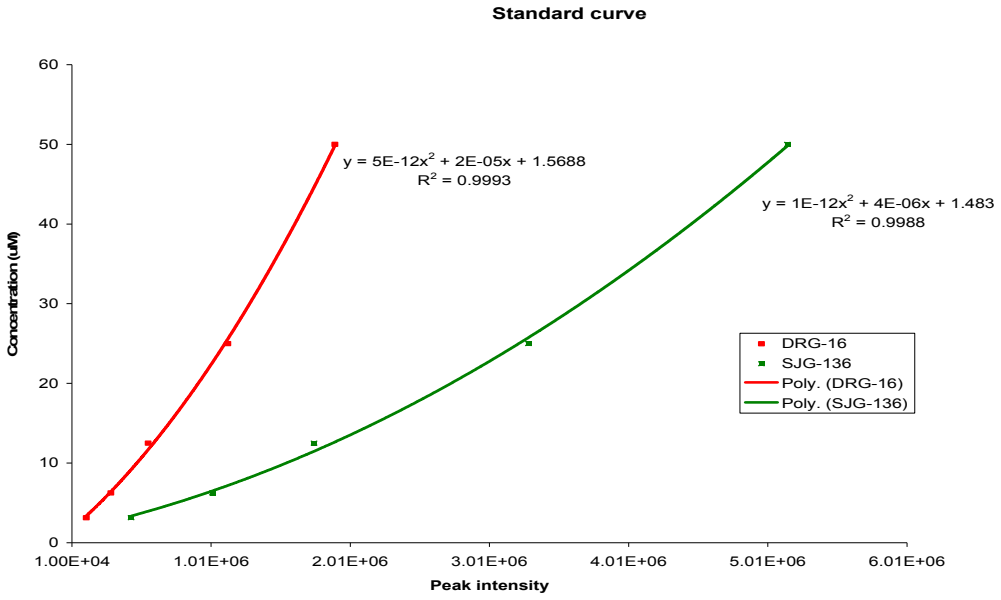

Figure 22. Relationship between the peak intensity determined by mass Spectrometer analysis and drug concentration of 2 PBD-dimers, DRG-16 and SJG-136. The PBDs were diluted at concentrations ranging from 50 µM to 3 µM in Hanks buffer. The standard curve of SJG-136 is represented in green. The standard curve for DRG-16 is represented in red. Results are replicate.

A polynomial function was used for the standard curves for the PBD-dimers ($r^2 > 0.99$ for both compounds) as opposed to linear function ($r^2 < 0.98$ for both compounds). In contrast, a linear function was used for the PBD-monomers ($r^2 > 0.99$) (data not shown). A volume of 10 µL of each chamber was then analysed by LC/MS and the concentration determined for each compound.

It has been shown that the permeability of a test compound can be defined by the following equation (Artursson and Karlsson 1991):

$$\mathbf{P}\boldsymbol{app} = \mathbf{(dQ/dt)/A\ C_0}$$

Where **A** is the surface area of the transwell membrane in cm^2 (= 0.31 cm^2), $\mathbf{C_0}$ is the molar drug concentration in the donor chamber at time = 0 (10 x 10^{-6} M for the PBD-dimers and 100 x 10^{-6} M for the PBD-monomers) and **dQ/dt** is the rate of transfer of the compound to the receiver chamber, determined from the slope of the graph concentration (dQ) versus time (dt) (= 7200 sec).

2.2.6.5 Determination of the mass balance

The mass balance (MB) of a compound is the percentage of original drug mass left at the end of the experiment at both apical and basal sides. It can be calculated with the following formula (Rautio, Humphreys et al. 2006):

$$\mathbf{MB = [(C_{at} \times V_a) + (C_{bt} \times V_b)] / (C_0 \times V_d)}$$

Where $\mathbf{C_{at}}$ is the concentration of the test compound at time = 120 min at the apical side, $\mathbf{V_a}$ is the volume in the apical chamber (0.3 mL), $\mathbf{C_{bt}}$ is the concentration of the test compound at time = 120 min at the basal side, $\mathbf{V_b}$ is the volume at the basal side, Where $\mathbf{C_0}$ is the concentration of the test compound at time = 120 min at the donor side and $\mathbf{V_d}$ is the volume in the donor chamber (0.3 mL). MB > 80% suggests that the intracellular metabolism did not lead to an erroneous evaluation of the impact of the transporters and that there was a minimal loss of drug substrate to plastic surfaces (Hu, Reddy et al. 2004; Rautio, Humphreys et al. 2006).

2.2.6.6 HPLC-Mass spectrometry analysis

The HPLC system comprised of a Dionex (Sunnyvale, CA, USA) 3000 Ultimate series LC connected to a 4000 Q Trap LC-MS/MS system (Applied Biosystems, Foster City, CA, USA) mass spectrometer, equipped with an orthogonal electrospray ion source. Data were acquired and processed with Chromeleon 6.1 and Analyst 1.4 chromatography manager software.

Compounds were separated on a Dionex Acclaim® C16 (150 x 2.0mm I.D.) and 3µm particle size column protected by a Phenomenex Gemini® C18 (4.0 x 2.0mm ID) and 3µm particle size guard cartridge (Phenomenex, Torrance, CA, USA). The HPLC method used gradient elution; mobile phase solvent A was water with 0.1% formic acid and mobile phase B was acetonitrile with 0.1% formic acid. The initial mobile phase composition of 99% solvent A and 1% solvent B was maintained for 3 min. Between 3 and 9 min the percentage of mobile phase B was increased to 75%, kept constant for 2 min and then back to initial the mobile phase composition within 2 min, with a total run time of 16 min. The column was set at a flow rate of 0.23 $mL.min^{-1}$ and a temperature of 33^{o}C. A sample volume of 6 µL was used for all LC-MS experiments.

The mass spectrometer was operated in electrospray mode. The source temperature was 450^{o}C and the spray voltage 3kV was used. The collision gas pressure was 1.5 mTorr. All analytes were optimised using the Analyst software auto tune facility for SRM transitions with dwell times set at 75 milliseconds.

2.2.6.7 Re-assessing membrane integrity with lucifer yellow.

At the end of the transwell assay, the integrity of the monolayer can be verified by measuring the amount of lucifer yellow (LY), a fluorophore, which has passed through the membrane (Hidalgo, Raub et al. 1989).

Concentration of LY should be proportional to its intensity. The concentration was assessed by measuring the OD value using a plate reader (Wallac EnVision reader, PerkinElmer, USA). A standard curve was determined with a range of concentrations 0-100 µM. Measurements were estimated at the excitation wavelength of 430 nM and emission wavelength of 536 nM. Overall, the concentration of lucifer yellow correlates with its intensity ($r^2 = 0.98$ and $P_{value} < 0.0001$) (Figure 23).

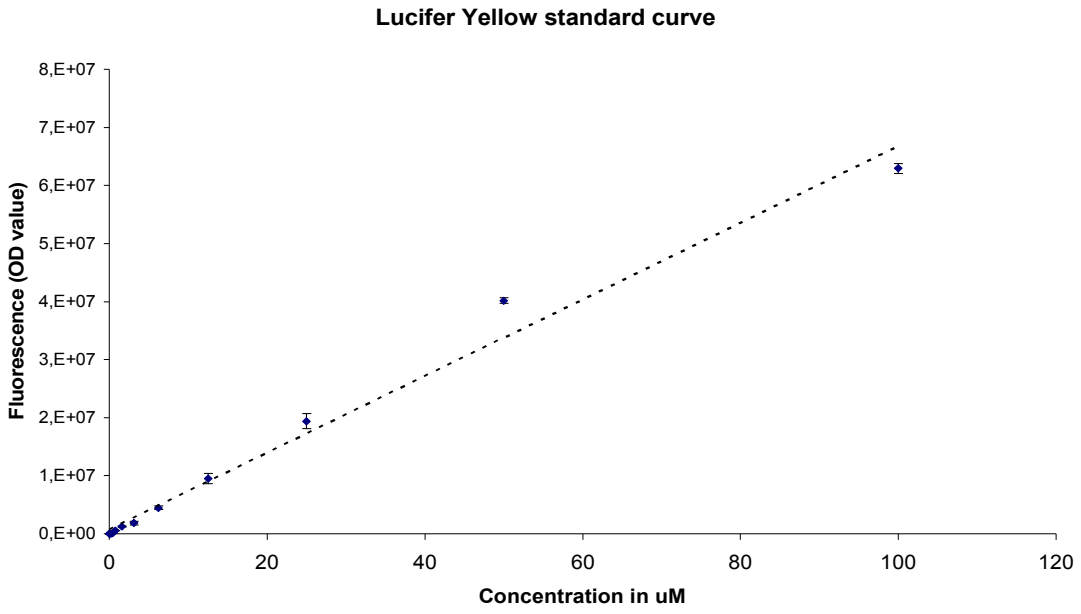

Figure 23. Standard curve of the fluorophore lucifer yellow. The intensity was plotted according to the range of concentration 0-100 µM. Results are means ± SEM of duplicate.

The concentration in the receiver chamber should represent < 2% of the concentration in the donor chamber (Samiulla, Vaidyanathan et al. 2005). The

integrity of the monolayer was assessed post drug transport as lucifer yellow may interfere with LC/MS analysis.

2.2.7 Determination of the level of P-gp mRNA

2.2.7.1 RNA extraction

Cells were lysed in tissue culture dishes with 1 mL of TRI reagent per 10 cm^2 of flask surface area. Cell pellets were transferred in stoppered tubes. 200 µL chroloroform was added per 1 mL of TRI reagent and left for 15 min at RT. The samples were centrifuged at 10 000 rpm using a SS34 rotor (pre-cooled) at 4°C for 15 min. The top phase was transferred to a fresh tube and 500 µL of isopropanol per mL of TRI was added. The samples were centrifuged at 10 000 rpm at 4°C for 10 min. Supernatants were removed, leaving the RNA in the pellet. 7.5 mL of cold 75% ethanol was added and the pellet was then re-suspended by vortex. The samples were transferred in sterile tubes and were centrifuged at 13 000 rpm at 4°C for 10 min. The ethanol was removed. The remaining sample was air dried for 5-10 minutes and re-suspended in distilled H_2O (50 µL).

2.2.7.2 The reverse transcription-PCR (RT-PCR) reaction

All transcripts were detected using Quantitect SYBR Green RT-PCR kits (Qiagen, Crawley, UK). P-gp mRNA expression was determined using forward primer mdr1E23 F: 50-aggccaacatacatgccttc and reverse primer mdr1E23 R: 50-ccttctctggctttgtccag. The reaction was carried out with 22.5 pmol of each primer. Mouse β2 microglobulin (mβ-2m) was used as reference gene to normalize the results in 3T3 fibroblasts using the following primers: mβ-2m F: 50-

gggaagccgaacatactgaa and mβ-2m R: 50-tgcttaactctgcaggcgtat. Standard curves were built from human liver RNA dilutions (BD Biosciences, Oxford, UK) for P-gp and mouse liver RNA for mβ-2m. Each cycle was 15 sec at 94°C (denaturation), 30 sec annealing and 30 sec at 72°C (extension) for 40 cycles. Fluorescence was recorded on the FAM channel (ExD470 nm, EmD510nm) at the end of the extension. Data were analyzed using Rotorgene 6 software.

2.2.8 Evaluation of the mRNA level of the ABC transporters

In order to evaluate the specific impact of ABC transporters, P-gp, MRP1 and ABCG2 on the anti-tumour activity of the PBD derivatives, several cell lines with a differential expression of the transporters were chosen according to their differential mRNA expression. The level of mRNA was determined for 14 different cell lines (data kindly generated by Janet McPherson, CRUK, Edinburgh, UK, personal communication) (Figure 24).

The colon cancer cell lines HCT 116 and HCT-15 were shown to be associated with a differential expression of P-gp only. Indeed, HCT 116 did not express the transporter in contrast to HCT-15. The level of MRP1 was similar in the 2 cell lines and ABCG2 was barely detectable in these 2 particular cell lines. These data confirmed the utility of the model to evaluate the impact of P-gp on the anti-tumour activity of the PBDs. Similarly, the ovarian cancer cell line A2780 and the doxorubicin resistant cell line, $A2780^{AD}$ showed massive difference in the level of P-gp mRNA expression and similar expression of the other 2 transporters, MRP1 and ABCG2.

The lung cancer cell line, A549 was associated with the highest level of MRP1 in contrast to any other cell lines and was therefore chosen to evaluate the impact of this particular transporter on the anti-tumour activity of the PBDs. ABCG2 is also expressed in A549, in low but not negligible mRNA levels and results should be considered in light of this finding.

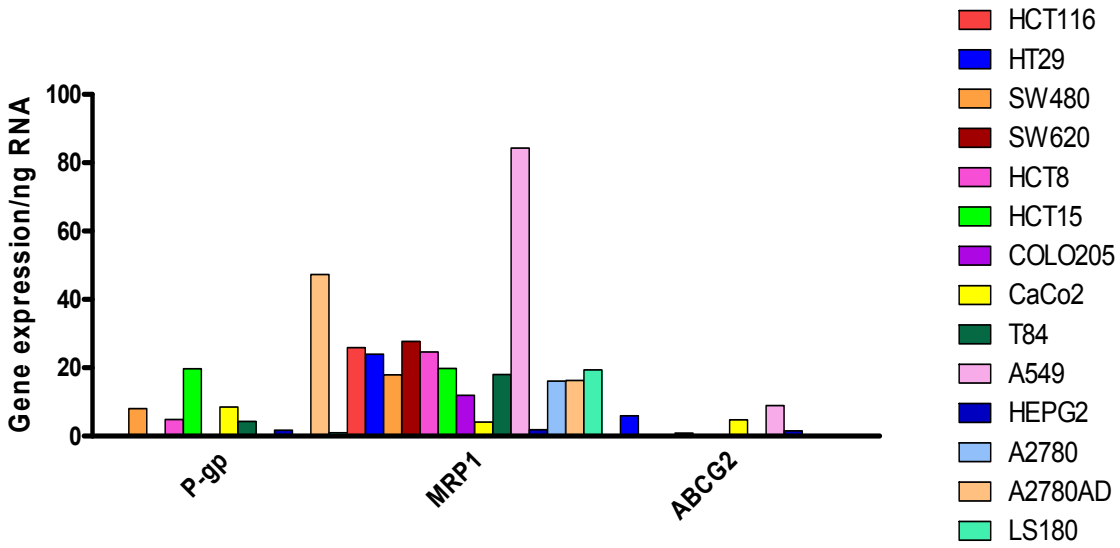

Figure 24. Level of mRNA of the three different ABC transporters, P-gp, MRP1 and ABCG2 among 14 cell lines. Resuts are means of triplicate. The SEM has not been represented for reasons of clarity.

2.2.9 Evaluation of the level of P-gp protein expression by flow cytometry

Cells (5 x 10^6) were resuspended in ice cold PBS. The mouse monoclonal antibody to an external P-gp epitope was added at 1/10 (4E3, Abcam, United Kingdom) containing 1% bovine serum albumin (BDH) and 5% goat serum (Jackson Immunolaboratories, West Grove, PA) for 30 min at RT. Cells were washed with ice cold PBS and incubated with secondary FITC-goat polyclonal to mouse antibody at 1/200 (Abcam, United Kingdom) in the dark for 30 minutes. Cells were washed

once more with ice cold PBS and analysed by fluorescence-activated cell sorting FACScalibur (BD Biosciences) using an excitation of 488 nm and an emission filter at 515 nm (FL-1 channel). Voltages were set up to display the population within the FSC and SSC channels. The population was gated to exclude debris and aggregates and the intensity of the histogram distribution of the FL-1 fluorescence in the population of cells analysed (10 000 cells) was recorded.

2.2.10 Evaluation of levels of MRP1 and ABCG2 protein expression by immunoblotting

Cells (1 x 10^6) were lysed with 200 µL lysis buffer (62.5 mM Tris pH 6.8, 6 M urea, 10% v/v glycerol, 2% w/v SDS, 0.003% w/v bromophenol blue) and sonicated on ice 3 times for 5 sec. Protein concentrations were determined using the bicinchonidic acid assay (Thermo Fisher Scientific, UK). 20 µg of protein was denatured at 45°C for 30 min in the presence of 5% v/v 2-mercaptoethanol, and 20 µg of protein was separated by 12% SDS–PAGE at 100 V for 1 hour and transferred to a PVDF Immobilon- P transfer membrane (Millipore) overnight at 4°C. The membrane was blocked in 5% w/v Marvel dried milk in Tris buffered saline pH 7.5 with 0.1% v/v Tween (TBS-T) for 1 h at room temperature, probed with MRP1 mouse monoclonal antibody (abcam, UK) at 1/500 or with BCRP mouse monoclonal antibody (BXP-21) (Alexis BioChemical) at 1/500 in 5% Marvel in TBS-T for 1 hour at RT and washed with TBS-T and TBS. After incubation with the secondary antibody Anti Mouse IgG-HRP (Santa Cruz Biotechnology, Santa Cruz, CA) at 1/200 in 5% Marvel in TBS-T for 1 h at RT and further washing with TBS-T and TBS. Blots were visualised by chemiluminescence using Western blotting Luminol

Reagent (Santa Cruz Biotechnology, Santa Cruz, CA). The same procedure was performed with actin and GAPDH antibody (1/120 000) and anti-mouse IgM secondary antibody (1/4000).

2.2.11 Surface activity

Experiments were carried out as described previously (Seelig, Gottschlich et al. 1994). Water used for buffers and solutions was nanopure with a resistivity of 17.5 MΩ/cm. Tris buffer (50 mM, containing 114 mM NaCl) was adjusted with HCl to the desired pH of 7.4. The surface pressure was measured at 23 ± 1°C using a Teflon trough (3-5 mL filling volume, Nima Technology Ltd, Coventry, UK) and a Wilhelmy plate covered by a Plexiglas hood to minimise evaporation and using drug concentrations ranging from 10^{-4} to 10^{-6} M. DMSO, used as a solvent was tested to correct for its own surface activity. The compounds which decreased the surface tension at 100 µM by > 5% were considered as being surface active. The measurements were monitored using a DST9005 tensiometer (Nima Technology Ltd, Coventry, UK). (Results generated with the help of Dr. Tony Gutierrez, Dunstaffnage Marine Laboratory, Oban, UK).

2.2.12 Analysis of the hydrogen bond acceptor patterns

The three-dimensional structures of compounds were modelled with a modified version of Allinger's MM2 force field approach (Burkert and Allinger 1982), using the software Chem*3D* (Cambridge Soft Corporation, Cambridge, MA, USA). The chemical structures were then screened for electron donor groups (*i.e.* O, N, S). The spatial distance between neighbouring atoms carrying the free electron

pair was measured. The hydrogen bond acceptor pattern was determined and quantified as formed either by two electron donor groups separated by a spatial distance of 2.5 ± 0.3 Å, or two electron donor groups separated by 4.6 ± 0.6 Å or three electron donor groups separated by 4.6 ± 0.6 Å, as described by Seelig *et al*. (Seelig 1998). In order to quantify the hydrogen bond acceptor pattern, relative hydrogen bond energy units were assigned: an oxygen-containing electron donor group (denoted **A)** = 1, while a weaker oxygen-free electron donor group such as tertiary amines (denoted **a)** = 0.5 (Seelig 1998).

2.2.13 Determination of LogP, PSA, surface accessible solvent area and the partial atomic charge

The hydrophobicity of the molecules, Log*P,* the polar surface area (PSA) defined by the sum of surfaces of polar atoms (usually oxygens, nitrogens and attached hydrogens), the solvent accessible surface area (SASA) defined by the surface area of a molecule that is accessible to a solvent, the partial charge as determined by the extended Hückel calculation, were also determined using Chem*3D*.

2.2.14 Determination of the electro-potential parameter

The chemical structures of the PBDs were first generated with Chem*3D*, converted as .Mol format files and exported to MarvinSketch / Chemaxon (Budapest, Hungary).

2.2.15 Molecular modelling

2.2.15.1 Preparation of DNA-drug complex for dynamic analysis.

The DNA duplex was generated with MAESTRO/MACROMODEL (version 7.5 Schrödinger 2006) with the sequence TATAGATCTATA and the .dat files were converted into AMBER (version 9). Ligands were initially built and minimized using MACROMODEL and converted into .Mol format files. They were then imported into AMBER. Ligands were prepared for AMBER using ANTECHAMBER program taking a .pdb as an input format and converting it into a .mol2 format applying GASTEIGER charging. Missing parameters for AMBER were applied using PARMCHK routine. AMBER (XLEAP) was used to combine ligands with the DNA. Parameters sets: PARM99.dat and GAFF (General AMBER Force Field) plus the additional parameters were added from the PARMCHK routine. The covalent bound was made manually using the graphic edit routine insuring that an S configuration of C11 was respected. Having made the construct, the topology file and the coordinates were saved for use in the minimization and the dynamics using AMBER. (Results kindly generated by Dr. Colin James, the School of Pharmacy, University of London, London, UK).

2.2.15.2 Energy minimization of the complex using AMBER

The DNA-ligand complex was minimized (energy minimization) to achieve the nearest stable low energy conformations using AMBER. The structures were subjected to 5000 steps over 10 ps. The MM-GBSA (molecular mechanics generalized-Born continuum solvent) or GB/SA approach was used as an implicit

solvent model. A concentration of 0.2 M of mobile counter ions was used. A long range non bonded cut off (100Å) was used

2.2.15.3 Molecular dynamics using AMBER

Similar MM-GBSA, concentration of counter ions and cut off were used with a time frame of 100 ps with 2 femtoseconds time step involving 50 000 steps. All the covalent bonds involving hydrogen were constrained using the SHAKE algorithm (allowing an increase of the dynamics time step). Langevin dynamics was used for temperature scaling.

2.2.15.4 Visualisation

Dynamics trajectory was visualised using VMD software (version 1.8.4) (Humphrey, Dalke et al. 1996) (VMD was developed by the Theoretical and Computational Biophysics Group in the Beckman Institute for Advanced Science and Technology at the University of Illinois at Urbana-Champaign) and using the PyMOL molecular graphics system (version 0.99) (San Carlos, CA Delano Scientific).

2.2.16 *In vivo* anti-tumour activity

Animal experiments were carried out under a project license issued by the UK home office, and UKCCCR guidelines were followed rigorously (1998). HCT 116 cells (10×10^6 cells) were injected subcutaneously into Nu/Nu mice. Treatment started when xenografts reached 50-100 mm^3. SG-2897 was prepared in 1% DMSO /Saline. Animals received SG-2897 intravenously (*i.v.*) at the dose of 300 μg/kg as

single or 120 μg/kg/d day x 5 according to the dose defined for SJG-136 by Alley and colleagues (Alley, Hollingshead et al. 2004). Weights were monitored daily from start of treatment to the end of study. Xenografts were measured 3 times a week. Tumour volumes were calculated from calliper measurements as width^2 x lengh/2. Relative tumour volumes (RTV) were calculated for each tumour dividing the tumour volume at a specific number of days after the start of treatment by the tumour volume at the start of treatment, day 0 multiplied by 100%. Results are means ± SE 5-10 animals. Specific growth delay (SGD) was calculated as follows: $[T_D \text{ (test)} - T_D \text{ (control)}] / T_D \text{ (control)}$ where T_D represents the time in which tumour has doubled or quadrupled. The tumour regression was determined as follows: T/C% = (mean RTV of treated group) / (mean RTV of control group) x 100. According to the National Cancer Institute standards, a T/C $\leq$ 42% is the minimum level for activity (Bissery and Chabot 1991; Plowman J 1997; Johnson, Decker et al. 2001).

3 Chapter 3: P-GP SUBSTRATE SPECIFICITY OF THE PBD DERIVATIVES

3.1 Introduction

Pyrrolo[2,1-*c*][1,4]benzodiazepines (PBDs) interact covalently within the minor groove of the DNA (Gregson, Howard et al. 2001). One of them, SJG-136 has a broad spectrum of cytotoxicity across the NCI60 cell line panel, and is highly potent in a number of xenograft models (Alley, Hollingshead et al. 2004; Pepper, Hambly et al. 2004). However, its cytotoxicity is reduced in cells expressing high levels of the transporter P-glycoprotein (P-gp), both *in vitro* and *in vivo* (Guichard, Macpherson et al. 2005).

P-gp is a member of the phylogenetically highly conserved super-family of ATP-Binding Cassette (ABC) transporter proteins. Increase in the expression of P-gp in tumour cells leads to cellular drug efflux and is a major factor for multidrug resistance (MDR) observed in many cancers. MDR can be intrinsic in some tumours (originating from tissues physiologically expressing high levels of P-gp such as colon, kidney and liver) or acquired after exposure to structurally unrelated anticancer drugs (Fojo, Ueda et al. 1987; Thiebaut, Tsuruo et al. 1987; Ambudkar, Dey et al. 1999; Silverman 1999).

Compounds that interact with the P-gp transporter belong to various therapeutic classes: anticancer drugs, HIV-protein inhibitors, detergents, antibiotics, immunosuppressant, antihypertensive drugs (Ambudkar, Dey et al. 1999). Their chemical structures are diverse. Knowledge of the factors that determine substrate specificity is crucial for the rational design of new drugs. Various attempts have

been made to find a common set of functional features that would predict the interaction of substrates with P-gp (Dellinger, Pressman et al. 1992; Ueda, Okamura et al. 1992; Gottesman and Pastan 1993; Bain and LeBlanc 1996; Schinkel, Wagenaar et al. 1996). However, these features have been validated for families of structurally related compounds and do not necessarily extend to other therapeutic classes (Didziapetris, Japertas et al. 2003). Novel PBD derivatives, PBD-dimers and PBD-monomers have shown significant growth inhibition *in vitro* (Thurston 1993). However, their potential interaction with P-gp is unknown. The influence of P-gp on the cytotoxic effect of PBDs was first assessed by measuring the relative cytotoxicity in different model systems expressing high and low levels of P-gp, in presence or absence of a P-gp blocker, verapamil. To confirm that the reduced uptake is a major factor impacting on the cytotoxic effect, the measure of drug-induced damage indicated by γH2AX foci formation was used as endpoint instead of growth inhibition. Finally, the activity of the transporter against different PBDs was assessed using a more specific study, the Caco-2 transwell assay. Once the differential dependency of PBDs to P-gp was established, the physico-chemical features responsible for the interaction with the transporter were evaluated as a basis for chemical synthesis of new chemical entities.

Inter-individual variations in the ABCB1 coding region have been extensively studied and several single nucleotide polymorphism (SNPs) have been identified: Two synonymous SNPs (C1236T in exon 12 and C3435T in exon 26) and a non-synonymous SNP (G2677T, Ala893Ser) in exon 21 were found to be associated with an altered protein expression as well as an altered function of the transporter which

could lead to redefine the spectrum of molecules recognised by the transporter (Hoffmeyer, Burk et al. 2000; Kim, Leake et al. 2001).

Data presented in this chapter identify key physicochemical properties influencing both the interaction of PBDs with P-gp in a series of novel PBD-dimers and PBD-monomers and, also the differential impact of the single or associated SNPs on the efflux of the PBD derivatives.

3.2 Results

3.2.1 Growth inhibition assay

3.2.1.1 Growth inhibition assay of the PBDS in colon cancer cells lines HCT-15 and HCT 116

The cytotoxic effect (IC_{50}) of the PBDs was determined using 2 colon cancer cell lines. HCT 116 expresses very low levels of P-gp and HCT-15 expresses high levels (Guichard, Macpherson et al. 2005). The PBD-dimers and the PBD-monomers exhibited a broad range of IC_{50} values: from 1.1 nM [SD = ± 0.3 nM] to 310 nM [± 72 nM] for the PBD-monomers and from 0.026 nM [± 0.01 nM] to 85 nM [± 32 nM] for the PBD-dimers (Table 4).

	HCT 116				HCT-15			
	-Ver		+Ver		-Ver		+Ver	
	IC_{50} (nM)	SD	**IC_{50} (nM)**	SD	**IC_{50} (nM)**	SD	**IC_{50} (nM)**	SD
SJG-136	0.72	0.24	0.44	0.24	2.5	0.46	0.59	0.21
DSB-120	42	18	24	11	85	32	20	10
DRG-16	0.044	0.015	0.025	0.012	0.22	0.09	0.038	0.006
ELB-21	0.026	0.01	0.017	0.001	0.19	0.12	0.030	0.024
SG-2796	6.4	0.3	n.d.	n.d.	6.4	1.9	n.d.	n.d.
SG-2797	9.8	2.8	11	4.5	8.6	2.2	7.3	2.5
SG-2781	20	8	n.d.	n.d.	24	12	n.d.	n.d.
SG-2819	13	4	n.d.	n.d.	13	3.3	n.d.	n.d.
SG-2820	26	4.5	24	4.9	30	8.9	16	2.2
SG-2823	10	0.8	9.5	2.7	7.6	1.9	5.8	2.1
SG-2825	120	16	n.d.	n.d.	110	16	n.d.	n.d.
SG-2897	1.1	0.3	n.d.	n.d.	1.5	0.3	n.d.	n.d.
SG-2900	120	27	n.d.	n.d.	96	10	n.d.	n.d.
SG-2901	190	25	176	21	200	29	220	58
SG-2902	65	7.3	n.d.	n.d.	46	3.4	n.d.	n.d.
SJG-244	260	60	280	38	310	72	290	65

Table 4. Sensitivity of HCT 116 and HCT-15 to the PBDs. Values are means ± SD of IC_{50} of n = 3 experiments performed in triplicate.

Since HCT-15 cells express P-glycoprotein while HCT 116 cells do not (Guichard, Macpherson et al. 2005), the ratio between the HCT-15 and HCT 116's IC_{50} was calculated and considered to be a potential indicator of P-gp dependency (Figure 25). A cut off value of 2 for the ratios (ratio between the IC_{50} in HCT-15 cells and the IC_{50} in HCT 116 cells) was considered as being significant based on the impact of the variability between the replicates. All 4 PBD-dimers have a ratio > 2. ELB-21 and DRG-16 showed the highest ratios (7.8 and 5.5, respectively). Conversely, all PBD-monomers show a ratio close to 1 (HCT-15 IC_{50}/HCT 116 IC_{50}) ranging from 0.72 for SG-2823 to 1.4 for SG-2897.

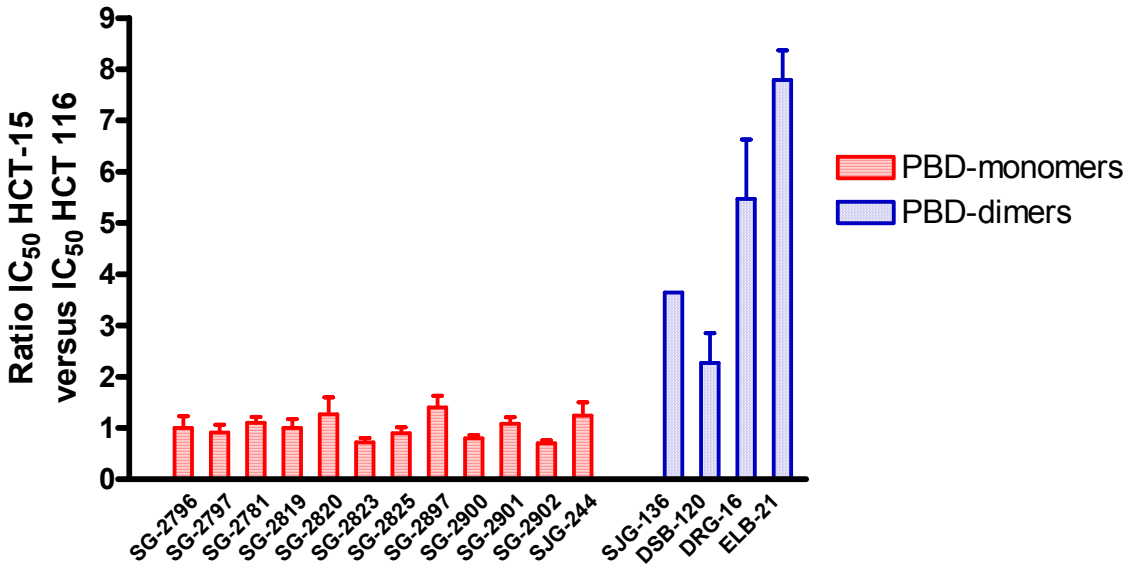

Figure 25. Ratio between HCT-15 and HCT 116's IC_{50}s. Results are means ± SEM of ratios of n = 3 experiments performed in triplicate.

These data suggests that P-gp expression would influence the growth inhibitory effect of PBD-dimers but not the PBD-monomers in colorectal cell lines.

3.2.1.2 Impact of verapamil on the growth inhibition of PBDs against HCT-15 and HCT 116 cells

Verapamil is a P-gp blocker that is used widely to study the impact of P-gp over-expression on drug uptake. In order to confirm, whether or not the compounds showing a high cytotoxic ratio between HCT-15 and HCT 116 cell lines, were influenced by P-gp expression, HCT-15 cells and HCT 116 cells were pre-incubated with verapamil, a P-gp inhibitor and the cytotoxic effect of PBDs was assessed. Cells were pre-incubated with 5 μg/ml of verapamil 1 h prior to the start of the exposure to the compounds. The concentration of verapamil was chosen according to

the recommendations of the Developmental Therapeutics Program of the NCI/NIH and was confirmed as inducing no significant in control cells (data not shown).

The impact of verapamil was evaluated on the cytotoxicity of the PBD-dimer, ELB-21. The IC_{50} following 24h exposure to ELB-21 decreased 4-fold when HCT-15 cells were pre-treated with verapamil (from 0.12 nM for ELB-21 alone to 0.047 nM in the presence of 5 µg/ml verapamil) (Figure 26). There was no significant difference when HCT 116 cells were pre-treated or not with verapamil (16 pM and 15 pM, respectively).

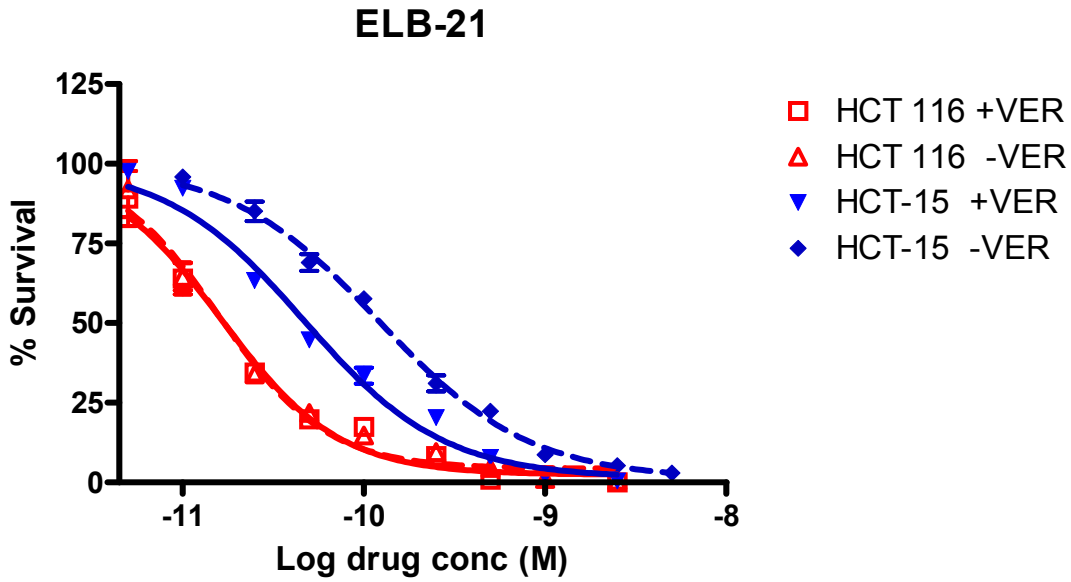

Figure 26. Impact of P-gp inhibition on the cytotoxic effect of ELB-21 in HCT 116 (red) and HCT-15 (blue) cells. Cells were treated with ELB-21 for 24 h with (□, ▼, plain connective lines) or without (Δ, ♦, dashed connective lines) pre-treatment with 5 µg/ml of verapamil. Results are means ± SEM of triplicate.

The impact of verapamil was also evaluated using the PBD-monomer, SJG-244. The IC_{50} following 24h exposure to SJG-244 was similar when HCT-15 cells were in absence or presence of verapamil (410 nM and 390 nM, respectively) (Figure

27). There was also no significant difference when HCT 116 cells were pre-treated or not with verapamil (230 nM and 220 nM, respectively).

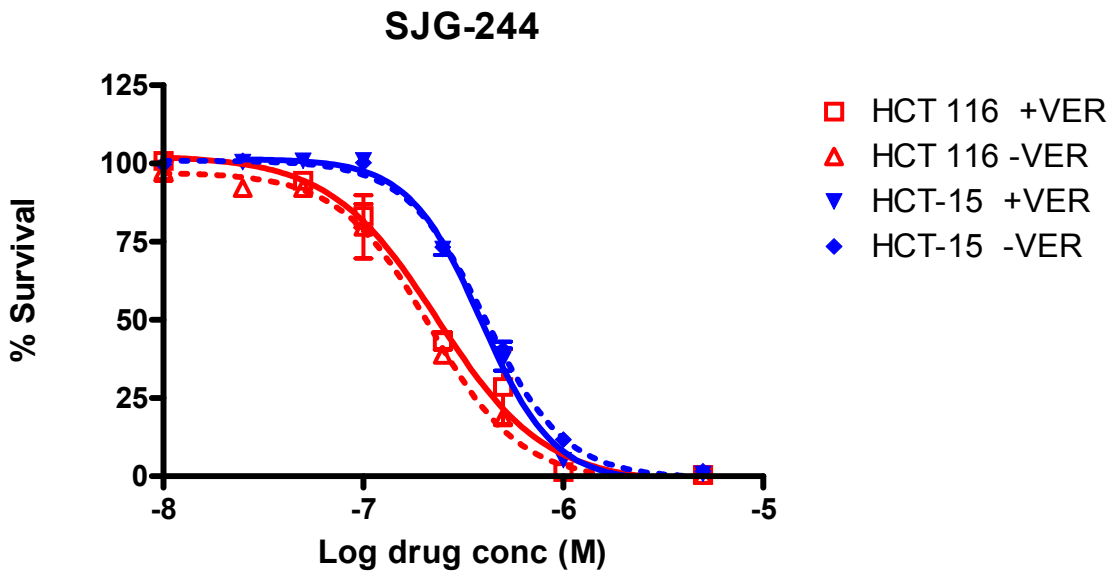

Figure 27. Impact of P-gp inhibition on the cytotoxic effect of SJG-244 in HCT 116 (open symbols) and HCT-15 (closed symbols) cells. Cells were treated with SJG-244 for 24 h with (□, ▼, plain connective lines) or without (Δ, ♦, dashed connective lines) pre-treatment with 5 µg/ml of verapamil. Results are means ± SEM of triplicate.

The impact of verapamil was also evaluated for all the PBD-dimers and 5 PBD-monomers. The pre-incubation of HCT-15 cells (high P-gp) with 5 µg/ml verapamil sensitised the cells to the PBD-dimers: from 0.19 [SD = ± 0.12 nM] to 85 nM [± 32 nM] without verapamil and from 0.030 [± 0.024 nM] to 20 nM [± 10 nM] with verapamil, representing a ~5-fold increase on average (Table 4). In contrast, the pre-treatment of HCT 116 cells (low P-gp) with verapamil had no effect on PBD-dimer growth inhibitory effect: from 0.017 nM [± 0.001 nM] to 24 nM [± 11 nM] and from 0.026 nM [± 0.01 nM] to 42 nM [± 18 nM] with and without verapamil, respectively (Table 4). PBD-monomers had similar cytotoxic effect in the colorectal

cell lines with or without pre-exposure to verapamil: from 7.6 nM [± 1.9 nM] to 310 nM [± 72 nM] without verapamil and, from 5.8 nM [± 2.1 nM] to 290 nM [± 65 nM] with verapamil in HCT-15 cells, thus providing further evidence that the PBD-monomers are not substrates for P-gp.

3.2.1.3 Growth inhibitory effect of the PBDs in ovarian cancer cell lines A2780 and A2780^{AD}

A2780^{AD} cells are derived from the parental A2780 cell line and are resistant to doxorubicin. Several studies have shown that resistance to doxorubicin is mediated by over-expression of P-glycoprotein (Rogan, Hamilton et al. 1984; Guichard, Macpherson et al. 2005).

The cytotoxic effect (IC_{50}) using the A2780 and the A2780^{AD} cells was determined for all PBDs. Overall the PBD-dimers were more potent in A2780 cells than the PBD-monomers: the most active compounds were ELB-21 and DRG-16 with an IC_{50} of 28 pM [± 1 pM] and 34 nM [± 2 pM], respectively in A2780 cells. The least active compounds were SJG-244 and SG-2901 (300 nM [± 9.6 nM] and 230 nM [± 38 nM], respectively) (Table 5).

	A2780		$A2780^{AD}$	
	IC_{50} (nM)	SD	**IC_{50} (nM)**	SD
SJG-136	0.16	0.1	13	8.5
DSB-120	8.2	1.2	420	110
DRG-16	0.034	0.02	1.7	0.6
ELB-21	0.028	0.01	1.6	0.69
SG-2781	12	1.7	10	4
SG-2796	7.1	2.1	8.2	0.1
SG-2797	10	2.9	13	2.9
SG-2819	17	2.3	20	1.2
SG-2820	12	3.3	20	10
SG-2823	5.5	0.4	12	2.1
SG-2825	110	30	130	45
SG-2897	1.2	0.4	4.5	0.9
SG-2900	140	98	110	55
SG-2901	230	38	330	190
SG-2902	60	26	84	15
SJG-244	300	9.6	460	4.1

Table. 5. Growth inhibitory effect of the PBDs in A2780 and $A2780^{AD}$ cells. Results are means ± SD of n = 3 experiments performed in triplicate.

$A2780^{AD}$ cells over-express P-gp in contrast to its parental cell line. Therefore, the differential growth inhibitory effect between the 2 cell lines, as expressed by the ratio of the IC_{50}s, was used to investigate the impact of the transporter.

Overall the PBD-dimers were associated with the highest ratio between the 2 cell lines: A2780 cells were 110-, 71- and 53-fold more sensitive to SJG-136, ELB-21, and DSB-120, respectively, than to the $A2780^{AD}$ cells (Figure 28). DRG-16 has shown the lowest differential of the PBD-dimers, between the 2 cell lines, with a ratio of 50.

The PBD-monomers have shown IC_{50}s ratios between the 2 cell lines ranging from 1.2 (SG-2825) up to 3.8 (SG-2897). The PBD-monomer SG-2897 is the most potent PBD-monomer towards A2780 (IC_{50}= 1.2 nM [± 0.2 nM]). $A2780^{AD}$ cells are derived from the parental A2780 cell line and are resistant to doxorubicin. It is likely other factors than the over-expression of the transporter in $A2780^{AD}$ may explain the cross-resistance to the PBDs such as SG-2897.

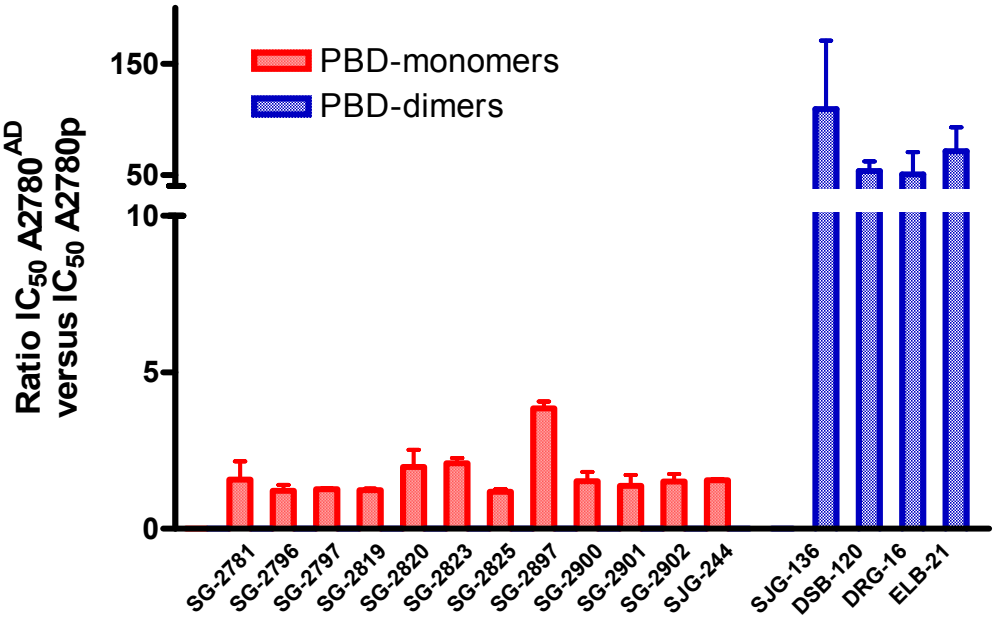

Figure 28. Ratio between the IC_{50} in $A2780^{AD}$ cells and the IC_{50} in A2780 parental cells. Results are means ± SEM of ratios of n = 3 experiments performed in triplicate.

As previously, the specific dependence on the P-gp transporter was assessed by co-incubation with verapamil.

A2780 cells were highly sensitive to ELB-21 (IC_{50} = 36 pM [95% confidence interval = 25 – 52 pM]) after 24 h exposure (Figure 29). The pre-treatment of A2780 cells with verapamil induced no significant variation in growth inhibitory effect

(IC_{50} = 27 pM [22 – 33 pM]). Using the same duration of exposure, ELB-21 induced a much lower cytotoxic effect against $A2780^{AD}$ cells (IC_{50} = 1.1 nM [0.8 – 1.4 nM]), but it was significantly increased by the presence of verapamil (IC_{50} = 0.18 nM [0.15 – 0.21 nM]) representing a ~6-fold increase in activity.

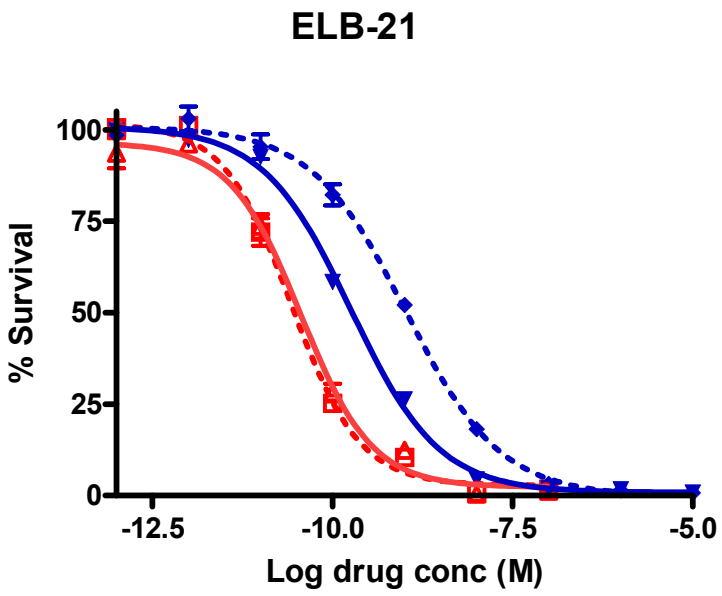

Figure 29. Impact of P-gp inhibition on the cytotoxic effect of ELB-21 in A2780 (open symbols) and $A2780^{AD}$ (closed symbols) cells. Cells were treated with ELB-21 for 24 h with (□, ▼, plain connective lines) or without (Δ, ♦, dashed connective lines) pre-treatment with 5 µg/ml of verapamil. Results are means ± SEM of triplicate.

The incubation of verapamil only partially reversed the resistance of the $A2780^{AD}$ to the PBD-dimers (Figure 30), again suggesting that an alternative resistance mechanism to the PBDs has been induced in the $A2780^{AD}$ cell line.

The IC_{50} in $A2780^{AD}$ was increased by ~5-fold when the cells were pre-incubated with verapamil: from 4.2 fold for SJG-136 up to 6.4 to DRG-16. The pre-

treatment of A2780^{AD} cells with verapamil induced no significant change in cytotoxicity of the PBD-monomers.

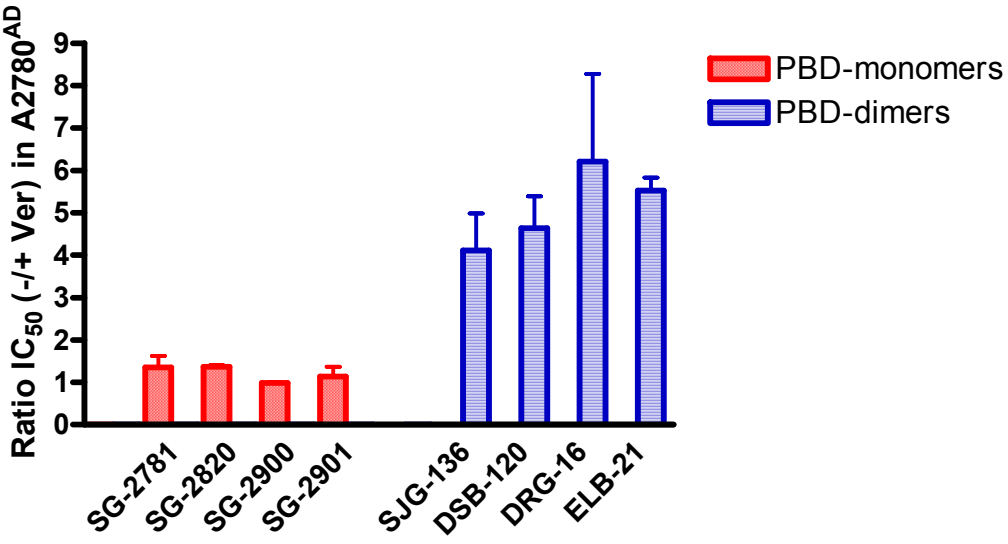

Figure 30. Impact of pre-incubation of verapamil on the growth inhibitory effect of 4 PBD-dimers and 4 PBD-monomers in A2780^{AD} cells. The cells were pre-treated for 24h with verapamil before PBD treatment. Results are means ± SEM of n = 3 experiments performed in triplicate.

3.2.1.4 Growth inhibitory effect of the PBDs in an isogenic 3T3 fibroblast model

To confirm P-gp dependency, 3T3 fibroblasts expressing either an empty vector (3T3 GP + E-86) or wild type mdr-1 (pHamdr-1) were exposed to the PBD-dimer DRG-16 and to the PBD-monomer SG-2797 (Figure 30). DRG-16 induced a greater cytotoxic effect against the 3T3 parental cell line (IC_{50} = 0.57 nM [95% confidence interval = 0.37-0.88 nM]) compared to pHamdr-1 cells (IC_{50} = 32 nM [19-52 nM]) (Figure 31.A.). Conversely, PBD-monomer SG-2797 induced a similar growth inhibition against 3T3 parental cells (IC_{50} = 12 nM [11-13 nM]) and pHamdr-1 (IC_{50} = 15 nM [14-16 nM]) (Figure 31.B).

A

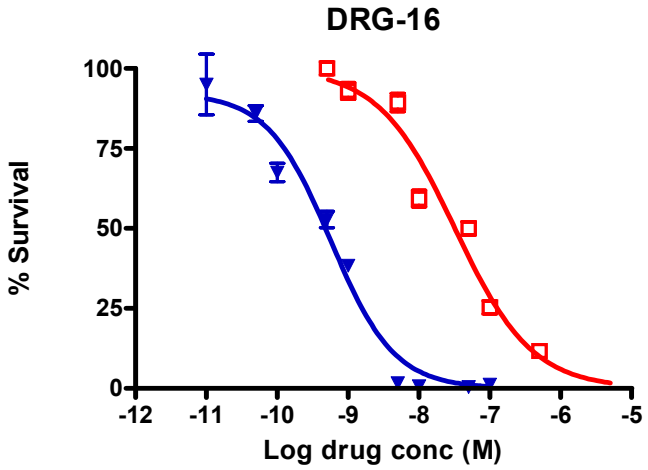

B

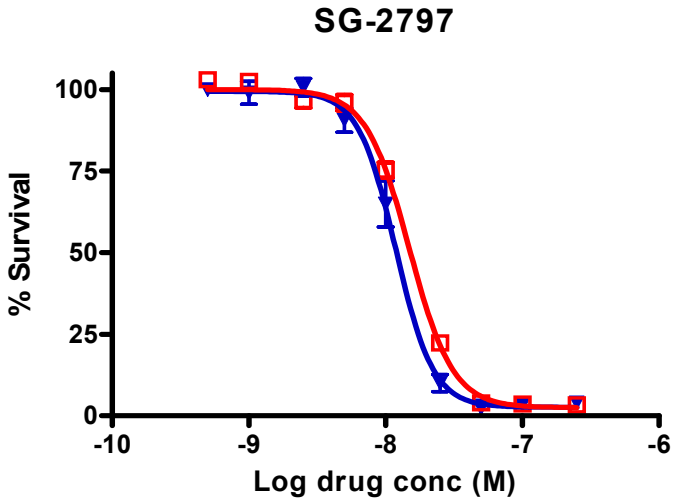

Figure 31. Impact of P-gp on the growth inhibition effet of the PBDs-dimers and the PBD-monomers in 3T3 and pHamdr-1 cells. Growth inhibitory effect observed in 3T3 (▼) and pHamdr-1 (□) cells after 24h exposure to (A) DRG-16 or (B) SG-2797. Results are means ± SEM of triplicate.

The cytototoxic effect (IC_{50}) using the 3T3 and the pHamdr1 cells was determined for all the PBDs. Overall, the PBD-dimers are more potent in the 3T3 cells than the PBD-monomers: the most active compounds were ELB-21 and DRG-

16 with an IC_{50} of 0.34 nM [± 0.26 nM] and 0.54 nM [± 0.32 nM], respectively in 3T3 cells (Table 6). The least active compounds were SJG-244 and SG-2901 (380 nM [± 33 nM] and 230 nM [± 65 nM], respectively).

	3T3		**pHamdr1**	
	IC_{50} (nM)	SD	**IC_{50} (nM)**	SD
SJG-136	1.3	0.3	50	21
DSB-120	54	18	1800	1000
DRG-16	0.54	0.32	20	13
ELB-21	0.34	0.26	14	8.6
SG-2781	13	7.9	19	11
SG-2796	7.4	1.3	8.1	1.5
SG-2797	9	2.5	15	0.9
SG-2819	15	1.6	38	18
SG-2820	21	3.1	34	2.8
SG-2823	8.9	0.9	17	5.2
SG-2825	160	10	190	2.3
SG-2897	2.5	0.29	5.7	0.5
SG-2900	140	16	240	85
SG-2901	230	65	310	50
SG-2902	120	54	150	76
SJG-244	380	33	750	240

Table 6. Growth inhibitory effect of the PBDs in 3T3 and in pHamdr1 cells. Results are means of n = 3 experiments performed in triplicate.

PHamdr1 cells over-express P-gp in contrast to its parental cell line. The differential growth inhibitory effect between the 2 cell lines, as expressed by the ratio of the IC_{50}s, was used to investigate the impact of the transporter. Overall, the PBD-dimers showed the highest ratio between the 2 cell lines: 3T3 cells were 46-, 44- and 40-fold more sensitive to ELB-21, DRG-16 and SJG-136, respectively, than to the pHamdr1 cells. DSB-120 has shown the lowest differential of the PBD-dimers, between the 2 cell lines, with a ratio close to 33 (Figure 32). The PBD-monomers

have demonstrated IC_{50s} ratios between the 2 cell lines ranging from 1.2 (SG-2825 and SG-2796) to 2.4 (SG-2819).

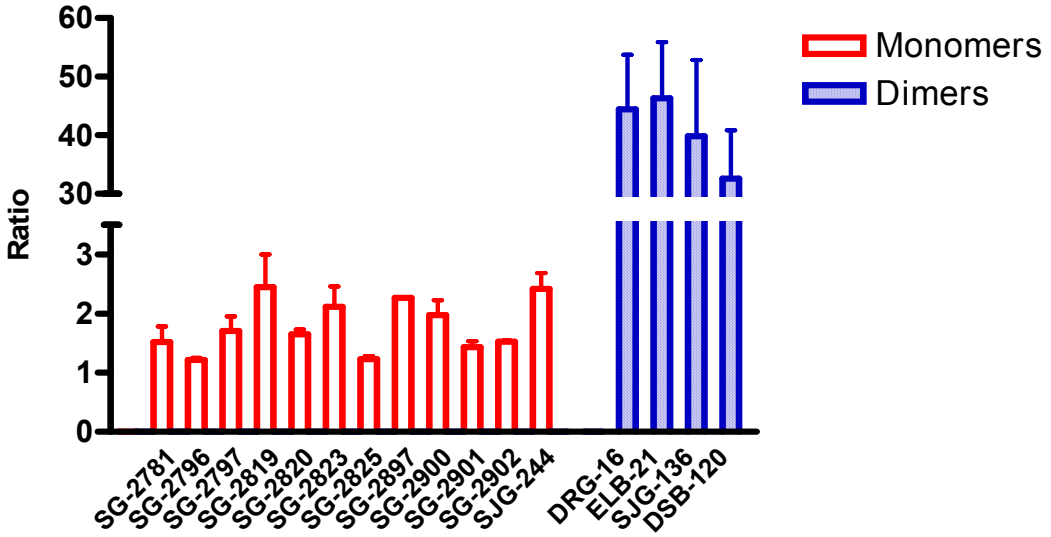

Figure 32. Ratio between the IC_{50} in pHamdr1 cells and the IC_{50} in 3T3 cells. Results are means ± SEM of n = 3 experiments performed in triplicate.

Previously, a cut off value of 2 for the ratios (ratio between the IC_{50} in HCT-15 cells and the IC_{50} in HCT 116 cells) was considered as being significant. The differential growth inhibition towards the 2 cell lines is greater than 2 for some PBD-monomers (SG-2823, SG-2819, SG-2897 and SJG-244). These compounds may be considered as low affinity substrates as opposed to the high affinity substrates, the PBD-dimers, associated with IC_{50} ratios ~33-46 times greater.

Verapamil could be used to confirm P-gp dependency of the PBDs in this isogenic system. However, as pHamdr1 cells over-express the transporter in supra-

physiological conditions, verapamil may not be able to block all the transporters and therefore the impact of the inhibitor may be misleading.

In this study, the ability for verapamil to inhibit the transport of substrates was assessed in pHamdr1 cells using the calcein-am assay. Calcein acetoxymethylester (Calcein-AM), a non-fluorescent dye, substrate of P-gp, is hydrolyzed by intracellular esterases into the fluorescent calcein. The impact of verapamil (at increasing concentrations) was evaluated on the related intracellular concentration of calcein, *i.e.* fluorescence. The minimum fluorescence was observed in pHamdr1 cells without any verapamil (65) (Figure 33). This is due to a maximum P-gp efflux activity of the Calcein-AM out of the cell. Therefore, the latter was not able to be converted into its fluorescent dye. The intracellular concentration of calcein correlated with the concentration of verapamil ($r^2 = 0.99$, $P_{value} < 0.001$) from 190, when the cells were incubated with 1.25 µM of verapamil to 1600 when the cells were incubated with 20 µM of the inhibitor, the maximum concentration used. The intra-cellular concentration of calcein in pHamdr1 cells has not reached the concentration in 3T3 cells (not expressing the transporter) (1800). Previously, an optimal concentration of 10 µM of verapamil was shown not to induce any cytotoxic effect (chapter 3.2.1.2) with suboptimal concentrations (20 µM) associated with a synergestic cytotoxic effect in a long term assay such as the SRB assay. Therefore, these results provide evidence that verapamil was unable to block all the transporters in pHamdr1 cells and can not be used to confirm P-gp substrate specificity of the PBDs in this particular system.

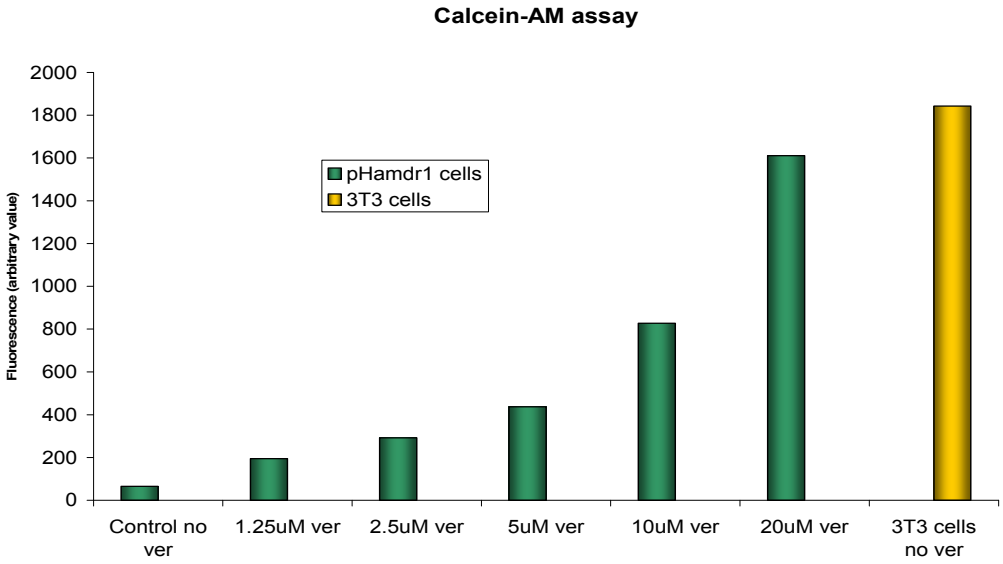

Figure 33. Impact of verapamil on the intra-cellular concentration of calcein in Phamdr1 and 3T3 cells. Replicate results.

In summary, these data confirm that the growth inhibitory effect of the PBD-dimers, in contrast to the PBD-monomers is highly influenced by the expression of P-gp.

3.2.2 H2AX phosphorylation (γH2AX) induced by the PBD-dimer DRG-16 in A2780 and A2780^{AD} cells

PBD-dimers can cross-link the DNA duplex. These cross-links can be detected using the comet assay or alkaline elution (Kohn 1991; Hartley, Spanswick et al. 1999), but more recent studies have identified the formation of γH2AX foci after exposure to the PBD-dimer SJG-136 (Arnould, Spanswick et al. 2006). γH2AX foci form at sites of DNA damage (Rogakou, Boon et al. 1999; Stojic, Mojas et al. 2004); therefore, their detection can be used as a marker of PBD dimer-DNA interaction.

In order to confirm that P-gp dependency, by limiting the uptake of the drugs, is the main factor related to the difference in drug efficacy, γH2AX foci formation was determined in cells with A2780 and A2780^{AD} in presence and absence of verapamil. In A2780 cells, exposure to PBD-dimer DRG-16 induced a ~2.5-fold increase in γH2AX foci (P_{value} <0.0001) (Figure 34).

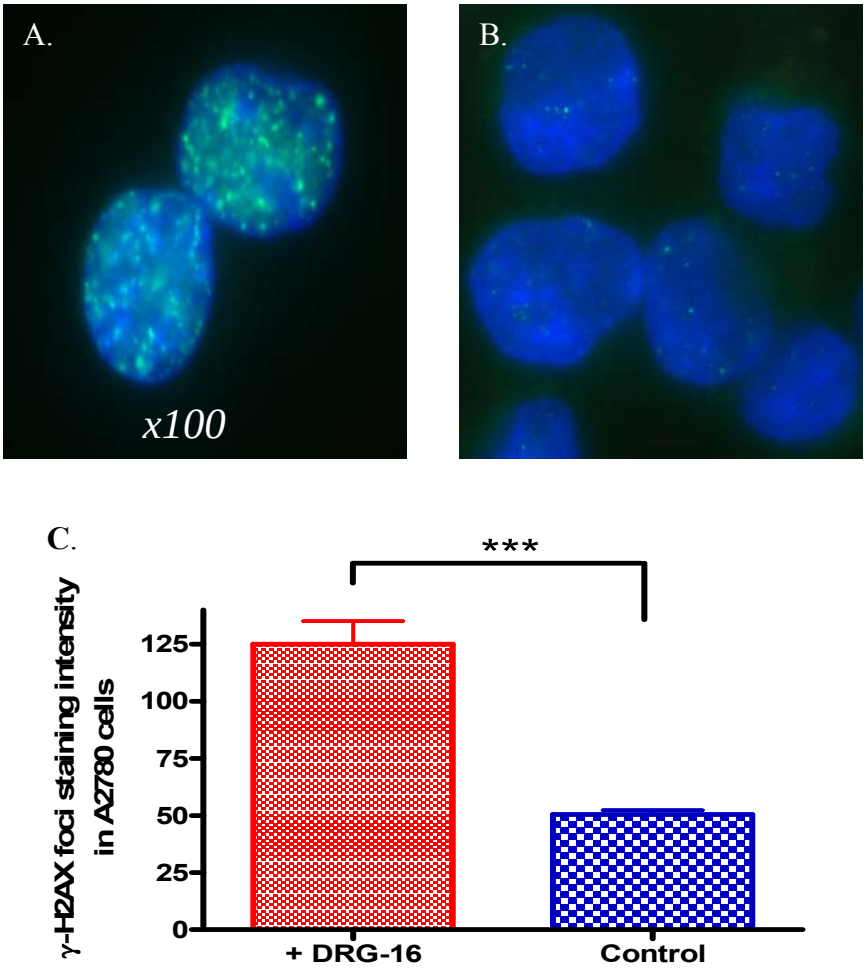

Figure 34. γH2AX foci formation observed in response to DRG-16 (A) compared to the control in A2780 cells (B). Cells were exposed to DRG-16 for 24h at 10 nM. A and B: representative pictures of γH2AX foci (represented in green). Counter-stain with DAPI (blue) confirms the nuclear localisation of γH2AX foci. C: γH2AX foci formation as expressed by staining intensity. Results are means ± SEM of 20 cells.

In A2780^{AD} cells, lower levels of γH2AX foci were observed than in A2780 cells following incubation in equimolar concentration of DRG-16 (data not shown). Following pre-treatment with verapamil a ~2-fold increased γH2AX foci formation was seen (P_{value} = 0.0003) (Figure 35).

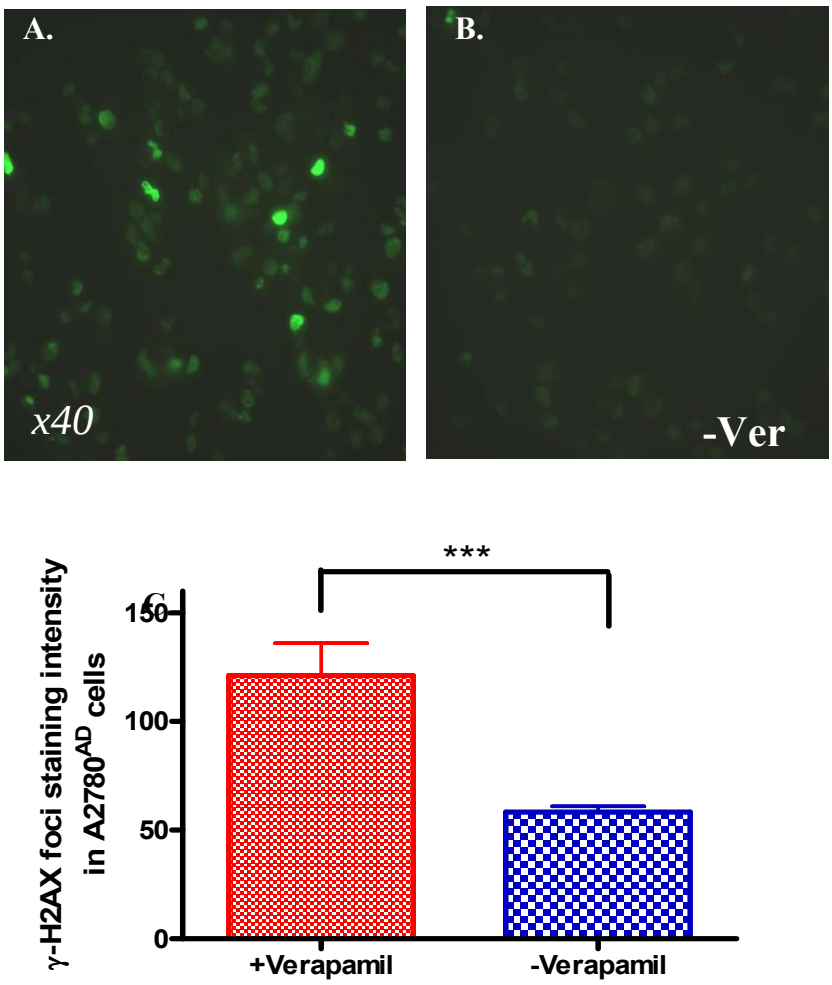

Figure 35. γH2AX foci formation observed in response to DRG-16 without (A) and with (B) pre-treatment with 5μg/ml verapamil. A2780 ^{AD} cells were exposed to DRG-16 for 24h at 10nM in presence or absence of verapamil. A and B: representative pictures of γH2AX foci (represented in green). C: γH2AX foci formation as expressed by staining intensity. Results are means ± SEM of 20 cells.

3.2.3 Permeability studies using the Caco-2 transwell assay

The Caco-2 model of permeability has been widely used to measure the rate of transfer of test compounds. The system has been optimised as described in Materials and Methods (chapter 2). The cells express P-gp at the apical side. It has been stated that if a compound exerts a ratio between the secretion (permeability from the basal to the apical side ($P_{app\ B\rightarrow A}$)) and the absorption (permeability from the apical to the basal side ($P_{app\ A\rightarrow B}$)) > 3, it can be considered as being actively effluxed by P-gp (Szakacs, Paterson et al. 2006).

The permeability of SJG-136 from the apical to the basal which represents absorption ($P_{app\ A\rightarrow B}$) is much lower than secretion (represented by the permeability from the basal to the apical side ($P_{app\ B\rightarrow A}$)): from 9.9 x 10^{-6} cm/sec [SD = ± 2.7 x 10^{-6} cm/sec] for the absorption to 64 x 10^{-6} cm/sec [± 27 x 10^{-6} cm/sec] for the secretion (Figure 36). This represents a ratio between $P_{app\ B\rightarrow A}$ and $P_{app\ A\rightarrow B}$ of ~6.4 suggesting that SJG-136 is actively transported by P-gp from the basal to the apical side. The Mass Balance was also evaluated for SJG-136 ($MB_{A\rightarrow B}$ = 69 ± 1%) suggesting that the compound may have potentially undergone metabolism and/or that it has been attached to plastic surface preventing the full recovery of the compound. However, $MB_{B\rightarrow A}$ = 105 ± 17% suggests a full recovery of SJG-136.

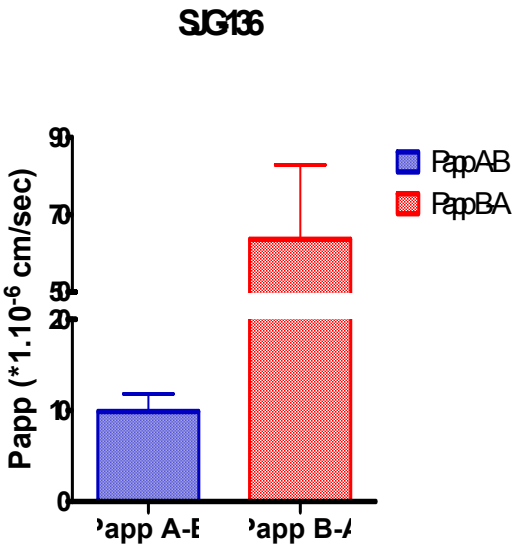

Figure 36. Permeability of the PBD-dimer, SJG-136. The permeability from the apical to the basal side (Papp $_{A\rightarrow B}$) is represented in blue. The permeability from the basal to the apical side (Papp $_{B\rightarrow A}$) is represented in red. Results are expressed as means ± SEM of triplicate.

Similarly, the PBD-dimer DRG-16 showed a differential permeability between the secretion (P*app* $_{A\rightarrow B}$) and the absorption (P*app* $_{B\rightarrow A}$) with permeability values of 9.8 x 10^{-6} cm/sec [± 4.7 x 10^{-6} cm/sec] and 2.8 x 10^{-6} cm/sec [± 0.7 x 10^{-6} cm/sec], respectively (Figure 37.A). This represents a ratio between P*app* $_{B\rightarrow A}$ and P*app* $_{A\rightarrow B}$ of ~3.5 suggesting that DRG-16 is also actively transported by P-gp from the basal to the apical side. Mass balance of DRG-16 was evaluated and was associated with a minimal drug metabolism/adherence to the system (MB $_{A\rightarrow B}$ = 85 ± 2.3%] and MB $_{B\rightarrow A}$ = 118 ± 16%).

Conversely, the PBD-monomer SG-2897 showed no difference between absorption (P*app* $_{A\rightarrow B}$ = 6.9 x 10^{-6} cm / sec) and secretion (P*app* $_{B\rightarrow A}$ = 6.9 x 10^{-6} cm / sec), suggesting that this particular compound is not actively transported from the basal to the apical side (Figure 37.B). Mass balance of SG-2897 was evaluated and

was also associated with minimal drug metabolism/adherence to the system (MB $_{A\rightarrow B}$ = 90 ± 10% and MB $_{B\rightarrow A}$ = 119 ± 18%)

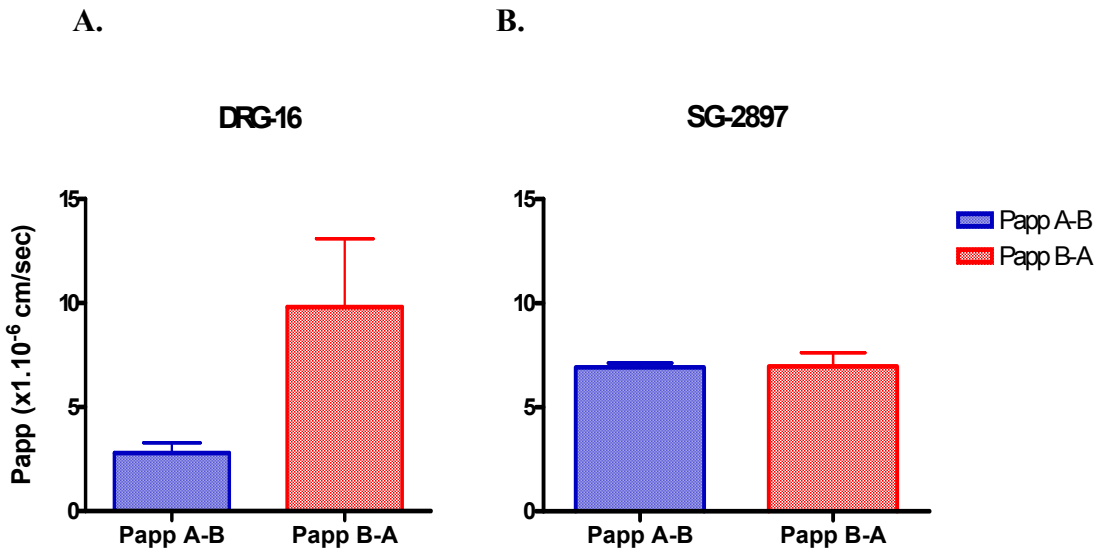

Figure 37. Permeability of the PBD-dimer, DRG-16 (A) and the PBD-monomer, SG-2897 (B). The permeability from the apical to the basal side (Papp $_{A\rightarrow B}$) is represented in blue. The permeability from the basal to the apical side (Papp $_{B\rightarrow A}$) is represented in red. Results are expressed as means ± SEM of triplicate.

Overall, the transwell assay has allowed us to confirm the active transport of the PBD-dimers, SJG-136 and DRG-16 from the basal to the apical side in contrast to the PBD-monomer, SG-2897.

3.2.4 Chemical structure analysis

3.2.4.1 General features involved in P-gp substrate specificity

From the literature, it is evident that P-gp substrates share a common set of physico-chemical properties. It has been stated that a compound, in order to be recognised by the transporter has to have some general parameters such as at least

one basic nitrogen, a molecular weight > 400, a number of (oxygen + nitrogen) atoms > 8 (with (N+O) < 4, predicting P-gp non substrates), a log*P* > -1, at least 2 aromatic rings and some more specific features (pharmacophores) such as, at least one hydrogen bond acceptor pattern. In addition, it has been suggested that P-gp substrates are surface active compounds.

There is a noticeable heterogeneity of the structures among the PBD derivatives. Some of them correspond to the features of being P-gp substrate as reported previously. Their chemical features are listed in Table 7.

Five of the 16 compounds have their molecular weight greater than 400 including 1 PBD-monomer (SG-2797, 402.4); 4 include ≥ 8 (N+O) atoms; 12 contain 2 aromatic rings including 8 PBD-monomers. All the compounds have a Log*P* ≥ -1 and contain basic nitrogen. However, all of them have a number of (N+O) > 4. This feature can therefore not be used to discriminate the compounds between substrates and non-substrates. All the compounds carry a hydrogen bond acceptor pattern and this feature can not be used either to discriminate them. The PBD-dimers differ from the PBD-monomers by a molecular weight greater than 400, a greater number of (N+O) and a greater polar surface area.

All compounds included in these studies contained at least one basic nitrogen. 12/16 compounds had more than 2 aromatic rings. Finally, all the PBD-dimers had a number of nitrogen and oxygen atoms (N+O) greater than 8, compared to the PBD-monomers.

	Molecular weight	Log*P*	Basic Nitrogen	(N+O)	PSA	2 Aromatic Rings
SJG-136	**556.608**	**1.383**	+	**10**	**102.2**	+
DRG-16	**584.662**	**2.254**	+	**10**	**102.2**	+
DSB-120	**532.587**	**1.295**	+	**10**	**102.2**	+
ELB-21	**612.715**	**2.989**	+	**10**	**102.2**	+
SJG-244	**348.395**	**2.493**	+	**5**	**51.1**	+
SG-2781	**377.436**	**2.494**	+	**6**	**54.4**	+
SG-2796	**360.405**	**2.844**	+	**5**	**51.1**	+
SG-2797	**402.366**	**3.13**	+	**5**	**51.1**	+
SG-2819	**376.448**	**3.443**	+	**5**	**51.1**	+
SG-2820	**359.377**	**2.242**	+	**6**	**74.9**	+
SG-2823	**362.378**	**1.956**	+	**6**	**68.2**	+
SG-2825	**340.416**	**2.788**	+	**5**	**51.1**	-
SG-2897	**385.415**	**2.292**	+	**6**	**64**	+
SG-2900	**354.442**	**3.205**	+	**5**	**51.1**	-
SG-2901	**368.469**	**3.622**	+	**5**	**51.1**	-
SG-2902	**340.416**	**2.753**	+	**5**	**51.1**	-

Table 7. Chemical features of the PBDs involved in P-gp substrate specificity. Previously suggested determinants for being substrates of P-gp are represented in green.

3.2.4.2 Hydrogen bond acceptor pattern

The chemical structures were screened for electron donor groups as described in Materials and Methods (Section 2.2.11).

Among the PBD-dimers, SJG-136 and DSB-120 were associated with the highest number of units of hydrogen bonding energy (17), followed by ELB-21 and DRG-16 with 15 units. All the PBD-monomers were assigned the same amount of hydrogen bonding energy units (7.5) (Table 8).

	Electron donor pattern (hydrogen bond acceptor pattern)			Units of H bonding energy (HBE)
SJG-136	Aaa(1,3,6) 4.186Å AA(1,6) 5.142 Å AA(1,4) 2.634 Å	Aa (1,5) 4.835 Å AA (1,4) 2.702 Å AA (1,6) 5.241Å	Aaa(1,3,6) 4.137Å Aa (1,5) 4.894Å AA (1,5) 4.818Å	17
DRG-16	Aaa(1,3,6) 4.129Å AA(1,6) 5.094 Å AA(1,4) 2.945 Å	Aa (1,5) 4.835Å AA (1,4) 2.920Å AA (1,6) 5.019Å	Aaa(1,3,6) 4.161 Å Aa (1,5) 4.841Å	15
DSB-120	Aaa(1,3,6) 4.129 Å AA(1,6) 5.154 Å AA(1,4) 2.770 Å	Aa (1,5) 4.835 Å AA (1,4) 2.940 Å AA (1,6) 5.051 Å	Aaa(1,3,6) 4.161 Å Aa (1,5) 4.841 Å AA (1,5) 4.807 Å	17
ELB-21	Aaa(1,3,6) 4.170 Å AA(1,6) 5.162 Å AA(1,4) 2.699 Å	Aa (1,5) 4.835 Å AA (1,4) 2.920 Å AA (1,6) 5.019 Å	Aaa(1,3,6) 4.161 Å Aa (1,5) 4.841 Å	15
SJG-244	Aaa (1,3,6) 4.137 Å AA (1,6) 5.193 Å	Aa (1,5) 4.866 Å AA (1,4) 2.690 Å		7.5
SG-2781 SG-2796 SG-2797 SG-2825 SG-2897 SG-2819 SG-2820 SG-2823 SG-2900 SG-2901 SG-2902	AA (1,4) 2.697 Å Aa (1,5) 4.927 Å Aaa(1,3,6) 4.035 Å AA (1,6) 5.256 Å			7.5

Table 8. Hydrogen bond acceptors patterns and units of hydrogen bonding energy of the PBDs. **A** denotes a hydrogen bonding acceptor group (electron donor group) containing oxygen and, **a** denotes a hydrogen bonding acceptor group containing no oxygen. The numbers in brackets indicate the first and the n^{th} atom with a free electron pair. The spatial distance between neighbouring atoms carrying the free electron pair was measured using the software Chem*3D*.

Since all the PBD-monomers follow the same pattern, no correlation could be established with the ratio. The PBD-dimers differ by two units of hydrogen bonding energy and the restricted number of compounds did not allow us to make any correlation either with the ratio. These results are consistent with previous reports suggesting that molecules with high HBE have increased likelihood of interacting with P-gp (Seelig 1998).

3.2.4.3 Polar surface area

The polar surface area (PSA) is defined as the sum of surfaces of polar atoms (usually oxygens, nitrogens and attached hydrogens). A cut-off of 75Å^2 has been suggested as a discriminator of P-gp substrates from non substrates (Varma, Sateesh et al. 2005). Our study showed that PBD- dimers have a PSA > 75 Å^2 while all the PBD-monomers have a PSA below the threshold, confirming the potential relevance of this parameter (Table 7).

3.2.4.4 Surface activity parameter

It has also been suggested that surface active properties, which allow the compounds to partition into the membrane and decrease the surface tension, influence P-gp dependency (Seelig 1998). Indeed, the amphiphilicity of a compound as reflected in its air-water partition coefficient, Kaw, has been shown to be correlated with the inverse of Michaelis-Menten constant, Km of the P-gp ATPase activation (Seelig and Landwojtowicz 2000).

The adsorption of an amphiphile at the air-water interface lowers the surface tension of the buffer, $\gamma_{0,}$ to a new value, γ. The difference, γ_0- γ is so called surface pressure or surface activity.

Among the PBD derivatives, some compounds were surface active and decreased the surface tension of TRIS such as SG-2825 (Figure 38). Others were not surface active and did not decrease the surface tension, such as SG-2781.

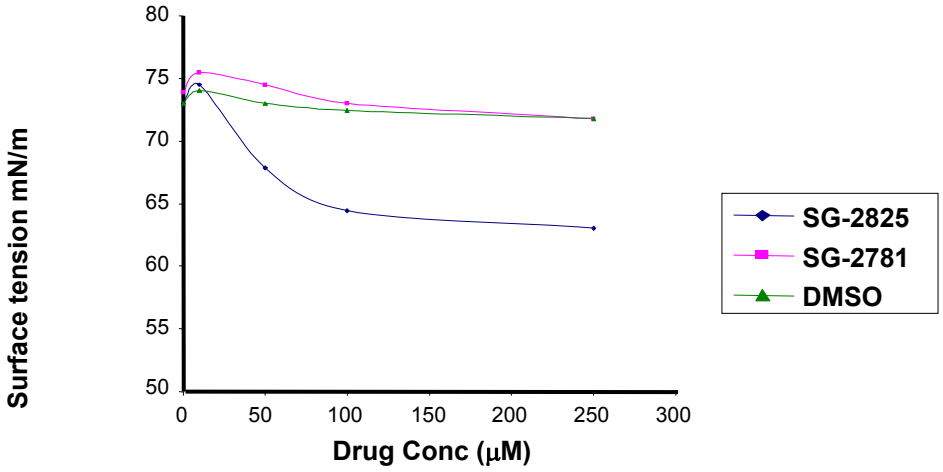

Figure 38. Surface activity of 2 PBD-monomers, SG-2825 and SG-2781 as determined by the wilhelmy plate method. Since all the PBDs are diluted in DMSO; its surface tension has been reported (green). SG-2825 does not decrease the surface tension and it is considered as being not surface active (blue). SG-2781 decreases the surface tension and is considered as being surface active (purple).

The surface activity was determined for all PBDs. As a result, all the PBD-dimers were non-surface active in the range of concentrations tested (10^{-9}-10^{-4} M). 7/12 PBD-monomers (SG-2797, SG-2819, SG-2825, SG-2900, SG-2901, SG-2902 and SJG-244) were surface active (Table 9), while their growth inhibitory effect was not influenced by P-gp. Therefore, the surface activity does not predict P-gp interaction for this class of compounds.

Surface active PBDs	Non surface active PBDs
SG-2797	SJG-136
SG-2819	DSB-120
SG-2825	DRG-16
SG-2900	ELB-21
SG-2901	SG-2781
SG-2902	SG-2796
SJG-244	SG-2820
	SG-2823
	SG-2897

Table 9. Surface activity of the PBDs. The PBD-monomers are represented in red and the PBD-dimers in blue.

3.2.4.5 Lipophilicity

The lipophilicity or Log*P* was greater than -1 for all the compounds. However, when the PBD-dimers were considered separately, the Log*P* correlated with the IC_{50} ratio between HCT-15 and HCT 116 (r^2 = 0.96, P value < 0.05), indicative of P-gp dependency (Figure 39).

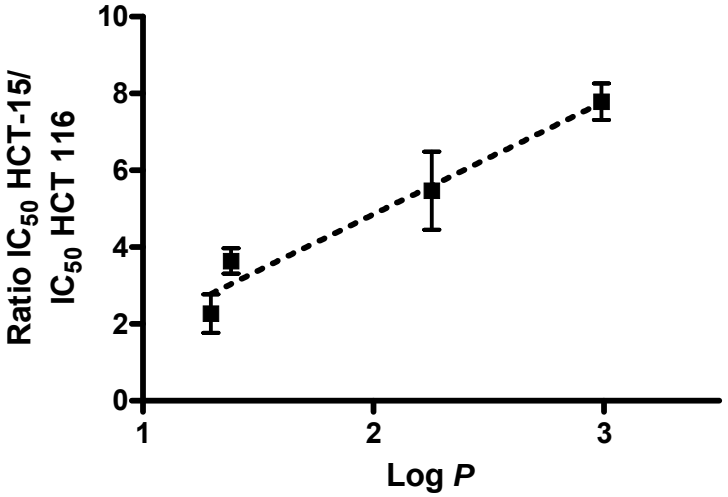

Figure 39. Relationship between (IC_{50} in HCT-15 versus IC_{50} in HCT 116) and Log*P*. Since the activity of the PBD-monomers has been shown to be not affected by the expression of P-gp, only the ratio for the PBD-dimers is represented. Results are means ± SEM of n = 5 experiments performed in triplicate.

3.2.4.6 Molecular weight

Molecular weight (MW) is a major factor related to P-gp interaction. In our series, all the PBD-dimers had a MW greater than the proposed threshold of 400, from 532.58 (SG-2018) to 612.71 (ELB-21), in addition to the PBD-monomer (SG-2797) (but only just > 400).

There was a highly significant correlation between molecular weight and the HCT- 15/HCT 116 IC_{50} ratio (r^2 = 0.99, P value < 0.001) when the dimers were evaluated in isolation, suggesting an impact on P-gp dependency (Figure 40).

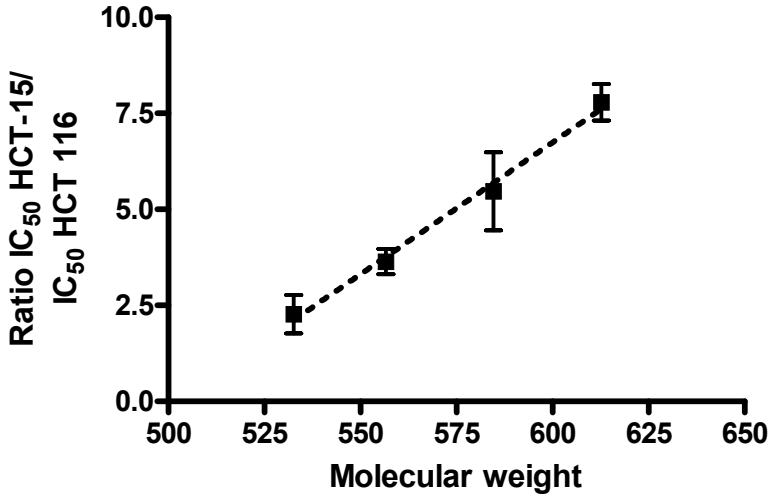

Figure 40. Relationship between (IC_{50} in HCT-15 versus IC_{50} in HCT 116) and the molecular weight. Since the activity of the PBD-monomers was shown not to be affected by the expression of P-gp, only the ratio for the PBD-dimers is represented. Results are means ± SEM of n = 5 experiments performed in triplicate.

3.2.5 Impact of ABCB1 polymorphism on P-gp substrate specificity of the PBD derivatives

ABCB1 genetic polymorphisms have been shown to modify both P-gp expression and also function though an effect on P-gp substrate specificity (Hoffmeyer, Burk et al. 2000; Aird, Thomson et al. 2007; Kimchi-Sarfaty, Oh et al. 2007). To evaluate the effect of different polymorphisms on the growth inhibitory effect of PBD derivatives, a series of isogenic fibroblast cell lines with mutations in positions 1236, 2677 and 3435 were used.

3.2.5.1 Determination of the level of P-gp mRNA

The level of mRNA was evaluated for all the 3T3 cell lines expressing the different genotypes of P-gp by quantitative RT-PCR.

The level of mRNA of P-gp is maximal in the 3T3 fibroblasts expressing the wild type form, (*pHamdr1*) (Figure 41). The presence of a G/T (*893*) or G/A (*2677*) mutation in position 2677 was associated with a decreased gene expression of ~1.5 and ~32-fold, respectively. The level of mRNA of P-gp was also reduced in cell lines expressing the combined mutations in positions 2677 (G/T) and 3435 (*893/3435*) (~2.8-fold). Combined mutations in position 1236 and 2677 (G/T) (*893/1236*) was associated with a decreased gene expression (~21.5-fold). Finally, the P-gp mRNA level was reduced in cell lines expressing the triple mutations in position 2677 (G/T), in position 1236 and in position 3435 (*893/1236/3435*) (~18-fold).

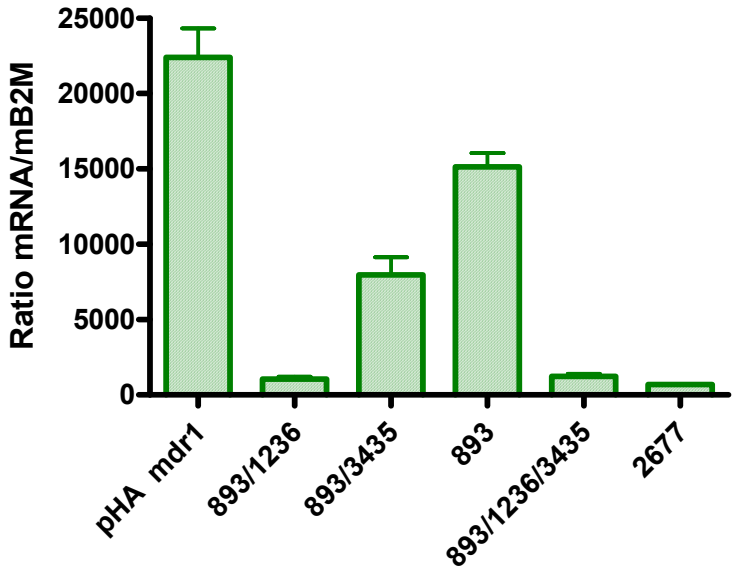

Figure 41. Level of mRNA of P-gp, in the 3T3 fibroblasts expressing different genotypes of the transporter. The levels of P-gp mRNA were corrected with the levels of mouse β-2-microglobulin (mB2M). The values are means ± SD of triplicate.

3.2.5.2 Determination of the level of P-gp protein expression

P-gp protein expression was measured by flow cytometry using a specific antibody (4E3 Ab) targeting the extracellular portion of the transporter. P-gp protein expression was maximal in pHamdr1 cells (Figure 42). The presence of a G/T (*893*) or G/A (*2677*) mutation in position 2677 was associated with a decreased protein expression of ~1.5- and ~4-fold, respectively. Combined mutations in positions 2677 (G/T) and 3435 (*893/3435*) also reduced P-gp expression (~2-fold). The level of protein expression was reduced in cell line expressing the mutations in position 1236 (~4-fold).

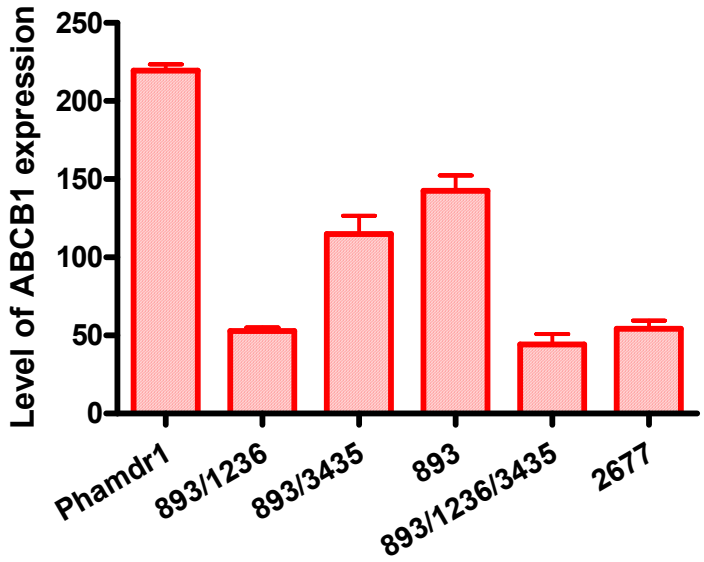

Figure 42. ABCB1 protein expression in cells lines transfected with wild type ABCB1 (pHamdr-1) and with mutations in positions 1236, 2677 and 3435 of the mdr-1 gene. Results are means ± SD of triplicate.

3.2.5.3 Relationship between the level of mRNA and protein expression of P-gp

The relationship between the level of protein expression and the level of mRNA has been evaluated and demonstrated significant correlation between gene and protein expression ($r^2 = 0.98$, $P_{value} = 0.0001$) (Figure 43).

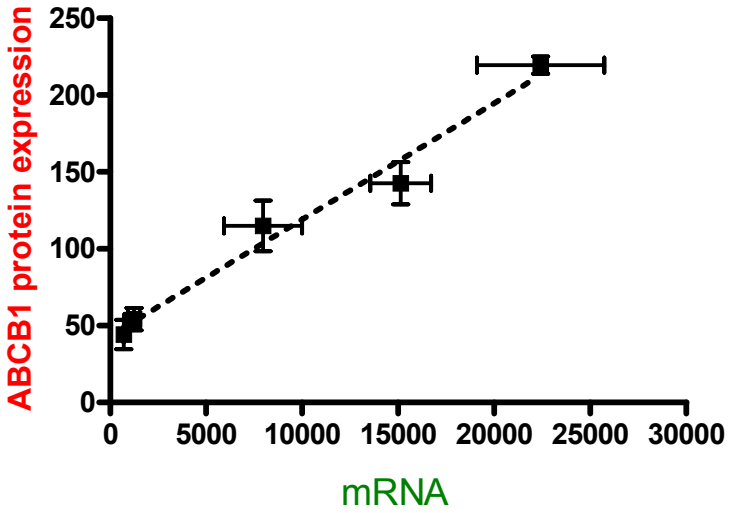

Figure 43. Relationship between the level of P-gp protein expression and the level of mRNA in the 3T3 fibroblasts expressing different mutations of ABCB1. Results are means ± SD of triplicate.

3.2.5.4 Growth inhibition studies using isogenic 3T3 cells expressing different genotypes of ABCB1

In order to evaluate the impact of ABCB1 polymorphism on P-gp substrate specificity of the PBDs, their growth inhibitory effect was evaluated against the 3T3 expressing mdr-1 cDNA with different mutations. The growth inhibitory effect of a PBD-dimer, SJG-136 was first evaluated. In the most resistant cell line, the 3T3 fibroblasts expressing ABCB1 with a mutation in position 2677 (G/T) (893 cells),

the IC_{50} = 79 nM [95% CI = 18 - 154 nM] (Figure 44). In contrast, the cell line expressing the wild type ABCB1 (pHamdr1) was more sensitive to SJG-136, than the 893 cells with an IC_{50} of 46 nM [28 - 75 nM]. Sensitivity to SJG-136 was enhanced further with combined mutations, with IC_{50} values of 37 nM [CI = 4 - 91 nM] and 9 nM [CI = 6.4 -13 nM], for 893-3435 and 893/1236 cell lines, respectively. Finally, the 3T3 fibroblasts transfected with cDNA containing the empty vector were the most sensitive cell line to SJG-136 with an IC_{50} = 4.8 nM [CI = 3.5 - 12 nM].

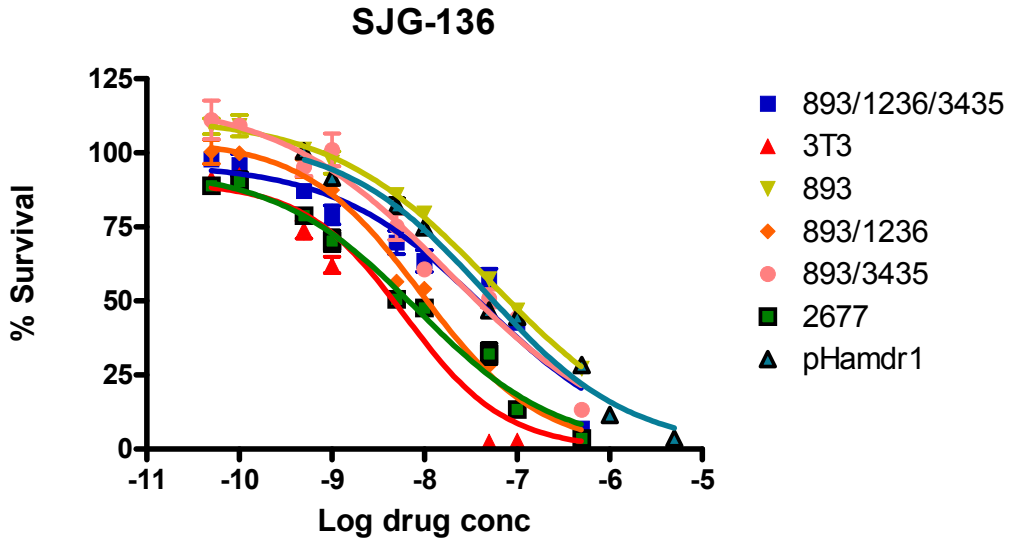

Figure 44. Growth inhibition curves of the PBD-dimer SJG-136 towards isogenic fibroblast cell lines expressing ABCB1 cDNA with different mutations in positions 1236, 2677 and 3435. Results are means ± SEM of triplicate.

The relationship between the protein expression of ABCB1 and the growth inhibitory effect of SJG-136 demonstrated a correlation (r^2 = 0.64 and P_{value} = 0.03) as described previously by Aird and colleagues (Aird, Thomson et al. 2008) (Figure 45). However, the growth inhibitory effect of SJG-136 associated with the mutation in position 893 (2677 (G/T)) is outside the 95% confidence interval and may be

considered as an outlier suggesting that the level of ABCB1 protein expression may not be the only factor modulating the anti-tumour activity of the PBD-dimer, SJG-136 (Figure 45).

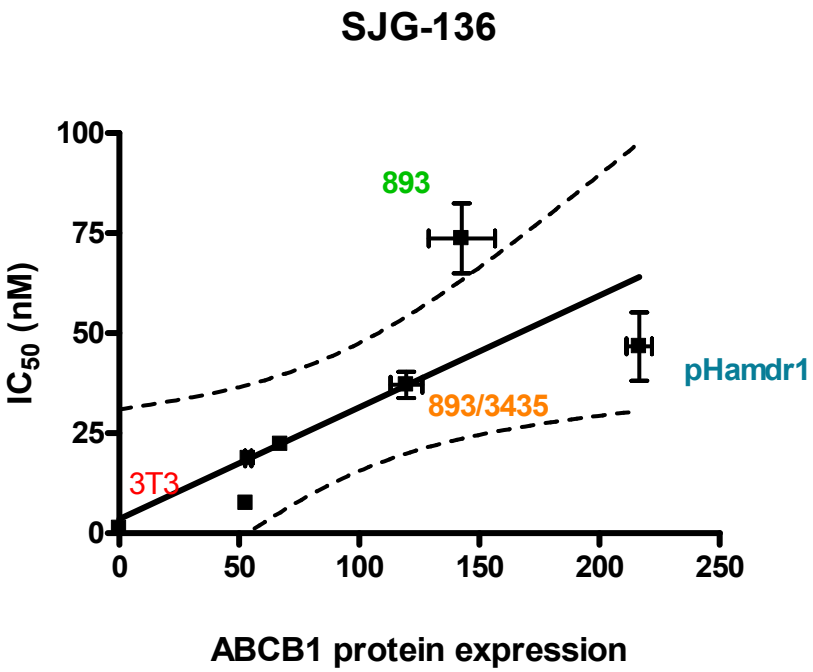

Figure 45. Relationship between ABCB1 protein expression and the growth inhibitory effect of the PBD-dimer, SJG-136. The IC_{50} values are means ± SD of n = 4 experiments performed in triplicate. The 95% Confidence interval is represented in dashed lines.

In order to investigate the specific impact of the different mutations on the function of the transporter, the IC_{50} values were "corrected" using the level of ABCB1 protein expression.

The ratio between the IC_{50} and the protein expression is the highest in cells expressing ABCB1 with a mutation in position 2677 (G/T) (893 cells): the cells expressing the mutated form were ~2.3-fold more resistant to SJG-136 than pHamdr1 while considering a similar level of protein expression of the transporter (Figure 46) ($P_{value} = 0.0077$). In other words, 893 cells were associated with a ~2.3-fold "gain of function".

With combined mutations in position 2677 (G/T) and 3435, this effect appears to be abrogated. When corrected for the level of protein expression, SJG-136 is ~1.8-fold more cytototoxic towards cell lines expressing the mutated form (893/3435) of the transporter than the cell line expressing only the mutated form in position 2677 (G/T) ($P_{value} = 0.048$).

The combination of the mutation in position 2677 (G/T) and the mutation in position 1236 (893/1236 cells) has abrogated the "gain of function" associated with the single mutation in position 2677 (G/T) further. Indeed, the corrected growth inhibitory effect of SJG-136 is similar in cell lines expressing the wild type form of the transporter and in cell lines expressing the combined mutations (893/1236).

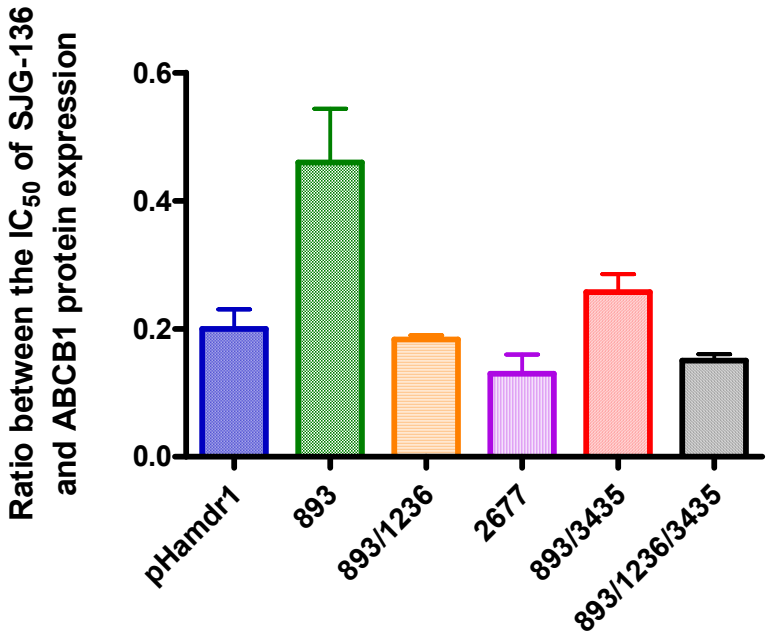

Figure 46. Impact of ABCB1 polymorphism on the growth inhibitory effect of SJG-136. The growth inhibition (IC_{50}) has been corrected with the level of ABCB1 protein expression. The IC_{50} values are means ± SEM of n = 4 experiments performed in triplicate.

These results provide evidence that ABCB1, incorporating specific mutations, induces a "gain of function". Previously, the PBD-monomers were

shown to be non substrates of the transporter. The following study evaluates whether the growth inhibitory effect of the PBD-monomers may be affected by some genetic polymorphisms of the transporter.

The growth inhibitory effect of PBD-monomer, SG-2897 was evaluated in the 3T3 cell lines expressing different genotypes of ABCB1. 893 cell line, expressing the mutated form of ABCB1 (2677 (G/T)) was the least sensitive to the PBD-monomer, SG-2897, with an IC_{50} = 9.6 nM [8.6 -10.5 nM] compared to the cell line expressing the wild type ABCB1 (pHamdr1), with an IC_{50} of 6.3 nM [5.6 – 6.9 nM] representing a ~1.5-fold increase in sensitivity (Figure 47). The cell line expressing ABCB1 with a combined mutation in position 2677(G/T) and 3435 (893/3435 cell line) was also more resistant to SG-2897 (with an IC_{50} = 7.8 nM [7.2 -8.3 nM]) than the pHamdr1 cell line.

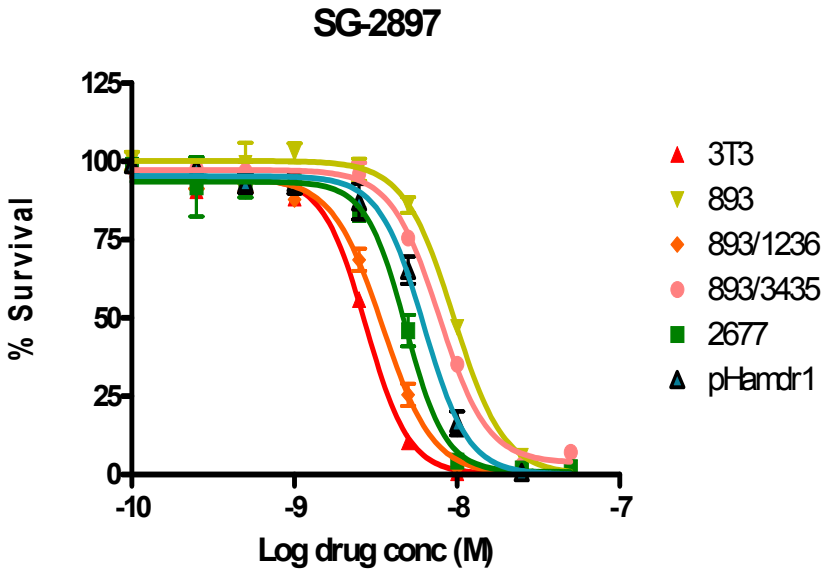

Figure 47. Cytotoxicity curves of a PBD-monomer SG-2897 towards isogenic fibroblast cell lines expressing ABCB1 cDNA with different mutations in positions 1236, 2677 and 3435. Results are means ± SEM of triplicate.

In contrast to the results with SJG-136, the relationship between the growth inhibitory effect of SG-2897 and the level of ABCB1 expression was not significant ($r^2 = 0.27$ and $P_{value} = 0.28$) (Figure 48).

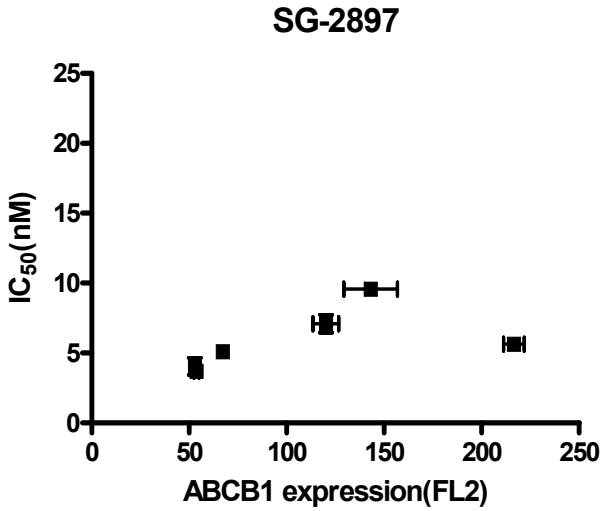

Figure 48. Relationship between ABCB1 protein expression and the growth inhibitory effect of the PBD-monomer, SG-2897. The IC_{50} values are means ± SEM of n = 3 experiments performed in triplicate.

The cell lines expressing the transporter with a mutation in position 2677 (G/T) and the transporter with a mutation associated in position 3435 were significantly more resistant to SG-2897 than the parental cell lines (3T3) ($P_{value} = 0.005$ and $P_{value} = 0.05$, respectively). The growth inhibition of SG-2897 was not affected by any other mutated form of the transporter (893/1236; 2677 and 893/1236/3435 cell lines) nor the wild type (pHamdr1) transporter.

In order to investigate whether these 2 particular forms of ABCB1 have had an impact on the function of the transporter, the IC_{50} values were corrected with the level of ABCB1 protein expression. When considering the corrected IC_{50} (corrected with the level of ABCB1 protein expression), the cell line expressing the mutated

form in positions 2677 (G/T) is on average ~2.5-fold more resistant to SG-2897 than the cell line expressing the wild type transporter (pHamdr1 cells) (P_{value} = 0.0002) (Figure 49). This "gain of function" has not significantly been abrogated by the presence of the associated mutation in position 3435 as the ratio between the corrected IC_{50} in the double mutant cell line and the corrected IC_{50} in the phamdr1 cells is ~2.4 (P_{value} = 0.006).

For the PBD-monomer, SG-2897, 3T3 cells expressing the mutated form of P-gp in position 2677 (G/T) were more resistant than the cells transfected with wild type P-gp, despite reduced expression. This suggests that the mutation has altered the substrate specificity of the compound. This is in contrast to the impact of the combined mutation in position 3435. The latter only abrogates the "gain of function" in the case of the PBD-dimer, SJG-136.

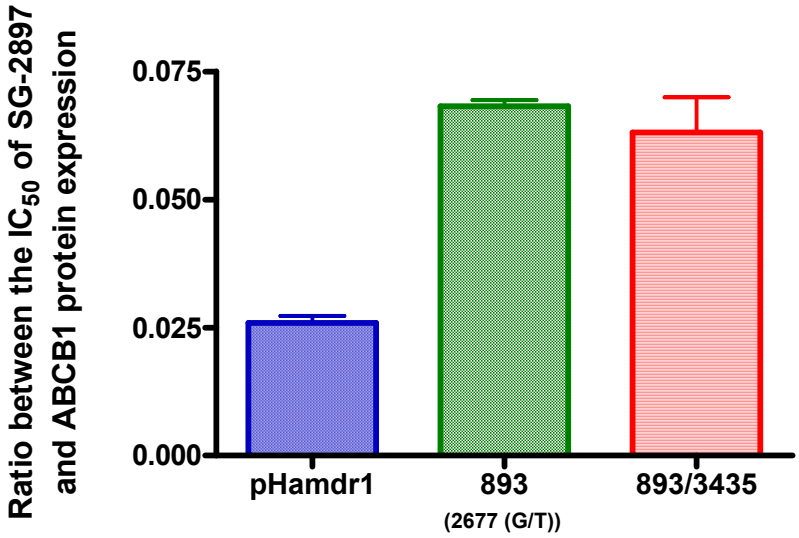

Figure 49. Impact of ABCB1 polymorphism on the growth inhibitory effect of SG-2897. The growth inhibition (IC_{50}) has been corrected with the level of protein expression as determined elsewhere. The IC_{50} values are means ± SEM of n = 3 experiments performed in triplicate.

The impact of the mutation in position 2677 (G/T) on the growth inhibitory effect of the PBD-monomer, SG-2897 was confirmed by pre-incubation with verapamil (Figure 50). The cytoxicity of SG-2897 in the cell lines expressing the mutated form of the transporter was increased by ~3-fold when the cells were pre-incubated with verapamil (from 9.6 nM [95% CI = 6.1-15 nM] alone to 2.9 nM [CI = 1.9-3.3 nM] when pre-treated with verapamil). The growth inhibitory effect of SG-2897 against the cells expressing the mutated form of the transporter, was similar when the cells were pre-incubated with verapamil to the parental cell lines which do not express the transporter (IC_{50} = 2.4 nM [CI = 2.2-2.6 nM]).

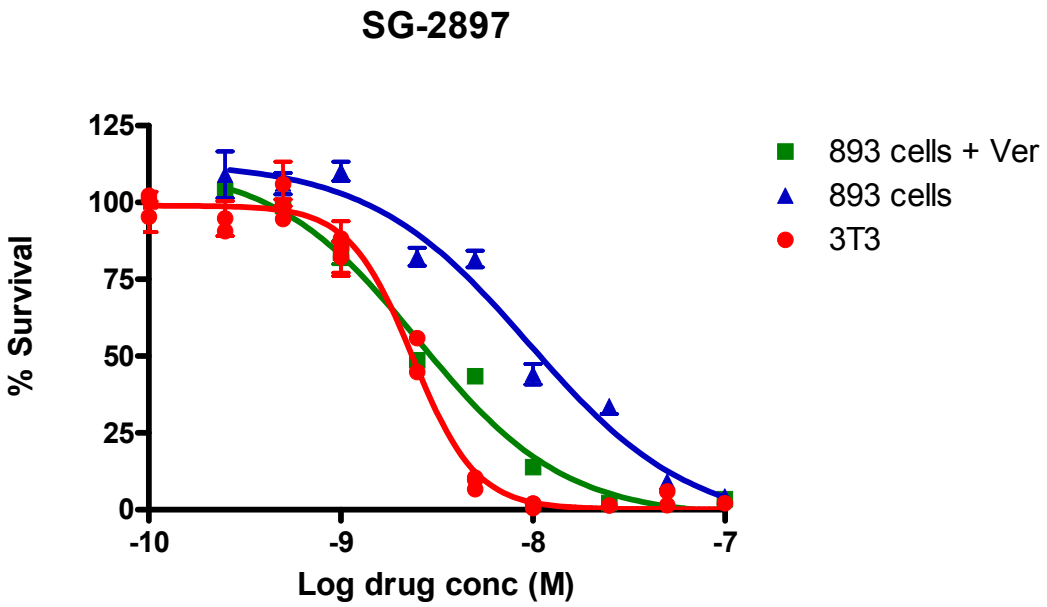

Figure 50. Impact of verapamil on the growth inhibitory effect of the PBD-monomer, SG-2897 in 3T3-893 fibroblasts expressing the mutated form of P-gp in position 2677(G/T). Cells were treated with SG-2897 for 24h with (■) or without (▲) pre-treatment with 10 µM verapamil. The growth inhibitory effect of SG-2897 in 3T3 cells is represented for comparison (●). Results are means ± SEM of triplicate.

The impact of the mutation in position 2677(G/T) was further investigated using other PBDs. The ratio between the IC_{50} in the cell line expressing the mutated form (893) of ABCB1 and the IC_{50} in the cell line expressing no transporter (3T3)

was plotted and compared to the ratio between the IC_{50} in the cell line expressing the wild type form (pHamdr1) and the IC_{50} in 3T3 for 4 PBD-dimers and 4 PBD-monomers. Overall, the ratios between the corrected IC_{50}s in the 893 cell line and the IC_{50}s in 3T3 are greater than the ratios between the corrected IC_{50}s in pHamdr1 and the IC_{50}s in 3T3, for both PBD-dimers and PBD-monomers (Figure 51). Therefore, the mutation at position 893 is associated with a reduced sensitivity of the PBD-dimers and the PBD-monomers tested than the wild type form.

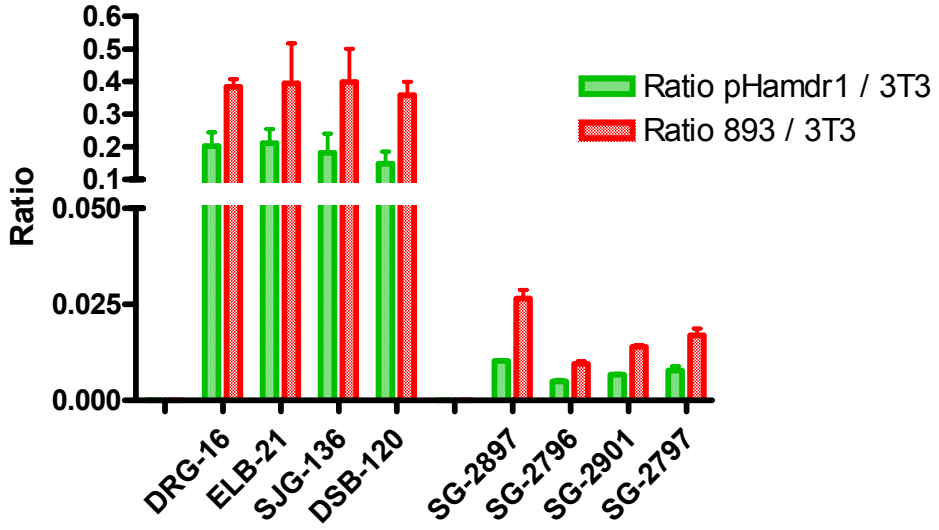

Figure 51. Ratios between the corrected IC_{50} in the pHamdr1 and the IC_{50} in the parental cell line, 3T3 (green) compared to the ratios between the corrected IC_{50} in the 893 cell line and the IC_{50} in 3T3 (red) for 4 PBD-dimers and 4 PBD-monomers. The values are means ± SD of 3 experiments, performed in triplicate.

The difference between the corrected IC_{50}s in the cell line expressing the wild type form of ABCB1 (pHamdr1) and the corrected IC_{50}s in the cell line expressing the mutated form of ABCB1 (893) have been evaluated among the PBD derivatives (data not shown) and the difference was significant ($P_{value} = 0.03$; $n = 25$).

However, the growth inhibitory effect of PBD derivatives was affected differentially by the presence of this specific mutation. The impact of the 893 mutation was evaluated by the ratio between the corrected IC_{50} in the 893 cell line and the corrected IC_{50} in the pHamdr1 cell line. Ratios were evaluated for 10 PBD-monomers and 4 PBD-dimers. When the IC_{50}s were corrected for ABCB1 protein expression, the pHamdr1 cells were on average ~2-fold more sensitive to the PBD-monomers than the 893 cells (Figure 52). The impact of the 893 mutation was greater for PBD-dimers (P_{value} = 0.0065). Indeed, the pHamdr1 cells were on average ~2.8-fold more sensitive to the PBD-dimers than the 893 cells.

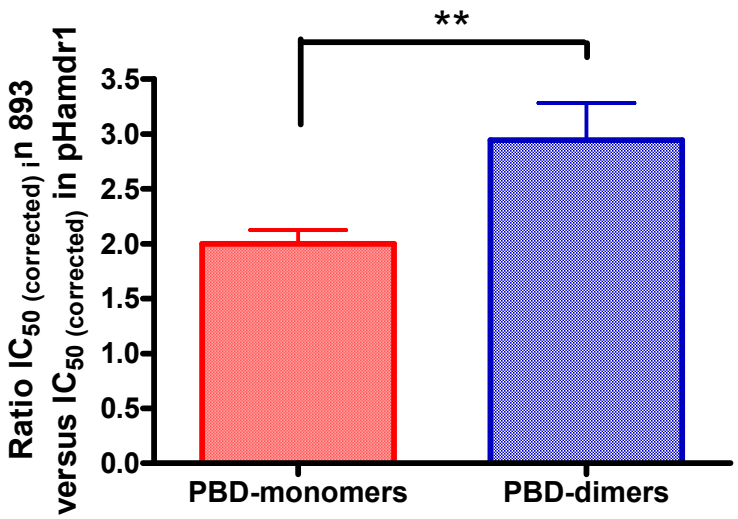

Figure 52. Differential impact of the mutation 2677 (G/A) on the growth inhibitory effect of the PBD-dimers and PBD-monomers. The values represent ratios between the corrected IC_{50} in 893 cells versus the corrected IC_{50} in the pHamdr1 cells. The mean ± SD of the ratios for the PBD-monomers is represented in red (n = 10). The mean of the ratios for the PBD-dimers is represented in blue (n = 4)

3.3 Discussion

PBD-dimers have shown promising preclinical results and SJG-136 is now in clinical development. SJG-136 has been shown to be a P-gp substrate and this study shows similar results for 3 other PBD-dimers. In contrast, the PBD monomers were shown to be non substrates in cell lines expressing physiological level of the transporter. This was demonstrated using different model systems: differential growth inhibition in mdr1 low (HCT 116 and A2780) and mdr1 high cell lines (HCT-15 and $A2780^{AD}$), inhibition of P-gp by verapamil, and with a Caco-2 model of permeability. Using isogenic cell lines (3T3 and pHamdr-1), expressing the transporter at a supra-physiological level, all PBD-dimers were confirmed to be high affinity substrate of P-gp while, some PBD-monomers (SG-2823, SG-2819, SG-2897 and SJG-244) were shown to low affinity substrate of the transporter. More importantly, this study showed how P-gp, by impairing drug uptake, may decrease the drug-DNA interaction of the PBD-dimers and therefore their growth inhibitory effect.

The growth inhibitory effect of the PBD-dimers was improved in $A2780^{AD}$ by pre-treatment with verapamil, although not reaching the growth inhibition observed in A2780. The inability for verapamil to reverse the resistance observed in $A2780^{AD}$ was also previously demonstrated with peloruside and paclitaxel (Gaitanos, Buey et al. 2004). Krasznai and colleagues have demonstrated that the intracellular accumulation of rhodamine 123 was greater when the cells were pre-treated with a more potent inhibitor of P-gp such as cyclosporine A than with the pre-treatment with verapamil in $A2780^{AD}$ cells (Krasznai, Peli-Szabo et al. 2006). The impact of more specific inhibitors could be the basis of further studies. $A2780^{AD}$ cell line has

been obtained by stepwise incubation with doxorubicin. It can be argued that over-expression of mdr-1 may not be the only factor that is up regulated in these cells that could contribute to the difference in growth inhibition not only for doxorubicin but, for the PBD derivatives as well. Several members of the ABC family are amplified in $A2780^{AD}$ cell line (Renes, de Vries et al. 1999). The investigation of other ABC transporters will be reported elsewhere (Cf. Chapter 4).

These studies suggest that P-gp dependency can be designed out. The molecular weight (MW), the polar surface activity (PSA), the number of (N+O) atoms and the hydrogen bonding energy were associated with P-gp substrates. Within the PBD-dimers, Log*P* and MW correlated with P-gp dependency and therefore could also be used to minimise the impact of P-gp over-expression. Small compounds with MW < 250 are suggested to be non substrates because of either a fast diffusion or the fact that P-gp has a large binding pocket with fuzzy specificity (Sharom 1997). One monomer had a MW slightly over a threshold suggested in the literature. However, this cut-off should take into account the pKa of the molecule. For larger molecules, the MW cut-off would be lowered (for bases (Lee, Paull et al. 1994)) or increased (for acids (Essodaigui, Broxterman et al. 1998; Lin 2003)) depending on the ionization of the compounds on the basis of the 400 cut-off defined by Didziapteris *et al* (Didziapetris, Japertas et al. 2003). The PBD derivatives are weak acids (pKa = 4.1). Therefore, the MW cut-off is probably higher for this class of compounds and a value between 402 and 533 would be suggested from our data.

Although the surface activity has been suggested to be a parameter involved in P-gp substrate specificity (Seelig and Landwojtowicz 2000), we found no evidence that this was the case with PBDs. All the substrates described by Seelig

and Landwojtowicz were relatively basic (pKa > 7.4) and more likely to be ionized in a relatively acid environment (Seelig and Landwojtowicz 2000). This ionized form is traditionally thought to be membrane impermeable. The lipophilicity as described among other parameters by the surface activity would compensate and allow these particular compounds (when pH < pKa) to interact with the membrane and being recognized by P-gp. The PBD-dimers which are not surface active are substrates of P-gp. It is likely that their relative acidity decreased the impact of the surface activity.

Hydrophobicity is thought to be a major determinant of P-gp substrate specificity (Ambudkar, Dey et al. 1999; Seelig and Landwojtowicz 2000; Osterberg and Norinder 2001). Molecules with Log*P* lower than 1 or greater than 5 are predicted to be non-substrate despite having some of the physico-chemical features of P-gp substrates, such as bromocriptin (BCT) using a MDCKII transwell assay similar to the one used in this study (Caco-2 system) (Varma, Sateesh et al. 2005). However, some of these compounds, have been shown to be P-gp substrates by others (such as BCT as determined *in vivo* in mdr1 -/- compared to mdr1 +/+ mice) (Mechetner, Kyshtoobayeva et al. 1998; Miyama, Takanaga et al. 1998; Vautier, Lacomblez et al. 2006). This study showed that although Log*P* failed to discriminate substrates from non substrates in all models tested, it could be used to evaluate the degree of P-gp dependency, in conjunction with MW.

The rate of transfer of 3 PBDs was investigated using a Caco-2 model of permeability and 2 PBD-dimers (DRG-16 and SJG-136) were shown to be actively secreted in contrast to the PBD-monomer SG-2897. The differentiated Caco-2 cells

express other ABC transporters such as ABCG2 at the apical side and MRP1 at the basal side. The specific impact of P-gp could not be verified by incubation with verapamil as it also blocks MRP1. Further studies are needed to investigate the specific contribution of the ABC transporters in the secretion of the PBD-dimers in the Caco-2 system.

The ability of the PBDs to act as P-gp inhibitors was also assessed using the calcein-AM assay. However, the affinity of calcein-AM for P-gp is much greater than the affinity of the PBDs and therefore no significant difference in the fluorescence could be observed.

The impact of ABCB1 polymorphism on the growth inhibitory effect of the PBDs was also assessed. The impact of the different mutations on the level of P-gp expression was evaluated first. The wild type pHamdr1 showed the greatest expression of the transporter, both at the level of mRNA and protein expression. The presence of single or combined mutations decreased the expression of P-gp. This is in accordance with the findings by many groups which demonstrated a relationship between ABCB1 polymorphism and lower expression in the human intestine (Hoffmeyer, Burk et al. 2000).

The growth inhibitory effect of the PBD-dimers correlated only poorly with the level of expression of P-gp using cell lines expressing the different genotypes of ABCB1 suggesting that the different mutations altered the function of the transporter. The cell line expressing the transporter associated with a mutation in position 2677 which changes the amino acid from an Alanine to a Serine (A893S)

was the least sensitive despite lower protein expression when compared to the cell line expressing the wild type transporter.

This finding is fully consistent with studies demonstrating an enhanced efflux transporting ability of the Ser 893 variant (Kim, Leake et al. 2001; Schaefer, Roots et al. 2006; Sakurai, Onishi et al. 2007). The exact mechanism by which this specific mutation enhances transport has been a matter of debate. It has been suggested that phosphorylation by protein kinase C of the serine residues might affect the activity of the transporter (Chambers, Pohl et al. 1993). A similar pattern could be seen with the PBD-monomers. Previously, some PBD-monomers were shown to be associated with a low affinity for the transporter (SG-2823, SG-2819, 2897 and SJG-244) in a system where supra-physiological conditions were observed. The Ser 893 variant was associated with an enhanced efflux in contrast to the wild type (Ala 893). Among the PBD-monomers, the differential growth inhibition between the cell lines expressing the different variants was not significant to develop a structure activity relationship. However, while considering both PBD-dimers and the PBD-monomers, we have shown a differential impact of this particular mutation. The Ser 893 variant is associated with a greater "gain of function" in relation to the PBD-dimers, high affinity substrates of the transporter.

The mutation in position 3435 was associated with the mutation in position 2677 (G/T), the former abrogated the "gain of function" in the efflux of the PBD-dimers only. Many laboratories have investigated the impact of this specific polymorphism revealing an altered drug phenotype without being able to reach a consensus (Lepper, Nooter et al. 2005). Recently, Gottesman and colleagues have suggested differential mRNA splicing associated with this particular polymorphism

leading to differential folding of the transporter in the membrane (Kimchi-Sarfaty, Oh et al. 2007). The "loss of function" was observed only among the PBD-dimers, which suggests that, the conformation of the protein (induced by the 3435 mutation) has diminished the substrate specificity to P-gp substrates.

The relatively low level of the transporter in the cell lines expressing the mutations in position 2677 (G/A), the double mutation in position 2677 (G/T) and 1236 and the triple mutation (893/1236/3435) did not allow discrimination of the impact of altered function from altered protein level of the transporter. Further studies are needed using cell lines or other system expressing identical levels of protein expression.

In summary, the 4 PBD-dimers were found to be substrates for P-gp in contrast to the 12 PBD-monomers in cell lines expressing physiological levels of the transporter. The 5 features identified, which may predict substrate specificity for PBD-derivatives, were MW, Log*P*, the number of (nitrogen + oxygen) atoms, hydrogen bonding energy, and PSA, When considered separately, MW and Log*P* correlated with the differential growth inhibitory effect of the dimers in the HCT 116 and HCT-15 cell lines. The impact of ABCB1 polymorphism was also investigated. The mutation in position 2677 (G/T) was associated with a "gain of function". An associated mutation in position 3435 abrogated this "gain of function".

Consideration of these factors may allow the rational design of new PBD analogues with reduced interaction with the P-gp transporter and this may enhance their anti-tumour activity.

4 Chapter 4: INFLUENCE OF OTHER ABC TRANSPORTERS ON THE GROWTH INHIBITORY EFFECT OF PBD DERIVATIVES

4.1 Introduction

The effect of the MDR phenomenon on anticancer agents is very variable. Agents may be recognised by P-gp as well as by the other proteins of the ABC super-family of transport proteins. Two other major proteins have been identified, conferring resistance to a number of anticancer agents: ABCC1, member of the ABC transporter subfamily C, member 1, commonly referred as the multidrug resistance protein 1 (MRP1) and ABCG2, member of the ABC transporter subfamily G, member 2, also named the breast cancer resistance protein (BCRP)

MRP1 recognises a wide range of anionic molecules which may or may not be conjugated to glutathione, sulphate or glucuronide in order to be extruded from the cell (Jedlitschky, Leier et al. 1996; Hipfner, Deeley et al. 1999; Konig, Nies et al. 1999). From the literature, it is not evident whether glutathione acts as a cofactor for the activity of the transporter as numerous studies have shown a direct coupling prior to the extrusion (Zaman, Lankelma et al. 1995; Rappa, Lorico et al. 1997). The conjugation of a compound to glutathione can occur spontaneously or enzymatically by the enzyme, glutathione-S-transferase or GST. This metabolic pathway needs a continual supply of glutathione which is produced by the enzyme, γ-Glu-Cys-synthetase or γ-GCS. Cancer drug resistance is often associated with up-regulation of MRP1, GST and GSH, simultaneously. In the last decade, much effort has been

made to define a structure activity relationship for compounds to be recognised by MRP1 without any success. Since the resistance mediated by MRP1 results from the combination of several factors (Cf .section 1.4.2.3.), it appears necessary to investigate the impact of each one of them to define any specific feature involved in MRP1 substrate specificity.

ABCG2 has shown overlapping substrate specificity to that of P-gp and MRP1. It recognises compounds which may or may not be conjugated with preferential substrate specificity for sulfate conjugates (Suzuki, Suzuki et al. 2003). ABCG2 substrates share a common set of properties such as a high polarity, a greater number of aromatic rings and hydrophilic groups. Such properties are common among chemotherapeutic agents. Defining more specific physico-chemical properties would help to predict ABCG2 substrate specificity.

Significant inter-individual variations in the ABCG2 gene have been reported altering the uptake of drugs. A single amino-acid change at position 482 from an arginine to a threonine has been shown to mediate this phenomenon. It has often been associated with a gain of function while a few studies have postulated the opposite (Honjo, Hrycyna et al. 2001; Ozvegy, Varadi et al. 2002). A structure activity relationship, based on a great number of compounds is required to find a consensus of the impact of this specific mutation.

PBDs have a broad spectrum of anti-tumour activity in a number of human cancer cell lines and xenograft models. All the PBD-dimers have been shown to be substrates for the ABC transporter, P-gp, potentially limiting their anti-tumour activity. In contrast, the growth inhibitory effect of the PBD-monomers has been shown not to be affected significantly by the over-expression of the transporter in

cancer cells. The affinity for PBDs interaction with other ABC transporters such as MRP1 and ABCG2 is unknown.

The work presented in this chapter investigates the impact of MRP1 and ABCG2 on the anti-tumour activity of the PBDs and identifies the key physico-chemical parameters involved in the resistance mediated by these 2 transporters. In addition, the impact of the SNP at position 482 on the efflux of the PBDs by ABCG2 will be addressed.

4.2 Results

4.2.1 MRP1 (ABCC1) substrate specificity of the PBD derivatives

4.2.1.1 Growth inhibition studies in the A549 cell line which expresses MRP1 highly

4.2.1.1.1 Determination of an optimal concentration of MK-571

MRP1 recognises a broad range of compounds and its substrate specificity has been shown to overlap P-gp substrate specificity (Zaman, Flens et al. 1994; Kruh and Belinsky 2003; Deeley and Cole 2006). In order to verify whether the PBD-dimers are substrates of MRP1 and the PBD-monomers non substrates, a cell line which expresses the transporter at high level, the human alveolar type II cell line A549 (non small cell lung cancer) was used in this study (Lehmann, Kohler et al. 2001; Stehfest, Torky et al. 2006).

As calcein-AM is a substrate of MRP1, the calcein assay was used to investigate the level of activity of MRP1 in A549 and the effect of its specific blocker MK-571 (Feller, Broxterman et al. 1995; Gekeler, Ise et al. 1995). A

concentration of the blocker retaining the maximum fluorescence within the cells was determined at 100µM (Figure 53).

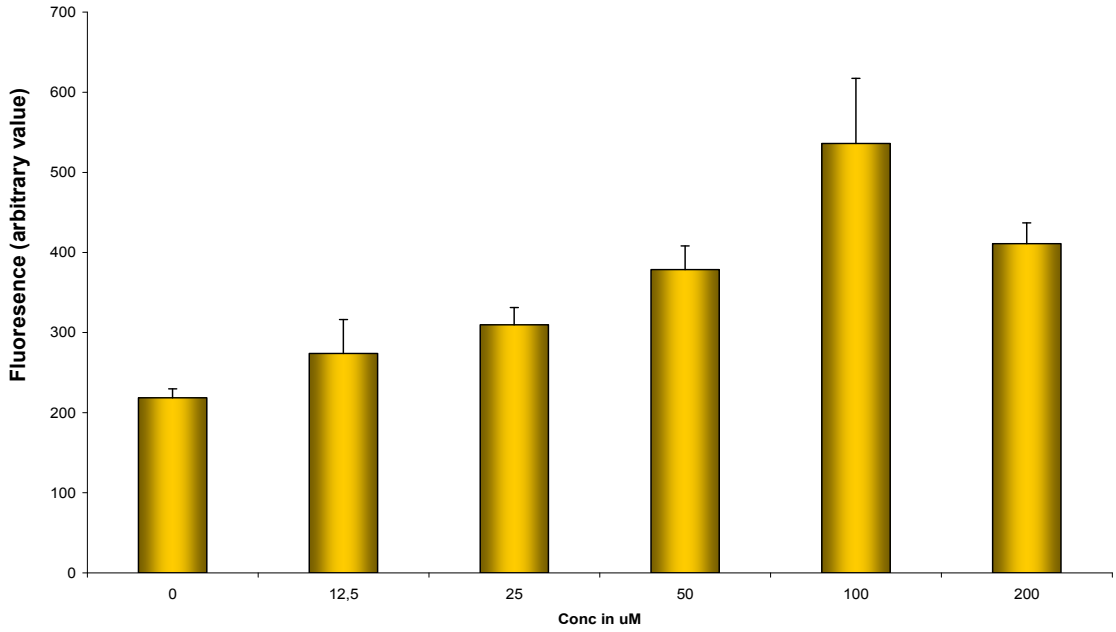

Figure 53. Dose dependent effect of MK-571 on the intracellular concentration of calcein as measured by the calcein-AM assay, in lung cancer cell line A549. Results are means ± SD of 3 experiments performed in duplicate.

However, the treatment with 100µM of MK-571 in A549 cells, using the SRB assay, has shown a significant effect on the survival of controls cells (Table 10).

	Vitality in A549 cells
Control	100 ± 2.3
50 uM MK-571	99.7 ± 2.9
100 uM MK-571	74.7 ± 4.7

Table 10. Impact of MK-571 on the viability of A549 cells. Results are means ± SD of triplicate.

The toxic effect following incubation with 100 µM is likely to be due to the difference in experimental conditions between the calcein AM assay and the SRB

assay. Indeed, the SRB assay is carried out over 6 days with the cells in contact with the inhibitor (MK-571) for 25 hours compared to the calcein AM assay for which cells are exposed to the inhibitor for less than 2 hours. Therefore, a concentration of 50 μM, associated with significant retention of calcein and, without any toxic effect was used for further experiments.

4.2.1.1.2 Impact of MK-571 on the growth inhibitory effect of the PBD derivatives

The impact of MK-571 was evaluated on the growth inhibitory effect of 2 PBD-monomers, SG-2823 and SJG-244. The IC_{50} following 24h exposure to SG-2823 decreased ~5-fold when A549 cells were pre-treated with MK-571 (From 52 nM [95% confidence interval = 49-55 nM] for SG-2823 alone to 10 nM [10-11 nM] in the presence of 50 μM MK-571 (Figure 54.A). The IC_{50} following 24h exposure to SJG-244 was similar when A549 cells were in presence or absence of MK-571 (410 nM [360-460 nM] and 420 nM [350-490 nM], respectively (Figure 54.B).

A.

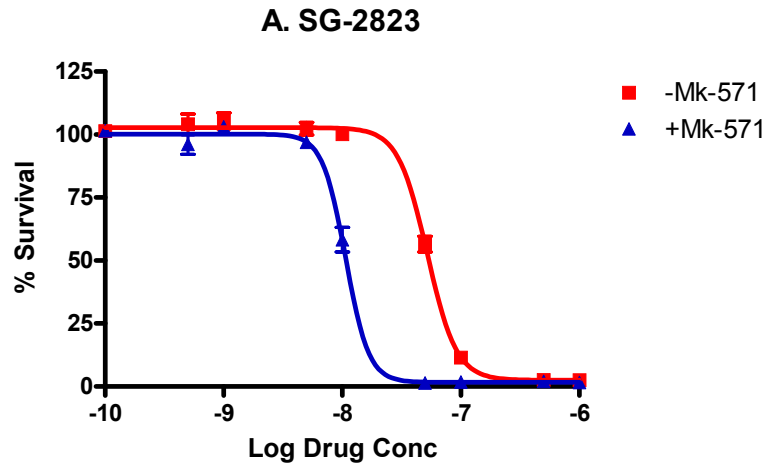

B.

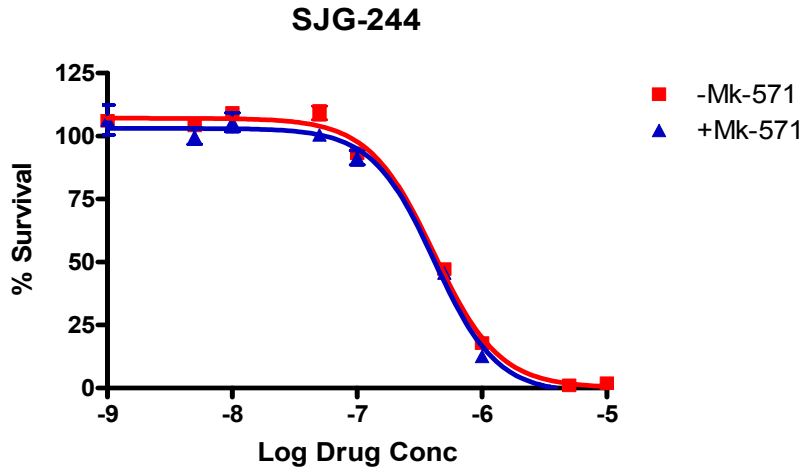

Figure 54. Impact of MRP1 on the cytotoxic effect of 2 PBD-monomers: SG-2823 (A) and SJG-244 (B) in lung cancer cell line A549. Cells were treated with SJG-244 for 24h with (▲) or without (■) pre-treatment with 50 µM MK-571. Results are means ± SEM of triplicate.

The cytotoxic effect (IC_{50}) of all PBD derivatives in A549 cells in presence or absence of MK-571 was evaluated for all PBDs. Overall, the PBD-dimers are more potent than the PBD-monomers in A549 cells (Table 11). The most active compounds were ELB-21 and DRG-16 with IC_{50} of 0.04 nM and 0.059 nM, respectively, without pre-treatment with MK-571. The least active compounds were

SJG-244, SG-2901, SG-2900 and SG-2825 (370 nM, 260 nM, 160 nM and 170 nM, respectively).

	Control		MK-571	
	IC_{50} (nM)	SD	IC_{50} (nM)	SD
SG-2781	15	4.7	17	1.4
SG-2796	8.8	1.2	8.5	2.0
SG-2797	14	2.0	11	0.3
SG-2819	21	6.0	19	1.8
SG-2820	30	0.8	21	0.9
SG-2823	47	4.8	10	2.0
SG-2825	170	24	160	8.9
SG-2897	1.9	0.3	1.4	0.2
SG-2900	160	22	150	35
SG-2901	260	59	290	13
SG-2902	98	7.8	79	0.2
SJG-244	370	34	350	75
DRG-16	0.052	0.020	0.022	0.011
ELB-21	0.040	0.014	0.015	0.007
SJG-136	0.46	0.11	0.21	0.06
DSB-120	75	29	28	4.3

Table 11. Pyrrolobenzodiazepine derivatives IC_{50}s in A549 lung cancer cell line. Cells were treated with different PBDs for 24h with or without pre-treatment with 50 μM MK-571. Results are means ± SD of 3 experiments performed in triplicate.

The ratio between the IC_{50} with or without MK-571 was determined for all the PBDs. Pre-treatment with MK-571 sensitised A549 cells to all 4 PBD-dimers and to one PBD-monomer, SG-2823 (Figure 55). Cells were ~5-fold more sensitive to SG-2823 and 2- to 3-fold more sensitive to the PBD-dimers. The pre-treatment of A549 cells with MK-571 had no effect on the growth inhibitory effect of the PBD-monomers (apart from SG-2823): the ratio was never greater than 2.

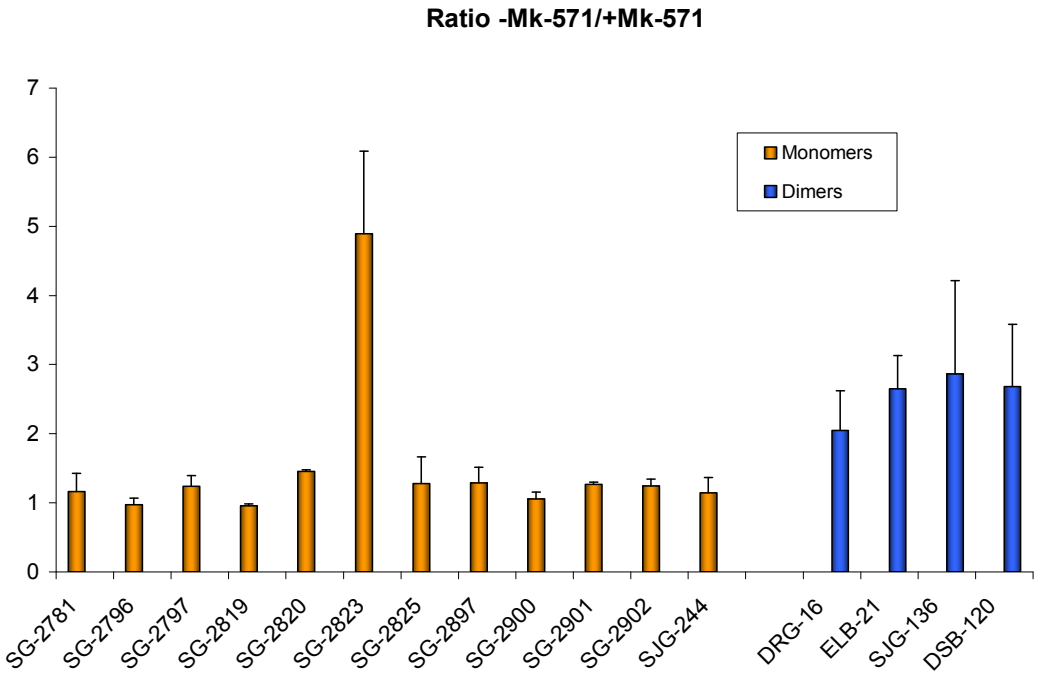

Figure 55. Ratio between the IC_{50} when A549 cells where pre-treated or not with 50 µM of MK-571 for the PBDs. Results are presented as ratio between – MK-571 versus + MK-571. The PBD-dimers are represented in blue and the PBD-monomers in orange. Results are means ± SEM of 3 experiments performed in triplicate.

4.2.1.1.3 Impact of dicumarol on the growth inhibitory effect of the PBD-derivatives

MRP1 can recognise a wide range of compounds. Some of them have to be conjugated to glucuronide, sulphate but mostly to glutathione prior to the efflux by MRP1 (Muller, Meijer et al. 1994; Jedlitschky, Leier et al. 1996; Barnouin, Leier et al. 1998; Loe, Deeley et al. 1998). In order to verify whether SG-2823 is conjugated to glutathione (GSH) by GST, the impact of a GST inhibitor, dicumarol, was evaluated in A549 cells. The cells were pre-incubated with 100 µM of dicumarol prior to the start of the exposure of the compound. This concentration of dicumarol

had been described elsewhere and was confirmed as inducing no significant growth inhibitory effect in control cells (Morrow, Diah et al. 1998).

The impact of dicumarol on A549 cells was assessed using 2 PBD-monomers, SG-2823 and SG-2781. The IC_{50} following 24h exposure to SG-2823 decreased ~4.5-fold when A549 cells were pre-treated with dicumarol (From 53 nM [95% confidence interval = 50 - 55nM] for SG-2823 alone to 11 nM [10-13 nM] in the presence of 100 μM dicumarol (Figure 56.A). The IC_{50} following 24h exposure to SG-2823 when the cells were treated with MK-571 (11 nM) was similar to the IC_{50} following 24h exposure to SG-2823 when the cells were treated with dicumarol (11 nM). The IC_{50} following 24h exposure to SG-2781 was similar in A549 cells in the absence or presence of dicumarol (8.1 nM [7.8 - 8.4 nM] and 6.4 nM [6 - 6.8 nM], respectively) (Figure 56.B).

A.

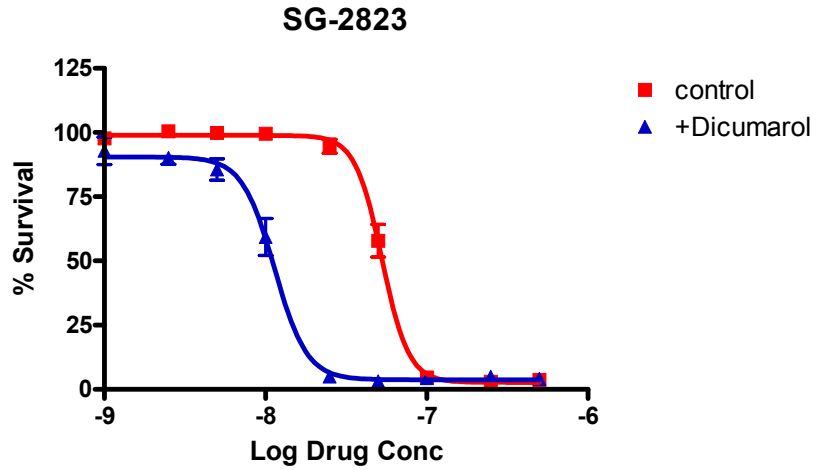

B.

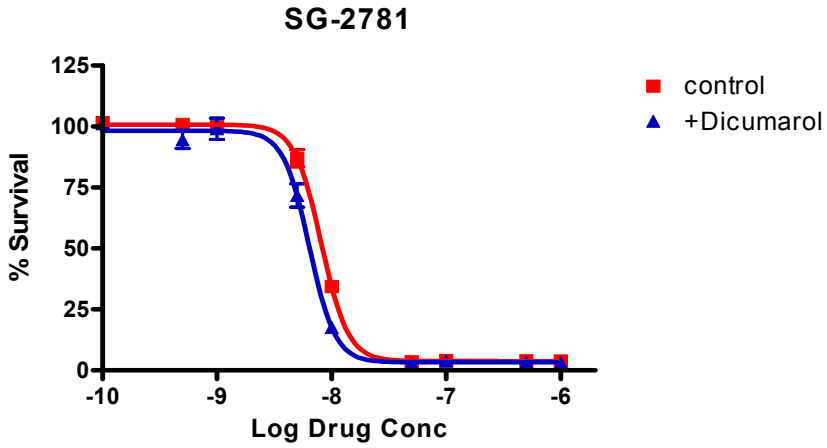

Figure 56. Impact of GST inhibition on the cytotoxic effect of 2 PBD-monomers: SG-2823 (A) and SG-2781 (B), in A549 cells. Cells were treated with SG-2823 or SG-2781 for 24h with (▲) or without (■) pre-treatment with 100µM Dicumarol. Results are means ± SEM of triplicate.

These results provide evidence that the resistance mediated by MRP1 to SG-2823 is reversed by the inhibition of GST in A549 cells.

Similar studies were also performed in a set of chemically different PBD-monomers and 1 PBD-dimer, DSB-120. The 4 chosen PBD-monomers differ by the presence of an electron donor group at the C2 extremity. The most active

compounds were SG-2819 and SG-2781 with an IC_{50} of 13 nM and 19 nM, respectively in A549 cells without pre-treatment with dicumarol (Table 12). The least active compounds were DSB-120, SG-2823 and SG-2820 (81 nM, 58 nM and 53 nM, respectively).

	Control		Dicumarol	
	IC_{50} (nM)	SD	**IC_{50} (nM)**	SD
SG-2781	19	4.9	17	5.9
SG-2819	13	3.7	11	2.6
SG-2820	53	0.1	37	7.3
SG-2823	58	15	11	0.1
DSB-120	81	32	44	16

Table 12. Pyrrolobenzodiazepine derivatives IC_{50}s, in A549 cell line. Cells were treated with PBDs for 24h with or without pre-treatment with 100 μM Dicumarol. Results are means ± SD of n = 3 experiments performed in triplicate.

The ratio between the IC_{50} with or without dicumarol was determined for the chosen PBD-monomers and PBD-dimer, DSB-120. The growth inhibitory effect of SG-2823 seemed to be the only one significantly affected by the presence of dicumarol (ratio of IC_{50}s between absence and presence of dicumarol greater than 2) (Figure 57).

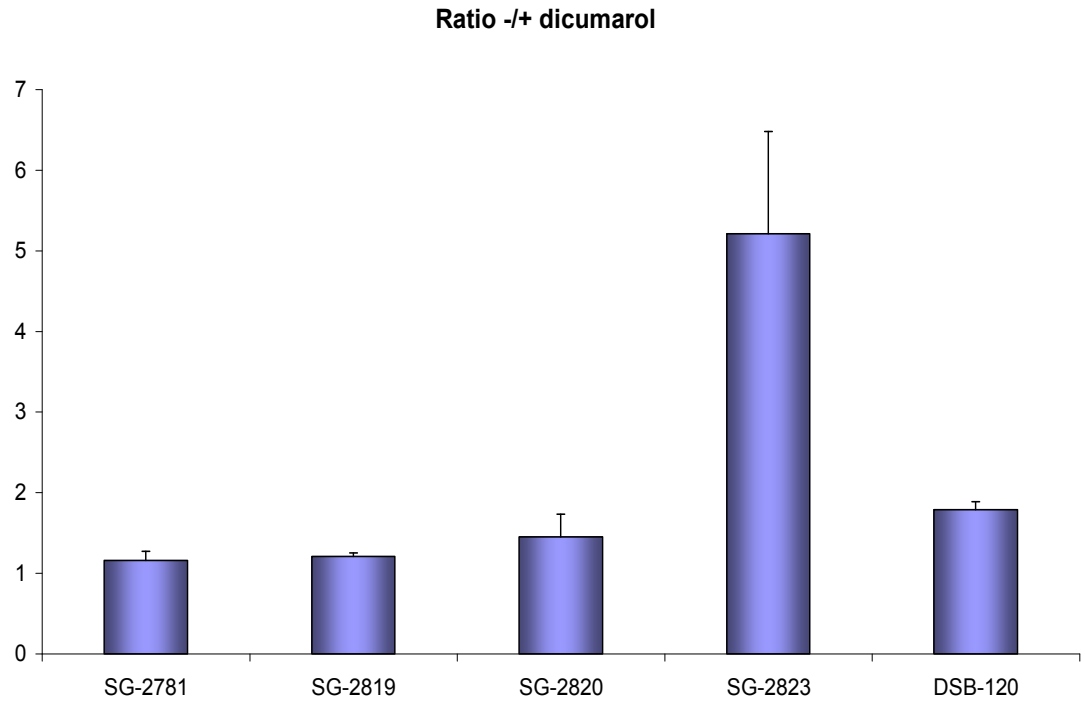

Figure 57. Ratio between the IC_{50} when A549 cells where pre-treated or not with 100 μM of dicumarol for a set of PBD derivatives. Results are presented as the ratio – dicumarol versus + dicumarol. Results are means ± SEM of n = 3 experiments performed in triplicate

4.2.1.1.4 Impact of BSO on the growth inhibitory effect of the PBD-derivatives

To compare the impact of inhibiting the conjugation of GSH to PBDs by GST (impact of dicumarol) to the impact of inhibiting GSH synthesis, the cells were treated with buthionine sulfoximine (BSO), a potent and specific inhibitor of γ-glutamylcysteine synthetase (γ-GCS), the rate-limiting enzyme in the synthesis of GSH (Dorr, Liddil et al. 1986). A concentration of 10 μM BSO was defined as sensitising the A549 cells to well known substrates of γ-GCS and was confirmed as inducing no significant growth inhibition in control cells (Roizin-Towle 1985).

The impact of BSO on A549 cells was evaluated with 2 PBD-monomers, SG-2823 and SG-2781. The IC_{50} following 24h exposure to SG-2823 decreased ~2.4-

fold when A549 cells were pre-treated with BSO (from 57 nM [95% confidence interval = 50-63 nM] for SG-2823 alone to 24 nM [20-28 nM], in presence of 10 µM BSO (Figure 58.A). The IC_{50} following 24h exposure to SG-2781 was similar when A549 cells were in the absence or presence of BSO (24 nM [19-32 nM] and 23 nM [17-28 nM], respectively) (Figure 58.B).

A.

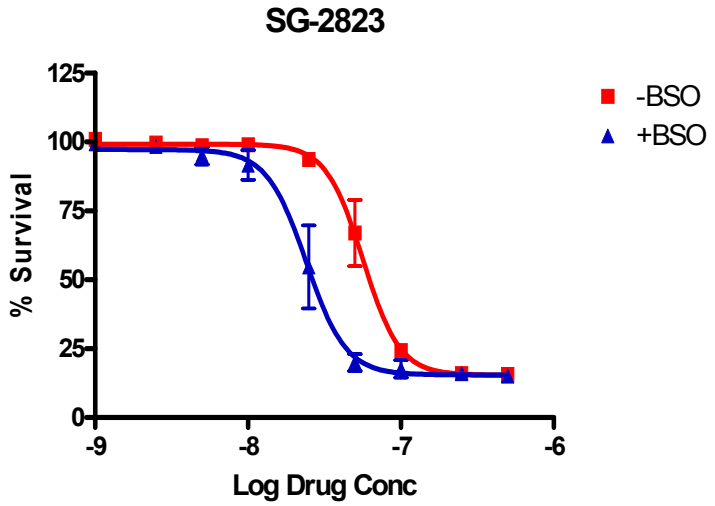

B.

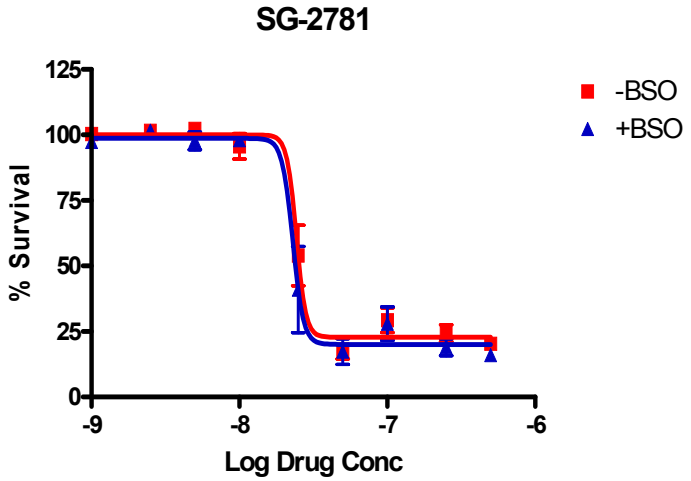

Figure 58. Impact of the inhibition of γ-GCS on the cytotoxic effect of SG-2823 (A) and SG-2781 (B), in A549 cells. Cells were treated with different PBD-monomers for 24h with (▲) or without (■) pre-treatment with 10 µM BSO. Results are means ± SEM of triplicate.

The ratio between the IC_{50} with or without BSO was determined for 5 PBD-monomers and 1 PBD-dimer (DSB-120). The PBD-dimer, DSB-120 also gave a ratio greater than 2 (Figure 59). Among the PBD-monomers, SG-2823 had the highest ratio (2.5) followed by SG-2820 (1.6). SG-2781 and SG-2825 have shown a ratio close to 1. Using an arbitrary cut-off value of 2, only DSB-120 and SG-2823 would be considered as being affected by the intracellular concentration of GSH.

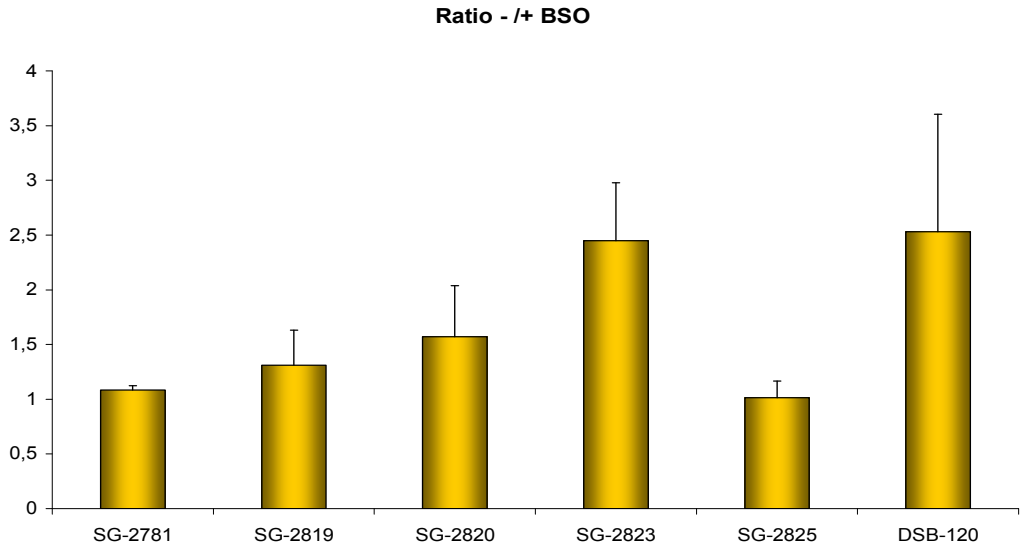

Figure 59. Ratio between the IC_{50} to PBD derivatives when A549 cells where pre-treated or not with 10 µM of BSO. Results are presented as the ratio – BSO versus + BSO. Results are means ± SEM of n = 3 experiments performed in triplicate.

4.2.1.2 Chemical structure analysis to explain variable MRP1 substrate specificity to PBD derivatives

All 4 PBD-dimers and SG-2823 are potential substrates of MRP1. This differential substrate specificity of the PBD derivatives towards MRP1 could be explained by differences in their chemical structure. Two chemical structures of

similar PBDs were compared: SG-2823, PBD-monomer substrate of MRP1 and SG-2819, PBD-monomer non substrate of the transporter. SG-2823 has a carbonyl moiety at the C2 aryl extremity in contrast to SG-2819 (Figure 60). No other difference could be seen.

SG 2823

SG 2819

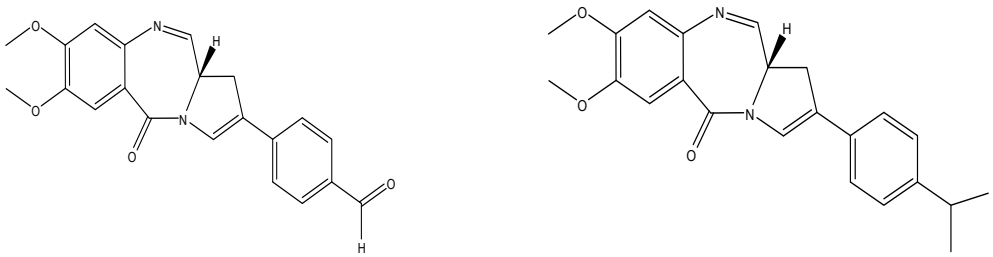

Figure 60. Chemical structure of 2 PBD-monomers SG-2823 and SG-2819.

PBD-dimers have a ratio between the IC_{50} with or without MK-571 greater than 2 suggesting an impact of MRP1 on their growth inhibition in A549 cells. However, there is no significant difference among them (similar ratio) and no conclusive structure activity relationship could be developed. Further experiments are needed to evaluate the differential substrate specificity of PBD-dimers to MRP1.

4.2.1.3 Conjugation of SG-2823 to glutathione

4.2.1.3.1 LC/MS analysis

To confirm a potential conjugation of SG-2823 to GSH, SG-2823 (10 µM) was incubated with GSH (1 mM) for 15 minutes at room temperature in Hanks buffer cell free. The products of the reaction were analysed by liquid chromatography / mass spectrometry (LC/MS). Briefly, the high performance liquid

chromatography separates the molecules according to their polarity; the less polar compounds being eluted earlier than the compounds with high polarity. The detection by mass spectrometry confirms the identity of the molecules based on their *m/z* values. The total ion chromatogram shows 3 different peaks corresponding to 3 compounds with different retention time, *i.e*. different polarity. The first peak eluted at 3.99 minutes (Figure 61.A) was identified as GSH $[M+H]^+$ 308.5 (Figure 61.B). The second peak eluted at 8.8 minutes corresponds to the conjugated form of SG-2823 to GSH $[M+H]^+$ 671.5 (Figure 61.C). Finally, a third peak at 9.77 minutes corresponds to SG-2823 $[M+H]^+$ 363.5 (Figure 61.D).

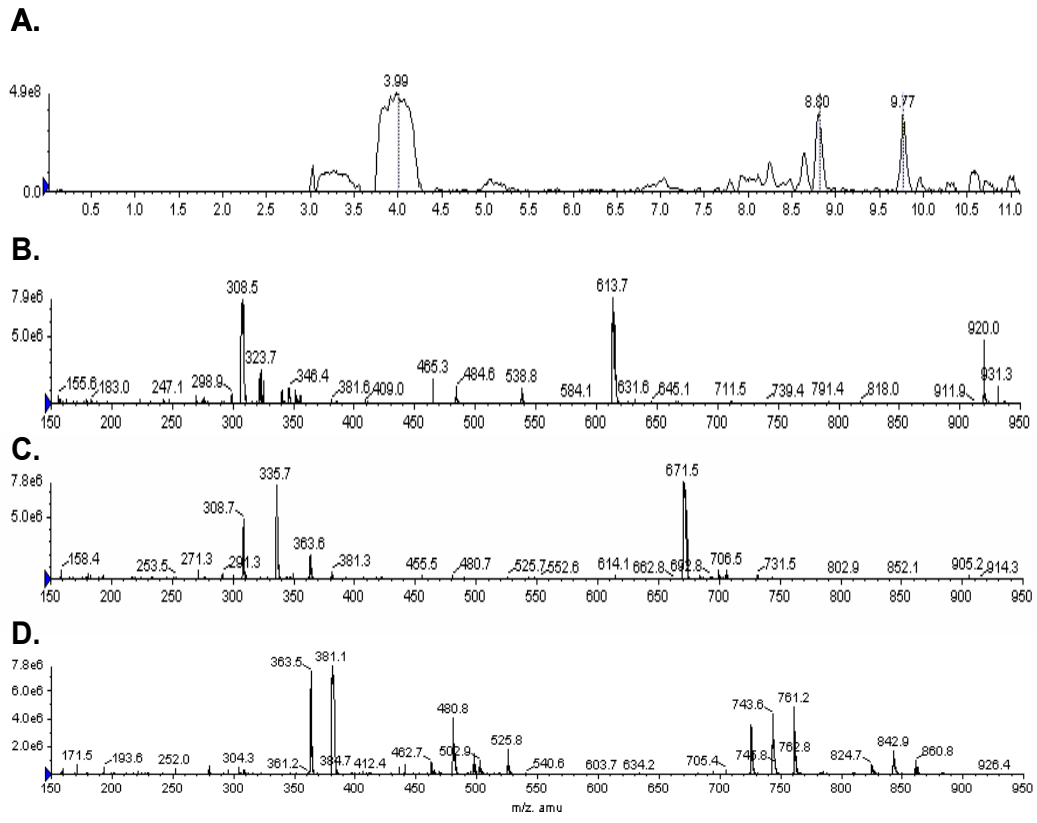

Figure 61. Conjugation of SG-2823 to glutathione. (A) Total ion chromatogram for the cell free analysis of GSH with SG-2823 (B) Spectra taken from the peak at 3.99 min which corresponds to GSH $[M+H]^+$ 308.5 (it also identifies the duplicate of GSH $[M+H]^+$ 613.7) (C). Spectra taken from the peak at 8.8 min which identifies the GSH conjugate $[M+H]^+$ 671.5 (D) Spectra taken from the peak at 9.77 min which identifies SG-2823 $[M+H]^+$ 363.5.

These results suggest that SG-2823 reacts in vitro with glutathione to form a conjugate with a molecular weight of 671.5 g/mol. The conjugation appears to be spontaneous as no GST has been added to the media. The conjugate, being less polar than SG-2823, would be expected to be extruded out of the cell by MRP1.

4.2.1.3.2 Kinetic activity of the formation of GS-PBD derivatives conjugates

To confirm the formation of the conjugate in a cell free system, GSH was incubated with SG-2823 and the intensity of the 671.5 peak was evaluated over-time (Figure 62). The peak intensity of GS-SG-2823 increases from time 0 (1.1×10^6) to time = 30 min (7.68×10^6) representing a ~7-fold increase in intensity. It is followed by a gradual increase up to 6 hours (2.32×10^7) representing a ~3-fold gain. The intensity remained steady up to 24 hours post incubation (2.33×10^7). Overall, the peak intensity was increased by ~21-fold over-time. The intensity of the free form of SG-2823 has also been evaluated (Figure 62). It is important to remember that the value of the peak intensity of the free form can not be compared directly to the value of the peak of the conjugated form. However, it can be reported that, as expected, the peak intensity was maximal at time = 0 (7.33×10^6). It then declined overtime up to 6 hours reaching its minimum value (4.6×10^6) representing a ~1.6-fold decrease.

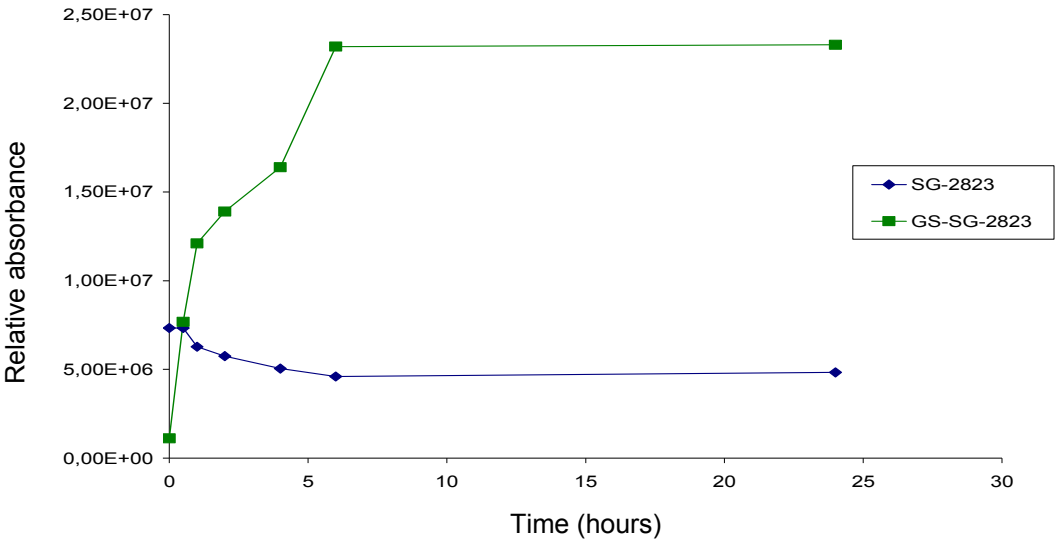

Figure 62. Conjugation of SG-2823 with GSH overtime. The spectra was taken from the peak at 8.8 min which identifies the GSH conjugate $[M+H]^+$ 671.5 (green) and compared to the spectra taken from the peak at 9.77 min which identifies SG-2823 $[M+H]^+$ 363.5 (blue). Results are replicate.

To confirm the ability of GSH to conjugate spontaneously only to SG-2823, the kinetics of another PBD-monomer SG-2819 were evaluated (it has been shown previously not to be affected by dicumarol (Cf. section 4.2.1.c.). Surprisingly, the formation of the conjugate seems also to be driven spontaneously at RT (Figure 63). The peak intensity of GSH-SG-2819 increases slightly from time 0 (3.27×10^6) to time = 30 min (4.78×10^6) representing a ~1.5-fold increase in intensity. It is followed by a gradual increase up to 6 hours (2.32×10^7) representing a ~3.4-fold gain. Overall, the peak intensity was increased by ~3.7-fold. The peak intensity of the free form of SG-2819 has also been evaluated. It followed a similar pattern as SG-2823: A maximal intensity at time = 0 (5.87×10^6). It then declined overtime reaching a minimal value after 24h (4.02×10^6) representing a ~1.5-fold decrease.

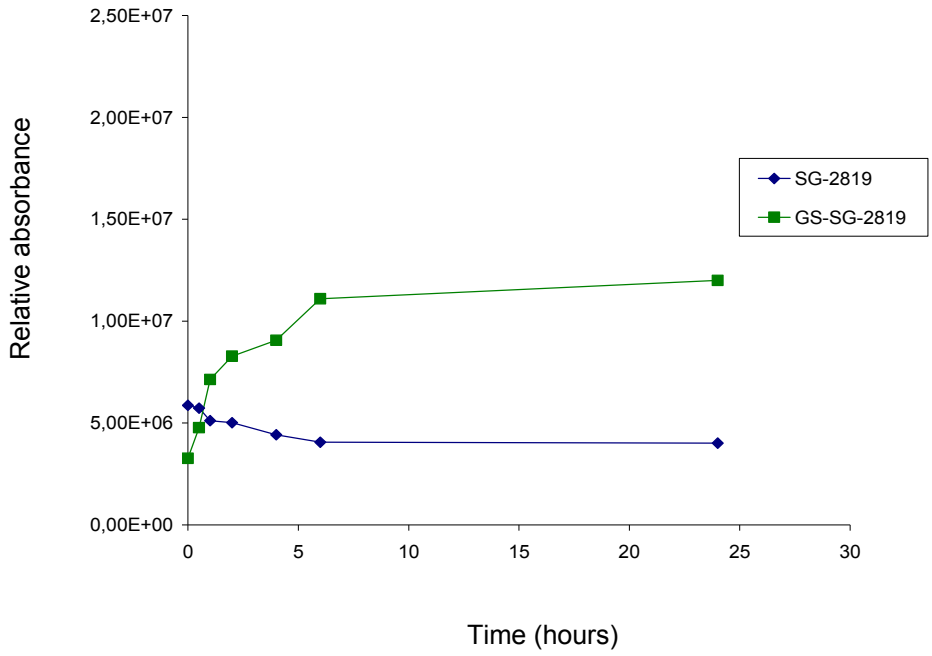

Figure 63. Conjugation of SG-2819 with GSH overtime. The spectra was taken from the peak at 9.46 min which identifies the GSH conjugate $[M+H]^+$ 684.7 (green) and compared to the spectra taken from the peak at 11.14 min which identifies SG-2819 $[M+H]^+$ 377.6 (blue). Results are replicate.

Taken together, these results provide evidence that both SG-2823 and SG-2819 are conjugated spontaneously to glutathione. However, the conjugation of GSH is enhanced for the compound with greater electrophilic potential.

The concentration of the conjugates could not be determined as no standard is available for this entity. Therefore, the determination of the kinetics (first/second order rate) of reaction may be misleading. A chemical synthesis of the conjugates may help defining these parameters.

4.2.2 ABCG2 (BRCP) substrate specificity of the PBD derivatives

4.2.2.1 Growth inhibition studies in MCF7 and MCF7-MX

4.2.2.1.1 Expression of ABCG2 in MCF7 and MCF7-MX breast cancer cell lines

MCF7-MX cells are derived from the parental MCF7 cell line and are resistant to mitoxantrone. Several studies have shown that the resistance to mitoxantrone is mediated by over-expression of the ABCG2 gene (Doyle, Yang et al. 1998; Ross, Yang et al. 1999).

The over-expression of ABCG2 in MCF7-MX cell line compared to MCF7 was confirmed by immunoblotting (Figure 64).

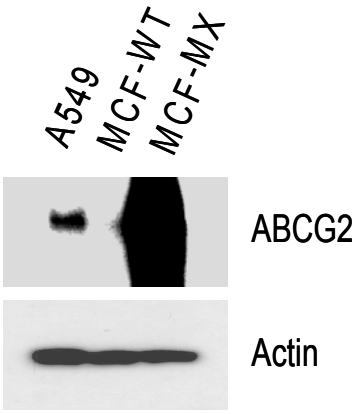

Figure 64. ABCG2 protein expression in MCF7-MX, and MCF7 breast cancer cell lines. The level of ABCG2 in A549 cell line has also been reported for comparison. ABCG2 protein migrated at ~72 kDa.

4.2.2.1.2 Growth inhibitory effect of the PBDs against MCF7 and MCF7-MX cell lines

Initially, the cytotoxic effect (IC_{50}) of 2 PBD derivatives, the PBD-dimer DRG-16 and the PBD-monomer SG-2901, was determined in both MCF7-MX (over-

expressing ABCG2) cells and MCF7 cells. DRG-16 was more potent against the MCF7 parental cell line (IC_{50} = 65 pM [95% confidence interval = 59–72 pM]) compared to MCF7-MX cells (IC_{50} = 2.2 nM [1.5–3.1 nM]) (Figure 65.A). Conversely, the PBD-monomer SG-2901 induced a similar growth inhibition against MCF7 parental cells (IC_{50} = 452 nM [130-1500 nM]) and MCF7-MX cells (IC_{50} = 780 nM [770-790 nM]) (Figure 65.B).

A.

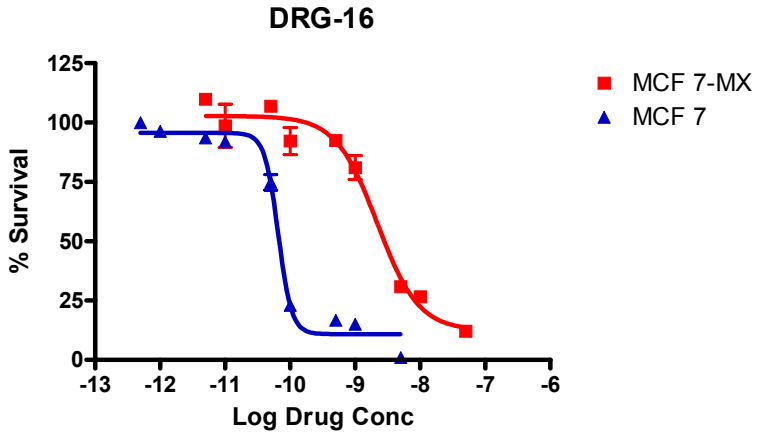

B.

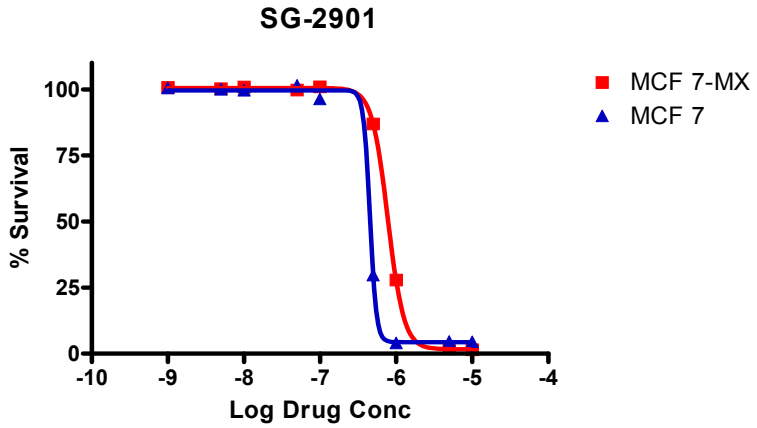

Figure 65. Impact of ABCG2 on the cytotoxic effect of DRG-16 (A) and SG-2901 (B) in MCF7-MX cells (over-expressing the transporter) (■) and in MCF7 parental cell line (▲). Results are means ± SEM of triplicate.

The study was extended to all PBD derivatives. Vinblastine is not a substrate of ABCG2 and was used as a negative control (Litman, Brangi et al. 2000). Mitoxantrone is a substrate of ABCG2 and was used as a positive control (Doyle, Yang et al. 1998). Overall, the PBD-dimers demonstrated greater growth inhibition than the PBD-monomers in MCF7 cells (Table 13). The most active compounds were ELB-21 and DRG-16 with an IC_{50} of 0.04 nM and 0.06 nM, respectively in MCF7 cells. The least active compounds were SG-2901 and SJG-244 (270 nM and 250 nM, respectively).

	MCF7-MX				MCF7			
	Control		+FTC		Control		+FTC	
	IC_{50} (nM)	SD	**IC_{50} (nM)**	SD	**IC_{50} (nM)**	SD	**IC_{50} (nM)**	SD
SG-2781	32	24	7.3	3.2	9.9	9.8	9	7.7
SG-2796	9	2.6	4.8	0.1	3.5	0.4	3.9	0.6
SG-2797	40	20	12	3.3	8.7	0.7	8.9	0.9
SG-2819	25	3.7	13	0.8	9.7	0.4	9.4	0.5
SG-2820	72	36	20	6.5	22	3.8	22	0.1
SG-2823	25	3.1	5.8	0.7	4.5	1.1	4.7	1.6
SG-2825	260	90	200	120	110	55	120	55
SG-2897	5.8	1.8	1.4	0.2	0.7	0.2	0.8	0.2
SG-2900	270	16	130	19	94	14	110	8.6
SG-2901	470	330	290	200	270	180	290	170
SG-2902	*n.d.*	*n.d.*	*n.d.*	*n.d.*	*n.d.*	*n.d.*	*n.d.*	*n.d.*
SJG-244	1200	410	460	220	250	160	280	140
SJG-136	26	4.3	2.4	0.6	0.6	0.1	0.6	0.0
DSB-120	470	33	46	7.4	28	4.6	30	6.5
DRG-16	1.8	0.3	0.2	0.03	0.06	0.01	0.06	0.01
ELB-21	1.4	0.2	0.1	0.01	0.04	0.01	0.04	0.01
Vinblastine	0.7	0.1	0.7	0.1	1.0	1.1	1.2	1.2
Mitoxantrone	2200	780	32	9.5	17	2.1	13	4.1

Table 13. Sensitivity of MCF7-MX and MCF7 to pyrrolobenzodiazepine derivatives. Values are means ± SD of IC_{50} of n = 3 experiments performed in triplicate.

The ratio of IC_{50} between the 2 cell lines was used as an indirect way to assess transporter dependency. The ratio for vinblastine, a negative control was close to 1 in contrast to the positive control, mitoxantrone with a ratio of 120 (Figure 66). Overall, the PBD-dimers had ratios of 37, 35 and 29 between MCF7-MX and MCF7 for DRG-16, ELB-21 and SJG-136, respectively. DSB-120 had the lowest ratio, 15.

The PBD-monomers had IC_{50}s ratios ranging from 2.4 (SG-2901) to 8.4 (SG-2897). SG-2897, the most potent PBD-monomer in MCF7 (IC_{50} = 0.7 nM) showed the highest ratio between MCF7-MX and MCF7. SG-2901, is the least potent PBD-monomer (IC_{50} = 270 nM) and had the lowest ratio. Similarly, DSB-120, the least potent PBD-dimer in MCF7 (IC_{50} = 28 nM) had the lowest ratio between the 2 cell lines (Figure 66).

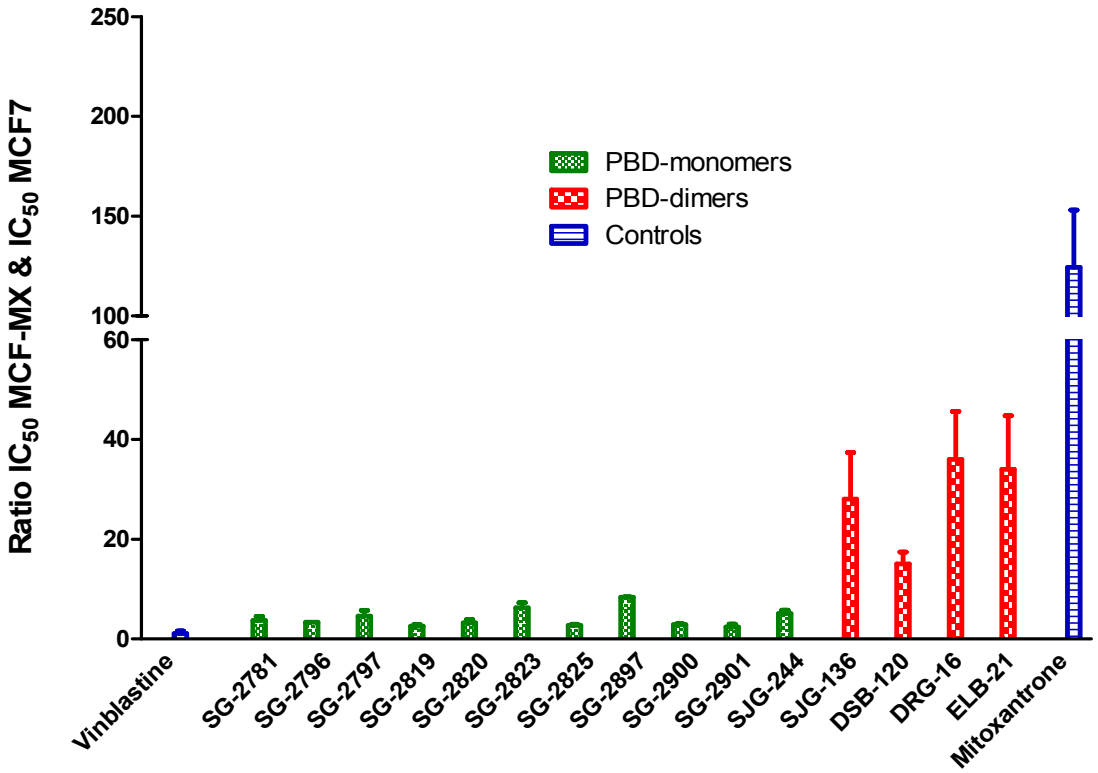

Figure 66. Ratio between the IC_{50} to the PBD derivatives in MCF7-MX and MCF7-WT. The PBD-dimers are represented in blue and the PBD-monomers in orange. The ratio between the IC_{50}s for vinblastine and mitoxantrone have also been reported as a negative and positive controls, respectively. Results are means ± SEM of n = 3 experiments performed in triplicate.

4.2.2.1.3 Impact of fumitremorgin C on the growth inhibitory effect of the PBDs

To confirm that the difference observed above was due to ABCG2 interaction, the growth inhibitory effect of the PBDs was determined in presence of absence of Fumitremorgin C (FTC), a specific ABCG2 inhibitor (Rabindran, Ross et al. 2000). A concentration of FTC of 10 μM inhibits the transporter and was confirmed as inducing no significant growth inhibition in the cell lines (Robey, Honjo et al. 2001).

The ratio between the IC_{50} of the PBDs was determined in presence or absence of FTC in MCF7-MX cells. Pre-exposure of MCF7-MX to FTC increased the growth inhibitory effect of the 4 PBD-dimers and 6/11 PBD-monomers. For instance, MCF7-MX cells were ~10-fold more sensitive to the PBD-dimers and ~2- to ~4-fold more sensitive to some PBD-monomers (SG-2781, SG-2797, SG-2820, SG-2823, SG-2897 and SJG-244).

Conversely, the pre-exposure of MCF7-MX cells to FTC had no effect on the growth inhibitory effect of the PBD-monomers SG-2796, SG-2819, SG-2825, SG-2900 and SG-2901: the ratio was never greater than 2 (Figure 67).

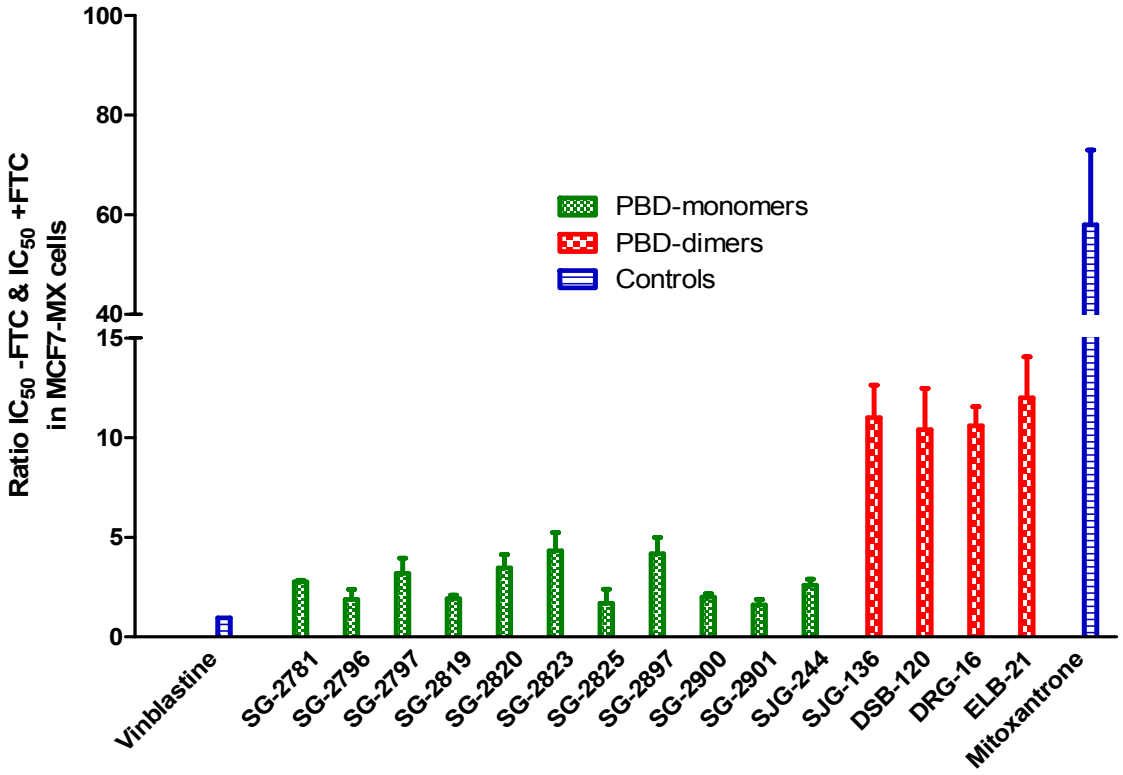

Figure 67. Ratio between the IC_{50} to the PBD derivatives when MCF7-MX cells where pre-treated or not with FTC. Results are presented as the ratio – FTC versus + FTC. Results are means ± SD of 3 experiments performed in triplicate.

Pre-treatment of MCF7 WT cells with FTC had no effect on the growth inhibitory effect of all PBDs (Table 13). These results provide evidence of the differential substrate specificity of the PBDs to ABCG2: The PBD-dimers are high affinity substrates of the transporter in contrast to the PBD–monomers, 6/11 being low affinity substrates. However, the affinity of the PBD-dimers for the transporter is ~3-fold lower than the positive control, mitoxantrone. The PBD-dimers may therefore be considered as substrate of ABCG2 with intermediate affinity when compared to the high affinity substrate, mitoxantrone. The PBD-monomeres may be considered as low affinity substrates.

4.2.2.2 Caco-2 model of permeability: Impact of FTC on the permeability of the PBD derivatives.

The Caco-2 transwell assay has been widely used to investigate the transport mediated by P-gp. However, the differentiated enterocytes also express other ABC transporters, such as ABCG2, localised at the apical side of the cells. Previously, the PBD dimers, SJG-136 and DRG-16, were shown to be actively transported from the basal to the apical side suggesting that the compounds are recognised by a transporter and extruded on the other side of the well. One way to investigate ABC transporter substrate specificity of PBD-dimers is to incubate the cells in this system together with a specific inhibitor.

Incubation with FTC blocks the ABCG2 transporter and if a test compound is a substrate of ABCG2, the apparent permeability from A to B (Papp $_{A\rightarrow B}$), *i.e*

absorption should be increased while the apparent permeability from B to A (Papp $_{B\rightarrow A}$), *i.e.* secretion will be decreased as represented in Figure 68.

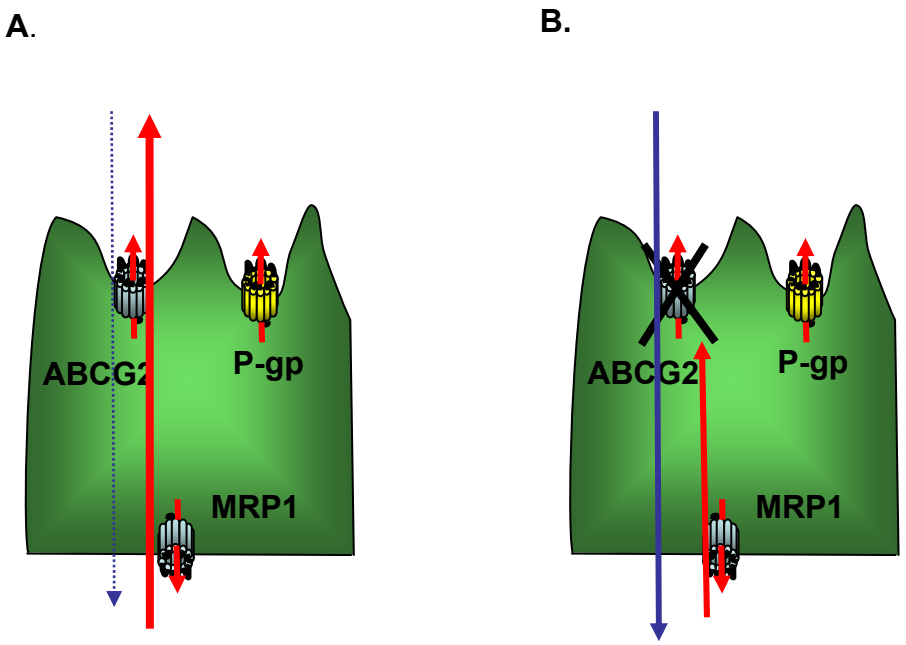

Figure 68. Hypothetical model of the impact of FTC on the transport of substrates of ABCG2. **A**. A test compound, passes through the membrane by passive diffusion from the apical to the basal chamber representing the absorption (↓). The secretion, the active transport from the basal to the apical side (↑) is greater than the absorption in the case of ABCG2 substrate specificity of the test compound. **B**. The cells are treated with FTC which blocks specifically the transporter ABCG2. In the case of ABCG2 substrate specificity of a test compound, the absorption should be increased and the secretion decreased.

The impact of the pre-treatment with FTC was evaluated on the transport activity of 2 PBD-dimers, SJG-136 and DRG-16 and, on the transport activity of the PBD-monomer SG-2897. The absorption of SJG-136 was increased when the cells were treated with FTC: from 9.9 ± 2.7 x 10^{-6} cm/sec for the control cells up to 16 ± 3.9 x 10^{-6} cm/sec, when the cells were pre-treated with FTC, so a ~1.6-fold increase in the absorption (no significant difference could have been seen with the secretion) (Figure 69). Similarly, the pre-exposure with FTC induced a higher absorption of the PBD-dimer, DRG-16, across the membrane (from 2.8 ± 0.7 x 10^{-6} cm/sec for the

control cells to 5.9 ± 0.5.x 10^{-6} cm/sec for the pre-treated cells), so a ~2.1-fold increase in the absorption. In addition, the pre-exposure with FTC also induced a slight decrease (~1.2-fold) of the secretion of DRG-16. Conversely, the pre-exposure with FTC did not modify the permeability of PBD-monomer SG-2897.

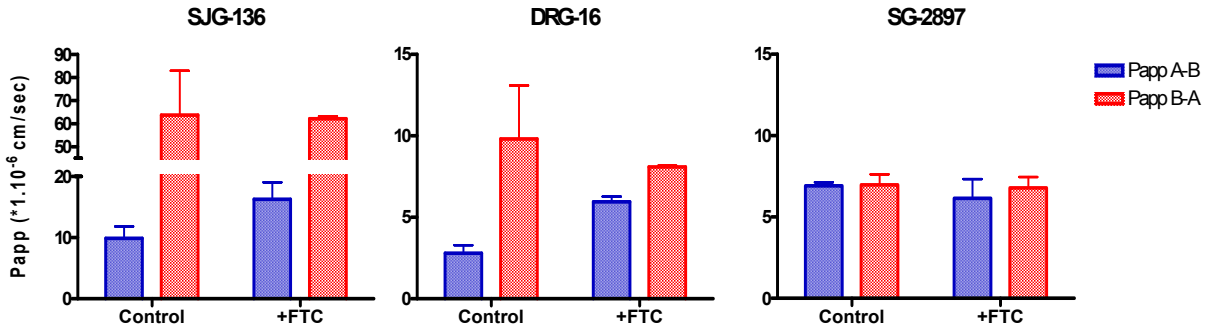

Figure 69. Impact of FTC on the permeability of the PBD derivatives as determined by the transwell assay. The permeability from the apical side to the apical side is represented in blue (Papp $_{A\rightarrow B}$) which corresponds to the absorption. The secretion, the permeability from the basal to the apical side (Papp $_{B\rightarrow A}$) is represented in red. Results are means ± SEM of triplicate.

These results provide evidence of ABCG2 substrate specificity of PBD-dimers as revealed by the impact of the FTC on the absorption of the compounds, in contrast to the PBD-monomer tested. The impact of FTC on secretion did not show a significant effect. One explanation may be that when the secretion was measured, FTC was incubated in the basal chamber. ABCG2 is localised at the apical side, significant amounts of FTC may not have reached the transporter to block it.

4.2.2.3 Chemical structure analysis to explain ABCG2 substrate specificity of the PBDs

ABCG2 substrates share a common set of physico-chemical properties such as a high polarity, a greater number of aromatic rings and hydrophilic groups (Nakagawa, Saito et al. 2006). Some of these features are present among some of the PBDs. In order to define the specific features relative to ABCG2 substrate specificity for the PBDs, the ratio between – FTC versus + FTC observed in MCF7-MX cells was plotted against the number of (N+O) atoms. There was a significant correlation between these 2 parameters suggesting that (N+O) was related to ABCG2 substrate specificity ($r^2 = 0.976$; $P_{value} < 0.0001$) (Figure 70).

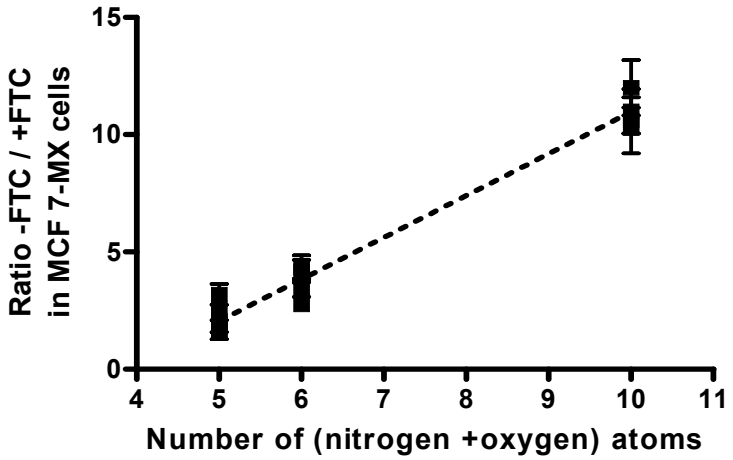

Figure 70. Relationship between the ratio (– FTC versus + FTC in MCF7-MX cells) for all PBDs and the number of (oxygen and nitrogen) atoms. Results are means ± SEM of n = 3 experiments performed in triplicate.

These results provide evidence of a relationship between the electrophilic characteristics of PBD derivatives and ABCG2 substrate specificity.

Oxygen atoms are more electronegative than nitrogen atoms. The potential interaction between a PBD-monomer and ABCG2 will be different according to the type of atoms. Therefore, arbitrary values have been attributed to nitrogen and oxygen atoms according to their electro-negativity. An arbitrary value of 1 is given for a nitrogen atom. A value of 2 is given to an oxygen atom.

The electronegativity of the fluoro group of SG-2797 was considered as similar as an atom of nitrogen and given an arbitrary value of 1. Indeed, the spatial distance between the different atoms of fluor is too limited for them to make an impact as separated entities. The ratio between (–/+ FTC) was plotted against the electronegativity of the different compounds and demonstrated a good correlation (r^2 = 0.985; $P_{value} < 0.0001$) (Figure 71).

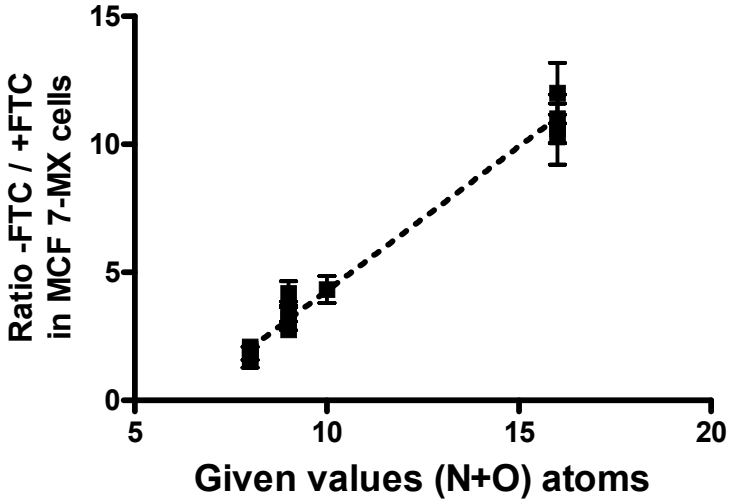

Figure 71. Relationship between the ratio (– FTC versus + FTC in MCF7-MX cells) for all the PBDs and the number of arbitrary values given for (oxygen and nitrogen) atoms. Results are means ± SEM of n = 3 experiments performed in triplicate.

However, the ratio of SG-2781 was ~2.8 while its structure contained 6 (N+O) atoms. The structure of SG-2897 had the same number of (N+O) atoms but a

ratio between – FTC / + FTC of ~4.2. The major difference is that the position of the nitrogen is within an aromatic ring and this may have generated a greater interaction with the transporter (Figure 72).

SG-2781

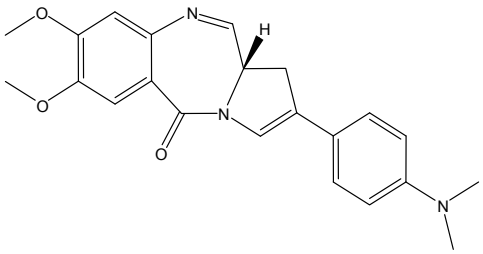

SG-2897

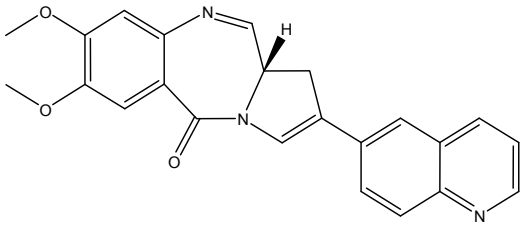

Figure 72. Chemical structure of 2 PBD-monomers SG-2781 and SG-2897.

It could be argued that the electronic environment of the nitrogen atom plays an important role in the electrostatic potential interaction with ABCG2. One way to investigate the chemical reactivity of an atom is to calculate its partial charge using the extended Hückel calculation. This parameter can be calculated *in silico* using Chem*3D*. As a result, the partial charge on the nitrogen (amine) of SG-2781 is positive (0.22). In contrast, the nitrogen (pyridine) of SG-2897 has a negative partial charge (- 0.23). When only the C2 extremity of the PBD-monomers was considered, the number (N+O) atoms, negatively charged, as determined by the extended Hückel calculation, was determined for all PBDs (Figure 73).

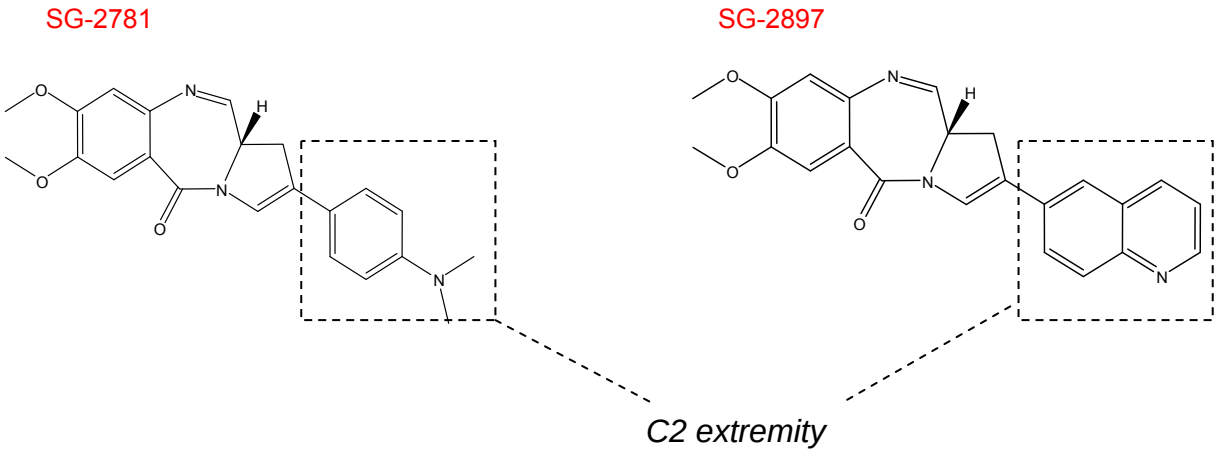

Figure 73. C2 extremity of the PBD-monomers, SG-2781 (*left*) and SG-2897 (*right*) involved in ABCG2 substrate specificity.

The electronic environment of the C2 extremity would therefore impact on the potential interaction with the transporter: Nitrogen, negatively charged in SG-2897, was considered to be associated with greater substrate specificity for the transporter. Therefore, arbitrary values of 1 and 2 were attributed for a nitrogen or an oxygen atom, respectively, which are negatively charged at the C2 extremity (in addition to the values (arbitrary values of (N+O) previously described). The potential interaction of the PBD derivatives with ABCG2 would follow the equation (1):

$$\mathbf{[(}\boldsymbol{n}\ \mathbf{(1/2N+O)}_{\boldsymbol{molecule}} + \boldsymbol{n}\ \mathbf{(1/2N^{-}+O^{-})}_{\boldsymbol{extremity}}\mathbf{]} \quad (1)$$

However, this equation can not be applied to all PBD-monomers as some of them have a similar number of [(N+O) atoms] and [(N+O) atoms negatively charged] at the C2 extremity and demonstrated a different ratio. For instance, SG-2820 has a

ratio between the IC_{50} (- /+ FTC) in MCF7-MX cells of ~3.23 despite having the same potential as SG-2897 as described by the equation (1) (ratio SG-2897 ~4.2). The major difference between the 2 compounds is the presence of a quinoline substituent in the chemical structure of SG-2897 (Figure 74).

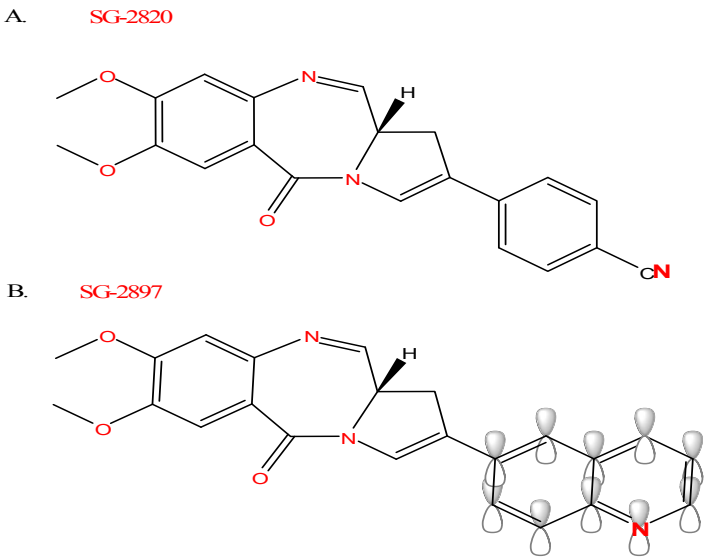

Figure 74. Chemical structure of two PBD-monomers SG-2820 (A) and SG-2897 (B). Atoms involved in ABCG2 interaction are represented in red (defined by a negative partial charge as determined by the extended Hückel calculation). The π orbitals of the quinoline substituent of SG-2897 have been represented and may participate in the overall interaction to the transporter.

In an aromatic system, by definition, the electrons are organised in π orbitals. Electrons of the quinoline substituent may be shared with the electrons of a surrounding planar group, thus inducing a greater interaction. This phenomenon represents the π-π stacking interaction. It can be argued that such interaction can also be found in benzene rings such as the one found in SG-2820 and other PBD-monomers. However, the presence of benzene only, was shown not to demonstrate any greater interaction with ABCG2. Two hypotheses can be proposed:

- The presence of shared π orbitals between two or more aromatic rings would be associated with greater interaction with a surrounding aromatic ring.
- The presence of an electronegative group within the ring may be the prerequisite for an enhanced interaction with the transporter.

The latter parameter has been incorporated into an equation trying to define the potential interaction with the transporter.

ABCG2 potential interaction=

$$\mathbf{[(}\boldsymbol{n}\ \mathbf{(1/2N+O)}_{\boldsymbol{molecule}} + \boldsymbol{n}\ \mathbf{(1/2N^{-}+O^{-})}_{\boldsymbol{C2\text{-}aryl\ extremity}} + \ \boldsymbol{n}\ \mathbf{(1/2N^{-}+O^{-})}_{\boldsymbol{aromatic\ ring}}\mathbf{]}\ (2)$$

The relationship between ABCG2 potential interaction as defined by equation (2) and the ratio between the IC_{50}s (-/+ FTC in MCF7-MX cells) demonstrated a significant correlation ($r^2 = 0.991$; $P_{value} < 0.0001$) (Figure 75).

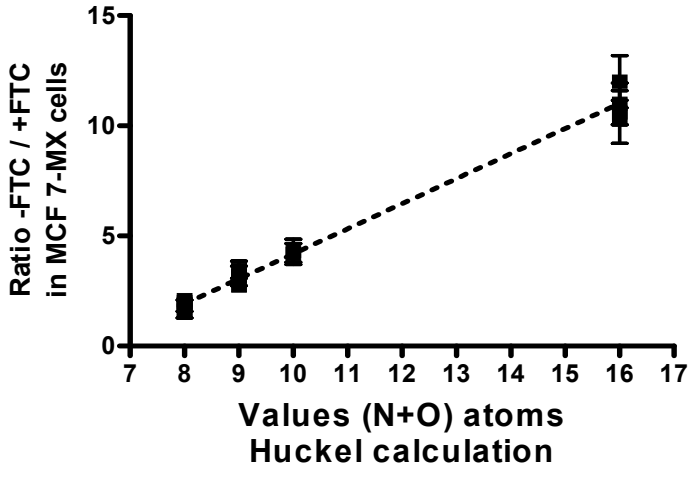

Figure 75. Relationship between the ratio (– FTC versus + FTC in MCF7-MX cells) for all PBDs and the number of arbitrary values given for (oxygen and nitrogen) atoms as determined by the equation (2). The ratio Results are means ± SEM of n = 3 experiments performed in triplicate.

These results support the hypothesis that the interaction between ABCG2 and the PBDs is driven by electrostatic forces and π-π interactions. The PBDs, with a greater electronegative potential, are more likely to interact with the transporter and to be transported out of the cell. It could be suggested that the interaction between the negatively charged atoms of the PBDs and ABCG2 is therefore likely to be due to the presence of electropositive residues within the binding pocket of the transporter.

4.2.2.4 Impact of ABCG2 polymorphism on substrate specificity of the PBDs

To date, three major variants of ABCG2 have been documented on the basis of changes in the amino acid moiety at position 482: the wild type form has arginine at that position (Allikmets, Schriml et al. 1998; Allen, Jackson et al. 2002), whereas the mutated forms have glycine or threonine (Doyle, Yang et al. 1998). It was shown that a mutation at position 482 can alter substrate specificity of a wide range of compounds such as rhodamine 123 (Honjo, Hrycyna et al. 2001), anthracyclines and mitoxantrone (Robey, Honjo et al. 2003).

In this study, the impact of the mutation at position 482 on the substrate specificity of the PBDs was evaluated in breast cancer cell lines MDA-MB-231 transfected with vector control (V8 cell line), plasmid containing the cDNA of ABCG2 wild type sequence at position 482 (R12 cell line) or the sequence mutated at position 482 (T3 cell line) (Kindly provided by Nakanishi T, University of Maryland, Baltimore).

4.2.2.4.1 Expression of ABCG2 in different isogenic MDA-MB-231 cell lines

The level of ABCG2 protein expression was confirmed by western blot. R12 and T3 cells express similar levels of ABCG2. In contrast, the V8 cells do not express the transporter (Figure 76).

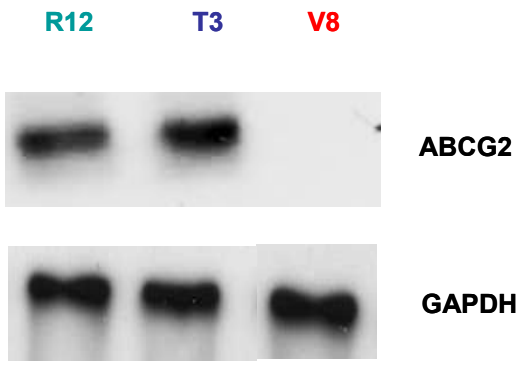

Figure 76. ABCG2 protein expression in the different MDA-MB-231 cell lines transfected with plasmid containing a wild type (R482) or mutated (T482) ABCG- *cDNA* with the appropriate vector control. R12 cell line expresses the wild type form of ABCG2 at position 482 (arginine). T3 cell line expresses the mutated form of the transporter at the position 484 (threonine). V8 cells have been transfected with the vector control. ABCG2 protein migrated at ~72 kDa.

4.2.2.4.2 Growth inhibition Assay of PBDs in MDA-MB-231 expressing ABCG2 with different amino acid at position 482

Initially, the cytotoxic effect (IC_{50}) of 2 PBD derivatives, one PBD-dimer DRG-16 and one PBD-monomer SG-2781 was determined using MDA-MB-231 cells expressing ABCG2 with different genotype at position 482 (Figure 77). DRG-16 induced a lower cytotoxic effect against the MDA-MB-231 / R12 cells transfected with wild type form of ABCG2 (R482) (IC_{50} = 0.13 nM [95% CI = 0.11 - 0.16 nM]) compared to MDA-MB-231 / V8 cells transfected with the empty vector (IC_{50} = 55 pM [44 – 67 pM]) *e.g.* ~2.4-fold decrease in sensitivity in the cell line expressing the transporter (Figure 77.A). A further decrease in sensitivity was seen in MDA-

MB-231 / T3 cells expressing the mutated form of ABCG2 (T482) (IC_{50} = 0.47 nM [0.22 - 0.99 nM]). This equals to a ~8.5-fold decrease in sensitivity compared to the MDA-MB-231 / V8 cells. The PBD-monomer SG-2781 induced a similar growth inhibition against MDA-MB-231 / V8 cells (IC_{50} = 14 nM [10-20 nM]), MDA-MB-231 / R12 cells (IC_{50} = 15 nM [11-21 nM]), and MDA-MB-231 / T3 cells (IC_{50} = 17 nM [5 - 56 nM]) (Figure 77.B).

A.

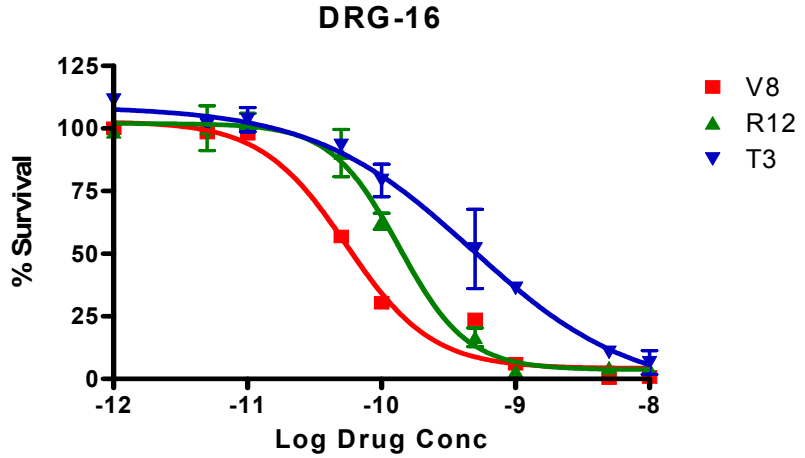

B.

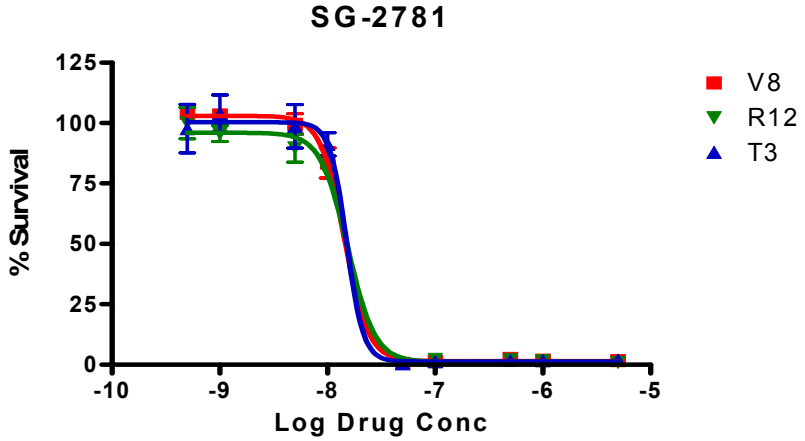

Figure 77. Impact of ABCG2 polymorphism on the cytotoxic effect of DRG-16 (A) and SG-2901 (B) as determined by the SRB assay using MDA-MB-231 / R12 cells expressing the wild type (R482) transporter (▼) or MDA-MB-231/ T3 cells expressing the mutated form (T482) (▲). MDA-MB-231 / V8 cells transfected with an empty vector have also been represented (■). Results are means ± SEM of triplicate.

Overall, the PBD dimers demonstrate greater potency in MDA-MB-231 cells than the PBD-monomers (Table 14). The most active compounds were DRG-16 and SJG-136 with an IC_{50} of 0.05 nM [± 0.01 nM] and 0.76 nM [± 0.18 nM], respectively. The least active compounds were SG-2825 and SJG-244 (990 nM [± 180 nM] and 380 nM [± 120 nM], respectively).

	V8		R12		T3	
	IC_{50} (nM)	SD	**IC_{50} (nM)**	SD	**IC_{50} (nM)**	SD
SG-2781	15	1.4	22	0.1	22	1.0
SG-2819	15	0.0	18	1.3	21	1.5
SG-2820	15	1.2	23	0.3	32	5.1
SG-2823	6.8	1.3	13	0.8	20	4.4
SG-2825	990	180	1200	140	1400	150
SG-2897	1.1	0.2	1.8	0.2	2.1	0.3
SG-2900	210	63	240	35	290	64
SG-2901	350	36	370	24	420	68
SJG-244	380	120	530	76	880	66
SJG-136	0.76	0.18	3.1	0.24	4.2	0.04
DSB-120	47	20	71	12	130	40
DRG-16	0.05	0.01	0.2	0.01	0.2	0.04
Vinblastine	1.4	0.2	1.2	0.08	n.d.	n.d.
Mitoxantrone	8.4	1.3	81	18	340	110

Table 14. Pyrrolobenzodiazepine derivatives IC_{50}s for MDA-MB-231 breast cancer cell lines expressing different genotypes of ABCG2. Results are means ± SD of n = 3 experiments performed in triplicate. N.d. not determined.

In order to evaluate the differential impact of the genetic polymorphism of ABCG2 among the PBDs, the ratio of the IC_{50}s between R12 and V8 as well as the ratio between T3 and V8 were calculated. PBD-dimers showed the highest R12/V8 ratios: 4.1, 3.6 and 3.4-fold for SJG-136, DRG-16 and DSB-120, respectively (Table 15). Among the PBD-monomers, only SG-2823 had a ratio of 2, suggesting a low affinity for ABCG2 for this compound. The rest of the PBD-monomers had similar

IC_{50}s in the 2 cell lines ranging from 1.1 for SG-2901 up to 1.6 for SG-2820 and SG-2897 considering PBD-monomers, apart from SG-2823, as being non substrate of the transporter.

	Ratio R12 / V8		Ratio T3 / V8		Ratio T3 / R12	
	Ratio	SD	**Ratio**	SD	**Ratio**	SD
SG-2781	1.4	0.1	1.5	0.0	1.0	0.1
SG-2819	1.2	0.1	1.5	0.1	1.2	0.2
SG-2820	1.6	0.1	2.2	0.2	1.4	0.3
SG-2823	2.0	0.1	2.9	0.3	1.4	0.3
SG-2825	1.2	0.2	1.4	0.1	1.2	0.4
SG-2897	1.6	0.0	1.9	0.1	1.2	0.1
SG-2900	1.4	0.0	1.2	0.1	1.2	0.1
SG-2901	1.1	0.1	1.2	0.3	1.2	0.4
SJG-244	1.4	0.1	2.4	0.4	1.7	0.2
SJG-136	4.1	1.7	5.6	0.4	1.4	0.8
DSB-120	3.4	0.7	3.5	0.8	1.4	0.2
DRG-16	3.6	0.3	4.9	1.1	1.4	0.5
Vinblastine	0.9	0.1	n.d.	n.d.	n.d.	n.d.
Mitoxantrone	9.7	1.4	40	7.4	4.3	1.3

Table 15. Pyrrolobenzodiazepine derivatives IC_{50}s ratios for MDA-MB-231 breast cancer cell lines expressing different genotypes of ABCG2. Results are means of ratios ± SD of n = 3 experiments performed in triplicate.

When considering the ratio T3 / V8, the PBD-dimers had again the highest ratios: 5.6-, 4.9- and 3.5-fold for SJG-136, DRG-16 and DSB-120, respectively, suggesting that the PBD-dimers are also substrates of the mutated form of ABCG2. The PBD-monomers, SG-2823, SJG-244 and SG-2820 were also affected with ratios of 2.9, 2.4 and 2.2, respectively. Among the other PBD-monomers, the ratios were ranging from 1.2 for SG-2901 up to 1.9 for SG-2897. These results show that 3 PBD-monomers could be substrates of the mutated form of ABCG2.

Taken together, these data suggest a differential impact of the mutated form of ABCG2 on the growth inhibitory effect of the PBD-monomers. SJG-244 has a minimal number of (oxygen and nitrogen) atoms and is predicted to be associated with minimal interaction with ABCG2 according to the equation (2). However, the ratio for SJG-244 between the IC_{50} in MDA-MB-231 / T3 cells and the IC_{50} in MDA-MB-231/ R12 cells was the highest among the PBDs (~1.7-fold) (Table 14). The presence of an aromatic ring with π orbitals, at the C8 extremity, appears to impact on the substrate specificity of the mutated form of ABCG2 (Figure 78).

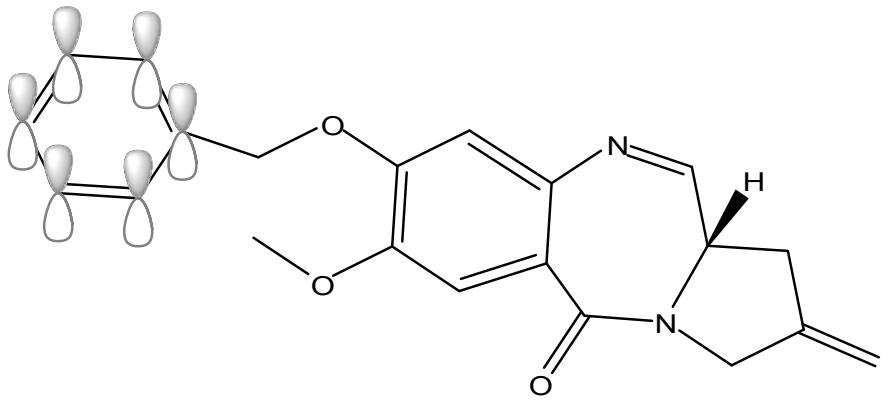

Figure 78. Chemical structure of PBD-monomer, SJG-244. The π orbitals have been represented at the C8 extremity which may participate in the overall affinity for ABCG2.

Overall, these results provide evidence that the PBD-dimers are substrates of ABCG2 for both the wild type and the mutated form. The latter seems to increase the resistance of this class of compounds. Similar increase in resistance was seen for most of the PBD-monomers. These results have been compared to well-known ABCG2 substrate: mitoxantrone. The impact of ABCG2 polymorphism on the growth inhibitory effect of mitoxantrone has been a matter of debate. In our hands, MDA-MB-231/ V8 cells were 9.7-fold more sensitive to mitoxantrone than MDA-

MB-231/ R12 cells confirming ABCG2 substrate specificity of this compound. In addition, MDA-MB-231/ V8 cells were 40.1-fold more sensitive to mitoxantrone than MDA-MB-231/ T3 cells representing a ~4.3-fold increase in resistance between the wild type and the mutated form the transporter. Also, it is noteworthy that the impact of the mutated form of ABCG2 on the sensitivity to mitoxantrone was ~10-fold greater than the impact on the sensitivity of the PBD-dimers suggesting that the former is associated with a higher affinity to the transporter.

Overall, these data suggest that the mutation at position 482 (threonine) increases ABCG2 efflux compared to the wild type form for compounds with a greater number of electrophilic atoms and aromatic rings.

4.2.2.4.3 Comparative study between the 2 models investigated: MCF7-MX cells and MDA-MB-231 cell lines.

Data in MCF7-MX cells suggested that all the PBD-dimers and some PBD-monomers (SG-2781, SG-2797, SG-2820, SG-2823, SG-2897 and SJG-244) might be substrates of ABCG2. ABCG2 substrate specificity of the PBD-dimers was confirmed using the MDA-MB-231 cells. In contrast to mitoxantrone, the PBD-dimers were associated with a low affinity to ABCG2. Only one PBD monomer, SG-2823, was suggested as low affinity substrate (ratio between the IC_{50} in cell line expressing the transporter and the IC_{50} in the cell line expressing no transporter > 2). The 2 cellular models MCF7-MX and MDA-MB-231/ABCG2 differ by multiple aspects but especially by the level of expression of the protein ABCG2. MCF7-MX

cells express higher levels than MDA-MB-231/ABCG2 and might therefore be more amenable to detect differences between the compounds.

A relationship between the ratios (-/+ FTC) in MCF7-MX cells and the ratios in the R12/V8 (described previously, section. 4.2.2.1.c) was plotted for all PBDs. The correlation was highly significant ($r^2 = 0.96$; $P_{value} < 0.0001$) (Figure 79). The relationship was less significant when considering the ratios in the T3/V8 ($r^2 = 0.87$; $P_{value} < 0.0001$). This is probably related to the expression of the wild type (arginine at position 482) transporter in MCF7-MX cells (Honjo, Hrycyna et al. 2001).

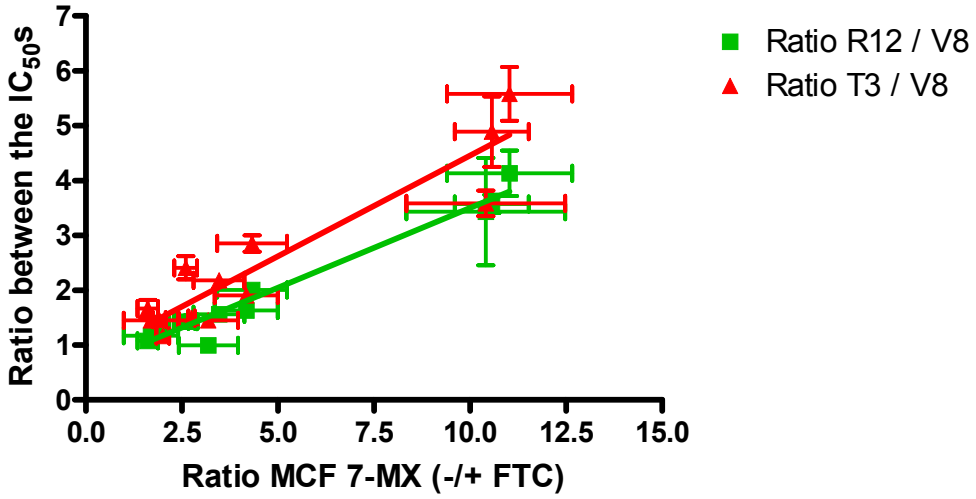

Figure 79. Relationship between the ratio (– FTC / + FTC in MCF7-MX cells) for all the PBDs and the ratio for MDA-MB-231 cell lines expressing different genotypes of ABCG2. The ratio between the IC_{50} in MDA-MB-231/ R12 cells expressing the wild type (R482) transporter and the IC_{50} in MB-231/ V8 cells (transfected with an empty vector) is represented in green. The ratio between the IC_{50}s in MDA-MB-231/ T3 cells expressing the mutated form (T482) of ABCG2 and the IC_{50}s in MB-231/ V8 cells is represented in red. Results are means ± SEM of n = 3 experiments performed in triplicate.

These results provide evidence that the factors related to substrate specificity of the PBD derivatives to ABCG2 (defined in MCF7-MX cells) can be applied to other cell lines expressing the wild type transporter such as the MDA-MB-231 cells transfected with plasmid containing a wild type (R482) ABCG2-*cDNA*.

4.3 Discussion

The experiments presented in this chapter evaluated the impact of the expression of 2 different ABC transporters, on the growth inhibitory effect of the PBD derivatives evaluated.

All PBD-dimers but only one PBD-monomer, SG-2823 were demonstrated to be substrates of MRP1 (ABCC1). This was shown using a cell line expressing the transporter highly (the lung cancer cell line A549) and, by pre-incubation with an optimal concentration of MK-571, a specific inhibitor of the transporter. The coupling of SG-2823 to glutathione by glutathione-S-transferase (GST) was also identified using inhibitors of both the synthesis of glutathione (BSO) and the enzymatic coupling (dicumarol). In both cases, the resistance to this particular compound was completely abrogated. These results provide evidence of a complimentary role of GSH / GST in the relative resistance mediated by MRP1 to the PBD-monomer SG-2823.

However, coupling to glutathione by GST was not involved in the mechanism of efflux of the PBD-dimer, DSB-120, as the treatment with dicumarol, did not sensitise the A549 cells significantly. The inhibition of the synthesis of glutathione by BSO affected the growth inhibitory effect of PBD-monomers differentially.

PBDs with a greater electrophilic potential at the C2 extremity, such as SG-2823, were more subject to the impact of glutathione. Similarly, the growth inhibitory effect of PBD-dimer, DSB-120 was affected by the concentration of GSH.

The reaction of the PBDs with glutathione was shown to occur spontaneously and / or by conjugation with GST depending on the electrophilicity at the C2 extremity. The fact that DSB-120 did not include an electrophilic extremity suggested that another entity within the structure is responsible for the coupling to GSH. These results were confirmed using a LC/MS method. The spontaneous formation of the conjugate GSH-PBD-monomer was demonstrated. Compounds with a greater electrophilic characteristic formed the conjugate more rapidly.

Indeed, the chemical structure of SG-2823 seems likely to play a major role in the ability of this compound to conjugate to GSH. SG-2823 has a carbonyl moiety at its extremity in contrast to SG-2819; the latter not being extruded by MRP1. GSH has a -SH moiety which is characterised as being a strong nucleophile. By definition, it may attack a surrounding compound at its electrophilic centre. Two models could be proposed. First, the carbonyl-carbon of SG-2823 is an electrophile and therefore may undergo nucleophile addition (Figure 80).

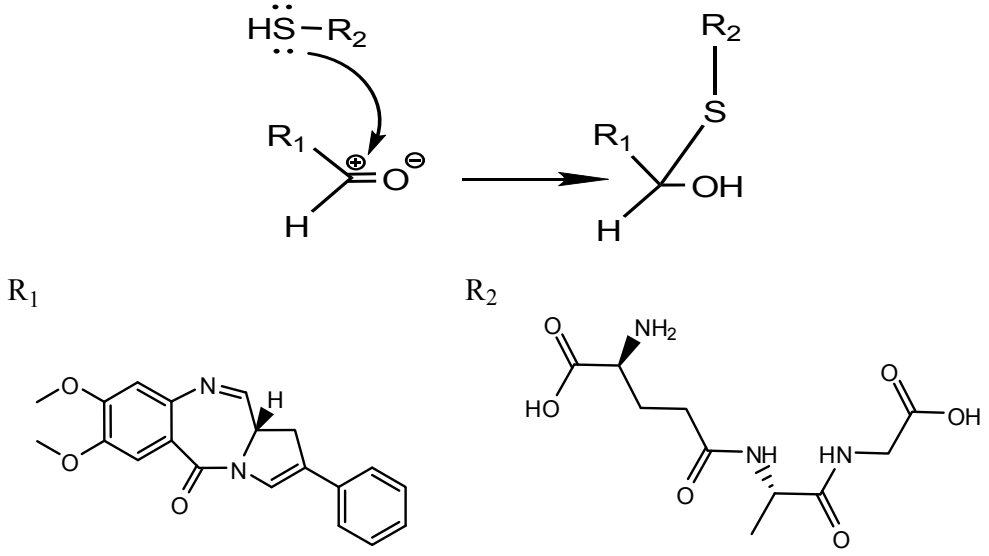

Figure 80. Proposed model of the conjugation of SG-2823 to GSH; a nucleophilic addition.

The nucleophilic addition may lead to the spontaneous formation of the GS-SG-2823 conjugate. Its hypothetical structure is represented in Figure 81.

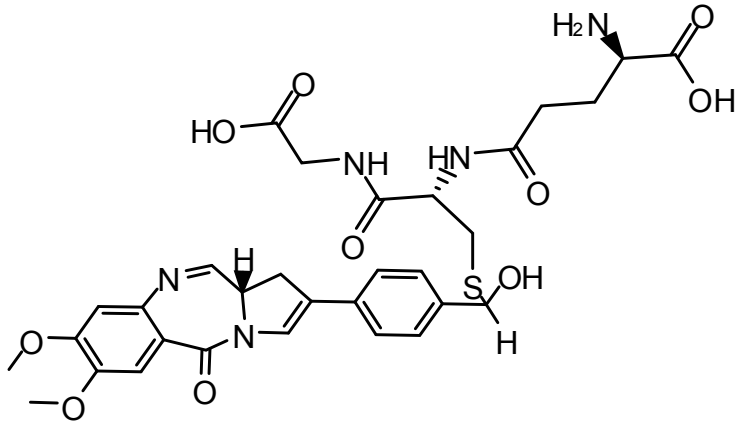

Figure 81. Proposed structure of the GS-SG-2823 conjugate.

However, hence formed, the SG moiety is very close to the phenol group which does not allow the former to remain attached; thus, the conjugated form is highly unstable.

SG-2823 also has an electrophilic centre at its C11 position. It may interconvert into the imine form and enable SG-2823 to alkylate the SH moiety of GSH (Figure 82).

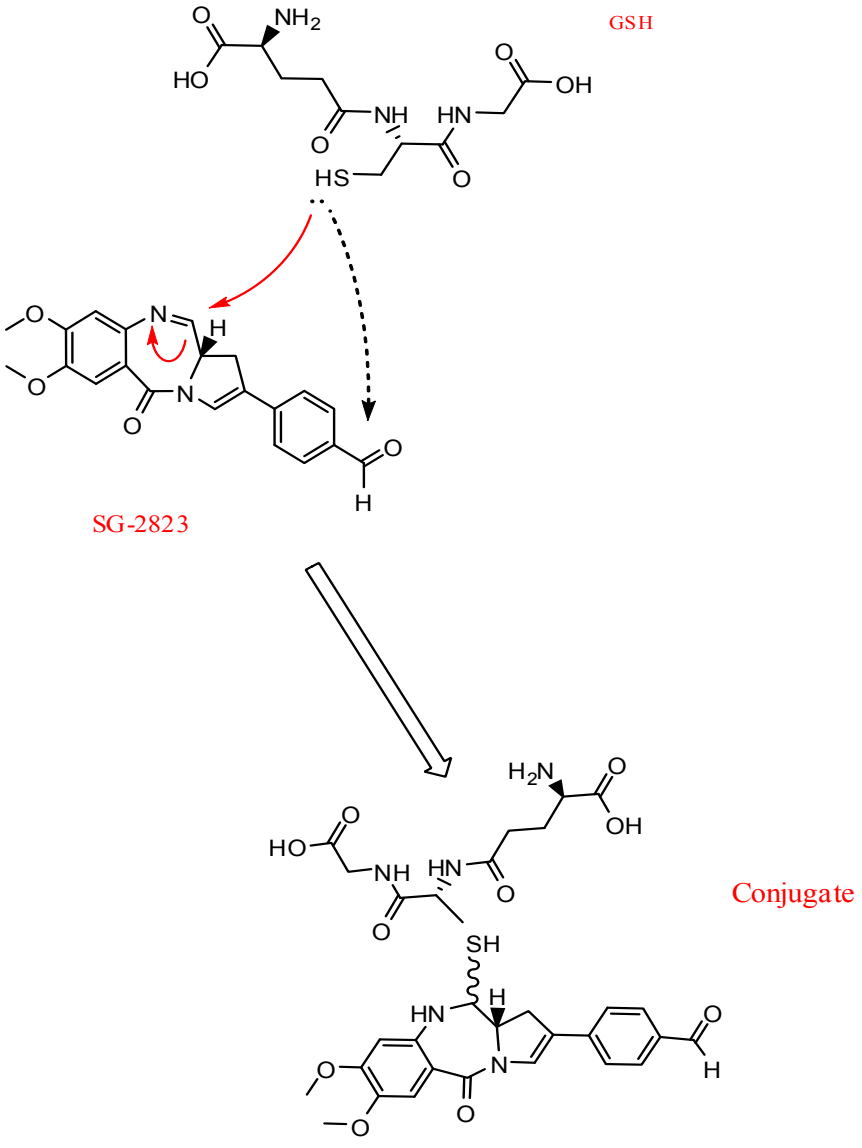

Figure 82: Hypothetical mechanism of SG-2823 binding to GSH: the N10-C11 imine / carbinolamine moiety of SG-2823 may bind to the SH moiety of GSH. The dashed line represents the primary attraction of GSH to SG-2823 by electrostatic interactions. The phenol group is negatively charged and may undergo a close contact interaction.

According to the hypothesis, the phenol group of SG-2823 is indirectly involved in the coupling:

- It may induce a delocalisation of the electrons, thus enhancing a greater electrophilicity of the C11.
- It may attract GSH at the carbonyl without creating any bond. This induced proximity (between GSH and SH-28230) may allow the SH group to interact with C11 of SG-2823 and create a covalent bond.

In both cases, GS-SG-2823 conjugate has a molecular weight of 669.7g/mol. The mass spectrometry analysis as described in Figure 61 identifies the intermediate compound with a molecular weight of 671.5 g/mol which corresponds to $[M+H]^+$ of the 2 proposed structures. Further NMR studies may be carried out in order to identify the unique structure / model.

According to the latter model, presence of a strong electrophilic group, *i.e.* a carbonyl moiety at the extremity of SG-2823 allowed a primary attraction to GSH in a cell free system. This entity was shown not to be absolutely necessary for the conjugation to occur as SG-2819 was associated with a minimal coupling with GSH although this did not translate into any biological difference (in presence or absence of dicoumarol). The PBDs, dimers and monomers, contain highly reactive imines in the diazepinone portions of the molecule. Cheung and colleagues have demonstrated that water or alcohol adds readily to the imino moiety of the PBD-dimer SJG-136, to form the corresponding carbinolamine or its alkyl ether, respectively (Cheung, Struble et al. 2005). Similar results have been demonstrated with the PBD-monomers by Antonow and colleagues (non published data). The imine of the PBDs reacts differentially with GSH, thus decreasing the potential for the entity to react

with the N2 of the guanine in the minor groove of the DNA. It is noteworthy that the PBD-dimers have two electrophilic centres (C11) which "doubly" enhance their affinity for GSH.

Using a series of various GST substrates, Satah has shown that the non enzymatic conjugation rate is influenced by the concentration of both GSH and its substrate, the pH and the temperature (Satoh 1995). Here, the kinetics of the coupling observed using the mass spectrometry analysis may overestimate the kinetics in normal physiological conditions since the PBDs were tested at a concentration of 10μM in a cell free assay, which represents, a 250-1000-fold increase in the concentration used (SG-2823) to determine the IC_{50} in A549 cells. The level of GSH has been shown to be relatively high in these cells and would not be considered as a limiting factor (Russo, DeGraff et al. 1986). Therefore, at relatively low concentration (nM), the conjugation of PBD-monomers, such as SG-2819, to GSH was considered as being not significant in A549 cells.

The impact of GST on the growth inhibitory effect of the PBDs was only demonstrated with SG-2823. The major characteristic of this particular PBD is the presence of a carbonyl moiety at the extremity which seems to be required for GST substrate specificity. Similarly, the chemical structure of GSH has a carbonyl group which has been suggested to be involved in GSH-GST binding (Jeppesen, Ortiz et al. 2003). GST may "recognise" the carbonyl functional groups of both GSH and SG-2823 and catalyse the conjugation.

GSTπ has been found to be the most predominant isoenzyme in a variety of tumours cell lines of the NCI60 panel, including A549 (O'Brien and Tew 1996) suggesting a substrate specificity of SG-2823 for GSTπ. However, the pre-

incubation of dicumarol inhibits not only GSTπ but other GST isoenzymes as well. Therefore, further studies are needed to elucidate the role of other isoenzymes in the conjugation of PBDs such as SG-2823.

MRP1 has been shown to require GSH as a cofactor in order to extrude drug substrates out of the cell. In some cases, the compounds need to be conjugated to GSH in order to be recognised by the transporter. In this study, only one PBD-monomer, SG-2823 was identified to be conjugated to GSH prior to its extrusion by MRP1. Its chemical structure differs from other PBDs by the presence of a carbonyl group which therefore, may interact with the transporter. GSH has also been shown to interact with the transporter but, from the literature, it is unclear which physico-chemical properties are involved in MRP1 binding. Although, it has been established that the sulfhydryl of the cysteine residue in GSH is not required for its MRP1 stimulatory activity (Loe, Deeley et al. 1998; Leslie, Mao et al. 2001; Qian, Song et al. 2001; Leslie, Deeley et al. 2003; Conseil, Deeley et al. 2005). The chemical structure of GSH has many carbonyl groups at the extremities and this may explain the affinity of GSH for the transporter. In addition, glutathione disulfide (GSSG), which has twice as many carbonyl groups has a 50- to 100-fold greater affinity for the transporter (Cole and Deeley 2006). Therefore, the presence of an additional carbonyl group at the extremity of the conjugate formed by SG-2823 and GSH may enhance significantly the binding affinity for MRP1.

The electrophilic centre of the PBDs at the C11 position allows these molecules to bind to DNA and exert their anti-tumour activity, thus limiting the electrophilic characteristic at the C2 extremity would appear to be the best strategy to limit the detoxification process mediated by GSH, GST and MRP1.

ABCG2 substrate specificity of the PBDs was also investigated. The PBDs with a greater number of electrophilic atoms were shown to have a greater affinity for the transporter. This was demonstrated using cell lines over-expressing the transporter; the breast cancer cell lines MCF7-MX and its parental counterpart and the breast cancer cell line MDA-MB-231 transfected with plasmid containing ABCG2-*cDNA*. ABCG2 substrate specificity of the PBDs was confirmed using fumitremorgin C, a specific inhibitor of the transporter, in MCF7-MX cells and in a Caco-2 transwell assay. In addition, a mutation at position 482 was shown to alter ABCG2 substrate specificity of PBDs. This was demonstrated using different MDA-MB-231 cell lines transfected with plasmid containing mutated (T482) or wild type form (R482) ABCG2-*cDNA*.

The activity of the PBDs was evaluated using mitoxantrone resistant breast cancer cell line MCF7-MX and its parental counterpart. The relative resistance for some of the PBDs could not be completely reversed using the specific ABCG2 inhibitor, FTC. The MCF7-MX cell line was obtained by stepwise incubation with mitoxantrone. It can be argued that other factors could contribute to the differential growth inhibition observed, not only for mitoxantrone but also for the PBD derivatives (Su, Lee et al. 2006). Mitoxantrone (MX) was shown to be conjugated by GSH and extruded out of the cell by MRP1 (Morrow, Peklak-Scott et al. 2006). The level of expression of both GSH and GSTs may be increased in this particular cell line contributing to the multidrug resistance phenotype. However, Morrow and colleagues have shown that the transport of MX by ABCG2 was independent of GSH. In addition, the structure affinity relationship for the PBDs has demonstrated that the carbonyl moiety, responsible for GSH coupling could not account for the

differential growth inhibition observed between the MCF7 and its MX resistant cell line. Further studies using BSO and dicumarol could confirm the lack of dependency of PBDs to GSH and GST in this particular cell line. The level of other members of the ABC family may be up-regulated in MCF7-MX cell line, apart from P-gp which has not been found (Nakagawa, Schneider et al. 1992)

A Caco-2 model of permeability was used to confirm the transport of the PBDs via ABCG2: reduced secretion was shown for the PBD-dimers, SJG-136 and DRG-16 following pre-incubation with FTC in contrast to the PBD-monomer SG-2897. However, the SG-2897 was associated with a ratio between the IC_{50} – FTC versus + FTC in MCF7-MX cells greater than 2, suggesting some substrate specificity towards ABCG2. MCF-7-MX over-expresses the transporter and therefore, any difference in ABCG2 substrate specificity should be apparent. Caco-2 cells express ABCG2 at more physiological levels. The impact of the transporter would therefore only be shown for high affinity substrates in the transwell assay. A similar statement could be made regarding the MDA-MB-231 cells transfected with plasmid containing ABCG2-c*DNA*. In summary, all the PBD-dimers were associated with a greater affinity for the transporter than the PBD-monomers. The PBD-monomers were differentially affected by ABCG2 expression.

The PBDs with a greater number of oxygen and nitrogen atoms that are negatively charged were shown to be associated with greater substrate specificity for ABCG2. This suggests that the PBDs bind to a positively charged binding pocket of ABCG2, thus enhancing electrostatic interactions. Similar findings have been reported for a series of camptothecin analogues (Nakagawa, Saito et al. 2006).

ABCG2 is a “half transporter” which needs to homo-dimerise in order to be fully activated. Studies have shown that ABCG2 has at least 2 symmetrical binding pockets (Clark, Kerr et al. 2006). PBD-dimers are high affinity substrates of the transporter with an arbitrary potential ABCG2 affinity value of 16 for all of them. Some PBD-monomers, without (N + O) atoms at the C2 extremity, and being considered as the mono-functional counterpart of PBD-dimers for this property, have an arbitrary potential ABCG2 affinity value of 8, half of the potential of PBD-dimers. These data suggest that PBD-dimers may bind to the 2 symmetrical binding pockets of ABCG2.

Physico-chemical properties, involved in ABCG2 substrate specificity, were extended to the known substrate, mitoxantrone and non substrate, vinblastine. Mitoxantrone has in its chemical structure a great number of oxygen and nitrogen atoms negatively charged at extremities, (potential ABCG2 affinity of 24 as defined by equation 2) which potentially could interact with the transporter. In addition, the chemical structure is relatively symmetrical suggesting its ability to bind to at least two binding pockets. It was associated with a maximal ratio between the different MDA-MB-231 cells transfected with plasmid ABCG2-*cDNA*.

In contrast, the chemical structure of vinblastine is relatively bulky without any planar groups with apparent π orbitals. No electrophilic atoms were found at extremities (Figure 83).

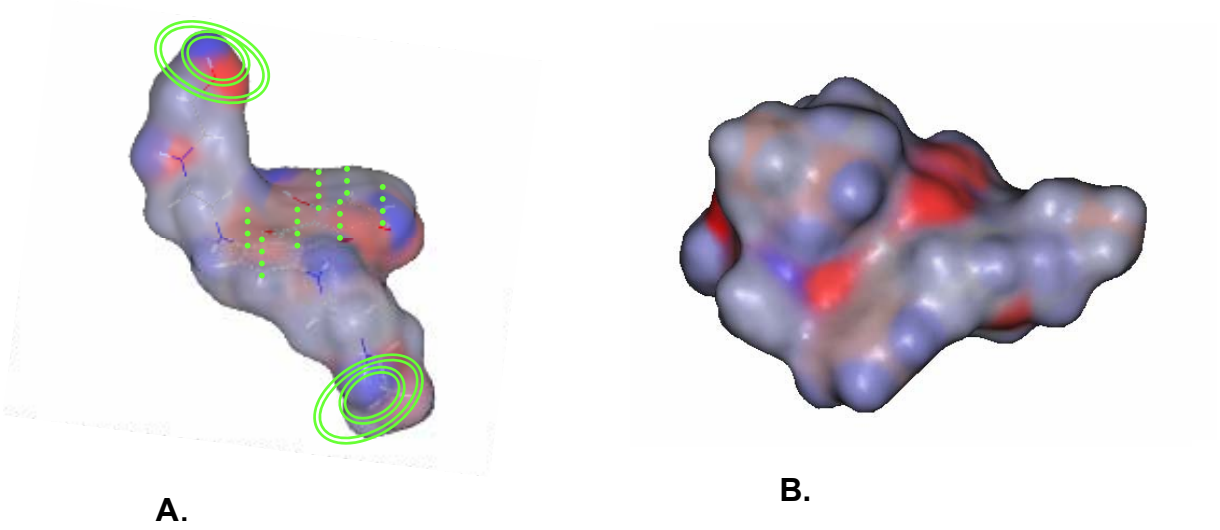

Figure 83. Chemical structures of known ABCG2 substrate, mitoxantrone (A) and known ABCG2 non substrate, vinblastine (B). Atoms with negative partial charge are represented in red. Atoms with positive partial charge are represented in blue. Dashes lines represent the predicted π stacking interactions involved in ABCG2 binding affinity. Circular lines represent the predicted electrostatic interactions involved in ABCG2 binding affinity.

These findings provide evidence that the chemical properties involved in ABCG2 substrate specificity to PBDs can also be applied to other classes of compounds.

The impact of a mutation at position 482 was also investigated. The mutated form of the transporter (threonine at position 482) was associated with a greater affinity for some PBDs, when compared to the wild type form of the transporter (arginine at the same position). No gain of affinity was shown with SG-2781, which has positive charged nitrogen at its C2 extremity which suggests that only the PBDs with positively charged atoms might be affected by this particular mutation among the C2 aryl derivatives. This neutral condition allowed a lower repulsion, thus a greater interaction with the transporter (Figure 84).

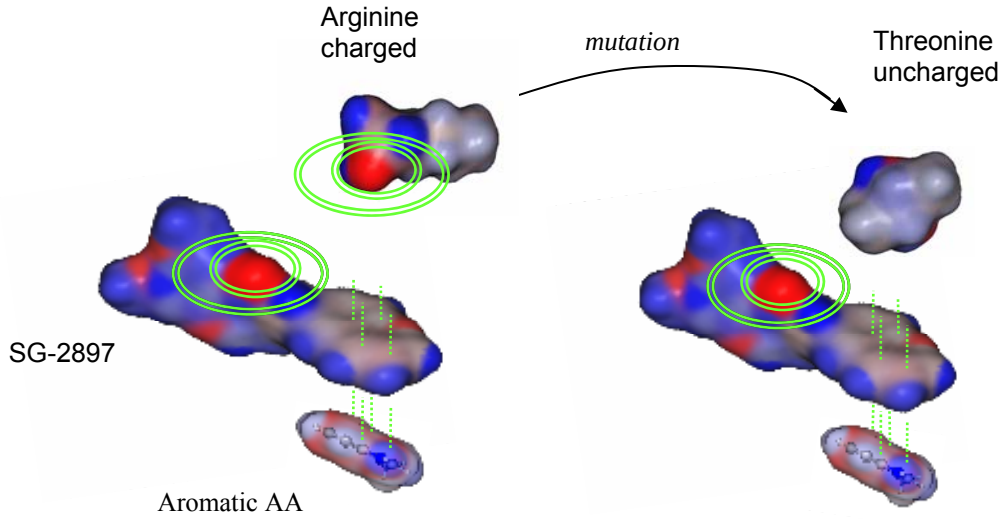

Figure 84. Hypothetical model of the impact of ABCG2 polymorphism on the substrate specificity of the PBDs. Atoms with negative partial charge are represented in red. Atoms with positive partial charge are represented in blue. Dashes lines represent the predicted π stacking interactions involved in ABCG2 binding affinity. Circular lines represent the predicted electrostatic interactions involved in ABCG2 binding affinity.

In addition, the mutated form of the transporter was associated with a similar "gain of function" with the PBD-dimers, high affinity substrates of the transporter, than the PBD-monomers, low affinity substrates of the transporter, despite having a greater number of electrophilic atoms, suggesting that other forces tend to participate in the overall affinity for the transporter.

The mutated form of the transporter was associated with a maximal "gain of function" with the PBD-monomer, SJG-244. SJG-244 has a minimal number of electrophilic atoms. However the presence of an aromatic ring with π orbitals at the C8 extremity seems to allow this particular compound to enhance substrate specificity to the mutated form of the transporter. The "gain of function" has been

maximal with mitoxantrone (~4.3-fold) which may be due to the presence in its chemical structure of 3 aromatic rings with conjugated π orbitals (Figure 83).

Overall, the interaction with ABCG2 is mainly driven by interaction forces due to the presence of charged amino acid in its binding pocket. When a particular mutation changes the amino acid sequence to an uncharged amino-acid, other close contact interactions such as the π-π interactions tend to participate in the overall binding affinity to the transporter.

In summary, all 4 PBD-dimers were identified to be substrates of MRP1 but only one PBD-monomer (SG-2823). The presence of a carbonyl moiety at the extremity of the PBD-monomer substrate was found sufficient to allow conjugation to GSH and further extrusion by the transporter. ABCG2 substrate specificity was also investigated. When compared to mitoxantrone, low affinities for ABCG2 were associated with all 4 PBD-dimers and, to a lesser extent for some PBD-monomers. The number of oxygen and nitrogen atoms, negatively charged, and the number of planar structures were identified as determinants of ABCG2 substrate specificity. The impact of ABCG2 polymorphism was also investigated. The T482 SNP was associated with a "gain of function".

Consideration of these factors may allow the rational design of new PBD analogues with minimal interaction with MRP1 and ABCG2 transporters and this may enhance even more their anti-tumour activity.

5 Chapter 5: ACTIVITY OF THE PBD-MONOMERS

5.1 Introduction

The pyrrolo[2,1-*c*][1,4]benzodiazepines (PBDs) are molecules which interact covalently within the minor groove of the DNA (Gregson, Howard et al. 2001). The PBD-monomers span 3 base pairs with preferential binding to Pu-G-Pu sequences. The PBD-dimers are interstrand cross-linkings (ICL) agents. They span a greater number of base pairs (6-7) with preferential binding to 5'-Pu-**G**A*(G/A)*TC-Py-3' sequences. Upon binding to their specific sequence, PBDs exert their anti-tumour activity by inducing stalled replication forks and blocking transcription by inhibiting RNA polymerase (Puvvada, Hartley et al. 1993; Puvvada, Forrow et al. 1997).

SJG-136, a PBD-dimer, has shown a broad spectrum of growth inhibition across the NCI60 cell line panel, and is highly potent in a number of xenograft models (Alley, Hollingshead et al. 2004; Pepper, Hambly et al. 2004). Other PBD-dimers have been synthesised and some have shown enhanced anti-tumour activity. However, their growth inhibitory effect is reduced in cells expressing high levels of the ABC transporters, P-glycoprotein, MRP1 and ABCG2 (chapter 3 and 4). Key physico-chemical properties have been defined as the determinants of the substrate specificity for the different transporters.

The anti-tumour activity of most of the PBD-monomers was shown not to be influenced by the expression of the ABC transporters. However, the PBD-monomers do not cross-link DNA and span only a minimum number of base pairs, it might be anticipated that the PBD-monomers would be less potent than the PBD-dimers.

The anti-tumour activity was evaluated in a wide range of cancer cell lines and some PBD-monomers were, surprisingly, highly cytotoxic, such as SG-2897 (chapter 3 and 4). In this chapter, data will be presented investigating the physico-chemical structures involved in the anti-tumour activity of the PBD-monomers, hence defining a structure activity relationship.

The ability of the cell to repair DNA damage is a critical factor determining growth inhibition. Mechanistic studies have revealed a unique interaction of the PBDs with the DNA repair machinery. The nucleotide excision repair (NER) pathway (XPF-ERCC1) and the homologous recombination (HR) repair pathway (Rad51 paralogues) were shown to be involved in the repair of ICLs (De Silva, McHugh et al. 2000). The PBD-monomers do not to produce ICLs in contrast to the PBD-dimers. However, a similar DNA repair pathway has been reported to be involved following exposure to the mono-functional counterpart of SJG-136, mmy-SJG (Clingen, De Silva et al. 2005). In this study, the impact of other proteins involved in the HR pathway, such as BRCA2 on the growth inhibitory effect of the PBD-monomers was evaluated.

Based on the biological evaluation of the PBD-monomers, new compounds with features leading to non recognition by the ABC transporters and with predicted enhanced anti-tumour activity were designed and tested *in silico.*

5.2 Results

5.2.1 Structure activity relationship of the PBD-monomers

Differential substrate specificity of the PBD-monomers towards ABC transporters was demonstrated using a range of cancer cell lines (chapter 3 and 4). Some PBD-monomers were highly cytotoxic (SG-2897) whereas some others were associated with a low anti-tumour activity (SJG-244). The physico-chemical structures involved in the anti-tumour activity of the PBD-monomers were evaluated in order to define a structure activity relationship (SAR).

There are major differences between cell lines: differences in membrane permeability, expression of ABC transporters, intracellular detoxification systems and many others. All these factors influence drug pharmacodynamics, limiting the desired cytotoxic effect. For this reason, a variety of cancer cell lines were used (human colon cancer cell line HCT-116, ovarian cancer cell line A2780, lung cancer cell line A549, leukemia cancer cell line K562, breast cancer cell line MCF7 and, mouse immortalised fibroblasts 3T3) in order to define a rational SAR for the PBD-monomers.

5.2.1.1 Thermal denaturation data

The PBD-monomers exert their anti-tumour activity by covalently binding to the Pu-G-Pu sequences in the minor groove of DNA. Therefore, the interaction with DNA may be the major determinant of the anti-tumour activity of this class of compounds. Reactivity towards double-stranded DNA was assessed by measuring

their effect on the melting behaviour (T_m) of calf thymus DNA (Antonow and coworkers, personal communication, Table 15).

		ΔTm (ºC)
C2 sibiromycin-aglycone analogues	SG-2825	2.4
	SG-2900	4.1
	SG-2901	2.5
	SG-2902	4.4
C2 aryl analogues	SG-2781	8
	SG-2796	9.2
	SG-2797	11.9
	SG-2819	6.9
	SG-2820	11
	SG-2823	10.8
C2 quinoline analogue	SG-2897	20.5

Table 15. Thermal denaturation data for the PBD-monomers. For CT-DNA alone, ΔTm = 67.82 ± 0.07°C. All ΔTm are ± 0.1-0.2°C after 18h post-incubation (No ΔTm data is available for SJG-244).

The sibiromycin-aglycone analogues (SAG) SG-2825, SG-2901, SG-2900 and SG-2902 showed the lowest stabilisation of the PBD-monomers with the DNA. These compounds differ in the length of the C2-*E*-alkenyl tail. Within this group, the PBD-monomer, with the shorter tail, SG-2902 appeared to generate the most stable complex with DNA as represented by a ΔTm at 18h = 4.4°C.

The C2 aryl substituent analogues seem to induce a greater stabilisation of the DNA: the thermal denaturation data (ΔTm at 18h) range from 6.9°C for SG-2819 to 11.9°C for SG-2797. Within the C2 aryl group, compounds with electron-withdrawing groups at the C2 extremity appear to outperform electron-donators. For example, SG-2797 (4-CF_3, ΔTm = 11.9°C) and SG-2820 (4-CN, ΔTm = 11°C)

confer greater DNA stabilisation than SG-2781 (4-N(CH_3)$_2$, ΔTm = 8°C) compared to SAG analogues.

Finally, the fused 6-membered aromatic system provide the greatest degree of stabilisation, with 6-quinolinyl (SG-2897) stabilising the double helix by 20.5°C. This high value is normally associated with the PBD-dimers such as DSB-120 (15°C) and SJG-136 (33°C), forming an ICL.

SJG-244 was not included in the structure activity relationship as no ΔTm was available for this compound and also because it is the only PBD-monomer derivative with a C8 substituent.

5.2.1.2 Relationship between ΔTm and the growth inhibitory effect of the PBD-monomers

The thermal denaturation data have been compared with the growth inhibition data among 6 different types of cancer cell lines.

5.2.1.2.1 Colon cancer cell line model

The PBD-monomers were tested against the colon cancer cell lines HCT-15 and HCT 116 and the IC_{50} were shown to be similar in activity in both cell lines (IC_{50} ratios close to 1) for all the PBD-monomers despite the differential expression of ABC transporters. Therefore, the data will be presented for only one cell line.

The PBD-monomers have shown a wide range of activity against HCT 116 cells ranging from 1.1 nM for SG-2897 to 260 nM for SJG-244 (Table 4).

The biological activity of the PBD-monomers correlated with the melting point temperature of the DNA (ΔTm as determined previously at 18h) with $r^2 = 0.85$ and $P_{value} < 0.0001$, for n = 11 (Figure 85). Therefore, the activity seems to be dependent upon the affinity for DNA. In addition, three classes of compounds among the PBD-monomers could be identified: the least cytotoxic compounds, corresponding to the sibiromycin analogues, with 1 aromatic ring in their structures. C2-aryls analogues were associated with an intermediate growth inhibitory effect and have 2 aromatic rings. Finally, the most cytotoxic PBD-monomer, SG-2897, contains the greatest number of aromatic rings

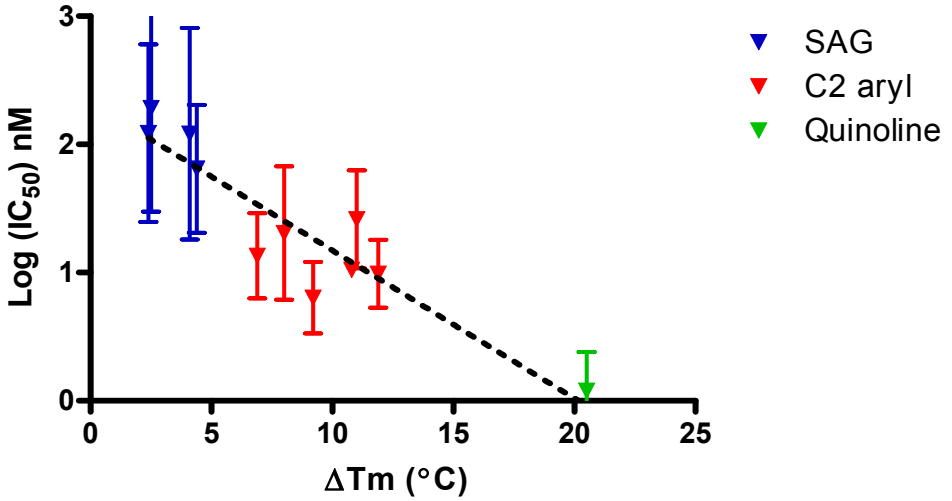

Figure 85. Relationship between the growth inhibitory effect of the PBD-monomers in colon cancer cells HCT 116 and the affinity for the DNA as determined by the ΔTm at 18h. The Log (IC_{50}) values are means ± SEM of n = 3 experiments performed in triplicate.

These data provide evidence that aromaticity has a major impact on the ΔTm and hence the biological activity of the PBD-monomers.

5.2.1.2.2 Ovarian cancer cell line model

The PBD-monomers have been tested against the ovarian cancer cell lines A2780 and $A2780^{AD}$ and the IC_{50} were similar in both cell lines (IC_{50} ratios close to 1) for all the PBD-monomers, despite the differential expression of ABC transporters. Only one cell line will be considered.

The PBD-monomers were associated with a broad spectrum of activity against the A2780 cell line ranging from 1.2 nM for SG-2897 to 300 nM for SJG-244 (Table 5). The relationship between the affinity for DNA as represented by ΔTm (at 18h) and the growth inhibitory effect of the PBD-monomers was evaluated and shown a good correlation ($r^2 = 0.88$ and $P_{value} < 0.0001$) for n = 10 (Figure 86). These results confirm that the activity of the PBD-monomers is mainly mediated by the affinity with the DNA.

Similarly, the number of aromatic rings correlated with the biological activity of the PBD-monomers ($P_{value} < 0.0001$).

In addition, the surface activity parameter, as determined previously seems to have an impact on the growth inhibitory effect of the PBD-monomers. Indeed, the non surface active PBD-monomers appear to be associated with the greatest interaction with the DNA and induced growth inhibition in contrast to the surface active ones (Figure 86).

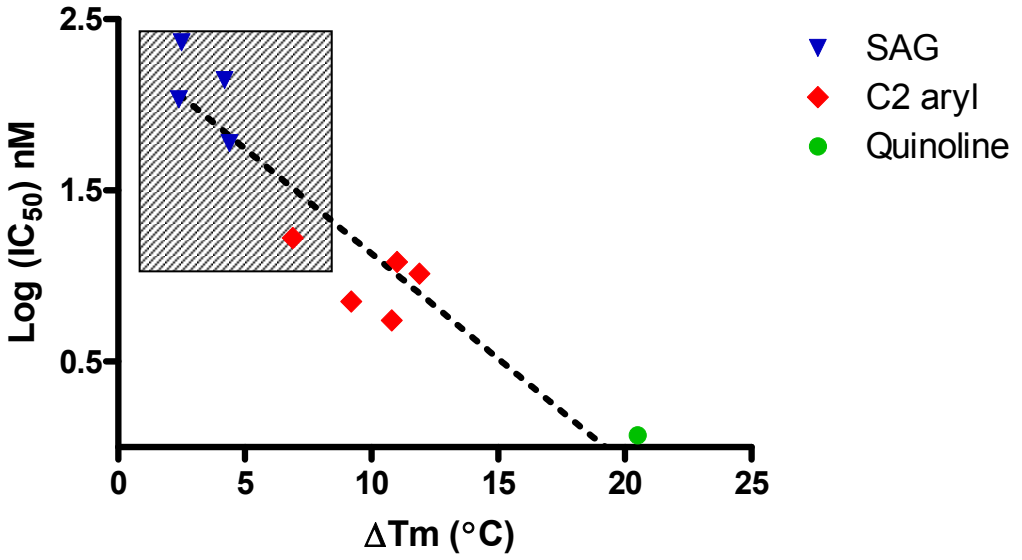

Figure 86. Relationship between the growth inhibitory effect of the PBD-monomers in ovarian cancer cells A2780 and the affinity for the DNA as determined by the ΔTm at 18h. The Log (IC_{50}) values are means of n = 3 experiments performed in triplicate. The SEM has not been reported in this graph for reasons of clarity. The surface active PBD-monomers are represented in dashed square.

5.2.1.2.3 Other cell lines models

The growth inhibitory effect of the PBD-monomers was evaluated in 6 different cancer cell lines. Overall, there was a correlation between the affinity for DNA and the biological activity of the PBD-monomers for all the cell lines tested which confirm the impact of the interaction with DNA on the biological activity of the PBD-monomers (Table 16). The growth inhibitory effect of SG-2823 in A549 has not been taken in account as the compound is a substrate of MRP1 reducing its anti-tumour activity. The growth inhibition in K562 was determined by Antonow and colleagues (personal communication).

	correlation with ΔTm	
	R^2	P_{value}
HCT 116	0.85	< 0.0001
A2780	0.88	< 0.0001
MCF7	0.78	< 0.0005
A549	0.85	< 0.0005
K562	0.83	< 0.0001
3T3	0.8	< 0.0001

Table 16. Relationship between the growth inhibitory effect of the PBD-monomers, in a panel of cancer cells, and the affinity for DNA, as determined by ΔTm at 18h. The Log (IC_{50}) values are means of n = 3 experiments performed in triplicate.

5.2.1.3 Physico-chemical properties involved in drug DNA binding and induced biological activity

Previously, the affinity for DNA has been shown to be a major factor involved in the biological activity of the PBD-monomers based on their aromaticity and surface activity.

The related physico-chemical parameters which may be involved in the PBD-DNA affinity were investigated using a computer based approach (Chem*3D*) (Table 17).

	ΔTm (ºC)	Log*P*	Critical volume (Å^3)	SASA (Å^2)
SG-2781	8	2.494	1058.5	674.2
SG-2796	9.2	2.844	1021.5	647.1
SG-2797	11.9	3.13	1027.5	642.7
SG-2819	6.9	3.443	1090.5	681.8
SG-2820	11	2.242	1010.5	629.3
SG-2823	10.8	1.956	1001.5	627.6
SG-2825	2.4	2.788	1016.5	665.5
SG-2897	20.5	2.292	1067.5	660.9
SG-2900	4.1	3.205	1072.5	692.7
SG-2901	2.5	3.622	1128.5	726.1
SG-2902	4.4	2.753	1005.5	644.8

Table 17. Physico-chemical properties of the PBD-monomers which may be involved in PBD-DNA affinity. SASA: Solvent accessible surface area.

5.2.1.3.1 Solvent accessible surface area

The solvent accessible surface area (SASA) is the surface area of a molecule that is accessible to a solvent. It has been defined as a way of quantifying the hydrophobic burial of a molecule (Lee and Richards 1971).

When considering 1 particular group of the PBD-monomers, the C2-sibiromycin-aglycone analogues (SAG) (SG-2825, SG-2901, SG-2900 and SG-2902), the SASA parameter has shown a highly significant correlation with the biological activity in A2780 cell line ($r^2 = 0.95$, $P_{value} = 0.02$) (Figure 87).

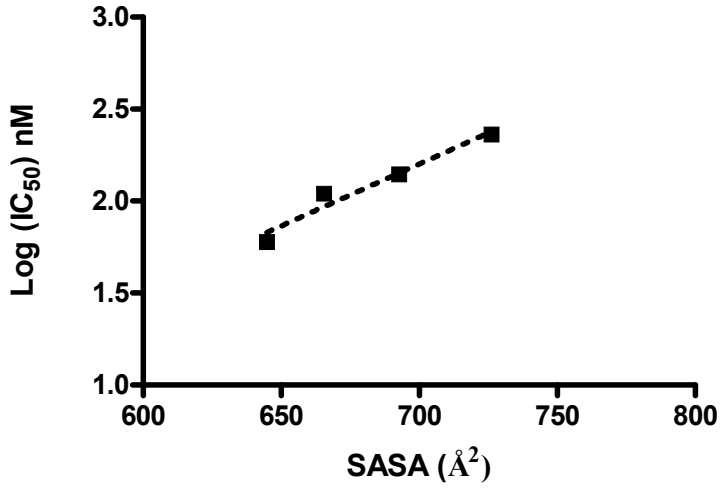

Figure 87. Relationship between the growth inhibitory effect of the C2-sibiromycin-aglycone analogues in A2780 cells and the solvent accessible surface area (SASA). The Log (IC_{50}) values are means of n = 3 experiments performed in triplicate. The SEM has not been reported in this graph for reasons of clarity.

The relationship between the growth inhibitory effect of the C2- sibiromycin-aglycone analogues against a panel of cell lines and SASA parameter has been evaluated and shown good correlations in 6/6 cell lines tested (Table 18).

	correlation with SASA	
	r^2	P_{value}
HCT 116	0.85	> 0,1
A2780	**0.95**	**< 0.05**
MCF7	0.81	> 0.1
A549	0.7	> 0.1
K562	**0.89**	**= 0.05**
3T3	0.5	> 0,1

Table 18. Relationship between the growth inhibitory effect of the C2-sibiromycin-aglycone analogues, in a panel of cancer cell lines and the solvent accessible surface area (SASA). The Log (IC_{50}) values are means of n = 3 experiments performed in triplicate.

In addition, the structure-activity-relationship was incorporated within the library of the PBD-monomers supplied by Antonow and colleagues. The biological activity (in K562 cells) of 6 C2-sibiromycin-aglycone analogues correlated with the SASA parameter ($r^2 = 0.95$, $P_{value} = 0.0008$).

The number of C2-sibiromycin-aglycone in our library did not allow us to define any other significant correlations between the biological activity towards the panel of cell lines and other physicochemical properties. When a greater number of C2-sibiromycin-aglycone analogues (6) were considered, 2 other parameters showed a significant impact: Log*P* correlated with the log scale of the IC_{50}s in K562 ($r^2 = 0.90$, $P_{value} = 0.0042$). Finally, the critical volume correlated with the biological activity of the C2-sibiromycin-aglycone analogues ($r^2 = 0.91$, $P_{value} = 0.0032$). These features seem to drive the growth inhibitory effect of this class of PBD-monomers independently of the interaction with DNA as no correlation could be shown with ΔTm.

5.2.1.3.2 π-π stacking interactions

π-π stacking is a popular chemistry concept describing how aromatic molecules are stabilized when oriented face-to-face as in a stack of coins. This phenomenon occurs when 2 surrounding aromatic rings have overlapping π orbitals and allows a strong close contact interaction.

Previously, the growth inhibitory effect (in the colon cancer cell line HCT 116) of the PBD-monomers was shown to be dependent on the number of aromatic rings (Cf. 5.2.1.2.a). In this study, this relationship was evaluated in 4 other cell lines (3T3, A549, MCF7, A2780 cells). The number of aromatic rings correlated with the growth inhibitory in the 5/5 cell lines tested (Table 19). It is noteworthy that SJG-244, the only PBD-monomer with an aromatic ring at the C8 extremity in contrast to the C2-aryl derivatives, did not show any correlation with the aromaticity. These data suggests that the aromaticity correlates with the growth inhibitory effect of the C2-aryl derivatives only.

	Correlation with n aromatic rings	
	r^2	P_{value}
3T3	0.92	< 0.0001
A2780	0.93	< 0.0001
HCT 116	0.92	< 0.0001
A549	0.90	< 0.0001
MCF7	0.92	< 0.0001

Table 19. Relationship between the growth inhibitory effect of the PBD-monomers and the number of aromatic rings, in a panel of cancer cell lines. The IC_{50} values are means of n = 3 experiments performed in triplicate.

The chemical structure of SG-2897 contains a quinoline based substituent at the C2 extremity, equivalent to a 6 member ring. The carbons of the ring are associated with conjugated π orbitals which theoretically, induce a greater stabilisation of the structure and also a greater interaction to other planar structures found in DNA as represented in Figure 88.

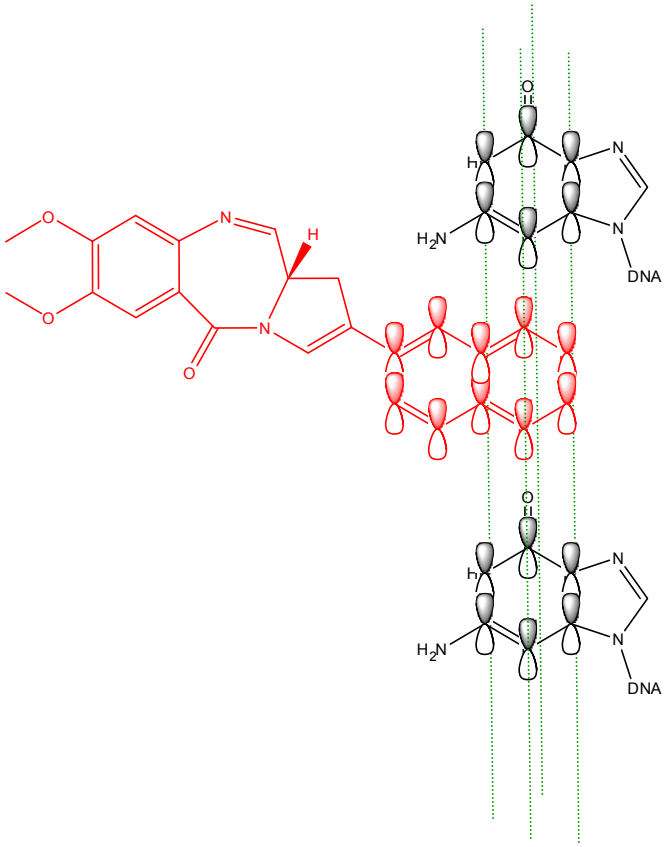

Figure 88. Hypothetical model of the π-π stacking interactions involved in PBD-monomers-DNA affinity. The PBD-monomer, SG-2897 has been represented in red. Guanines bases have represented in black. All the π orbitals involved in PBD-DNA interaction have been represented, and for reasons of clarity are not overlapping in the figure. The π-π stacking interactions are represented in green.

5.2.1.3.3 Hydrogen bonding

The electrostatic forces impact on close contact interactions between intermolecular complexes. Previously, the PBD-monomers, with a greater

electrostatic potential, were shown to be associated with a greater interaction to proteins such as ABCG2 (Cf. Section 4.2.2.). In this section, the impact of the electrostatic forces on the overall affinity for DNA associated with the biological activity of the PBD-monomers was evaluated. Using a series of PBD-monomers with C2-aryl substituent, *i.e.* with a similar aromaticity, the impact of the electrophilicity was determined on the interaction with DNA and also on the biological activity. The 3 PBD-monomers of interest have been chosen because of the presence of electron-withdrawing groups at the C2-aryl extremity (SG-28. The nitrogen atom at the extremity of SG-2781 was shown previously to be positively charged in contrast to the nitrogen at the extremity of SG-2820 (Figure 89).

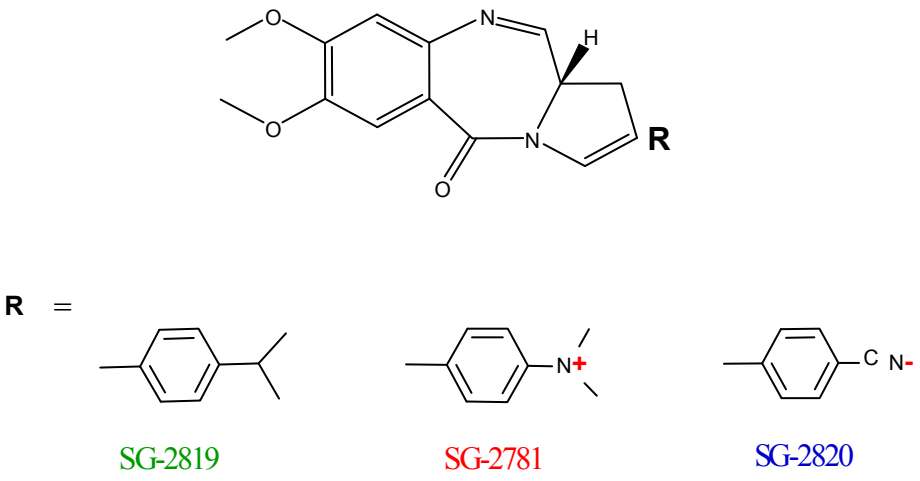

Figure 89: Chemical structure of the PBD-monomers with different C2-aryl substituent.

The biological activity of the 3 PBD-monomers was evaluated in 5 cell lines (3T3, A549, HCT 116, MCF7, A2780 cells). As expected, the presence of a nitrogen atom at the C2 extremity was associated with a greater affinity for DNA: SG-2819

(no nitrogen at C2) stabilises the helix by 6.9 °C whereas SG-2781 stabilises the DNA by 8°C (Figure 90). The presence of nitrogen, in the chemical structure of SG-2820, with a negative partial charge, (electron withdrawing group) stabilises the DNA (ΔTm of 11 °C) even further. This is in accordance with the physico-chemical parameters involved in PBD-"protein" interaction.

However, SG-2820, being associated with the greatest affinity for DNA, has shown the lowest growth inhibitory effect among the 5 different cell lines tested (3T3, A549, HCT 116, MCF7, A2780 cells) with a mean IC_{50} = 22 nM [SD ± 6.7 nM]). The difference between the growth inhibitory effect of SG-2781 and SG-2820 is statistically significant (paired t-test, P_{value} = 0.03). No significant difference could have been seen between the growth inhibitory effect of SG-2819 (mean IC_{50} = 15 nM [SD ± 4.3 nM] and the growth inhibitory effect of SG-2781 (mean IC_{50} = 14 nM [SD ± 4.1 nM].

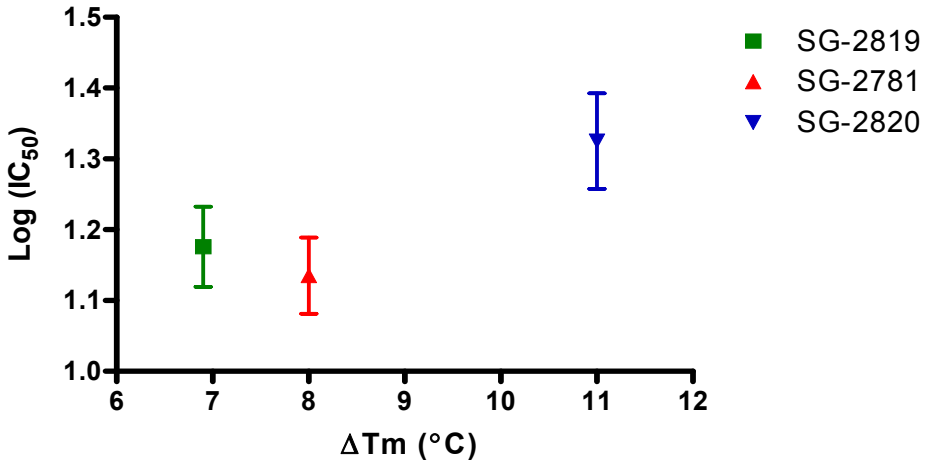

Figure 90. Impact of the electrophilicity on the biological activity of the C2 aryl derivatives. Results are expressed as relationship between the affinity for DNA as determined by ΔTm (at 18h) and the biological activity for SG-2819 (■), SG-2781 (▲) and SG-2820 (▼) in a range of cancer cell lines (A549, HCT 116, MCF7, A2780 cells). The Log (IC_{50}) values are means ± SEM of at least n = 5 experiments performed in triplicate.

The position of the electron-withdrawing groups was also investigated. One PBD-monomer (SG-2896) was synthesised by Antonow and colleagues with similar physico-chemical properties to SG-2897 (SASA, aromaticity, number of nitrogen and oxygen atoms, similar electrostatic potential) (Figure 91).

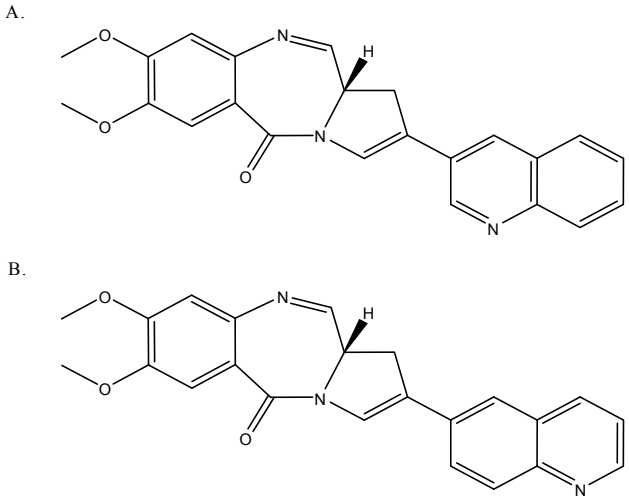

Figure 91. Chemical structure of SG-2896 (A) compared to the chemical structure of SG-2897 (B).

However, SG-2896 was associated with a lesser interaction with DNA (ΔTm = 18.6 °C) and has showed a ~6 fold decrease in anti-tumour activity (IC_{50} = 8.5 nM) towards K562 cell line (Antonow and colleagues, personal communication) compared to SG-2897 (ΔTm = 20.5 °C, IC_{50} = 1.4 nM). Therefore, the position of the nitrogen atom appears to enhance close contact interactions with DNA.

A molecular modelling approach was used to evaluate the impact of the position of the nitrogen atom on close contact interactions with DNA. By definition, a hydrogen bond could be formed, when the spatial distance between an electron donor group and an electron acceptor group is lower than ~3.5 Å. The spatial distances between the nitrogen of the 6 member ring of SG-2897 and the surrounding hydrogen of the adenine and the hydrogen of a deoxyribose base are 2.9 Å and 2.6 Å, respectively (Figure 92.B). These data confirm the close contact interactions

generated by the presence of nitrogen within the 6 member ring of SG-2897. In contrast, the distance between the nitrogen of the 6 member ring of SG-2896 and any surrounding hydrogen is never lower than 3.5 Å which suggests limited hydrogen bonding (Figure 94.C).

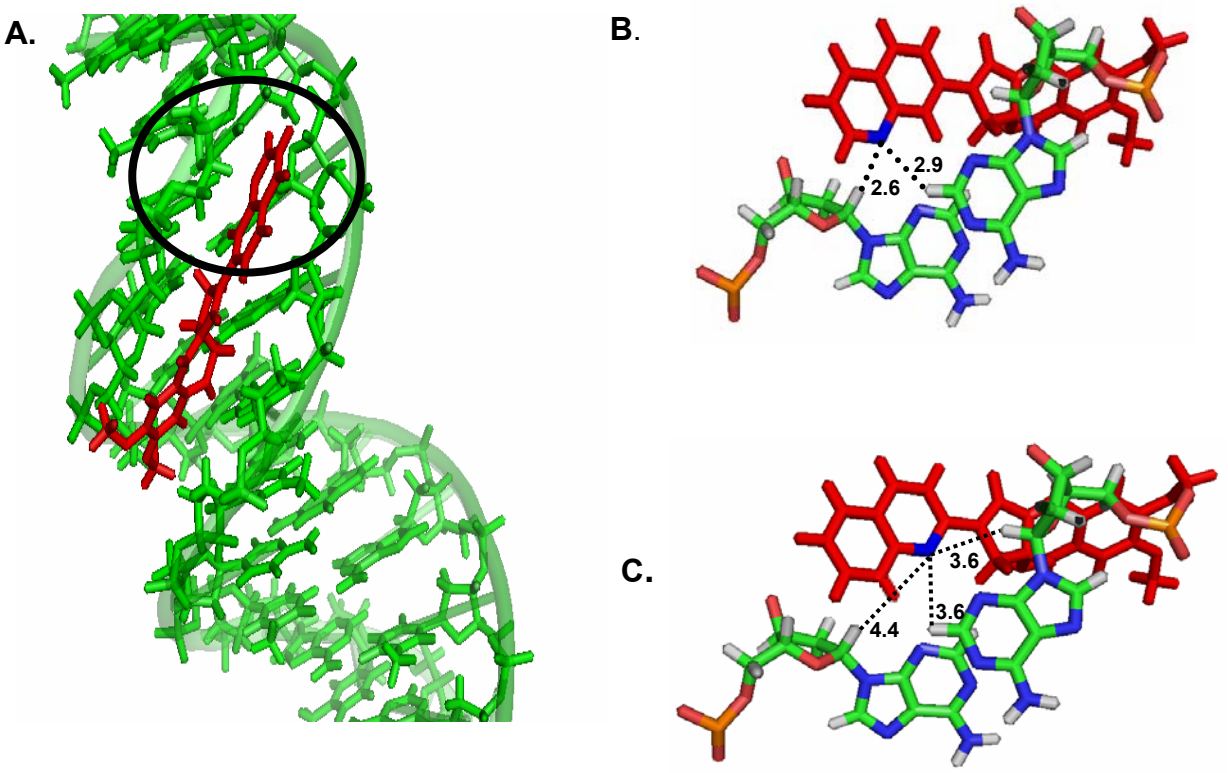

Figure 92. Close contact interactions of two PBD-monomers, SG-2897 and SG-2896, with DNA. **A.** Molecular modelling of the interaction of a quinoline based PBD-monomer (red) within DNA (green). **B.** Close contact interactions of SG-2897 (red) with DNA. The nitrogen of the 6 member ring is represented in blue **C.** Close contact interactions of SG-2896 (red) with DNA.

These data provide evidence that SG-2897 can interact, through the nitrogen of its 6 member ring, with both strands of DNA with a preferential interaction for the opposite strand, where the covalent bound is formed with guanine (Figure 93).

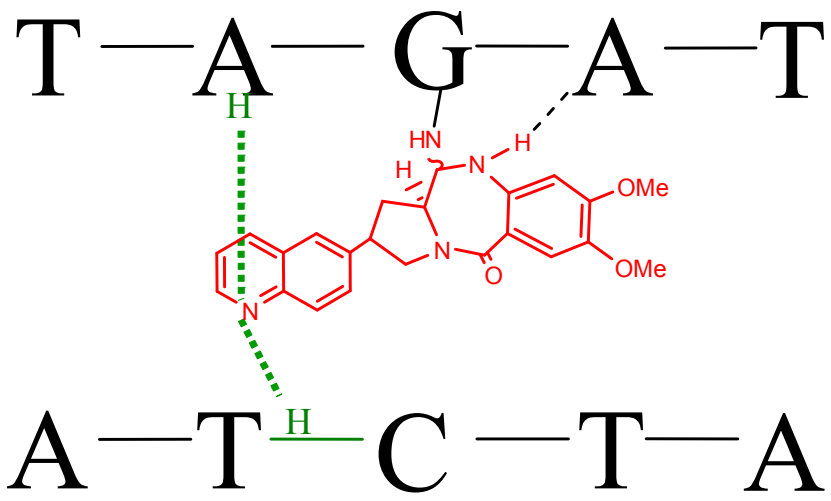

Figure 93. Hypothetical model of the interaction of SG-2897 with the 2 strands of DNA. The carbolamine interacts covalently with guanine. The nitrogen of the 6 member ring interacts with the hydrogen of the backbone of the opposite strand of DNA. The same nitrogen interacts also with hydrogen of adenine.

5.2.1.4 Structure activity relationship of the PBD-monomers in a larger library of PBD monomers

The structure activity relationship study was extended to the library synthesised by Antonow *et al*,. The growth inhibitory effect of 82 compounds was evaluated in the K562 cell line and showed a wide range of activity ranging from < 0.1 nM to 920 nM (Antonow and colleagues, personal communication). ΔTm associated with the affinity for DNA showed only a poor correlation ($r^2 = 0.33$, $P_{value} = 0.0014$) due to a very large heterogeneity of the structures. This correlation was increased considering molecules with similar PSA ($r^2 = 0.49$, $P_{value} = 0.0012$). This

correlation was slightly improved with Log*P* parameter ($r^2 = 0.51$, $P_{value} = 0.0018$); an increase of the lipophilicity decreasing the growth inhibitory effect. Finally (with similar PSA), the growth inhibitory effect correlates significantly and inversely with SASA ($r^2 = 0.81$, $P_{value} < 0.0001$).

Furthermore, the position of the C2-phenyl substituent appears to have a major impact on the growth inhibitory effect. The para-substituted C2-phenyl derivatives have a greater cytotoxic effect than the meta-substituted counterparts ($P_{value} = 0.04$).

5.2.2 Anti-tumour activity of the most potent PBD-monomer, SG-2897

Previously, PBD-monomers were shown to be associated with a low affinity to ABC transporters (Chapter 3 and 4). Among the PBD-monomers, SG-2897 was also associated with a maximal growth inhibition similar to the PBD-dimer SJG-136 (nM range), substrate of the ABC transporters. SG-2897, as a lead compound, was chosen for further biological evaluation.

5.2.2.1 Cell line screening of SG-2897

The anti-tumour activity of the most potent PBD-monomer, SG-2897 was evaluated in a series of colon cancer cell lines to allow further comparison with SJG-136 (Guichard, Macpherson et al. 2005). Overall, SG-2897 was associated with similar growth inhibition among the different cell lines tested (Table 20). The most sensitive cell line was HCT 116 with an IC_{50} of 1.2 nM in contrast to the least

sensitive cell line, the Caco-2 with an IC_{50} of 3.4 nM. The former was chosen for further evaluation of SG-2897 *in vivo.*

	IC_{50} (nM)	SD
HCT-116	1.2	0.3
HCT-15	1.6	0.3
HT-29	1.9	0.1
HCT-8	2.5	0.3
Caco-2	3.4	0.9
Colo-205	1.9	0.7
SW-480	1.7	0.6
SW-620	1.8	0.5

Table 20. SG-2897 IC_{50}s for a panel of colon cancer cell lines. Results are means ± SD of n = 3 experiments performed in triplicate.

5.2.2.2 *In vivo* antitumor activity of SG-2897, HCT 116 xenograft model

The HCT 116 cell line was chosen as the xenograft model among the panel of colon cancer cell lines because of its high sensitivity to SG-2897 *in vitro*. Its anti-tumour activity was tested using 2 schedules of administration as in previous studies with SJG-136: a single *i.v*. injection and 5 daily *i.v*. injections.

The specific growth delay (SGD) of 0.68 for animals treated with 120 µg/kg/d for 5 days could not confirm the anti-tumour activity of SG-2897 in this particular model (Figure 94). In addition, the tumour regression (T/C%) was ranging from 55% at day 4 up to 62% at day 9 when the animals were treated with 120

µg/kg/d for 5 days, never achieving the significant 42% threshold (Bissery and Chabot 1991; Plowman J 1997; Mohammad, Dugan et al. 1998; Johnson, Decker et al. 2001). The bolus injection was associated with a T/C ranging from 82% at day 9 up to 88% at day 2.

These results were compared with the data obtained with the PBD-dimer SJG-136 (Guichard and colleagues, personal communication). Similarly, the anti-tumour activity of SJG-136 was associated with a SGD < 1 at the dose of 120 µg/kg/d. In addition, the tumour regression (T/C%) was ranging from 70% at day 2 up to 80% at day 7 when the animals were treated with 120 µg/kg/d for 5 days, never achieving the significant 42% threshold. The bolus injection was associated with a T/C ranging from 93% at day 2 up to 104% at day 11.

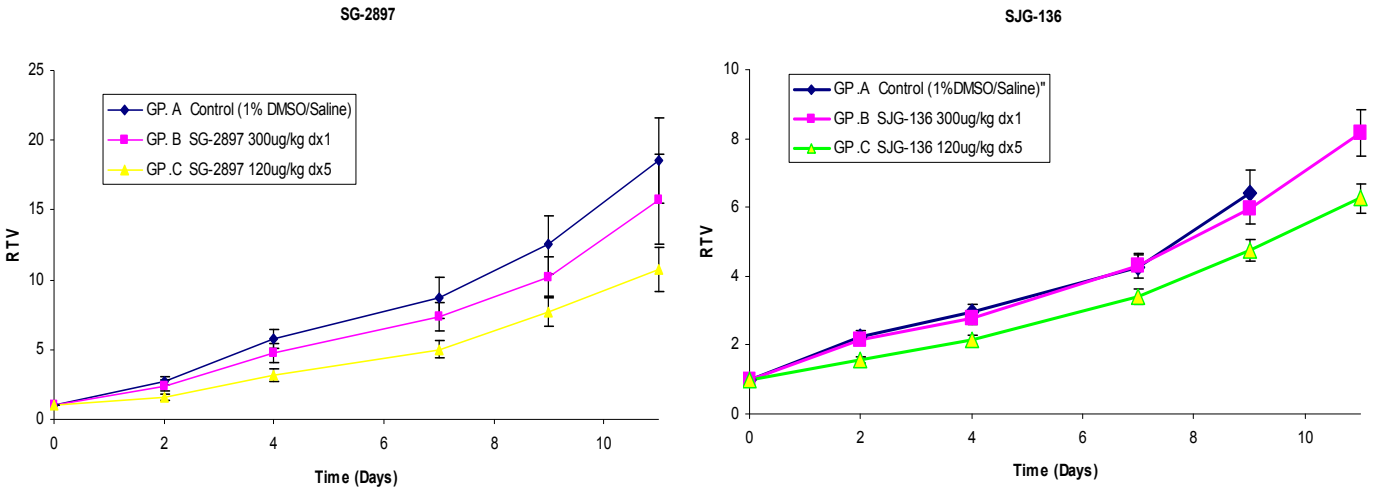

Figure 94. Results of the *In vivo* study with SG-2897 compared to SJG-136 towards animals bearing HCT 116 xenograft.

Taken together, the anti-tumour activity of SG-2897 was not demonstrated in this model where SJG-136 was not active either.

5.2.3 Activity of the PBD derivatives in cell lines deficient in DNA repair machinery: VC8 Chinese hamster cells (CHO) compared to the proficient V-79 CHO cells

DSB can be repaired by two pathways, homologous recombination repair (HR) and non-homologous end joining (NHEJ). It has been shown that the growth inhibitory effect of the PBD-dimer, SJG-136 and the growth inhibitory effect of its mono-functional (PBD-monomer) counterpart, mmy-SJG were dependent on HR factors such as the Rad51 paralogues (Clingen, De Silva et al. 2005). DSB are also detected by ATM, which triggers a downstream signal to the BRCA proteins allowing the Rad51 complex to arrange a nucleo-filament around the damaged strands in order for DNA to be repaired.

5.2.3.1 Growth inhibition studies

In this experiment, the impact of BRCA2 deficiency on the sensitivity of the PBDs was investigated using a cell line deficient in BRCA2 (VC-8) and its parental counterpart (V-79). The growth inhibitory effect of the PBD-dimer (SJG-136) and the PBD-monomer (SG-2897) in the 2 cell lines were evaluated. SJG-136 induced a greater cytotoxic effect against the VC-8, BRCA2 deficient cell line (IC_{50} = 52 pM [95% confidence interval = 46 – 49 pM]) compared to parental cells (IC_{50} = 1.3 nM [1 – 1.7 nM]) representing a ~25 fold increase in sensitivity (Figure 95.A). Similarly, the PBD-monomer SG-2897 induced a greater cytotoxic effect against the VC-8 (IC_{50} = 72 pM [95% confidence interval = 60 – 86 pM]) compared to parental cells (IC_{50} = 3 nM [2.4- 3.8 nM]) representing a ~42 fold increase in sensitivity (Figure 95.B.).

A.

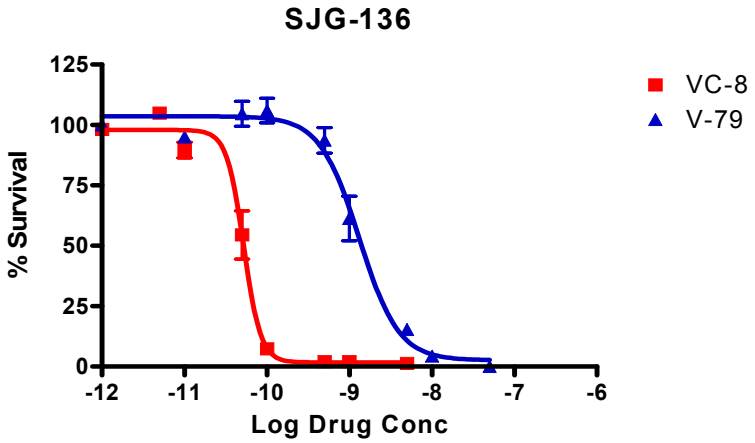

B.

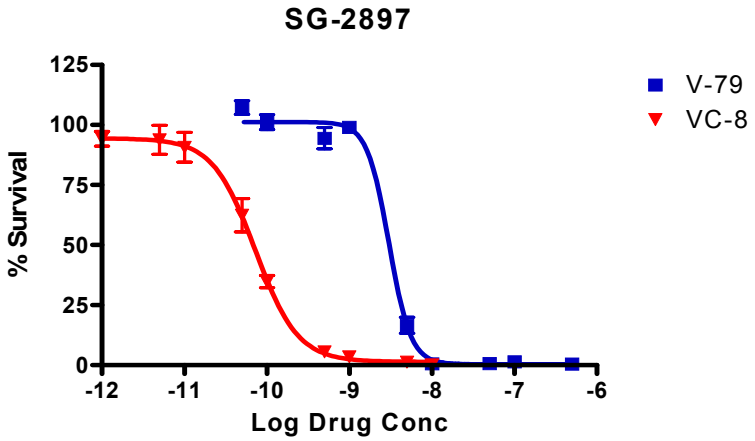

Figure 95. Impact of BRCA2 on the cytotoxic effect of SJG-136 (A) and SG-2897 (B) on VC-8 cells, deficient in BRCA2 (▼) and, on V-79 parental cell line (■). Results are means ± SEM of triplicate.

The ratio between the 2 cell lines for SJG-136 and SG-2897 was determined from 3 independent experiments. Overall, VC-8 cells were ~50 fold more sensitive to the PBD-monomer SG-2897, than to the parental cell line V-79 (Figure 96). The differential growth inhibitory effect was significantly lower for the PBD-dimer, SJG-136 (unpaired t test, $P_{value} = 0.042$). VC-8 cells were on average ~20 fold, more sensitive than the parental cell line to SJG-136.

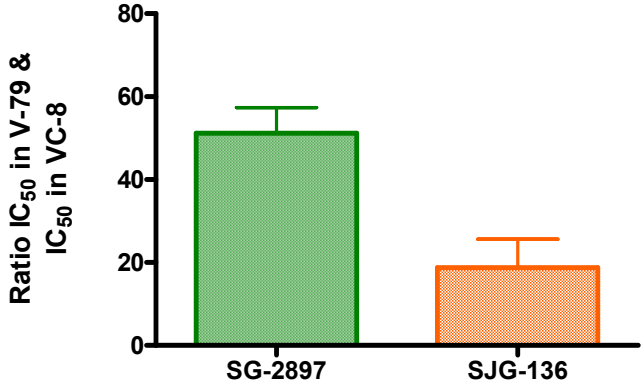

Figure 96. Ratio between the IC_{50} in VC-8 (BRCA2 deficient) cells and the IC_{50} in the parental cell line V-79. Results are means ± SEM of n = 3 experiments performed in triplicate.

These data provide additional evidence that the growth inhibitory effect of the PBD derivatives is dependent on HR proteins such as BRCA2. The higher ratio associated with SG-2897 suggests that the impact of this protein may be more important in the repair of the damage caused by the PBD-monomers than the PBD-dimers although further confirmation studies are required.

5.2.3.2 H2AX phosphorylation (γH2AX)

Previously, γH2AX foci formation was shown to be a surrogate marker of DNA damage caused by the PBDs (Cf. section 3.2.2**)**. As BRCA2 is involved in the repair of the damage caused by this class of molecules, γH2AX foci might be increased in BRCA2 deficient cells.

The CHO cell lines, VC-8 and V-79, were treated with the PBD-monomer, SG-2897, for 24h and stained for γH2AX foci. The number of V-79 cells *(*Figure 97-A*),* as represented by their nuclei (colored in blue by DAPI) is greater than the

number of VC-8 cells deficient in BRCA2 (Figure 97-A) after treatment with the same concentration of SG-2897.

In addition, there are almost no γH2AX foci in V-79 cells (Figure 97-A). Only few sporadic spots can be seen and represent the spontaneous formation of γH2AX foci. Conversely, there are a greater proportion (~5-fold) of the VC-8 cells with γH2AX foci (Figure 97-B and C) (Pvalue = 0.0002).

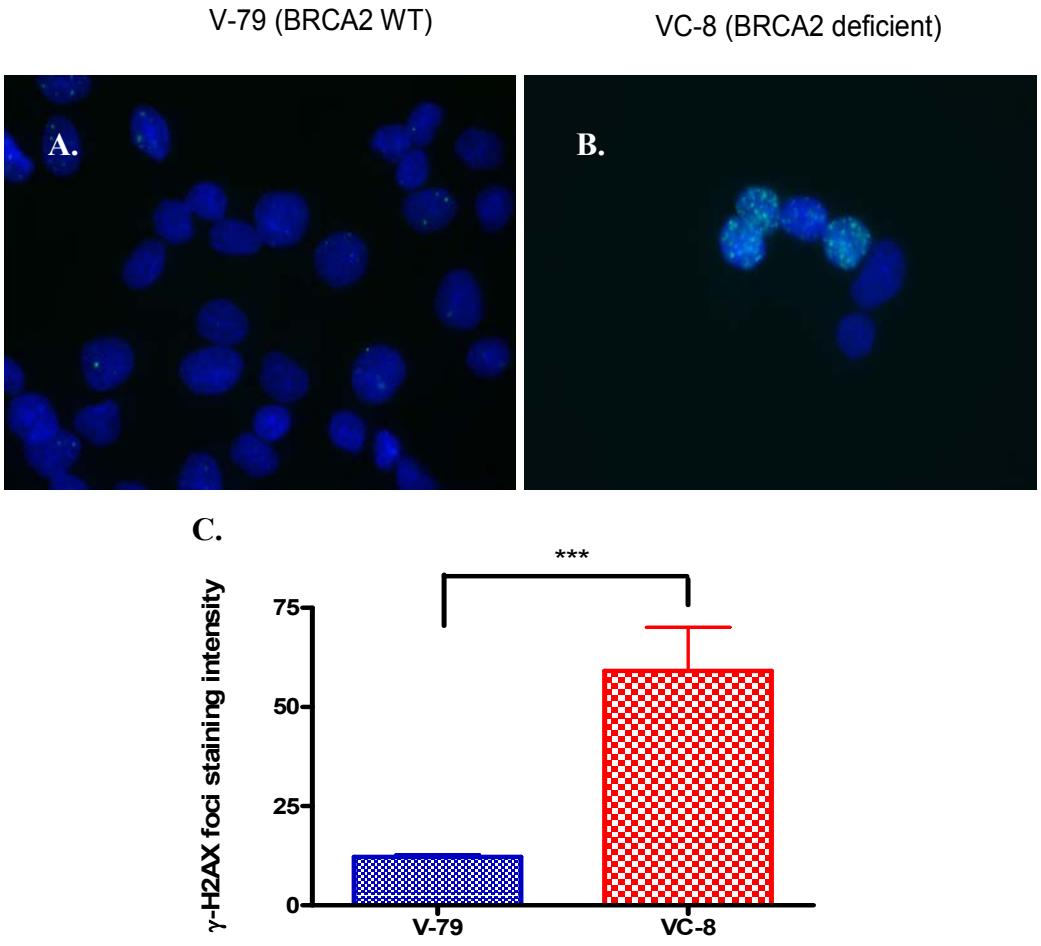

Figure 97. γH2AX foci formation observed in response to SG-2897 in V-C8, BRCA2 deficient cells (A) and in V-79, BRCA2 proficient cells (B). CHO cells were exposed to SG-2897 for 24h at 0.1 nM. A and B: representative pictures of γH2AX foci (represented in green). Counter-stain with DAPI (blue) confirms the nuclear localisation of γH2AX foci. C: γH2AX foci formation as expressed by staining intensity. Results are means ± SEM of 20 cells.

These results confirm the importance of BRCA2 in the repair of DNA damage caused by the PBD-monomers.

5.2.4 Computer based approach to design new PBD derivatives with enhanced growth inhibitory effect

The DNA/drug interaction was shown previously to be the dominant feature related to the growth inhibitory effect of the PBD-monomers (Section 5.2.1.2). In this section, a computer-based approach was used to assess the molecular docking of the different PBD-monomers within the DNA. The different parameters defining "the optimal fit" were compared to the experimental data (ΔTm) and a predictive model was developed. This strategy may allow to the design of new PBD derivatives with enhanced growth inhibitory effect.

It has been shown previously that SJG-136 spans 6bp and preferentially binds to Pu-GATC-Py sequences (Hartley, Spanswick et al. 2004). The PBD-monomers span 3bp and bind to Pu-G-Pu sequences (Hurley, Reck et al. 1988). Therefore, a specific sequence (TATA*GATC*TATA) was used in this experiment (Figure 98).

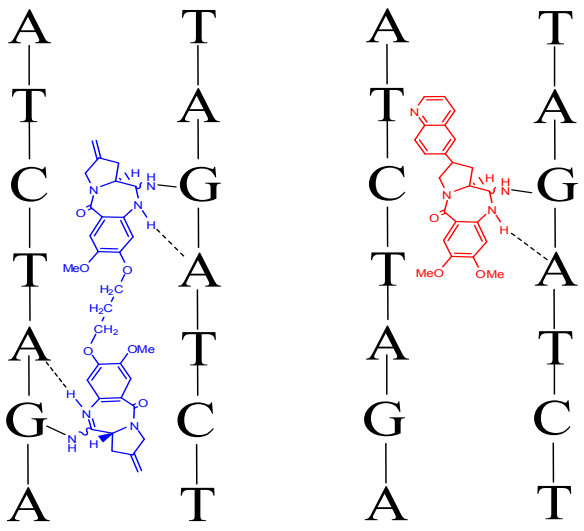

Figure 98. Mechanism of interstrand cross-linking of DNA by the PBD-dimer SJG-136 (A) and mono-alkylating of DNA by the PBD-monomer SG-2897 (B). The sequence selectivity of the PBD-dimer is due to (1) the covalent bound between the C11 of the PBD moieties and the N2 groups of the Guanine on opposite strands and (2) hydrogen bonds formed between the proton of the dimer moieties and the ring acceptor of the Adenine. The same sequence has been used for the monomer in order to normalize the data.

A set of PBD-monomers were chosen for the *in silico* approach, to achieve a wide range of physicochemical properties (number of aromatic rings, number of nitrogen and oxygen atoms, electrostatic potential) and growth inhibition *in vitro.*

Minimisation of DNA/Drug complex led to an optimal conformation defined by several parameters: the van-der-waals energy, the electrostatic forces and the sum of the bonded forces (Table 21).

	VdW	EELS	∑ bonded forces
DNA alone	-442.6	3111.51	574.87
SG-2781	-507.6	3426.62	626.78
SG-2819	-504.9	3398.22	621.91
SG-2820	-505.1	3417.61	624.86
SG-2825	-502.8	3409.13	628.85
SG-2897	-510.6	3418.86	624.42

Table 21. Physical Parameters generated *in silico* by the optimisation of the complex drug-DNA for 5 PBD-monomers: the van-der-waals energy (VdW), the electrostatic forces (EELS) and the sum of the bonded forced (the torsion and the dihedral angles).

5.2.4.1 The van-der-waals energy

The van-der-waals (VdW) energy is a close contact interaction. When 2 atoms or molecules are separated by a distance r they exert a close contact interaction (Figure 99). This attractive force increases inversely with the distance until reaching a limit when the force becomes repulsive.

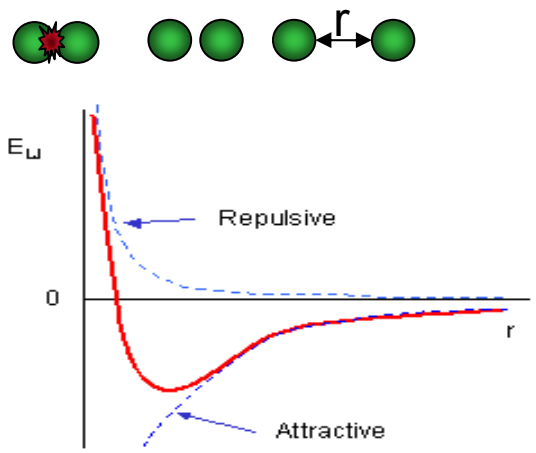

Figure 99. Representation of the van-der-waals energy.

SG-2897 was associated with the lowest VdW energy (-510.6) in contrast to SG-2819 (-502.8) (Table 21). These data suggest that SG-2897 has generated greater close contact interactions than SG-2819.

The interaction with DNA was measured physically previously by ΔTm. In order to investigate whether the VdW forces participate in the overall drug-DNA affinity, the relationship between the VdW and ΔTm was evaluated. The VdW interactions correlate with the melting point (ΔTm) value (r^2 = 0.8, P_{value} = 0.04) (Figure 100). SG-2897 was associated with the highest ΔTm (20.8) and has generated the lowest VdW energy (-510.6). In contrast, SG-2825 was associated with the lowest ΔTm (2.4) and has generated the greatest VdW energy (-502.8). However, 2 PBD-monomers deviate from the linear correlation (SG-2781 and SG-2819). This deviation may be explained by the impact of other forces in the overall affinity.

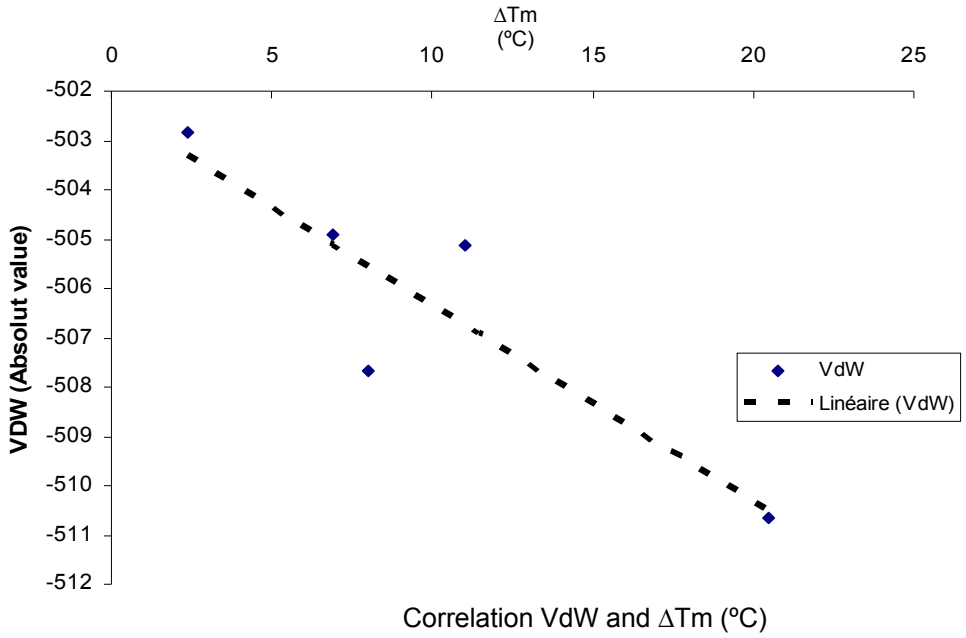

Figure 100. Relationship between the van-der-waals energy as determined by a computer based approach after minimization of the complex DNA-drug.

5.2.4.2 The electrostatic forces

Electrostatic forces (EELS) are generated between 2 charged atoms or molecules. Repulsion will occur between 2 atoms or molecules that are similarly charged. In contrast, 2 atoms or molecules with opposite charges will be attracted to each other.

SG-2819 and SG-2820 have shown similar VdW energies, (-504.9 and -505.1, respectively) (Table 21). However, SG-2820 was associated with a greater affinity for DNA as measured by the ΔTm (11) than SG-2819 (6.9). SG-2820 generated greater EELS forces (3417) than SG-2819 (3398), inducing greater close contact interactions with DNA. This is accordance with the fact that SG-2820 has a

negatively charged nitrogen atom at the extremity in contrast to SG-2819 (Figure 101).

SG-2820

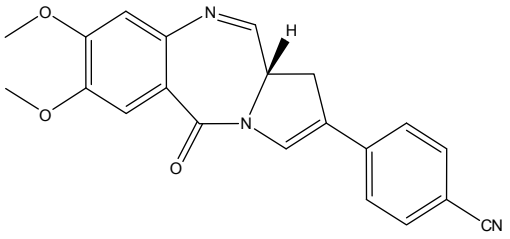

SG-2819

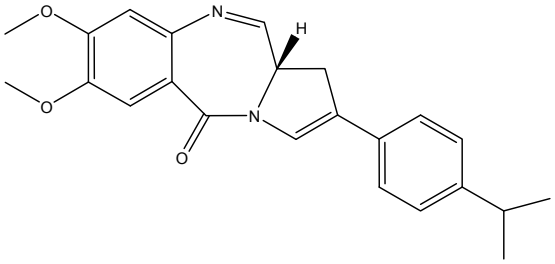

Figure 101. chemical structure of 2 PBD-monomers SG-2820 and SG-2819

Conversely, SG-2781 was associated with a lower ΔTm (8) despite having generated a relatively low VdW energy (-507.6). SG-2781 has a nitrogen atom at the extremity (Figure 102). However it is surrounded by other carbons. It has been shown, by the extended Hückel calculation that this nitrogen is predicted to be positively charged.

SG-2781

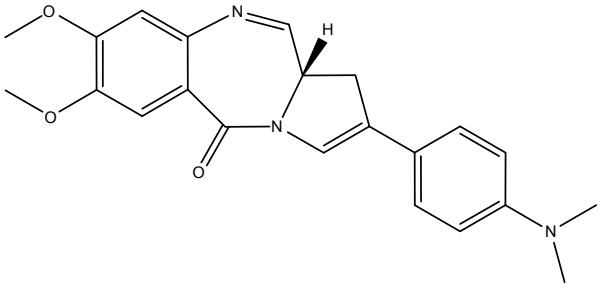

Figure 102. Chemical structure of SG-2781

5.2.4.3 The bonded forces

The bonded forces are generated by PBD-DNA complex and represent the mechanical distortions induced by the minimisation (spatial optimisation) of the complex. The components are the bond stretching, bond bending, bond torsion and chirality of the bond. The minimisation of the complex should lead to a minimal distortion. In other words, PBDs with a better fit within DNA would induce a lower distortion.

The sums of the different bonded forces have been determined for the PBD-monomers of interest (Table 21). As a result, SG-2819 was associated with the lowest distortion of the PBD-DNA complex with a sum of bonded forces of 621 in contrast to SG-2825 which was associated with the greatest distortion (628.5).

The latter was associated with a low affinity for DNA ($\Delta Tm = 2.4$). SG-2825 has a chemical structure with a long tail of unsaturated carbons at the C2 extremity (Figure 103). The bulkiness of its structure might explain the low affinity for DNA and the maximal distortion induced *in silico.*

SG-2825

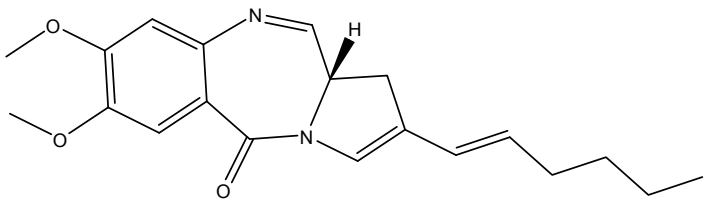

Figure 103. Chemical structure of SG-2825.

5.2.4.4 Design of new PBD derivatives with greater affinity for DNA

The growth inhibitory effect of the PBDs was shown to be mainly related to their interaction with DNA. However, the expression of ABC transporters may also affect their anti-tumour activity. Therefore, the consideration of both the factors related to PBD-DNA binding and to substrate specificity to ABC transporters should allow the rational design of new PBD derivatives with enhanced anti-tumour activity.

Two strategies were investigated: One was to increase the length of the C2 substituent in the PBD-monomers; the other was to decrease the second moiety of the PBD-dimers in C8. Suggested potential structures are shown in Figure 104.

All the new PBD derivatives are predicted to be associated with a limited interaction with the ABC transporters. In order to be P-gp non substrate, they have a molecular weight lower than 500, a number of (nitrogen + oxygen) atoms lower than 8, a log *P* ranging from 1.387 to 3.225, a number of hydrogen bonding energy lower than 10. In order to be non substrate of MRP1, none of the new derivatives have a carbonyl group at the C2 extremity. Finally, all new PBDs have a limited number of (N+O) atoms, negatively charged as determined by the Hückel calculation, in order to prevent ABCG2 substrate specificity.

104.A.

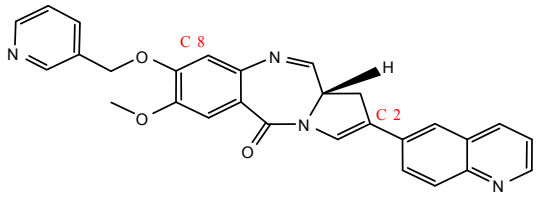

LogP = 2.688
Mol Weight = 462.49

104.B

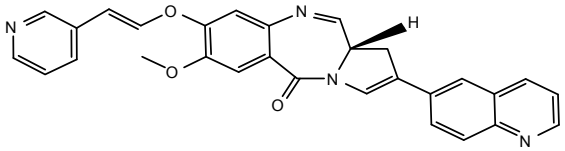

LogP = 3.096
Mol Weight = 474.51

104.C.

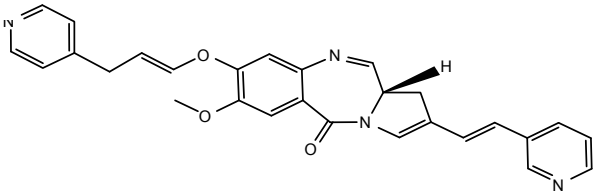

LogP = 2.608
Mol Weight = 464.51

104.D.

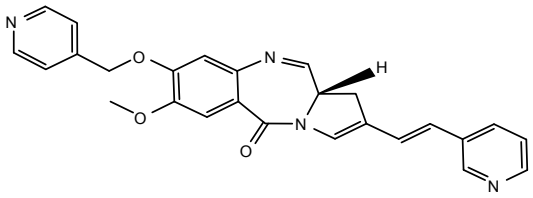

LogP = 1.782
Mol Weight = 438.48

104.E.

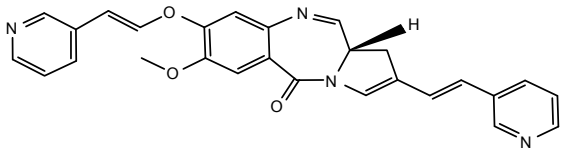

LogP = 2.8
Mol Weight: 450,49

104.F.

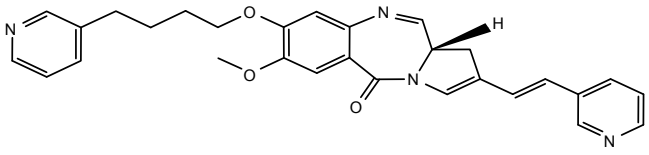

LogP = 2.897
Mol Weight = 480.55

104.G.

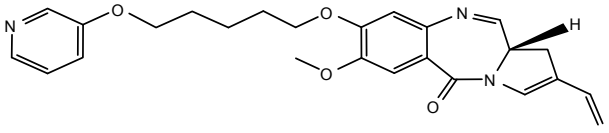

LogP = 2.472
Mol Weight = 433.49

Figure 104. Proposed structures of new PBD derivatives anticipated to be non-substrates for neither P-gp nor MRP1 and associated with a low affinity to ABCG2.

In order to test whether the new PBD derivatives would be associated with a greater interaction with DNA, 2 were tested using the molecular modelling approach (104.A. and 104.B). The modelling of SG-2819 was reported for comparison. All three molecules appear to fit well in the minor groove of DNA (Figure 105). The C8 substituent of 104.A. allows the molecule to span a greater length of DNA than SG-2819 thus, increasing the close contact interactions. In addition, the specific layout of the C8 moiety of 104.B. allows the molecule to fit perfectly in the minor groove of DNA limiting the distortion of the helix.

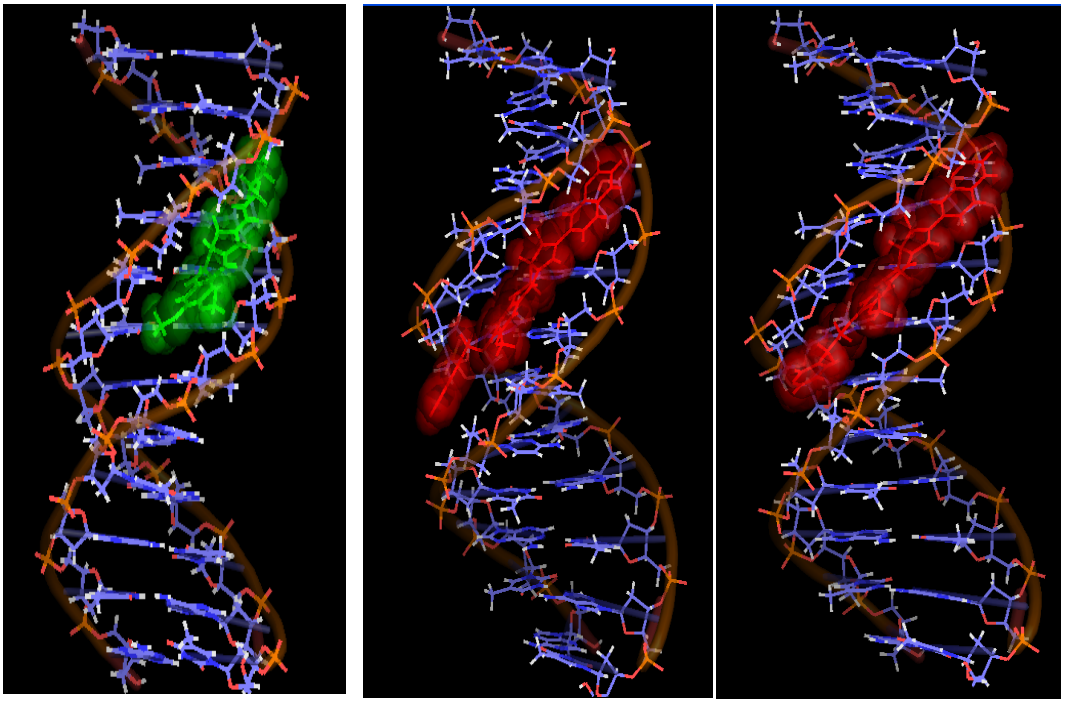

SG-2819 104.A. 104.B.

Figure 105. Molecular modelling of the new PBD derivatives with DNA. The new PBD derivatives (red), 104.A. (middle picture) and 104.B. (right picture), are predicted to be non substrates for any of the ABC transporters (P-gp, MRP1 nor ABCG2). The molecular modelling of SG-2819 (green) within DNA has been shown for comparison (left picture).

The general parameters defining the minimisation of the complex such as the van-der-waals energy was evaluated for the 2 new derivatives. 104.A. was associated with the lowest VdW energy (-526.7) followed by 104.B. (-515.5) (Figure 106). Since the VdW energy has been shown to be a major factor involved in the drug-DNA interaction, 104.A. and 104.B. are predicted be associated with a maximal interaction with DNA (predicted ΔTm of 61.3 and 33.7, respectively).

For comparison, SG-2897 is associated with a ΔTm of 20.8 which represents a ~3 fold lower affinity for DNA. This particular compound has been shown to be the most cytotoxic PBD-monomer among a panel of cell lines. Since, the interaction with DNA has been shown to be a major factor in the PBD-monomers driven growth inhibitory effect, the new derivatives (especially 104.B.) are predicted to be associated with maximal anti-tumour activity.

SJG-136, a PBD-dimer has shown a ΔTm of 31 which represents a ~2 fold lower affinity for DNA. In addition, its growth inhibitory effect has been shown to be reduced by the expression of the ABC transporters. In contrast, 104.B. would have a greater affinity for DNA and a limited interaction with the ABC transporters, thus associated with a maximal anti-tumour activity.

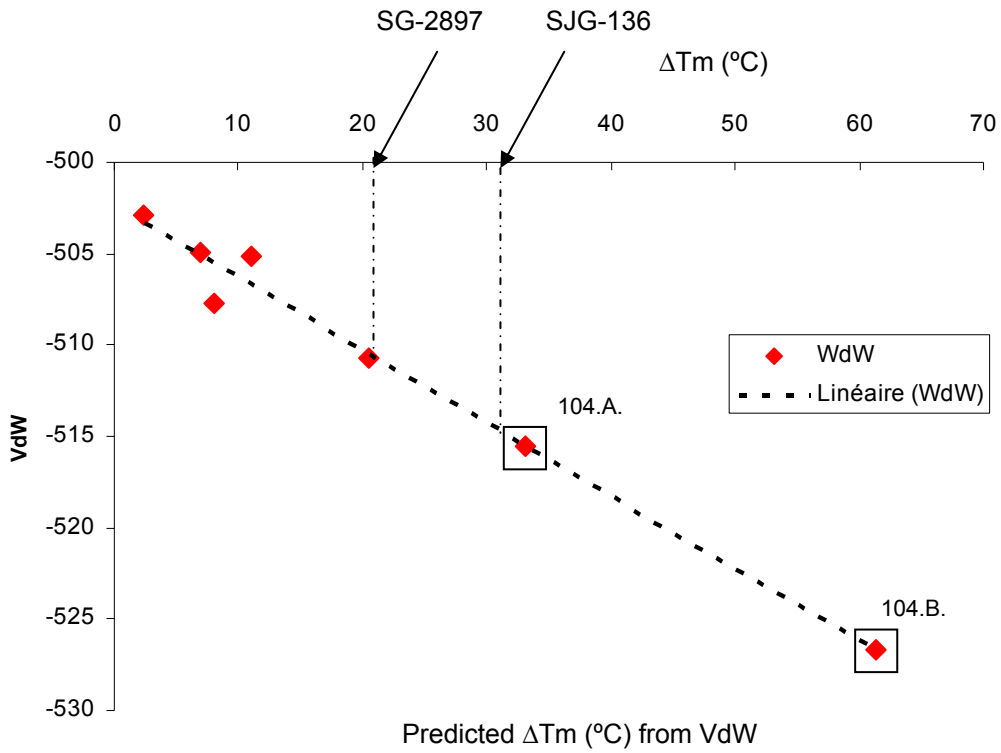

Figure 106. Prediction of the interaction with DNA of the 2 PBD-new derivatives. The interaction with DNA is represented as ΔTm. The VdW energies for 104.A. and 104.B. have been evaluated by molecular modelling after minimisation of the PBD-DNA complex. Predicted ΔTm of the PBD new derivatives have been determined according to the linearity defined previously for a range of PBD-monomers. ΔTm for SJG-136 has been reported for comparison (ΔTm = 31).

5.3 Discussion

Interstrand cross-linking (ICL) agents have shown utility in the treatment of many cancers. A novel ICL agent, SJG-136, a PBD-dimer, has been shown to be active *in vitro* and *in vivo* and is in clinical development. However its growth inhibitory effect can be decreased by the expression of many ABC transporters.

The PBD-monomers may not be considered to be the best candidates for further development as they do not cross-link DNA and are generally less potent that the PBD-dimers. However, the PBD-monomers only demonstrate a limited

interaction with ABC transporters and one of them has shown a level of growth inhibitory effect similar to SJG-136. In this chapter, physico-chemical properties involved in the biological activity of the PBD-monomers were defined, hence defining a structure activity relationship. The interaction with DNA, as measured by ΔTm and the growth inhibitory effect of the PBD-monomers has been shown to be highly correlated in a panel of cancer cell lines.

It is well known that that due to its phosphate group, DNA is negatively charged. Moreover, the electrostatic potential is more negative for the deep, narrow minor groove than for the major groove of B-form DNA (Pullman, Lavery et al. 1982; Nelson, Finch et al. 1987).

PBD-monomers are positively charged at physiological pH and it appears that long-range electrostatic attractions allow an initial approach of the PBDs to DNA.

The surface buried in the minor groove of DNA has been shown to be fundamentally hydrophobic. As a consequence, molecules with a greater hydrophobicity are predicted to generate a greater affinity within the binding pocket of DNA. The PBD-monomers are all hydrophobic as determined by their Log *P* ranging from 1.9 to 3.7. This property allows them to fit within DNA.

In addition, the presence of the imine form containing the C11-electrophilic carbon is ubiquitous among the PBD-monomers. The imine allows the PBD-monomers to form a covalent bond with DNA. Other physico-chemical parameters may also impact on the drug-DNA affinity. When bound to one strand of DNA, the lipophilicity as represented by the surface activity, the solvent accessible surface area and log *P* were negative determinants for additional interaction with DNA and the induced growth inhibition. This phenomenon could be explained by the fact that

when 2 entities are hydrophobic, they attract one another. However, a repulsive force tends to appear once the 2 entities get too close (when they are inside each others VdW radii).

In contrast, the molecular aromaticity (number of 6 menber rings) was identified as a positive determinant for the interaction of the PBDs to DNA. The molecular aromaticity has been further analysed and the role of the stacking interactions between the C2 moiety of the PBD-monomers and the different bases of DNA was revealed. The stacking interactions represent the most important close contact interactions which allow the 2 strands of DNA to be held together. The strength of the base stacking interactions depends on the bases. It is strongest for stacks of G/C base pairs and weakest for stacks of A/T base pairs, which explains why it is easier to melt A/T rich DNA at high temperature. The PBD-monomers of our library may generate a greater interaction with DNA when surrounded by GC sequences. By minimising the PBD-monomer-DNA complex *in silico*, the spatial arrangement of the C2-aryl substituent did not allow the molecule to fit in between the nucleotides and undergo the optimal stacking interaction. However, during replication, DNA is subject to relaxation. The modified spatial arrangement of the nucleotides may allow the aromatic ring to become available for an optimal stacking interaction with the PBD-monomers. Further studies will be needed to confirm this hypothesis. For example, the denaturation data (ΔTm) may be re-evaluated using G/C-rich sequences (Ha-*ras* oncogene) or A/T-rich (estrogen receptor (ER)) amplified by Polymerase chain reaction (PCR).

The aromaticity, of SJG-244 should have predicted potent growth inhibitory effect. However, the latter has an aromatic ring at the C8 extremity and has shown

the lowest growth inhibitory effect among the panel of cell lines tested. When the complex between SJG-244 was modelled *in silico* the C8 extremity was found pointing towards the outer surface of DNA (data not shown) preventing a good fit within the minor groove of the double helix. SJG-244-DNA adducts may be recognised and removed more readily by DNA repair machinery, thus limiting its anti-tumour activity.

In addition, electrophicity was shown to be a major determinant of the interaction of the PBD-monomers with DNA. SG-2820 has, at its C2 extremity, a nitrogen atom with a negative partial charge in contrast to SG-2781. It may form hydrogen bonds, more readily, with DNA, thus enhancing a greater interaction with the double helix. However, the anti-tumour activity of SG-2820 did not correlate with the interaction with DNA as determined by the thermal denaturation data. Therefore, other cellular factors may influence the biological activity of the C2-aryl substituent derivatives. Compounds with a greater electrophilic potential may be associated with a greater interaction with cellular proteins or may be detoxified more easily by conjugation therefore, reaching DNA less readily, resulting in a reduced anti-tumour activity. Consideration of these factors may allow a rational design of new PBDs with enhanced anti-tumour activity. PBD-electrophilic-site, involved in PBD-DNA interaction may be hidden by the addition of chemical groups. The pro-drug may be easily recognised by nuclear lytic enzymes which could release the active form more readily, preventing detoxification processes. Such strategy has already been tested with the PBD derivatives. For instance, "N10 protected" PBD molecules pro-drugs were associated with a limited anti-tumour activity in contrast to

the active form, obtained by the lytic activity of the nitroreductase enzyme (Sagnou, Howard et al. 2000).

The position of the electrophilic atom has also been shown to be of importance in PBD-DNA complex formation and in the related activity of the PBD-monomers. Indeed, SG-2897 is associated with a greater interaction with DNA and greater anti-tumour activity than its 6 member ring counterpart SG-2896. The nitrogen, with a particular spatial arrangement, may interact with both strands of DNA, thus increasing PBD-DNA interaction. These results provide evidence that the PBD-monomer, SG-2897, which does not cross-link DNA, may generate significantly close contact interactions which could "mimic" the cross-link, induced by the PBD-dimers.

The anti-tumour activity of SG-2897 has also been tested *in vivo* and compared to the anti-tumour activity of SJG-136 using Nu/Nu mice. The choice of the doses for SG-2897 was based on the maximum tolerated dose (MTD) that was determined previously for SJG-136 (0.6 mg/kg). The drug was given ***i.v.*** in a single (0.3 mg/kg) or 0.12 mg/kg in a Qdx5 schedule. The single administration schedule was less effective, but the total dose administered with the Qdx5 schedule is twice the single dose (0.3 mg/kg). A specific growth delay < 1 and a tumour regression (T/C) > 42% suggested that the inhibition of the tumour growth with SG-2897 was not significant. However, the activity of SJG-136 was also not significant in this particular model. The potency of SG-2897 is similar to SJG-136, *in vitro* and it can be argued that further investigations of the anti-tumour activity in more appropriate models may lead to more convincing results. The NCI60 screen has identified the melanoma SK-Mel 5 cell line as being the most sensitive cell line model to SG-2897.

Experiments were carried out in order to determine the MTD for this particular compound using CD-1 nude mice. A 0.25 mg/kg dose in a Qdx5 schedule was not tolerated and the mice had to be culled after 3 days of treatment. When the mice were treated back with 0.12 mg/kg dose in a Qdx5 schedule, a body weight loss was first observed; suggesting toxicity, followed by death after 5 days. The necroscopy revealed hepatitis. These results suggest a hypersensitivity reaction rather than a true toxic effect which may be strain related. Therefore, evaluation of the MTD using the Nu/Nu mouse strain, originally tested, would be the next step.

The recognition and the repair of the DSB generated by the PBD derivatives have been shown to involve the recruitment of proteins of the homologous recombination (HR) repair pathway such as XRCC2 and XRCC3. In this chapter, the impact of another protein in the HR pathway, BRCA2 was investigated. A cell line deficient for BRCA2, was more sensitive to the PBD-dimer, SJG-136 and to the PBD-monomer SG-2897. The ratio between the IC_{50}s in the proficient cell line V-79 and the IC_{50} in the deficient cell line was > 20 for SJG-136 and > 50 for SG-2897. These results demonstrate the impact of BRCA2 in DNA repair machinery associated with PBDs. When these results are compared to the study by Clingen and colleagues, the ratio between the IC_{50} in XRCC3 and XRCC2 proficient and deficient cell lines was 7.5 and 3.5, respectively, demonstrating a limited impact of these factors on DNA repair in contrast to BRCA2 (Clingen, De Silva et al. 2005). Moreover, the growth inhibitory effect of SG-2897 was more enhanced by the deletion of BRCA2 than the growth inhibitory effect of SJG-136. In vivo experiments were carried out to confirm the impact of BRCA2 but since the CD-1 nude mice used were hypersensitive, no conclusive result could be obtained.

Other studies have also reported differential impact of the proteins of the HR pathway in the repair of the damage induced by cytotoxic agents. The HR induced by ET-743, has been shown to be mediated mostly by XRCC3 in contrast to XRCC2 (Soares, Escargueil et al. 2007). In contrast, XRCC2 and XRCC3 were both recruited after treatment with melphalan, Mitomycin C and tirapazamine (Cui, Brenneman et al. 1999; Clingen, De Silva et al. 2005; Evans, Chernikova et al. 2008).

Taken together, the different HR proteins may be acting as in an equilibrium model to trigger efficiently the signal for the repair of damaged DNA.

There are a great number of cancers associated with mutations of proteins of the HR pathway. For instance, 50% of all breast cancers are associated with loss of HR(Venkitaraman 2002). Targeting the HR-defective tumours with specific chemotherapeutics such as the PBDs appears to be a realistic clinical strategy, underlying the concept of "synthetic lethality". Recently, Bryant and colleagues have demonstrated the relevance of this strategy using inhibitors of poly(ADP-ribose) polymerase 1 in the killing of BRCA2 deficient tumours (Bryant, Schultz et al. 2005). Similarly, a benefit in cisplatin based chemotherapy was seen among patients with ERCC1 negative tumours (Olaussen, Dunant et al. 2006).

The PBD-monomer, SG-2897 was associated with a significant anti-tumour activity *in vitro* without being able to reproduce similar potency *in vivo*. The rational design of new PBD-monomers that are not substrates for ABC transporters and with enhanced anti-tumour activity may generate PBD derivatives associated with sufficient *in vivo* anti-tumour activity to merit their preclinical evaluation. To facilitate the design of new molecules, a computer based approach has been used to

evaluate the potential potency of new derivatives. Minimisation of the PBD-monomer-DNA complex has identified the van-der-waals energy and the electrostatic forces as determinants of the interaction with DNA. *C*ompounds that have generated the greatest VdW energy, by minimisation of the complex were associated with the greatest affinity for DNA. This is in accordance with the findings from Bielawski and colleagues who analysed a series of carbocyclic analogues of netropsin which are also minor-groove binders (Bielawski, Bielawska et al. 2000). Some might argue that VdW interactions could also generate repulsive forces. In this case, a greater value of VdW would be associated with greater steric constraints and more bonded forces after optimisation of the complex. SG-2897 was associated with the greatest VdW energy but with limited bonded forces.

Many PBD-derivatives have been synthesised in order to improve their affinity for DNA and related growth inhibitory effect (Kamal, Babu et al. 2005; Kamal, Reddy et al. 2006; Wang, Shen et al. 2006). These studies have focussed on modification of the C8 subsituents. For instance, a series of PBD-polypyrrole conjugates reported by Baraldi and Lown (Damayanthi, Praveen Reddy et al. 1999) and modified by Wells and colleagues have been associated with a significant interaction with DNA and growth inhibition in the nanomolar range against K562 cell line (Wells, Martin et al. 2006). However, all of these analogues share the physico-chemical features for recognition by the ABC transporters: the number of (N+O) atoms > 10, a log*P* > -1, a PSA > 75 $Å^2$ and the presence of carbonyl at the extremity. Therefore, their anti-tumour activity is predicted to be reduced in cell lines expressing different ABC transporters. In addition, the presence of an carbonyl moiety may lead to a greater detoxification through the conjugation to glutathione by

glutathione-S-transferase for example, limiting even further their anti-tumour activity.

Another strategy has been investigated by Antonow and colleagues. They have synthesised a series of PBD-derivatives, with modifications at the C2 substituent. A few were associated with a high affinity for DNA as determined by ΔTm thus, inducing a greater cytotoxic effect. Similarly, though some of these PBD derivatives are predicted to be ABC transporter and GST substrates.

In this chapter, 2 strategies were combined: new PBD derivatives were designed by modifying the substituent at position C2 and C8 based on their ability to interact with DNA and simultaneously limited potential interaction with the ABC transporters.

Unfortunately, it became apparent that the chemical synthesis of the new analogues with combined modifications at C2 and C8 is challenging chemistry as novel synthetic pathways will have to be developed. Therefore, synthesis of new analogues was not achieved within the time scale of the project.

6 Chapter 6: CONCLUSIONS

The aims of the work presented in this thesis were to identify the structural factors responsible for ABC transporter (P-gp, MRP1 and ABCG2) dependency of the pyrrolo [2, 1-c][1,4]benzodiazepines (PBDs), to evaluate the impact of ABCB1 and ABCG2 polymorphisms and to determine the structural features associated with PBD activity. Using this information, new PBD entities would be designed with potentially enhanced anti-tumour activity.

6.1 Features involved in ABC transporters substrate specificity of the PBD derivatives

6.1.1 P-gp (ABCB1)

Molecular weight (MW), the polar surface activity (PSA), the number of (N+O) atoms and the hydrogen bonding energy were associated with P-gp substrate specificity of the PBDs (Table 22). When the PBD-dimers were considered independently, Log*P* and MW correlated with P-gp dependency and therefore could be used to further minimise the impact of P-gp over-expression. However, all PBD-dimers have a MW > 532.5 and no approach is feasible to diminish their size without losing "the dimer property". The PBD-monomers were only shown to be low affinity substrates in supraphysiological conditions. In a clinical context, optimising their structures is therefore not required.

6.1.2 MRP1 (ABCC1)

The presence of a carbonyl moiety at the C2 extremity of the PBD derivatives (SG-2823) was shown to be required for a spontaneous and enzymatic (glutathione-S-transferase) coupling to glutathione, prior to the extrusion by MRP1, out of the cell (Table 22). The spontaneous conjugation of GSH to the PBDs was suggested to occur at the carbinolamine moiety ubiquitous among the PBDs. This detoxification process (conjugation to glutathione) is, as well as the expression of the ABC transporters, involved in MDR. Consideration of the factors involved in the GSH / coupling such as the electrophilicity of the PBDs should be taken in account in the rational design of new entities. The specific impact of the different members of the GST family on the detoxification process mediated by MRP1 may be the basis for further work.

6.1.3 ABCG2 (BCRP)

It has been shown that ABCG2 substrates share a common set of properties such as high polarity and a large number of hydrophilic groups which can be seen among both the PBD-dimers and PBD-monomers. The work presented in this thesis demonstrated that PBDs with a greater number of aromatic rings and (nitrogen and oxygen) negatively charged atoms were shown to be associated with greater substrate specificity to ABCG2 (Table 22). Minimising these features should allow the design of new PBD derivatives with minimal interaction for the transporter.

6.2 Impact of the major ABC transporters polymorphisms

Inter-individual differences as described by ABC transporters polymorphism may also alter the specificity of PBDs for the transporters. The work presented in this thesis evaluated the impact of the major mutations on the substrate specificity of the PBDs to ABC transporters.

6.2.1 ABCB1 polymorphism

An enhanced efflux transport ability associated with the 2677 (G/T) variant (Ser 893), *i.e.* "gain of function" mutation for the PBD-dimers, high affinity substrates of the transporter was demonstrated. When a mutation in position 3435 was associated with a mutation in position 2677 (G/T), the former abrogated the "gain of function" identified in the efflux of the PBD-dimers. The anti-tumour activity of the PBD-monomers, low affinity substrates, would be less subject to inter-individual variability of the transporter than the PBD-dimers. A phase one trial is being conducted with SJG-136 and preliminary data have demonstrated an impact of ABCB1 polymorphism (personal communication).

6.2.2 MRP1 polymorphism

Functional single nucleotide polymorphisms of MRP1 have not yet been reported and further studies are needed to evaluate the impact of inter-individual variability on PBD efflux mediated by MRP1. In addition, the role of glutathione-S-transferase polymorphism on clinical outcome has been reported recently and in light of the data presented in this thesis it may be appropriate to investigate the impact of

the different variants on PBD susceptibility to detoxification (Moradi, Mojtahedzadeh et al. 2008).

6.2.3 ABCG2 polymorphism

A "gain of function" was associated with the presence of a threonine as supposed to an arginine. PBDs, with a greater number of aromatic rings and electron withdrawing groups were more affected by this particular mutation. These preclinical data may guide further evaluations of the PBD-monomers and PBD-dimers and establish a link with the clinical impact of the 482 SNP.

6.3 PBD-monomer related activity

The PBD-monomers do not appear to be high affinity substrates of P-gp or MRP1 (apart from SG-2823) and have shown a minimal interaction with ABCG2 in contrast to the PBD-dimers. It can be argued that the PBD-monomers might be associated with a minimal interaction for the ABC transporters, but as they do not cross-link DNA, they would be less potent than the PBD-dimers.

These studies demonstrate that the PBD-monomer, SG-2897 is as active as the PBD-dimer, SJG-136 *in vitro*. To study this further, the physico-chemical properties involved in the PBD-monomer/DNA binding affinity and to the related anti-tumour activity were investigated. The number of aromatic rings correlated with the anti-tumour activity of the PBD-monomers. The number of electrophilic atoms and the lipophilicity as represented by the surface accessible solvent area and log*P,* inversely correlated with the anti-tumour activity. In addition, the fitting of the

PBDs (preventing bulkiness) within DNA was shown to be a critical factor for the activity of the PBD-monomers as well as the position of the electrophilic atoms at the C2 extremity, thus enhancing greater close contact interactions (Table 22).

Overall, the results presented in this thesis allowed the rational design of a new PBD derivative (104.B.) based on the features associated with the affinity for the different ABC transporters and on the features involved in the anti-tumour activity of the PBDs (Table 22). Few parameters such as the aromaticity were optimised in order to prevent ABCG2 substrate specificity but also to allow a sufficient anti-tumour activity. Parameters such as Log *P* and the number of (N+O), negatively charged were decreased in order to promote the anti-tumour activity of the PBDs.

Features	P-gp	MRP1	ABCG2	Anti-tumour activity
PSA	+			
MW	+			
Log *P*	+			-
HBE	+			
(N+O)	+		+	
(N+O)-			+	-
(N+O)+				
Aromatic rings			+	+
Surface activity				-
bulkiness				-
SASA				-
C=O at extremity		+		

Table 22. Features involved in the anti-tumour activity of the PBDs and the features involved in ABC transporters dependency. PSA: Polar surface area, MW: Molecular weight, HBE: Hydrogen bonding energy, (N+O), (N+O)- and (N+O)+: number of oxygen and nitrogen atom, negatively charged and positively charged, respectively. SASA: Solvent accessible surface area. (+) show a positive contribution of the features to PBD dependency to ABC transporters. (-) show a negative contribution to the anti-tumour activity of the PBDs. (+) show a positive contribution to the anti-tumour activity of the PBDs.

Further work is needed to confirm the relevance of the different features, *i.e.* optimised structure on drug absorption, distribution, metabolism and elimination, hence defining the pharmacokinetics of the PBD-monomers. The PBDs, due to their high electrophilic characteristic (C11), may potentially undergo a high metabolism and a significant protein binding preventing the molecule to reach the tumour site. Alternative deliver strategies, such as prodrugs with "hidden electrophilic moiety" should be undertaken in order to allow a significant *in vivo* anti-tumour activity. Such strategy may only be applied to the PBD-monomers as the addition of the "hiding groups" would increase the molecular weight of the derivatives associated with P-gp substrate specificity.

H2AX foci formation correlated with activity of the PBD-monomers. Therefore, the formation of γH2AX foci may be used to evaluate the efficacy of the drug treatment. The DNA repair machinery following the treatment with the PBD-monomers was also investigated and BRCA2 was identified as a predictive biomarker. Therefore, the potential anti-tumour activity of the PBDs may be enhanced in tumours mutated or deficient in this particular protein.

To conclude, in the work presented in this thesis, I have identified the chemical features involved in ABC transporter dependency of the PBDs. I have also been able to link structural features of the PBD monomers to activity and this has allowed me to design a novel PBD derivative, predicted to show enhanced anti-tumour activity. Unfortunately, the complexity of the synthesis of this chemical entity did not allow it to be synthesised within the time scale of this project

References

Aird, R. E., M. Thomson, et al. (2007). "ABCB1 genetic polymorphism influences the pharmacology of the new pyrrolobenzodiazepine derivative SJG-136." Pharmacogenomics J.

Aird, R. E., M. Thomson, et al. (2008). "ABCB1 genetic polymorphism influences the pharmacology of the new pyrrolobenzodiazepine derivative SJG-136." Pharmacogenomics J **8**(4): 289-96.

Akkari, Y. M., R. L. Bateman, et al. (2000). "DNA replication is required To elicit cellular responses to psoralen-induced DNA interstrand cross-links." Mol Cell Biol **20**(21): 8283-9.

Allen, J. D., S. C. Jackson, et al. (2002). "A mutation hot spot in the Bcrp1 (Abcg2) multidrug transporter in mouse cell lines selected for Doxorubicin resistance." Cancer Res **62**(8): 2294-9.

Alley, M. C., M. G. Hollingshead, et al. (2004). "SJG-136 (NSC 694501), a novel rationally designed DNA minor groove interstrand cross-linking agent with potent and broad spectrum antitumor activity: part 2: efficacy evaluations." Cancer Res **64**(18): 6700-6.

Allikmets, R., L. M. Schriml, et al. (1998). "A human placenta-specific ATP-binding cassette gene (ABCP) on chromosome 4q22 that is involved in multidrug resistance." Cancer Res **58**(23): 5337-9.

Ambudkar, S. V., S. Dey, et al. (1999). "Biochemical, cellular, and pharmacological aspects of the multidrug transporter." Annu Rev Pharmacol Toxicol **39**: 361-98.

Anderle, P., E. Niederer, et al. (1998). "P-Glycoprotein (P-gp) mediated efflux in Caco-2 cell monolayers: the influence of culturing conditions and drug exposure on P-gp expression levels." J Pharm Sci **87**(6): 757-62.

Antonow, D., N. Cooper, et al. (2007). "Parallel synthesis of a novel C2-aryl pyrrolo[2,1-c][1,4]benzodiazepine (PBD) library." J Comb Chem **9**(3): 437-45.

Arnould, S., V. J. Spanswick, et al. (2006). "Time-dependent cytotoxicity induced by SJG-136 (NSC 694501): influence of the rate of interstrand cross-link formation on DNA damage signaling." Mol Cancer Ther **5**(6): 1602-9.

Artursson, P. and J. Karlsson (1991). "Correlation between oral drug absorption in humans and apparent drug permeability coefficients in human intestinal epithelial (Caco-2) cells." Biochem Biophys Res Commun **175**(3): 880-5.

Bain, L. J. and G. A. LeBlanc (1996). "Interaction of structurally diverse pesticides with the human MDR1 gene product P-glycoprotein." Toxicol Appl Pharmacol **141**(1): 288-98.

Baraldi, P. G., B. Cacciari, et al. (2000). "[2,1-c][1,4]benzodiazepine (PBD)-distamycin hybrid inhibits DNA binding to transcription factor Sp1." Nucleosides Nucleotides Nucleic Acids **19**(8): 1219-29.

Barnouin, K., I. Leier, et al. (1998). "Multidrug resistance protein-mediated transport of chlorambucil and melphalan conjugated to glutathione." Br J Cancer **77**(2): 201-9.

Benderra, Z., A. M. Faussat, et al. (2004). "Breast cancer resistance protein and P-glycoprotein in 149 adult acute myeloid leukemias." Clin Cancer Res **10**(23): 7896-902.

Berhane, K., X. Y. Hao, et al. (1993). "Contribution of glutathione transferase M3-3 to 1,3-bis(2-chloroethyl)-1-nitrosourea resistance in a human non-small cell lung cancer cell line." Cancer Res **53**(18): 4257-61.

Bielawski, K., A. Bielawska, et al. (2000). "Molecular modelling of the interaction of carbocyclic analogues of netropsin and distamycin with d(CGCGAATTCGCG)2." Acta Pol Pharm **57 Suppl**: 110-2.

Bissery, M. C. and G. G. Chabot (1991). "[History and new development of screening and evaluation methods of anticancer drugs used in vivo and in vitro]." Bull Cancer **78**(7): 587-602.

Bolton, M. G., O. M. Colvin, et al. (1991). "Specificity of isozymes of murine hepatic glutathione S-transferase for the conjugation of glutathione with L-phenylalanine mustard." Cancer Res **51**(9): 2410-5.

Bryant, H. E., N. Schultz, et al. (2005). "Specific killing of BRCA2-deficient tumours with inhibitors of poly(ADP-ribose) polymerase." Nature **434**(7035): 913-7.

Burger, H., J. A. Foekens, et al. (2003). "RNA expression of breast cancer resistance protein, lung resistance-related protein, multidrug resistance-associated proteins 1 and 2, and multidrug resistance gene 1 in breast cancer: correlation with chemotherapeutic response." Clin Cancer Res **9**(2): 827-36.

Burkert, U. and N. L. Allinger (1982). " Molecular MechanicsACS Monograph 177." American Chemical Society, Washington, DC.

Chambers, T. C., J. Pohl, et al. (1993). "Identification of specific sites in human P-glycoprotein phosphorylated by protein kinase C." J Biol Chem **268**(7): 4592-5.

Chan, L. M., S. Lowes, et al. (2004). "The ABCs of drug transport in intestine and liver: efflux proteins limiting drug absorption and bioavailability." Eur J Pharm Sci **21**(1): 25-51.

Chen, C. J., J. E. Chin, et al. (1986). "Internal duplication and homology with bacterial transport proteins in the mdr1 (P-glycoprotein) gene from multidrug-resistant human cells." Cell **47**(3): 381-9.

Chen, Z. S., R. W. Robey, et al. (2003). "Transport of methotrexate, methotrexate polyglutamates, and 17beta-estradiol 17-(beta-D-glucuronide) by ABCG2: effects of acquired mutations at R482 on methotrexate transport." Cancer Res **63**(14): 4048-54.

Cheung, A., E. Struble, et al. (2005). "Direct liquid chromatography determination of the reactive imine SJG-136 (NSC 694501)." J Chromatogr B Analyt Technol Biomed Life Sci **822**(1-2): 10-20.

Choi, C. H. (2005). "ABC transporters as multidrug resistance mechanisms and the development of chemosensitizers for their reversal." Cancer Cell Int **5**: 30.

Ciaccio, P. J., K. D. Tew, et al. (1990). "The spontaneous and glutathione S-transferase-mediated reaction of chlorambucil with glutathione." Cancer Commun **2**(8): 279-85.

Ciaccio, P. J., K. D. Tew, et al. (1991). "Enzymatic conjugation of chlorambucil with glutathione by human glutathione S-transferases and inhibition by ethacrynic acid." Biochem Pharmacol **42**(7): 1504-7.

Clark, A. G., J. N. Smith, et al. (1973). "Cross specificity in some vertebrate and insect glutathione-transferases with methyl parathion (dimethyl p-nitrophenyl phosphorothionate), 1-chloro-2,4-dinitro-benzene and s-crotonyl-N-acetylcysteamine as substrates." Biochem J **135**(3): 385-92.
Clark, R., I. D. Kerr, et al. (2006). "Multiple drugbinding sites on the R482G isoform of the ABCG2 transporter." Br J Pharmacol **149**(5): 506-15.
Clingen, P. H., I. U. De Silva, et al. (2005). "The XPF-ERCC1 endonuclease and homologous recombination contribute to the repair of minor groove DNA interstrand crosslinks in mammalian cells produced by the pyrrolo[2,1-c][1,4]benzodiazepine dimer SJG-136." Nucleic Acids Res **33**(10): 3283-91.
Cole, S. P. (1990). "Patterns of cross-resistance in a multidrug-resistant small-cell lung carcinoma cell line." Cancer Chemother Pharmacol **26**(4): 250-6.
Cole, S. P., G. Bhardwaj, et al. (1992). "Overexpression of a transporter gene in a multidrug-resistant human lung cancer cell line." Science **258**(5088): 1650-4.
Cole, S. P. and R. G. Deeley (2006). "Transport of glutathione and glutathione conjugates by MRP1." Trends Pharmacol Sci **27**(8): 438-46.
Conseil, G., R. G. Deeley, et al. (2005). "Polymorphisms of MRP1 (ABCC1) and related ATP-dependent drug transporters." Pharmacogenet Genomics **15**(8): 523-33.
Cooper, N., D. R. Hagan, et al. (2002). "Synthesis of novel C2-aryl pyrrolobenzodiazepines (PBDs) as potential antitumour agents." Chem Commun (Camb)(16): 1764-5.
Crowe, A. and M. Lemaire (1998). "In vitro and in situ absorption of SDZ-RAD using a human intestinal cell line (Caco-2) and a single pass perfusion model in rats: comparison with rapamycin." Pharm Res **15**(11): 1666-72.
Cruet-Hennequart, S., M. T. Glynn, et al. (2008). "Enhanced DNA-PK-mediated RPA2 hyperphosphorylation in DNA polymerase eta-deficient human cells treated with cisplatin and oxaliplatin." DNA Repair (Amst) **7**(4): 582-96.
Cui, X., M. Brenneman, et al. (1999). "The XRCC2 and XRCC3 repair genes are required for chromosome stability in mammalian cells." Mutat Res **434**(2): 75-88.
Damayanthi, Y., B. S. Praveen Reddy, et al. (1999). "Design and Synthesis of Novel Pyrrolo[2,1-c][1,4]benzodiazepine-Lexitropsin Conjugates." J Org Chem **64**(1): 290-292.
Damia, G., L. Imperatori, et al. (1996). "Sensitivity of CHO mutant cell lines with specific defects in nucleotide excision repair to different anti-cancer agents." Int J Cancer **66**(6): 779-83.
De Silva, I. U., P. J. McHugh, et al. (2000). "Defining the roles of nucleotide excision repair and recombination in the repair of DNA interstrand cross-links in mammalian cells." Mol Cell Biol **20**(21): 7980-90.
Deeley, R. G. and S. P. Cole (2006). "Substrate recognition and transport by multidrug resistance protein 1 (ABCC1)." FEBS Lett **580**(4): 1103-11.
Dellinger, M., B. C. Pressman, et al. (1992). "Structural requirements of simple organic cations for recognition by multidrug-resistant cells." Cancer Res **52**(22): 6385-9.
Didziapetris, R., P. Japertas, et al. (2003). "Classification analysis of P-glycoprotein substrate specificity." J Drug Target **11**(7): 391-406.

Diestra, J. E., E. Condom, et al. (2003). "Expression of multidrug resistance proteins P-glycoprotein, multidrug resistance protein 1, breast cancer resistance protein and lung resistance related protein in locally advanced bladder cancer treated with neoadjuvant chemotherapy: biological and clinical implications." J Urol **170**(4 Pt 1): 1383-7.

Dip, R., U. Camenisch, et al. (2004). "Mechanisms of DNA damage recognition and strand discrimination in human nucleotide excision repair." DNA Repair (Amst) **3**(11): 1409-23.

Dirven, H. A., E. L. Dictus, et al. (1995). "The role of human glutathione S-transferase isoenzymes in the formation of glutathione conjugates of the alkylating cytostatic drug thiotepa." Cancer Res **55**(8): 1701-6.

Dorr, R. T., J. D. Liddil, et al. (1986). "Cytotoxic effects of glutathione synthesis inhibition by L-buthionine-(SR)-sulfoximine on human and murine tumor cells." Invest New Drugs **4**(4): 305-13.

Doyle, L. A., W. Yang, et al. (1998). "A multidrug resistance transporter from human MCF-7 breast cancer cells." Proc Natl Acad Sci U S A **95**(26): 15665-70.

Drescher, S., E. Schaeffeler, et al. (2002). "MDR1 gene polymorphisms and disposition of the P-glycoprotein substrate fexofenadine." Br J Clin Pharmacol **53**(5): 526-34.

Dronkert, M. L. and R. Kanaar (2001). "Repair of DNA interstrand cross-links." Mutat Res **486**(4): 217-47.

Dulik, D. M., C. Fenselau, et al. (1986). "Characterization of melphalan-glutathione adducts whose formation is catalyzed by glutathione transferases." Biochem Pharmacol **35**(19): 3405-9.

Essodaigui, M., H. J. Broxterman, et al. (1998). "Kinetic analysis of calcein and calcein-acetoxymethylester efflux mediated by the multidrug resistance protein and P-glycoprotein." Biochemistry **37**(8): 2243-50.

Evans, J. W., S. B. Chernikova, et al. (2008). "Homologous recombination is the principal pathway for the repair of DNA damage induced by tirapazamine in mammalian cells." Cancer Res **68**(1): 257-65.

Evers, R., G. J. Zaman, et al. (1996). "Basolateral localization and export activity of the human multidrug resistance-associated protein in polarized pig kidney cells." J Clin Invest **97**(5): 1211-8.

Fairchild, C. R., J. A. Moscow, et al. (1990). "Multidrug resistance in cells transfected with human genes encoding a variant P-glycoprotein and glutathione S-transferase-pi." Mol Pharmacol **37**(6): 801-9.

Faneyte, I. F., P. M. Kristel, et al. (2002). "Expression of the breast cancer resistance protein in breast cancer." Clin Cancer Res **8**(4): 1068-74.

Feller, N., H. J. Broxterman, et al. (1995). "ATP-dependent efflux of calcein by the multidrug resistance protein (MRP): no inhibition by intracellular glutathione depletion." FEBS Lett **368**(2): 385-8.

Fichtinger-Schepman, A. M., J. L. van der Veer, et al. (1985). "Adducts of the antitumor drug cis-diamminedichloroplatinum(II) with DNA: formation, identification, and quantitation." Biochemistry **24**(3): 707-13.

Fojo, A. T., K. Ueda, et al. (1987). "Expression of a multidrug-resistance gene in human tumors and tissues." Proc Natl Acad Sci U S A **84**(1): 265-9.

Fukuyama, T. L., G.; Linton, S. D.; Lin, S. C.; Nishino, H. (1993). "Total Synthesis of (+)-Porothramycin-B." Tetrahedron Lett
(34): 2577-2580.
Gaitanos, T. N., R. M. Buey, et al. (2004). "Peloruside A does not bind to the taxoid site on beta-tubulin and retains its activity in multidrug-resistant cell lines." Cancer Res **64**(15): 5063-7.
Galimberti, S., F. Guerrini, et al. (2004). "Evaluation of BCRP and MDR-1 co-expression by quantitative molecular assessment in AML patients." Leuk Res **28**(4): 367-72.
Gekeler, V., W. Ise, et al. (1995). "The leukotriene LTD4 receptor antagonist MK571 specifically modulates MRP associated multidrug resistance." Biochem Biophys Res Commun **208**(1): 345-52.
Germann, U. A. (1996). "P-glycoprotein--a mediator of multidrug resistance in tumour cells." Eur J Cancer **32A**(6): 927-44.
Germann, U. A., P. V. Schoenlein, et al. (1994). "Putative "MDR enhancer" is located on human chromosome 20 and not linked to the MDR1 gene on chromosome 7." Genes Chromosomes Cancer **10**(4): 267-74.
Gervasini, G., J. A. Carrillo, et al. (2006). "Adenosine triphosphate-binding cassette B1 (ABCB1) (multidrug resistance 1) G2677T/A gene polymorphism is associated with high risk of lung cancer." Cancer **107**(12): 2850-7.
Goto, M., S. Masuda, et al. (2002). "C3435T polymorphism in the MDR1 gene affects the enterocyte expression level of CYP3A4 rather than Pgp in recipients of living-donor liver transplantation." Pharmacogenetics **12**(6): 451-7.
Goto, S., Y. Ihara, et al. (2001). "Doxorubicin-induced DNA intercalation and scavenging by nuclear glutathione S-transferase pi." Faseb J **15**(14): 2702-14.
Gottesman, M. M. and I. Pastan (1993). "Biochemistry of multidrug resistance mediated by the multidrug transporter." Annu Rev Biochem **62**: 385-427.
Grant, C. E., G. Valdimarsson, et al. (1994). "Overexpression of multidrug resistance-associated protein (MRP) increases resistance to natural product drugs." Cancer Res **54**(2): 357-61.
Gregson, S. J., P. W. Howard, et al. (2001). "Synthesis of the first example of a C2-C3/C2'-C3'-endo unsaturated pyrrolo[2,1-c][1,4]benzodiazepine dimer." Bioorg Med Chem Lett **11**(21): 2859-62.
Gregson, S. J., P. W. Howard, et al. (2004). "Linker length modulates DNA cross-linking reactivity and cytotoxic potency of C8/C8' ether-linked C2-exo-unsaturated pyrrolo[2,1-c][1,4]benzodiazepine (PBD) dimers." J Med Chem **47**(5): 1161-74.
Gregson, S. J., P. W. Howard, et al. (2001). "Design, synthesis, and evaluation of a novel pyrrolobenzodiazepine DNA-interactive agent with highly efficient cross-linking ability and potent cytotoxicity." J Med Chem **44**(5): 737-48.
Greiner, B., M. Eichelbaum, et al. (1999). "The role of intestinal P-glycoprotein in the interaction of digoxin and rifampin." J Clin Invest **104**(2): 147-53.
Guichard, S. M., J. S. Macpherson, et al. (2005). "Influence of P-glycoprotein expression on in vitro cytotoxicity and in vivo antitumour activity of the novel pyrrolobenzodiazepine dimer SJG-136." Eur J Cancer **41**(12): 1811-8.

Gupta, A., Y. Zhang, et al. (2004). "HIV protease inhibitors are inhibitors but not substrates of the human breast cancer resistance protein (BCRP/ABCG2)." J Pharmacol Exp Ther **310**(1): 334-41.
Hadjivassileva, T., D. E. Thurston, et al. (2005). "Pyrrolobenzodiazepine dimers: novel sequence-selective, DNA-interactive, cross-linking agents with activity against Gram-positive bacteria." J Antimicrob Chemother **56**(3): 513-8.
Hafkemeyer, P., S. Dey, et al. (1998). "Contribution to substrate specificity and transport of nonconserved residues in transmembrane domain 12 of human P-glycoprotein." Biochemistry **37**(46): 16400-9.
Hamilton, K. O., M. A. Yazdanian, et al. (2001). "Modulation of P-glycoprotein activity in Calu-3 cells using steroids and beta-ligands." Int J Pharm **228**(1-2): 171-9.
Hamilton, T. C., M. A. Winker, et al. (1985). "Augmentation of adriamycin, melphalan, and cisplatin cytotoxicity in drug-resistant and -sensitive human ovarian carcinoma cell lines by buthionine sulfoximine mediated glutathione depletion." Biochem Pharmacol **34**(14): 2583-6.
Han, K., J. Kahng, et al. (2000). "Expression of functional markers in acute nonlymphoblastic leukemia." Acta Haematol **104**(4): 174-80.
Hansen, M., S. Yun, et al. (1995). "Hedamycin intercalates the DNA helix and, through carbohydrate-mediated recognition in the minor groove, directs N7-alkylation of guanine in the major groove in a sequence-specific manner." Chem Biol **2**(4): 229-40.
Hartley, J. A., V. J. Spanswick, et al. (2004). "SJG-136 (NSC 694501), a novel rationally designed DNA minor groove interstrand cross-linking agent with potent and broad spectrum antitumor activity: part 1: cellular pharmacology, in vitro and initial in vivo antitumor activity." Cancer Res **64**(18): 6693-9.
Hartley, J. M., V. J. Spanswick, et al. (1999). "Measurement of DNA cross-linking in patients on ifosfamide therapy using the single cell gel electrophoresis (comet) assay." Clin Cancer Res **5**(3): 507-12.
Hayes, J. D., J. U. Flanagan, et al. (2005). "Glutathione transferases." Annu Rev Pharmacol Toxicol **45**: 51-88.
Hazlehurst, L. A., N. E. Foley, et al. (1999). "Multiple mechanisms confer drug resistance to mitoxantrone in the human 8226 myeloma cell line." Cancer Res **59**(5): 1021-8.
Hidalgo, I. J., T. J. Raub, et al. (1989). "Characterization of the human colon carcinoma cell line (Caco-2) as a model system for intestinal epithelial permeability." Gastroenterology **96**(3): 736-49.
Hipfner, D. R., K. C. Almquist, et al. (1997). "Membrane topology of the multidrug resistance protein (MRP). A study of glycosylation-site mutants reveals an extracytosolic NH2 terminus." J Biol Chem **272**(38): 23623-30.
Hipfner, D. R., R. G. Deeley, et al. (1999). "Structural, mechanistic and clinical aspects of MRP1." Biochim Biophys Acta **1461**(2): 359-76.
Hitzl, M., S. Drescher, et al. (2001). "The C3435T mutation in the human MDR1 gene is associated with altered efflux of the P-glycoprotein substrate rhodamine 123 from CD56+ natural killer cells." Pharmacogenetics **11**(4): 293-8.
Hoffmeyer, S., O. Burk, et al. (2000). "Functional polymorphisms of the human multidrug-resistance gene: multiple sequence variations and correlation of

one allele with P-glycoprotein expression and activity in vivo." Proc Natl Acad Sci U S A **97**(7): 3473-8.
Honjo, Y., C. A. Hrycyna, et al. (2001). "Acquired mutations in the MXR/BCRP/ABCP gene alter substrate specificity in MXR/BCRP/ABCP-overexpressing cells." Cancer Res **61**(18): 6635-9.
Hou, L., M. T. Honaker, et al. (2007). "Functional promiscuity correlates with conformational heterogeneity in A-class glutathione S-transferases." J Biol Chem **282**(32): 23264-74.
Hu, J., M. B. Reddy, et al. (2004). "Soyasaponin I and sapongenol B have limited absorption by Caco-2 intestinal cells and limited bioavailability in women." J Nutr **134**(8): 1867-73.
Humphrey, W., A. Dalke, et al. (1996). "VMD: visual molecular dynamics." J Mol Graph **14**(1): 33-8, 27-8.
Hurley, L. H., T. Reck, et al. (1988). "Pyrrolo[1,4]benzodiazepine antitumor antibiotics: relationship of DNA alkylation and sequence specificity to the biological activity of natural and synthetic compounds." Chem Res Toxicol **1**(5): 258-68.
Imai, Y., S. Asada, et al. (2003). "Breast cancer resistance protein exports sulfated estrogens but not free estrogens." Mol Pharmacol **64**(3): 610-8.
Ishikawa, T., C. D. Wright, et al. (1994). "GS-X pump is functionally overexpressed in cis-diamminedichloroplatinum (II)-resistant human leukemia HL-60 cells and down-regulated by cell differentiation." J Biol Chem **269**(46): 29085-93.
Iyer, V. N. and W. Szybalski (1963). "A Molecular Mechanism of Mitomycin Action: Linking of Complementary DNA Strands." Proc Natl Acad Sci U S A **50**: 355-62.
Iyer, V. N. and W. Szybalski (1964). "Mitomycins and Porfiromycin: Chemical Mechanism of Activation and Cross-Linking of DNA." Science **145**: 55-8.
Janvilisri, T., S. Shahi, et al. (2005). "Arginine-482 is not essential for transport of antibiotics, primary bile acids and unconjugated sterols by the human breast cancer resistance protein (ABCG2)." Biochem J **385**(Pt 2): 419-26.
Jedlitschky, G., I. Leier, et al. (1996). "Transport of glutathione, glucuronate, and sulfate conjugates by the MRP gene-encoded conjugate export pump." Cancer Res **56**(5): 988-94.
Jedlitschky, G., I. Leier, et al. (1994). "ATP-dependent transport of glutathione S-conjugates by the multidrug resistance-associated protein." Cancer Res **54**(18): 4833-6.
Jeppesen, M. G., P. Ortiz, et al. (2003). "The crystal structure of the glutathione S-transferase-like domain of elongation factor 1Bgamma from Saccharomyces cerevisiae." J Biol Chem **278**(47): 47190-8.
Johnson, J. I., S. Decker, et al. (2001). "Relationships between drug activity in NCI preclinical in vitro and in vivo models and early clinical trials." Br J Cancer **84**(10): 1424-31.
Juliano, R. L. and V. Ling (1976). "A surface glycoprotein modulating drug permeability in Chinese hamster ovary cell mutants." Biochim Biophys Acta **455**(1): 152-62.
Kage, K., S. Tsukahara, et al. (2002). "Dominant-negative inhibition of breast cancer resistance protein as drug efflux pump through the inhibition of S-S dependent homodimerization." Int J Cancer **97**(5): 626-30.

Kamal, A., A. H. Babu, et al. (2005). "Synthesis of pyrrolo[2,1-c][1,4]benzodiazepines and their conjugates by azido reductive cyclization strategy as potential DNA-binding agents." Bioorg Med Chem Lett **15**(10): 2621-3.
Kamal, A., D. R. Reddy, et al. (2006). "Synthesis and DNA-binding ability of pyrrolo[2,1-c][1,4]benzodiazepine-azepane conjugates." Bioorg Med Chem Lett **16**(5): 1160-3.
Kanzaki, A., M. Toi, et al. (2001). "Expression of multidrug resistance-related transporters in human breast carcinoma." Jpn J Cancer Res **92**(4): 452-8.
Kelner, M. J., T. C. McMorris, et al. (1987). "Preclinical evaluation of illudins as anticancer agents." Cancer Res **47**(12): 3186-9.
Keppler, D., I. Leier, et al. (1997). "Transport of glutathione conjugates and glucuronides by the multidrug resistance proteins MRP1 and MRP2." Biol Chem **378**(8): 787-91.
Kim, D. W., M. Kim, et al. (2006). "Lack of association between C3435T nucleotide MDR1 genetic polymorphism and multidrug-resistant epilepsy." Seizure **15**(5): 344-7.
Kim, R. B., B. F. Leake, et al. (2001). "Identification of functionally variant MDR1 alleles among European Americans and African Americans." Clin Pharmacol Ther **70**(2): 189-99.
Kimchi-Sarfaty, C., J. M. Oh, et al. (2007). "A "silent" polymorphism in the MDR1 gene changes substrate specificity." Science **315**(5811): 525-8.
Klimecki, W. T., B. W. Futscher, et al. (1994). "P-glycoprotein expression and function in circulating blood cells from normal volunteers." Blood **83**(9): 2451-8.
Kohn, K. W. (1991). "Principles and practice of DNA filter elution." Pharmacol Ther **49**(1-2): 55-77.
Konig, J., A. T. Nies, et al. (1999). "Conjugate export pumps of the multidrug resistance protein (MRP) family: localization, substrate specificity, and MRP2-mediated drug resistance." Biochim Biophys Acta **1461**(2): 377-94.
Krasznai, Z. T., J. Peli-Szabo, et al. (2006). "Paclitaxel modifies the accumulation of tumor-diagnostic tracers in different ways in P-glycoprotein-positive and negative cancer cells." Eur J Pharm Sci **28**(3): 249-56.
Krishna, R. and L. D. Mayer (2000). "Multidrug resistance (MDR) in cancer. Mechanisms, reversal using modulators of MDR and the role of MDR modulators in influencing the pharmacokinetics of anticancer drugs." Eur J Pharm Sci **11**(4): 265-83.
Krishnamurthy, P. and J. D. Schuetz (2006). "Role of ABCG2/BCRP in biology and medicine." Annu Rev Pharmacol Toxicol **46**: 381-410.
Kroetz, D. L., C. Pauli-Magnus, et al. (2003). "Sequence diversity and haplotype structure in the human ABCB1 (MDR1, multidrug resistance transporter) gene." Pharmacogenetics **13**(8): 481-94.
Kruh, G. D. and M. G. Belinsky (2003). "The MRP family of drug efflux pumps." Oncogene **22**(47): 7537-52.
Kurnik, D., G. G. Sofowora, et al. (2008). "Tariquidar, a selective P-glycoprotein inhibitor, does not potentiate loperamide's opioid brain effects in humans despite full inhibition of lymphocyte P-glycoprotein." Anesthesiology **109**(6): 1092-9.

Lai, S. L., L. J. Goldstein, et al. (1989). "MDR1 gene expression in lung cancer." J Natl Cancer Inst **81**(15): 1144-50.
Larbcharoensub, N., J. Leopairat, et al. (2008). "Association between multidrug resistance-associated protein 1 and poor prognosis in patients with nasopharyngeal carcinoma treated with radiotherapy and concurrent chemotherapy." Hum Pathol **39**(6): 837-45.
Lautier, D., Y. Canitrot, et al. (1996). "Multidrug resistance mediated by the multidrug resistance protein (MRP) gene." Biochem Pharmacol **52**(7): 967-77.
Lawley, P. D. and D. H. Phillips (1996). "DNA adducts from chemotherapeutic agents." Mutat Res **355**(1-2): 13-40.
Lee, B. and F. M. Richards (1971). "The interpretation of protein structures: estimation of static accessibility." J Mol Biol **55**(3): 379-400.
Lee, J. S., K. Paull, et al. (1994). "Rhodamine efflux patterns predict P-glycoprotein substrates in the National Cancer Institute drug screen." Mol Pharmacol **46**(4): 627-38.
Lehmann, T., C. Kohler, et al. (2001). "Expression of MRP1 and related transporters in human lung cells in culture." Toxicology **167**(1): 59-72.
Leier, I., G. Jedlitschky, et al. (1994). "The MRP gene encodes an ATP-dependent export pump for leukotriene C4 and structurally related conjugates." J Biol Chem **269**(45): 27807-10.
Lepper, E. R., K. Nooter, et al. (2005). "Mechanisms of resistance to anticancer drugs: the role of the polymorphic ABC transporters ABCB1 and ABCG2." Pharmacogenomics **6**(2): 115-38.
Leslie, E. M., R. G. Deeley, et al. (2003). "Bioflavonoid stimulation of glutathione transport by the 190-kDa multidrug resistance protein 1 (MRP1)." Drug Metab Dispos **31**(1): 11-5.
Leslie, E. M., R. G. Deeley, et al. (2005). "Multidrug resistance proteins: role of P-glycoprotein, MRP1, MRP2, and BCRP (ABCG2) in tissue defense." Toxicol Appl Pharmacol **204**(3): 216-37.
Leslie, E. M., Q. Mao, et al. (2001). "Modulation of multidrug resistance protein 1 (MRP1/ABCC1) transport and atpase activities by interaction with dietary flavonoids." Mol Pharmacol **59**(5): 1171-80.
Lin, J. H. (2003). "Drug-drug interaction mediated by inhibition and induction of P-glycoprotein." Adv Drug Deliv Rev **55**(1): 53-81.
Litman, T., M. Brangi, et al. (2000). "The multidrug-resistant phenotype associated with overexpression of the new ABC half-transporter, MXR (ABCG2)." J Cell Sci **113 (Pt 11)**: 2011-21.
Loe, D. W., R. G. Deeley, et al. (1998). "Characterization of vincristine transport by the M(r) 190,000 multidrug resistance protein (MRP): evidence for cotransport with reduced glutathione." Cancer Res **58**(22): 5130-6.
Lorke, D. E., M. Kruger, et al. (2001). "In vitro and in vivo tracer characteristics of an established multidrug-resistant human colon cancer cell line." J Nucl Med **42**(4): 646-54.
Malago, J. J., J. F. Koninkx, et al. (2003). "Expression levels of heat shock proteins in enterocyte-like Caco-2 cells after exposure to Salmonella enteritidis." Cell Stress Chaperones **8**(2): 194-203.

Markowska, M., R. Oberle, et al. (2001). "Optimizing Caco-2 cell monolayers to increase throughput in drug intestinal absorption analysis." J Pharmacol Toxicol Methods **46**(1): 51-5.
Martin, C., T. Ellis, et al. (2005). "Sequence-selective interaction of the minor-groove interstrand cross-linking agent SJG-136 with naked and cellular DNA: footprinting and enzyme inhibition studies." Biochemistry **44**(11): 4135-47.
Mechetner, E., A. Kyshtoobayeva, et al. (1998). "Levels of multidrug resistance (MDR1) P-glycoprotein expression by human breast cancer correlate with in vitro resistance to taxol and doxorubicin." Clin Cancer Res **4**(2): 389-98.
Meyer, D. J., K. S. Gilmore, et al. (1992). "Chlorambucil-monoglutathionyl conjugate is sequestered by human alpha class glutathione S-transferases." Br J Cancer **66**(3): 433-8.
Mirski, S. E., J. H. Gerlach, et al. (1987). "Multidrug resistance in a human small cell lung cancer cell line selected in adriamycin." Cancer Res **47**(10): 2594-8.
Mitomo, H., R. Kato, et al. (2003). "A functional study on polymorphism of the ATP-binding cassette transporter ABCG2: critical role of arginine-482 in methotrexate transport." Biochem J **373**(Pt 3): 767-74.
Miyake, K., L. Mickley, et al. (1999). "Molecular cloning of cDNAs which are highly overexpressed in mitoxantrone-resistant cells: demonstration of homology to ABC transport genes." Cancer Res **59**(1): 8-13.
Miyama, T., H. Takanaga, et al. (1998). "P-glycoprotein-mediated transport of itraconazole across the blood-brain barrier." Antimicrob Agents Chemother **42**(7): 1738-44.
Mohammad, R. M., M. C. Dugan, et al. (1998). "Establishment of a human pancreatic tumor xenograft model: potential application for preclinical evaluation of novel therapeutic agents." Pancreas **16**(1): 19-25.
Moradi, M., M. Mojtahedzadeh, et al. (2008). "The role of glutathione-S-transferase polymorphisms on clinical outcome of ALI/ARDS patient treated with N-acetylcysteine." Respir Med.
Morrow, C. S., S. Diah, et al. (1998). "Multidrug resistance protein and glutathione S-transferase P1-1 act in synergy to confer protection from 4-nitroquinoline 1-oxide toxicity." Carcinogenesis **19**(1): 109-15.
Morrow, C. S., C. Peklak-Scott, et al. (2006). "Multidrug resistance protein 1 (MRP1, ABCC1) mediates resistance to mitoxantrone via glutathione-dependent drug efflux." Mol Pharmacol **69**(4): 1499-505.
Muller, M., E. Bakos, et al. (1996). "Altered drug-stimulated ATPase activity in mutants of the human multidrug resistance protein." J Biol Chem **271**(4): 1877-83.
Muller, M., C. Meijer, et al. (1994). "Overexpression of the gene encoding the multidrug resistance-associated protein results in increased ATP-dependent glutathione S-conjugate transport." Proc Natl Acad Sci U S A **91**(26): 13033-7.
Nakagawa, H., H. Saito, et al. (2006). "Molecular modeling of new camptothecin analogues to circumvent ABCG2-mediated drug resistance in cancer." Cancer Lett **234**(1): 81-9.
Nakagawa, M., E. Schneider, et al. (1992). "Reduced intracellular drug accumulation in the absence of P-glycoprotein (mdr1) overexpression in mitoxantrone-resistant human MCF-7 breast cancer cells." Cancer Res **52**(22): 6175-81.

Nelson, H. C., J. T. Finch, et al. (1987). "The structure of an oligo(dA).oligo(dT) tract and its biological implications." Nature **330**(6145): 221-6.
Niedernhofer, L. J., H. Odijk, et al. (2004). "The structure-specific endonuclease Ercc1-Xpf is required to resolve DNA interstrand cross-link-induced double-strand breaks." Mol Cell Biol **24**(13): 5776-87.
O'Brien, M. L. and K. D. Tew (1996). "Glutathione and related enzymes in multidrug resistance." Eur J Cancer **32A**(6): 967-78.
Ohishi, Y., Y. Oda, et al. (2002). "ATP-binding cassette superfamily transporter gene expression in human primary ovarian carcinoma." Clin Cancer Res **8**(12): 3767-75.
Olaussen, K. A., A. Dunant, et al. (2006). "DNA repair by ERCC1 in non-small-cell lung cancer and cisplatin-based adjuvant chemotherapy." N Engl J Med **355**(10): 983-91.
Osterberg, T. and U. Norinder (2001). "Prediction of drug transport processes using simple parameters and PLS statistics. The use of ACD/logP and ACD/ChemSketch descriptors." Eur J Pharm Sci **12**(3): 327-37.
Ozvegy, C., A. Varadi, et al. (2002). "Characterization of drug transport, ATP hydrolysis, and nucleotide trapping by the human ABCG2 multidrug transporter. Modulation of substrate specificity by a point mutation." J Biol Chem **277**(50): 47980-90.
Paull, T. T., E. P. Rogakou, et al. (2000). "A critical role for histone H2AX in recruitment of repair factors to nuclear foci after DNA damage." Curr Biol **10**(15): 886-95.
Peng, K. C., F. Cluzeaud, et al. (1999). "Tissue and cell distribution of the multidrug resistance-associated protein (MRP) in mouse intestine and kidney." J Histochem Cytochem **47**(6): 757-68.
Pepper, C. J., R. M. Hambly, et al. (2004). "The novel sequence-specific DNA cross-linking agent SJG-136 (NSC 694501) has potent and selective in vitro cytotoxicity in human B-cell chronic lymphocytic leukemia cells with evidence of a p53-independent mechanism of cell kill." Cancer Res **64**(18): 6750-5.
Plowman J, D. D., Hollingshead M, Simpson-Herren L, Alley MC (1997). Human tumor xenograft models in NCI drug development. Anticancer drug development guide : preclinical screening, clinical trials, and approval. T. B. (ed). Totowa, New Jersey

Pullman, B., R. Lavery, et al. (1982). "Two aspects of DNA polymorphism and microheterogeneity: molecular electrostatic potential and steric accessibility." Eur J Biochem **124**(2): 229-38.
Puvvada, M. S., S. A. Forrow, et al. (1997). "Inhibition of bacteriophage T7 RNA polymerase in vitro transcription by DNA-binding pyrrolo[2,1-c][1,4]benzodiazepines." Biochemistry **36**(9): 2478-84.
Puvvada, M. S., J. A. Hartley, et al. (1993). "A quantitative assay to measure the relative DNA-binding affinity of pyrrolo[2,1-c] [1,4]benzodiazepine (PBD) antitumour antibiotics based on the inhibition of restriction endonuclease BamHI." Nucleic Acids Res **21**(16): 3671-5.
Qian, Y. M., W. C. Song, et al. (2001). "Glutathione stimulates sulfated estrogen transport by multidrug resistance protein 1." J Biol Chem **276**(9): 6404-11.

Rabindran, S. K., D. D. Ross, et al. (2000). "Fumitremorgin C reverses multidrug resistance in cells transfected with the breast cancer resistance protein." Cancer Res **60**(1): 47-50.
Ranaldi, G., K. Islam, et al. (1992). "Epithelial cells in culture as a model for the intestinal transport of antimicrobial agents." Antimicrob Agents Chemother **36**(7): 1374-81.
Rappa, G., A. Lorico, et al. (1997). "Evidence that the multidrug resistance protein (MRP) functions as a co-transporter of glutathione and natural product toxins." Cancer Res **57**(23): 5232-7.
Rautio, J., J. E. Humphreys, et al. (2006). "In vitro p-glycoprotein inhibition assays for assessment of clinical drug interaction potential of new drug candidates: a recommendation for probe substrates." Drug Metab Dispos **34**(5): 786-92.
Reeve, J. G., P. H. Rabbitts, et al. (1990). "Non-P-glycoprotein-mediated multidrug resistance with reduced EGF receptor expression in a human large cell lung cancer cell line." Br J Cancer **61**(6): 851-5.
Renes, J., E. G. de Vries, et al. (1999). "ATP- and glutathione-dependent transport of chemotherapeutic drugs by the multidrug resistance protein MRP1." Br J Pharmacol **126**(3): 681-8.
Robey, R. W., Y. Honjo, et al. (2003). "Mutations at amino-acid 482 in the ABCG2 gene affect substrate and antagonist specificity." Br J Cancer **89**(10): 1971-8.
Robey, R. W., Y. Honjo, et al. (2001). "A functional assay for detection of the mitoxantrone resistance protein, MXR (ABCG2)." Biochim Biophys Acta **1512**(2): 171-82.
Robey, R. W., K. Steadman, et al. (2004). "Pheophorbide a is a specific probe for ABCG2 function and inhibition." Cancer Res **64**(4): 1242-6.
Roepe, P. D. (1995). "The role of the MDR protein in altered drug translocation across tumor cell membranes." Biochim Biophys Acta **1241**(3): 385-405.
Rogakou, E. P., C. Boon, et al. (1999). "Megabase chromatin domains involved in DNA double-strand breaks in vivo." J Cell Biol **146**(5): 905-16.
Rogakou, E. P., D. R. Pilch, et al. (1998). "DNA double-stranded breaks induce histone H2AX phosphorylation on serine 139." J Biol Chem **273**(10): 5858-68.
Rogan, A. M., T. C. Hamilton, et al. (1984). "Reversal of adriamycin resistance by verapamil in human ovarian cancer." Science **224**(4652): 994-6.
Roizin-Towle, L. (1985). "Selective enhancement of hypoxic cell killing by melphalan via thiol depletion: in vitro studies with hypoxic cell sensitizers and buthionine sulfoximine." J Natl Cancer Inst **74**(1): 151-7.
Ross, D. D., W. Yang, et al. (1999). "Atypical multidrug resistance: breast cancer resistance protein messenger RNA expression in mitoxantrone-selected cell lines." J Natl Cancer Inst **91**(5): 429-33.
Russo, A., W. DeGraff, et al. (1986). "Selective modulation of glutathione levels in human normal versus tumor cells and subsequent differential response to chemotherapy drugs." Cancer Res **46**(6): 2845-8.
Sagnou, M. J., P. W. Howard, et al. (2000). "Design and synthesis of novel pyrrolobenzodiazepine (PBD) prodrugs for ADEPT and GDEPT." Bioorg Med Chem Lett **10**(18): 2083-6.

Saito, S., A. Iida, et al. (2002). "Three hundred twenty-six genetic variations in genes encoding nine members of ATP-binding cassette, subfamily B (ABCB/MDR/TAP), in the Japanese population." J Hum Genet **47**(1): 38-50.
Sakurai, A., Y. Onishi, et al. (2007). "Quantitative structure--activity relationship analysis and molecular dynamics simulation to functionally validate nonsynonymous polymorphisms of human ABC transporter ABCB1 (P-glycoprotein/MDR1)." Biochemistry **46**(26): 7678-93.
Salinas, A. E. and M. G. Wong (1999). "Glutathione S-transferases--a review." Curr Med Chem **6**(4): 279-309.
Samiulla, D. S., V. V. Vaidyanathan, et al. (2005). "Rational selection of structurally diverse natural product scaffolds with favorable ADME properties for drug discovery." Mol Divers **9**(1-3): 131-9.
Sato, K. (1989). "Glutathione transferases as markers of preneoplasia and neoplasia." Adv Cancer Res **52**: 205-55.
Satoh, K. (1995). "The high non-enzymatic conjugation rates of some glutathione S-transferase (GST) substrates at high glutathione concentrations." Carcinogenesis **16**(4): 869-74.
Satoh, T., M. Nishida, et al. (2001). "Expression of glutathione S-transferase pi (GST-pi) in human malignant ovarian tumors." Eur J Obstet Gynecol Reprod Biol **96**(2): 202-8.
Sauerbrey, A., W. Sell, et al. (2002). "Expression of the BCRP gene (ABCG2/MXR/ABCP) in childhood acute lymphoblastic leukaemia." Br J Haematol **118**(1): 147-50.
Schaefer, M., I. Roots, et al. (2006). "In-vitro transport characteristics discriminate wild-type ABCB1 (MDR1) from ALA893SER and ALA893THR polymorphisms." Pharmacogenet Genomics **16**(12): 855-61.
Schaich, M., L. Kestel, et al. (2008). "A MDR1 (ABCB1) gene single nucleotide polymorphism predicts outcome of temozolomide treatment in glioblastoma patients." Ann Oncol.
Schaich, M., S. Soucek, et al. (2005). "MDR1 and MRP1 gene expression are independent predictors for treatment outcome in adult acute myeloid leukaemia." Br J Haematol **128**(3): 324-32.
Schinkel, A. H., E. Wagenaar, et al. (1996). "P-glycoprotein in the blood-brain barrier of mice influences the brain penetration and pharmacological activity of many drugs." J Clin Invest **97**(11): 2517-24.
Seelig, A. (1998). "A general pattern for substrate recognition by P-glycoprotein." Eur J Biochem **251**(1-2): 252-61.
Seelig, A., R. Gottschlich, et al. (1994). "A method to determine the ability of drugs to diffuse through the blood-brain barrier." Proc Natl Acad Sci U S A **91**(1): 68-72.
Seelig, A. and E. Landwojtowicz (2000). "Structure-activity relationship of P-glycoprotein substrates and modifiers." Eur J Pharm Sci **12**(1): 31-40.
Shafran, A., I. Ifergan, et al. (2005). "ABCG2 harboring the Gly482 mutation confers high-level resistance to various hydrophilic antifolates." Cancer Res **65**(18): 8414-22.
Shah, R. B. and M. A. Khan (2004). "Regional permeability of salmon calcitonin in isolated rat gastrointestinal tracts: transport mechanism using Caco-2 cell monolayer." Aaps J **6**(4): e31.

Sharom, F. J. (1997). "The P-glycoprotein efflux pump: how does it transport drugs?" J Membr Biol **160**(3): 161-75.
Shen LZ, W. W. (1999). "Expression of P-glycoprotein and estrogen receptor in human primary colorectal carcinoma." Nanjing Med University **13**: 61-69.
Sills, G. J., R. Mohanraj, et al. (2005). "Lack of association between the C3435T polymorphism in the human multidrug resistance (MDR1) gene and response to antiepileptic drug treatment." Epilepsia **46**(5): 643-7.
Silverman, J. A. (1999). "Multidrug-resistance transporters." Pharm Biotechnol **12**: 353-86.
Skehan, P., R. Storeng, et al. (1990). "New colorimetric cytotoxicity assay for anticancer-drug screening." J Natl Cancer Inst **82**(13): 1107-12.
Slovak, M. L., G. A. Hoeltge, et al. (1988). "Pharmacological and biological evidence for differing mechanisms of doxorubicin resistance in two human tumor cell lines." Cancer Res **48**(10): 2793-7.
Smellie, M., D. S. Bose, et al. (2003). "Sequence-selective recognition of duplex DNA through covalent interstrand cross-linking: kinetic and molecular modeling studies with pyrrolobenzodiazepine dimers." Biochemistry **42**(27): 8232-9.
Smith, M. T., C. G. Evans, et al. (1989). "Denitrosation of 1,3-bis(2-chloroethyl)-1-nitrosourea by class mu glutathione transferases and its role in cellular resistance in rat brain tumor cells." Cancer Res **49**(10): 2621-5.
Soares, D. G., A. E. Escargueil, et al. (2007). "Replication and homologous recombination repair regulate DNA double-strand break formation by the antitumor alkylator ecteinascidin 743." Proc Natl Acad Sci U S A **104**(32): 13062-7.
Stehfest, E., A. Torky, et al. (2006). "Non-destructive micromethod for MRP1 functional assay in human lung tumor cells." Arch Toxicol **80**(3): 125-33.
Stojic, L., N. Mojas, et al. (2004). "Mismatch repair-dependent G2 checkpoint induced by low doses of SN1 type methylating agents requires the ATR kinase." Genes Dev **18**(11): 1331-44.
Su, Y., S. H. Lee, et al. (2006). "Inhibition of efflux transporter ABCG2/BCRP does not restore mitoxantrone sensitivity in irinotecan-selected human leukemia CPT-K5 cells: evidence for multifactorial multidrug resistance." Eur J Pharm Sci **29**(2): 102-10.
Suzuki, M., H. Suzuki, et al. (2003). "ABCG2 transports sulfated conjugates of steroids and xenobiotics." J Biol Chem **278**(25): 22644-9.
Szakacs, G., J. K. Paterson, et al. (2006). "Targeting multidrug resistance in cancer." Nat Rev Drug Discov **5**(3): 219-34.
Szakacs, G., A. Varadi, et al. (2008). "The role of ABC transporters in drug absorption, distribution, metabolism, excretion and toxicity (ADME-Tox)." Drug Discov Today **13**(9-10): 379-93.
Taguchi, Y., K. Kino, et al. (1997). "Alteration of substrate specificity by mutations at the His61 position in predicted transmembrane domain 1 of human MDR1/P-glycoprotein." Biochemistry **36**(29): 8883-9.
Taguchi, Y., M. Morishima, et al. (1997). "Amino acid substitutions in the first transmembrane domain (TM1) of P-glycoprotein that alter substrate specificity." FEBS Lett **413**(1): 142-6.

Takahashi, Y., H. Kondo, et al. (2002). "Common solubilizers to estimate the Caco-2 transport of poorly water-soluble drugs." Int J Pharm **246**(1-2): 85-94.
Tan, K. H., D. J. Meyer, et al. (1988). "Detoxification of DNA hydroperoxide by glutathione transferases and the purification and characterization of glutathione transferases of the rat liver nucleus." Biochem J **254**(3): 841-5.
Taylor, C. W., W. S. Dalton, et al. (1991). "Different mechanisms of decreased drug accumulation in doxorubicin and mitoxantrone resistant variants of the MCF7 human breast cancer cell line." Br J Cancer **63**(6): 923-9.
Tercero, J. A. and J. F. Diffley (2001). "Regulation of DNA replication fork progression through damaged DNA by the Mec1/Rad53 checkpoint." Nature **412**(6846): 553-7.
Tew, K. D., A. Monks, et al. (1996). "Glutathione-associated enzymes in the human cell lines of the National Cancer Institute Drug Screening Program." Mol Pharmacol **50**(1): 149-59.
Thiebaut, F., T. Tsuruo, et al. (1987). "Cellular localization of the multidrug-resistance gene product P-glycoprotein in normal human tissues." Proc Natl Acad Sci U S A **84**(21): 7735-8.
Thompson, A. S. and L. H. Hurley (1995). "Solution conformation of a bizelesin A-tract duplex adduct: DNA-DNA cross-linking of an A-tract straightens out bent DNA." J Mol Biol **252**(1): 86-101.
Thompson, L. H. and D. Schild (2002). "Recombinational DNA repair and human disease." Mutat Res **509**(1-2): 49-78.
Thurston, D. E. (1993). Advances in the Study of Pyrrolo[2,1-c][1,4]benzodiazepine (PBD) Antitumour Antibiotics. Molecular Aspects of Anticancer Drug-DNA Interactions. London, The Macmillan Press Ltd. **Vol. 1:** pp 54-88.
Tirumalasetty, P. P. and J. G. Eley (2006). "Permeability enhancing effects of the alkylglycoside, octylglucoside, on insulin permeation across epithelial membrane in vitro." J Pharm Pharm Sci **9**(1): 32-9.
Townsend, D. and K. Tew (2003). "Cancer drugs, genetic variation and the glutathione-S-transferase gene family." Am J Pharmacogenomics **3**(3): 157-72.
Tsuchida, S. and K. Sato (1992). "Glutathione transferases and cancer." Crit Rev Biochem Mol Biol **27**(4-5): 337-84.
Ueda, K., N. Okamura, et al. (1992). "Human P-glycoprotein transports cortisol, aldosterone, and dexamethasone, but not progesterone." J Biol Chem **267**(34): 24248-52.
Varma, M. V., K. Sateesh, et al. (2005). "Functional role of P-glycoprotein in limiting intestinal absorption of drugs: contribution of passive permeability to P-glycoprotein mediated efflux transport." Mol Pharm **2**(1): 12-21.
Vautier, S., L. Lacomblez, et al. (2006). "Interactions between the dopamine agonist, bromocriptine and the efflux protein, P-glycoprotein at the blood-brain barrier in the mouse." Eur J Pharm Sci **27**(2-3): 167-74.
Venkitaraman, A. R. (2002). "Cancer susceptibility and the functions of BRCA1 and BRCA2." Cell **108**(2): 171-82.
Volk, E. L., K. M. Farley, et al. (2002). "Overexpression of wild-type breast cancer resistance protein mediates methotrexate resistance." Cancer Res **62**(17): 5035-40.

Walton, M. I., P. Goddard, et al. (1996). "Preclinical pharmacology and antitumour activity of the novel sequence-selective DNA minor-groove cross-linking agent DSB-120." Cancer Chemother Pharmacol **38**(5): 431-8.
Wang, J. J., Y. K. Shen, et al. (2006). "Design, synthesis, and biological evaluation of pyrrolo[2,1-c][1,4]benzodiazepine and indole conjugates as anticancer agents." J Med Chem **49**(4): 1442-9.
Weinshilboum, R. (2003). "Richard Weinshilboum: Pharmacogenetics: The future is here!" Mol Interv **3**(3): 118-22.
Wells, G., C. R. Martin, et al. (2006). "Design, synthesis, and biophysical and biological evaluation of a series of pyrrolobenzodiazepine-poly(N-methylpyrrole) conjugates." J Med Chem **49**(18): 5442-61.
Westlake, C. J., S. P. Cole, et al. (2005). "Role of the NH2-terminal membrane spanning domain of multidrug resistance protein 1/ABCC1 in protein processing and trafficking." Mol Biol Cell **16**(5): 2483-92.
Xia, C. Q., N. Liu, et al. (2005). "Expression, localization, and functional characteristics of breast cancer resistance protein in Caco-2 cells." Drug Metab Dispos **33**(5): 637-43.
Yoh, K., G. Ishii, et al. (2004). "Breast cancer resistance protein impacts clinical outcome in platinum-based chemotherapy for advanced non-small cell lung cancer." Clin Cancer Res **10**(5): 1691-7.
Yoshimoto, K., H. Iwahana, et al. (1988). "A polymorphic HindIII site within the human multidrug resistance gene 1 (MDR1)." Nucleic Acids Res **16**(24): 11850.
Yuan, Z. M., P. B. Smith, et al. (1991). "Glutathione conjugation with phosphoramide mustard and cyclophosphamide. A mechanistic study using tandem mass spectrometry." Drug Metab Dispos **19**(3): 625-9.
Zaman, G. J., N. H. Cnubben, et al. (1996). "Transport of the glutathione conjugate of ethacrynic acid by the human multidrug resistance protein MRP." FEBS Lett **391**(1-2): 126-30.
Zaman, G. J., M. J. Flens, et al. (1994). "The human multidrug resistance-associated protein MRP is a plasma membrane drug-efflux pump." Proc Natl Acad Sci U S A **91**(19): 8822-6.
Zaman, G. J., J. Lankelma, et al. (1995). "Role of glutathione in the export of compounds from cells by the multidrug-resistance-associated protein." Proc Natl Acad Sci U S A **92**(17): 7690-4.
Zeng, H., Z. S. Chen, et al. (2001). "Transport of methotrexate (MTX) and folates by multidrug resistance protein (MRP) 3 and MRP1: effect of polyglutamylation on MTX transport." Cancer Res **61**(19): 7225-32.
Zewail-Foote, M. and L. H. Hurley (1999). "Ecteinascidin 743: a minor groove alkylator that bends DNA toward the major groove." J Med Chem **42**(14): 2493-7.